REMOTE SENSING AND GEOGRAPHICAL INFORMATION SYSTEM (GIS) MODELLING OF LANDUSE/LANDCOVER AND CLIMATE CHANGE IN THE DERIVED SAVANNAH REGION OF NIGERIA

AKINTUYI Akinlabi Oluyemi (029082030)
B.Sc. (Geography & Regional planning) LASU, M.Sc. (Geography) Lagos

A thesis submitted to the School of Postgraduate Studies, University of Lagos in partial fulfilment for the award of the degree of Doctor of Philosophy (PhD) in Geography

February, 2015

UNIVERSITY OF LAGOS
SCHOOL OF POSTGRADUATE STUDIES
DEPARTMENT OF GEOGRAPHY

This is to certify that this thesis:

Remote Sensing and Geographical Information System (GIS) Modelling of Landuse/Landcover and Climate Change in the Derived Savannah Region of Nigeria

SUBMITTED TO SCHOOL OF POSTGRADUATE STUDIES

For the
DEGREE DOCTOR OF PHILOSOPHY (PhD)

Is a record of original research carried out by

AKINTUYI, AKINLABI OLUYEMI

In the Department of Geography

Author's name	signature	Date
Supervisor's name	signature	Date
Supervisor's name	signature	Date
Supervisor's name	signature	Date
Internal Examiner's name	signature	Date
Internal Examiner's name	signature	Date
External Examiner's name	signature	Date
PG School Representative	signature	Date

DEDICATION

I dedicate this thesis to Almighty **GOD**, the Author and the Finisher of my Faith who enabled me to successfully complete this programme, and also, to the memory of my late father,
CHIEF Christopher Olufemi AKINTUYI

ACKNOWLEDGEMENTS

First of all, Glory and Hallelujah to the Almighty God in the highest for the knowledge, understanding and wisdom given to me for the successful completion of this thesis. I appreciate You for being there for me throughout this programme. "*Thank You"* heavenly Lord for the grace and mercy shower on me and my family.

My appreciation goes to my supervisors, Drs A.S.O. Soneye and M.J. Fasona and our Baba, Prof. Adeniyi for their valuable guidance, patience and criticism, despite their busy schedules. I can now understand the love and the pain felt by Dr. Soneye when he would call me to know my whereabout or give a deadline that I thought was impossible. Thank you sir and "God will continually take care of your own garden as you have done to me and my family". Also, Dr. Fasona (*Fash*) thank you once again for your time and help right from conceptualization of this research to the last page. I really appreciate your effort towards the success of this work; you have been more than a supervisor, but a brother. Thanks for your brotherly love and care. God bless you and your family.

I am really indebted to Prof Omojola and his family, who is not only an uncle, but a father; thank you for seeing the vision when the future looks bleak and standing by me through the realization of it. I am grateful for your support both financially and mentally without which I would not be where I am. I pray that God will continue to shower His blessing on you and your family and take you to a most enviable position.

Also, Prof. Oni has been wonderful to me and family, *my HOD;* I will say a big thank you for your wealth of experience, criticism and willingness to always assist at any point in time. Furthermore, to all staff of the department who see me as their brother, Drs Babatola, Balogun, Uluocha, Feyi Oni, Ogunkunle, Adeaga, Odunuga, Adedayo, Ege, Elias, Omenai, Ojekunle and others, thank you for the job well-done. Dr. Odunuga, thank you for the private discussions, encouragement and challenge to do a standard work. In addition, Mr. Ogunkunle, *my course adviser*, thank you sir for the time taken to read through my GRY 901 seminar paper and your contributions really enriched this work, once again thank you.

Similarly, *My coordinator*, Dr. Adeaga I do not know how to appreciate you for being wonderful, all the same, thank you for being our own professor and coordinator of coordinators.

I also appreciate the contribution of my colleagues, especially, the *Resource Group*, which include Dr. Ayeni, Isaiah Akoteyon, Bola Daramola, K.K. Biney, Emmanuel Wunude and Kayode Fashuan and others not mentioned here. Thanks and God bless you all. Furthermore, to other M.Phil/PhD candidates, Mrs. Oni, Emily Ojukwu, Uma Odim, Messers S. Muyiolu, Olorunmibe and Onyekuwelu and Kemi Efunsade; your contributions are highly appreciated. Special thanks to Mr. Seun Raji for his encouragement, Remote Sensing software and interpretation.

My parents, Late (Chief) and Mrs. Akintuyi have been wonderful, thanks for your prayers and parental care. Also, Alhaji Azeez Olaseni, my uncle, thank you for laying the foundation. I could remember the short period (1984 – 1985) that I stayed with you; it was very informative, educative and interesting. Special Thanks also go to my brothers, Pastor Abiodun Akintuyi and Dayo Omojola, and my sisters Yinka, Bolaji, Abike and Kemi. Thanks once again, I really appreciate your contributions.

Special thanks go to Dr. Nurayn Alimi of English Dept., UNILAG, my language editor, for a job well done in spite of his busy schedule and to my friends, Alli-Balogun, Emmanuel, Ope, Femi (Doggy), Faithy, Lola, Wale, Timlock Wazhi, Toyin Makinde and Joy, thanks for your understanding and for not being with you when I was supposed to be. I wish you all good luck and happiness in future endeavours. Mention should also be made of Miss Tope Alimi for her contributions and the support, thanks girl.

This acknowledgement will not be accepted if Dr. Alex Uriri is not mentioned, *my personal person*, thank you and I appreciate your contributions and the zeal to win, regards to Nicole and the mum.

Finally, my family has been very supportive, caring and prayerful, Mrs. Funmi Akintuyi, my love and a woman made from my ribs, thank you for taking care of the home front and keeping vigils whenever I come home very late and also for other excesses of mine. To my kids, Oreoluwa and Oluwatamilore, thank you for your understanding, for not dedicating enough time for you; that will change from now. God will continue to unite us with His love and we will wax stronger by the day. Thanks once again and God bless.

TABLE OF CONTENTS

Page

LIST OF TABLES

LIST OF FIGURES

ABSTRACT

The interaction of landuse/Landcover (LULC) and climate change, to a large extent, involves anthropogenic activities. This interaction has brought about a complex global environmental change which includes biodiversity loss, land degradation, deforestation, afforestation and forest degradation among others. Such change is manifested through the dual nature of landuse/landcover both as causal factor and as effect of climate change. LULC is initiated through human activities such as forest harvesting for logging, fuelwood and charcoal production without forest regeneration of these forest resources, bush fires, overgrazing, as well as urban and agricultural expansion that tends to increase the concentration of greenhouse gases (GHGs). This study was carried out in a delicate ecological zone where the interaction of LULC and climate change could be well appreciated. The zone is an interface between the forest and savannah zones experiencing drastic environmental change as it impacts on desert encroachment and resource conflicts. The study evaluated coupled interaction between LULC and climate change within the derived savannah zone of Nigeria. It assessed the changes in the landuse/landcover patterns for the periods 1972, 1986, 2002 and 2010, and evaluated the variability in rainfall and temperature as the dominant climatic parameters within the study area over the area from 1941 to 2010. In addition, an attempt was made to predict the interaction between LULC and climate change and to estimate the changes in carbon stock resulting from LULCC. The study further employed remote sensing and GIS techniques to interpret and analyse Landsat satellite imageries for the period under study while the multivariate statistical analysis was used to analyse the historical and downscaled climate data for the present and future climates. In predicting the nature of interaction between LULC and climate for future climate within the region, the study adopted both statistical and Land Change Modeller (LCM) techniques. The study revealed that the built up area, farmland, waterbody and woodland experienced a rapid increase of about 1,134.69%, 1,202.85%, 631.51% and 188.09%, respectively, while the forest cover, degraded surfaces and grassland lost about 19.32%, 72.76% and 0.05% respectively between 1972 and 2010. The study thus confirmed the sinusoidal nature of the climatic pattern with 2.03mm (0.02%) and 0.15mm (0.01%) increase per annum for mean annual rainfall and rainfall anomaly respectively with annual mean rainfall of 1,316mm for the present climate. The future climate was predicted to increase at a rate of 3.13mm (0.2%) per annum for mean annual rainfall with an annual mean of 1,393mm. Also, the rainfall variability index during the present climate ranges between 15 and 23% and 9 – 13% for future climate, which indicated that rainfall will be more stable in the future climate, while temperature variability indices range from 1.42 – 2.41% and 1.26 – 1.33% for both the present and future climates respectively. Due to the short temperature range predicted for the future climate, temperature will be more stable with higher intensity. Furthermore, the study predicted 40.28% and 37.84% reduction in the forested area between 1986 and 2050 and 2010 and 2050 respectively. In addition, the study estimated that about 298,767,040 tons of CO_2 will be emitted due to the deforestation and forest degradation induced by the interaction of LULC and climate. The study concludes that climate parameters, especially rainfall will be the major driver of LULC change within the study area and calls for further studies on the implications of rainfall variability and change during future climate.

DEFINITION OF TERMS

Remote Sensing and GIS: Remote Sensing is the science and art of acquiring information without coming into physical contact with the objects, or area, or phenomenon while GIS (Geographical Information Systems) can be manual or computer based set of procedures used to store and manipulates geographically referenced data.

Landuse - This refers to the natural and man-made features on the earth's surface with emphasis on the types and economic value of use.

Landcover – This refers to the natural and man-made features on the earth's surface, be it waterbodies, vegetal cover, rock outcrops, built-up area.

Landuse/Landcover (LULC) change – This is the process of conversion in the type of LULC due to human and/or natural activities.

Climate, Variability and Change – Climate is the average atmospheric condition of a place or region over a period of time, 30 – 35 years. Climate variability is the fluctuation in climatic parameters over or below the long time average value, while climate change is regarded as the consistent variation in the climate of a region for a comparable period of time, whether due to natural variability or as a result of anthropogenic activities.

Deforestation – This is a process of forest conversion to other land uses (farmland, grassland, woodland, etc) excluding conversion to surface, which cannot support vegetation growth.

Forest Degradation –This is a situation where forest land is converted to another surfaces or landuse classes like built-up area, road construction, eroded surface, etc, which cannot supports vegetation or plant grow.

Transition Potential – This is an index of land change model that shows the tendency of a landcover class to change to another.

Land Change Modeler – This is a land change analysis algorithm. The Land Change Modeler adopted in this study was developed by Clark laboratory for landcover analysis and prediction, estimation of GHG emission reductions, land change implication on biodiversity and planning interventions.

Idrisi Selva/ArcGIS – This is the Latest version of Remote sensing and GIS software used for integration of data, coupling of model and prediction of future landuse/ landcover

Derived Savannah: Derived savannah constitutes the transition region between the northern boundary of forest zones and the southern boundary of Guinea Savannah.

CHAPTER ONE

INTRODUCTION

1.1 Background to the Study

There has been increasing interest in the events of climatic variations and their implications on natural systems and human activities globally in recent time (Braganza *et al.,* 2002; IPCC, 2007 and Rosenzweig *et al*., 2007). The climatic variations termed variously as climate change, according to the Intergovernmental Panel on Climate Change (IPCC) (2001), refer to change in the climate of a region for a comparable period of time, whether due to natural variability or as a result of anthropogenic activities such as landuse/landcover (LULC) changes, burning of fossil fuel, urbanisation and industrialisation. When the fluctuations in climatic parameters such as temperature, precipitation, winds, clouds and humidity revolve around their normal averages, the variations are regarded as normal. However, variations are regarded as abnormal when they deviate significantly from their long time normal averages.

Historical records show evidences of climate variability and change (Mahoney *et al*., 2003). Odekunle *et al.* (2005) and Odjugo (2011) assert that Nigeria's climate has been witnessing increasing temperature at the rate of about 0.15^0C per decade and decreasing amount of rainfall in the last 70 years. Also, Braganza *et al.* (2002) used the historical records of surface air temperature for about 120 years to conclude that the observed indices of climate variability and change simulated well and fit into the trend of the climate of 1700 to 1900. Amongst others, anthropogenic factors such as deforestation and burning of fossil fuel are concrete activities of man that contribute significantly to increase in the concentration of Greenhouse Gases (GHGs) (Soneye, 2012). On the other hand, the natural factors are phenomena of volcanic eruptions and changes in the Earth's orbit, the sun's intensity and the

circulation of ocean and atmosphere constitute the natural factors leading to the heightened concentration of Greenhouse Gases (GHGs).

The stocks and flows approach adopted by IPCC (2001) and Le Treut *et al.* (2007), presents the globe as four interacting systems, made up of four sub-systems representing (i) society and the economy, (ii) atmospheric concentrations, (iii) climate and (iv) natural systems. The interactions and feedbacks within these systems are complex and are capable of leading to extreme events such as climate change, critical thresholds and shocks. For instance, there are three feedbacks and interactions within these systems. The first is the feedback from sea temperature rise to atmospheric concentrations, because the sea absorbs less carbon dioxide (CO_2) at higher temperature (Dale, 1997; Barker, 2003). The second is the possibility of some feedbacks from the changes in the natural systems to the climate system, such as albedo effects from changing LULC or land surface characteristics, and other larger interactions between the natural systems and atmospheric concentrations. The third, termed the climate system, is defined by Baede, *et al.* (2001) as an interacting system consisting of five major components namely, the atmosphere, the hydrosphere, the cryosphere, the land surface and the biosphere which is forcefully influenced by various external mechanisms, the most important of which is the sun. Although, all these affect human activities, the external forcing mechanisms is the most dominant.

Climate plays crucial roles in the distribution and development of land resources by determining the flora and fauna found on the land surface. However, LULC is one of the human activities influencing the climate of an area (Turner, 1993 and Dale, 1997). The impacts of LULC changes on climate are locally significant in some regions, but are negligible at the global scale when compared to GHGs warming. In spite of this, changes in

the land surface cover such as vegetation, soils and water resulting from human activities can affect local climate significantly through shifts in radiation, cloudiness, surface roughness and surface temperatures and eventually, the surface energy and water balance (Solomon *et al.,* 2007). Landcover is defined as the attributes of the earth's land surface and immediate subsurface, including biota, soil, topography, surface and groundwater, and human structures (Lambin *et al*., 2003). Landuse is simply regarded as the types of use or activities and management practices put into a piece of land. The visible evidence of landuse include both the vegetative and non-vegetative features even though the concept emphasises management and economic functions (Campbell, 1996). Landuse is largely influenced by both underlying and proximate factors such as agricultural intensification, infrastructural expansion, demographic change, economics, socio-cultural, institutional and policies (Geist and Lambin, 2002; 2004).

The implication of the forgoing is that spatial differentiation in landcover and its use in an area are induced by both the natural and anthropogenic factors. Landuse/landcover change is also by implication both a driver and effect of climate change because of its multi-stressor effects in terms of changing characteristics of the surface and exchange of fluxes between land surface and atmosphere (Turner, 1993; Dale, 1997; Mahoney *et al.,* 2003; Pielke and Avissar, 1990). Consequent upon this, Landuse/landcover changes are taking place at unprecedented magnitude, rate and spatial scales (Turner II *et al.,* 1994) and are becoming significant contributors to climate variability and change due to the strong linkages between the land surface and climate (Solomon, *et al.,* 2007). For example, studies by Xue and Shukla (1993); and Dale (1997) have demonstrated the importance of LULC to regional rainfall distribution. However, most of these studies are one-sided because they emphasise only the

rainfall distribution over other climate parameters like temperature, relative humidity, wind, etc., which are also very important to the climate patterns or variability of region.

1.2 Statement of the Problem

Global changes in arid, semi-arid and dry sub-humid areas are not necessarily driven by climatologically-induced variables. Rather, they are triggered by anthropogenic activities in an attempt by man to adjust to human needs and aspirations (Matthew, 1982). Although, the increase in the concentration of greenhouse gases in the atmosphere is the best known impact of human activities on climate change, variations in landuse/landcover may be of equal importance (Pielke, 1997; Pitman, 2000). Thus, a basic understanding of the characteristics of climatic parameters and atmospheric conditions over a place for some periods of time would provide an understanding of the significance of LULC changes to climatic variability and change. Large scale LULC change modifies the surface albedo and surface–atmosphere energy exchanges (Pielke and Avissar, 1990). Consequently, it has an effect on the atmospheric flux of carbon dioxide (CO_2) and determines the contribution of evapo-transpiration to the precipitation recycling, which has impacts on both the local, regional and global climate. Due to the complex interaction between LULC and climate, therefore, there is the need to develop new models that will link climate variability and change with socio-economic drivers for better understanding (Loveland *et al.,* 2003).

The interaction between LULC and climate is complex, it can be viewed from three dimensions. First, the interaction of LULC or vegetation on climate - LULC determines or modifies climate or induce changes in climate of a region as it is a factor of climate. Second, the interaction of climate on LULC or vegetation - change in climate induced LULC change or modifies LULC of a place being an effect of climate. Finally, it can be viewed from the

feedbacks from the interaction. To this end, most studies have emphasized the interaction of LULC on regional climate and considered LULC as a factor of climate. Previous studies in Africa and globally have either not fully integrated or have downplayed the importance of LULC change to climate and climate variability. Also, focus has largely been on the landscape or land fragmentation and vegetation distribution, without any consideration of the human impacts (Pielke *et al.,* 2007; Pielke and Avissar, 1990; Matthews, 1982). In few instances where LULC were integrated to model scenarios, emphasize have been put on the global or regional scale and at a coarse resolution (Zheng and Eltahir, 1997; Pitman *et al.,* 2000; Wang *et al*., 2004; Zeng *et al*., 1999). For example, Zheng and Eltahir (1997) modelled the response of the West Africa monsoon to deforestation and desertification at horizontal and vertical resolutions of about 2^0 and 1km respectively.

In addition, Pitman *et al.* (2000) investigated the role of the land surface in determining weather and climate. They concluded that land surface affects the partitioning of water and energy and do cause changes in the atmosphere. However, they queried if these changes are large enough to determine the weather and climate of a place. This query was answered by stating the examples of drying experienced after large scale deforestation in Africa and Western Ghats of India; changes in US landuse and changes in the microclimate that followed the Amazon deforestation. Pitman *et al.* (2000) noted the fundamental gap in the importance of changing land surface to climate and weather. Because measurement is generally too short on the time scale to determine the roles of land surface in climate, modeling studies have tended to rely on unrealistically large perturbations. The fact that LULC change plays a major role in the balancing of radiation of the earth and in maintaining a number of biogeochemical cycles related to climate and climate change justify the need to downscale existing models on the trend and cycle of LULC and climate changes to finer resolution.

Until recently, generating temporal data on LULC had been difficult due to non-availability of the required data at such a digital format and at fine resolution. With the advent of spatial technology, large volume of dataset can be processed, analyzed and stored in retrieval devices consistently both in format and resolution. Most studies in Nigeria have not taken the advantages offered by the spatial techniques such as Remote Sensing and Geographic Information System (GIS) to generate, integrate and manipulate the large volume of data on the static and dynamic attributes of LULC over time and space (Adeniyi *et al*., 1992; Soneye and Akintuyi, 2013). In terms of climate variability and change, most existing studies have focused on vulnerability, impacts and adaptation to the neglect of the interaction and feedback between landcover and climate (Odjugo and Ikhuoria, 2005; Odjugo, 2011).

LULC characteristics in Nigeria are closely linked to vegetation distribution and are controlled by the interaction of the variables of climate, soils and human activities. In broad terms, the different vegetation zones are savannahs and forests. Comparatively, more expanse savannah zone receives lower rainfall over a shorter period, the higher the temperature over a longer period comparatively. The savannah zone can however be subdivided into three natural savannah types. These are the Guinea, Sudan and Sahel. They are significant for animal grazing and farming.

The Nigeria savannah zone is prone to desert encroachment, increasing temperature and decreasing rainfall, increasing human and animal population, overgrazing and lack of rangeland for grazing. These have predisposed the area to the dangers of environmental change which include climate change. For instance, changes in landcover patterns are one way in which the effects of climate change are expressed (Dale, 1997). Other ways are land degradation, flooding, such as the recent experience in substantial part of Kogi State in 2012, etc. In addition to these problems, are the downward spread of desert encroachment and

reducing farm yield, land-cum-resource conflict between cattle herders from the Sudan and Sahel savanna zones and local farmers of the Guinea savanna zone. These have acted as the push factors for the local human and animal population to migrate southward to Derived Savannah, which they consider to be more habitable and conducive due to long rainy season.

Derived savannah is the transition region between the northern boundary of forest zones and the southern boundary of guinea savannah (Clayton, 1962). This region is originally the drier part of the high forest zone, but has been destroyed as a result of deforestation, bush burning, overgrazing, cultivation and human activities over a long period and replaced with a mixture of tall grasses and scattered trees. Consequently, the ecological balance of the derived savannah has come under threat as could be seen in recent events within the area. Fasona & Omojola (2005) revealed that 35% of the conflict reported between 1991 and 2005 within the zone are land resources driven and as evidence from the recent conflict between Hausa-Fulani and Tivs in Benue State. This scenario may be attributed to the downward movement of nomads from the main savannah zone for greener pasture for their cattle. The nomads have turned this zone to their permanent abode as they are found grazing animals all year round in such places like Oshogbo, Ado Ekiti, Ikole, Igbagun, etc. Unlike the practice in the past, the nomads are now usually seen during the dry season, while they leave at the onset of the rainy season.

This situation has provoked the local farmers. This is because the activities of the nomads have affected or compounded their economic problems or reduced food production by destroying or reducing returns from their farm holdings. Nomads' activities have also an effect on the land surface characteristics as farmers have resulted to shifting cultivation, shortened bush fallowing or deforestation (Geist & Lambin, 2004) to increase their farm holdings. For example, Nigeria has lost about 55% of primary forest between 2000 and 2005

due to deforestation, the highest in the world. The country is also one of the two largest losers of natural forest in Africa (FAO, 2006). Also, as a consequence of this, the country had 2.7% and 3.7% annual forest lost during 1990 to 2000 and 2000 to 2010 respectively (FAO, 2011). Furthermore, the Derived Savannah region is important to economy of Nigeria being the region where food crops - both tuber and cereal crops are grown. In spite of this the fragile ecosystem has been under pressure from increased human activities, and downward desert encroachment. Also, increasing population and urbanization, large scale charcoal production in the study area such as in the Oke Ogun area, which involves processes that cause large scale deforestation and land degradation, rain-fed farming as well as shifting cultivation system have upset landuse practices. The shifting cultivation system in particular has contributed to the complex interaction of LULC and climate change of the study area.

The interaction of LULC and climate change has been found both at regional and global scales to have environmental feedbacks. However, there still remains the uncertainty in the coupling of the coupled models (Randall *et al.*, 2007), which is an important aspect. The evaluation of the land surface component in coupled models is often severely limited by lack of suitable observations. The terrestrial surface plays key climatic roles in influencing the partitioning of available energy between sensible and latent heat fluxes. It specially determines whether water drains or remains, or whether it is available for evaporation. Terrestial surfaces, in addition determines the surface albedo and whether snow melts or remains frozen, and also influences surface fluxes of carbon and momentum. In Africa, some of these models have been evaluated at regional and local scales with high level of confidence in their performance reported (Hewitson and Crane, 1996). However, at the local scale, more observations are still required. To this end, there is the need to incorporate studies at the local scale in the observation and evaluation of these models. This research is, therefore, an attempt to model the complex interactions of LULC and climate change in the

Derived Savannah region of Nigeria. The study used historical climate data for the present climate, statistical downscaling of one of the global climatic models (GCMs) under A2 climate Special Report on Emission Scenarios (SRES) for the future climate and coupled it with interactive remotely sensed data at a relative fine resolution of 30metres (1arcsecond) to simulate LULC patterns for the future climate.

1.3 Aim and Objectives

The aim of the study is to model the interaction of LULC and climate change in the derived savannah region of Nigeria using satellite Remote Sensing data and Geographical Information System (GIS) techniques.

The specific objectives are to:

i. Assess the changes in the LULC patterns within the study area for the periods 1972, 1986, 2002 and 2010;
ii. Evaluate the variability in Rainfall and Temperature over the study area between 1941 and 2010 for present climate and 2011 and 2050 for future climate;
iii. Model the impact of climate change on landuse/landcover changes within the study area, and
iv. Estimate the changes in carbon stock resulting from interaction of landcover change and climate change during the present and future climate of the study area.

1.4 Research Questions

The following are the research questions:

i. What are the extent, rate and direction of landcover and landuse changes in the derived savannah area of Nigeria?
ii. What are the trends in the dominant climatic variables within the area as local, regional and global change induced factors?

iii. How can the interaction between climatic variability and LULC be modeled to explain the changes in the spatial distribution and pattern of LULC of the area?

iv. What are the implications of the climate – LULC interaction on the human and environmental systems in the study area?

1.5 Justification and Significance of the Study

The interaction between climate and LULC is complex in nature and interwoven. There is the need for proper understanding of the coupling and feedbacks between the climate variability and change and LULC variables. The contributions of LULC to the global climate change might be minute, however, it is significant at the local level when considering the role it plays in the modification of surface albedo, landscape fragmentation, burning of biomass and generally its anthropogenic effects on the concentration of greenhouse gases (GHGs).

The study area plays an important role in the economy of the country being an ecological zone where food and cash crops are grown. Also, the area is fragile ecologically and it is an interface between the forest and savannah ecological zones, which is presently generating environmental and sustainability concerns relative to population growth and means of livelihood. There is the need to appreciate the socioeconomic dynamics and challenges posed by the recent environmental changes taking place within and around the derived savannah region of Nigeria. These environmental changes include illegal lumbering, large scale charcoal production, deforestation and forest degradation, resource driven conflicts between the traditional subsistence farmers and immigrant herdsmen.

The study evaluates the interaction of climate change and LULC by assessing the variability in the observed climatic data between 1941 and 2010 and statistically downscales climatic

data from one of the GCMs (MRI-CGCM2-3-2 model) under the SRES A2 and B1 coupled with the past LULC changes to simulate the spatial distribution and patterns of LULC during the present and future climate. This is done in the study with a view to providing a better understanding and developing a model which links the climatic parameters with other drivers of change within the region in order to predict the patterns of LULC during the future climate, The study generates the baseline characterization on the static and temporal LULC in order to provide an insight to the magnitude and rate of past changes in the LULC within the area. In addition, the study reaffirmes the predicted patterns and directions of climate variability and change for the present and future climates within the tropical region on which adaptation and mitigation strategies could be developed. It further generates empirical/quantitative information on the carbon stock resulting from the changes in the LULC in order to draw attention to the need to develop an approach or strategy to cut down on human induced LULC change. Finally, the study triggers the need for more research on sustainable development of land resources within the region under study.

1.6 Scope and Limitation

This study focuses and demonstrates the interaction of climate change and LULC to predict the nature of spatial patterns of LULC for the present and future climates. The study relies on Landsat images for 1972, 1986, 2002 and 2010, which were downloaded from the website of the Global Land Cover Facility (GLCF) of the University of Maryland and integrated with the topographical maps produced from aerial photographs between 1956 and 1972 (Soneye & Akintuyi, 2013). They are in analogue format, which are not suitable for digital analysis (Soneye, 1999). However, they are used as ancillary data to aid the interpretation of the archived satellite imageries. The study would have assessed the LULC for later years (i.e. 2003 – 2010) but, Landsat 7 satellite imageries or data were not available for the study area

for these periods due to the Scan Line error (or SLC error) that occurred in 2003 to the sensor of Landsat 7 (http://landsat.usgs.gov/products_slcoffbackground.php). The quality of the satellite data for 2010 affected the result of the LULC for 2010, but was used for model validation. Therefore, the study relies on the LULC data for 1972, 1986 and 2002 to achieve other objectives.

Climatic data for the period between 1941 and 2010 were sourced from six synoptic stations in Ilorin, Oshogbo, Lokoja, Bida, Akure and Ondo for the assessment of the present climate variability and change. Empirical data for temperature and rainfall for 2011 to 2050 from MRI-CGCM2.3.2 model were downscaled under emission scenarios (SRES A2) to assess the future climate variability and change. MRI-CGCM2.3.2 was developed by the Meteorological Research Institute, Japan and was used for this study because the GCM simulated monthly precipitation and temperature relatively well for the Nigerian environment (Ringler *et al.*, 2010 and Abiodun *et al.*, 2013). Also, it maintains stable control run without using surface flux corrections (Dia, 2006).

The study adopts remote sensing and GIS techniques for the classification and interpretation of satellite imageries for the LULCC analysis. Multivariate statistical techniques were used for analyzing climatic parameters, while factor analysis was used to identify the controlling variables of LULC during the present and future climates. In modelling LULC for the present and future climates, the climatic variables were used as the dynamic and the main drivers of LULC within the study area. However, other proximate and underlying drivers of LULC were used as static variables during both climates.

The major limitation of the study is the non availability of the remotely sensed data of the same resolutions and climatic data of the same periods. There are also some gaps in the

climatic data on the synoptic stations. These issues were resolved by resampling the image cells and resolutions to a common resolution that was used for the analysis. The climatic data gaps were filled by performing a regression analysis between the nearest stations with and without gaps after considering the correlation between the stations.

1.7 The Study Area

1.7.1 Vegetation Distribution in Nigeria

The vegetation distribution in Nigeria is based on the combined effects of the amount of rainfall, temperature and relative humidity - i.e. climate and soil formation across the country. However, these factors have been modified by the interaction of human activities and patterns of landuse (Oyenuga, 1967 & Iloeje, 2001). Nigerian vegetation zones were classified into nine ecological zones by Oyeunga (1967), namely, mangrove forest and coastal vegetation, freshwater swamp communities, tropical high forest zone, derived guinea savannah with relict of forest, southern Guinea savannah zone, northern Guinea savannah, Sudan savannah and Sahel savannah. Keay (1959) and Iloeje (2001) in their own classifications grouped Nigerian vegetation into two broad categories using the same factors, which were further divided into smaller units or zones, namely, the Forest zone – mangrove/saltwater swamp, freshwater swamp and lowland forest or rain forest and Savannah zone - Guinea savannah, Sudan savannah and Sahel as shown in figure.1.1. However, derived savannah would be the focus of this work.

1.7.2 Derived Savannah

The southern guinea savannah zone is one of the four (4) major zones into which Keay (1959) divided the savannah regions of Nigeria. The northern and southern guinea savannah zones occupy about 40% of the area of Nigeria while the derived savannah occupies slightly over 10% of the country's land area and extends southwards from the southern guinea zone into the forest zone. Jones (1945) and Keay (1959) described the derived savannah as a belt

of vegetation that stretches from east to west across the width of Nigeria. Along the southern boundary there is a transition, often remarkably abrupt, to Rain forest, while to the north it merges with the Southern Guinea type of savanna. It is an area that is thinly populated with great potentialities for agricultural development (Adegbola and Onayinka, 1976).

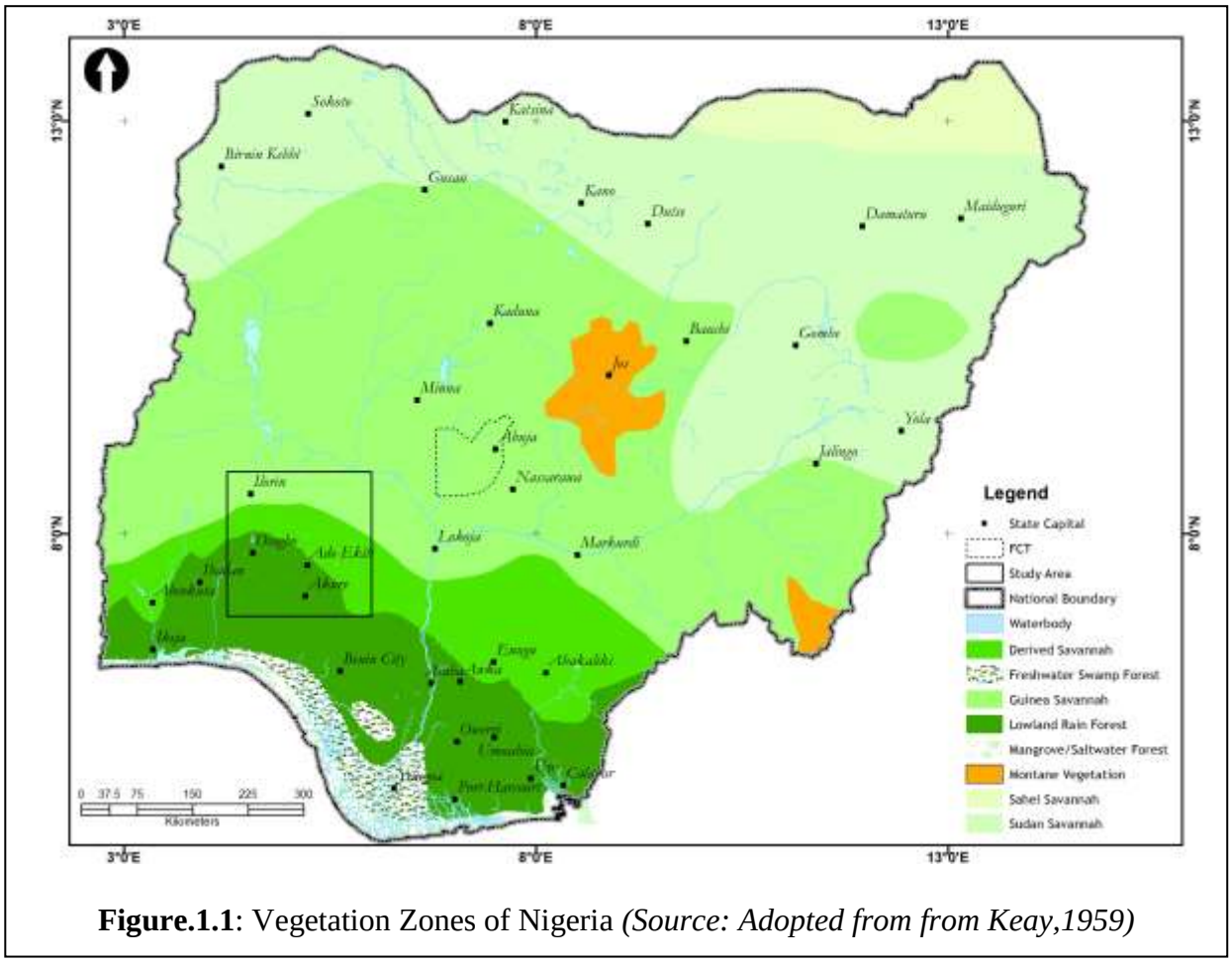

Figure.1.1: Vegetation Zones of Nigeria *(Source: Adopted from from Keay,1959)*

The rainfall in Derived Savannah is greatly influenced by orographic factors due to the presence of ridges. The rainfall is of the 'two peak' type, with peaks in July and September; mean annual rainfall of 50 inches (1270mm), and lowest mean monthly relative humidity of 9hours of not less than 70%. Clayton (1962) stated that as the rainfall decreases, the dry season increases in severity from south to north. Pullan (1962) also confirmed that the length of the dry season is the most important climatic factor in the zone, with rainfall varying between 1,000mm in the northern end to 1,800mm in the southeast end of the derived savannah zone.

The geomorphology and soil of the zone are underlain by pre-Cambrian metamorphic rocks. Its topography is dominated by blocks of dissected hills and level plains alternating with the belts of the dissected country (Clayton, 1961). The soils are developed over the rather variable metamorphic rocks of the basement complex. Also, the soils of the plains typically consist of 18 inches (46cm) of greyish-buff slightly clayey sand overlying vesicular or pisolitic ironstone. The depth of the soil, however, is very variable, ranging from 2-3 ft (0.6 – 0.9m) to a mere 3 inches 98cm) where the ironstone approaches the surface. The soils of the dissected country are mostly skeletal, consisting of pale brown to orange-brown sands or grits with many quartz stones, interspersed with pockets of deeper sandwash (Clayton, 1961). A full description of the soil series in the zone have been published in the Annual Reports of the Agricultural Department for the years 1951-52 and 1952-53, and Vine *et al.* (1954) have grouped the soil series into '**fascs**'. Clayton (1958), however, grouped them into three empirical classes as follows:

a) Clayey soils: including Olorunda, Mamu, Effon and Iregun Series.

b) Sandy soils: including Ibadan, Apomu and Gambari Series.

c) Poorly drained and swampy soils: including Matako, Jago and Osun Series.

In addition, Vegetation varies a great deal in this zone. The southern area of the derived savannah zone contains relic patches of high forest or forest trees including oil palms (*Elaeis guineensis*). This is as a result of bush burning and overgrazing, cultivation and hunting activities over a long period, which are replaced with scattered trees, tall grasses and climbers growing on relatively dry ground which receives water only from rain. Other tree species associated with the derived savannah zone include, Locus Beans (*Parkia filicoidea*), Shea Butter (*Butyrospermum parkii*) and Mango (*Mangifera indica*). Tall grasses common to the region include *Pennistum, Andropogon, Panicum, Chloris, Melinis,* etc.

1.7.3 Geography of the Study Area

1.7.3.1 Geographic location and extent

The study area covers the Derived Savannah region of Nigeria spanning from longitude 4.25^0 to 6.0^0E and latitude 7.0^0 to 8.75^0N. It is about 37,751.91km^2 in area and covers the present Ekiti State in its entirety and parts of Kwara, Ondo, Oyo, Osun, Kogi, and Edo States (Figure 1.2). As shown in figure 1.2 and table1.1, all the sixteen LGAs of Ekiti and about forty-one others in the remaining states, including Kwara (14), Ondo (13), Oyo (5), Kogi (4), Edo (3), Niger (1) and Ogun (1) are covered in the study area. The area covered in this study extends into the upper part of the forest ecological zone. This is to be able to capture the interactions of landuse/landcover change and climate at the fringes of the ecological zone. The derived savannah is a delicate zone that is undergoing continuous encroachment due to the interplay of climate change and anthropogenic activities over time. It is noted that the zone has been encroaching into the rain forest zone due to the continued pressure from both natural and anthropogenic activities (FME, 2004) as illustrated in the figures 1.3, 1.4 and 1.5.

1.7.3.2 The Physical Setting

The annual mean distribution of rainfall decreases from about 1,600mm in the south to 1,200mm north around Ondo and Pategi respectively. The pattern shows that it is influenced by the orography as evident around the southwest of Effon ridges and other highlands within the region. The derived savannah usually records two-peak rainfall in July and September, and a relative short dry break in August. The low volumes of rainfall are usually recorded between November and March of every year, which account for dry season in the area.

The mean minimum and maximum annual temperatures range from 21.5 to 22.8^0C and 30.6 to 33.6^0C, respectively. Mean daily minimum and maximum are 22.2^0C and 32.1^0C while the annual mean is about 27.8^0C. As depicted in figure 1.6, the temperature anomaly shows a sinusoidal pattern, even though the values are relatively high and uniform all the year round.

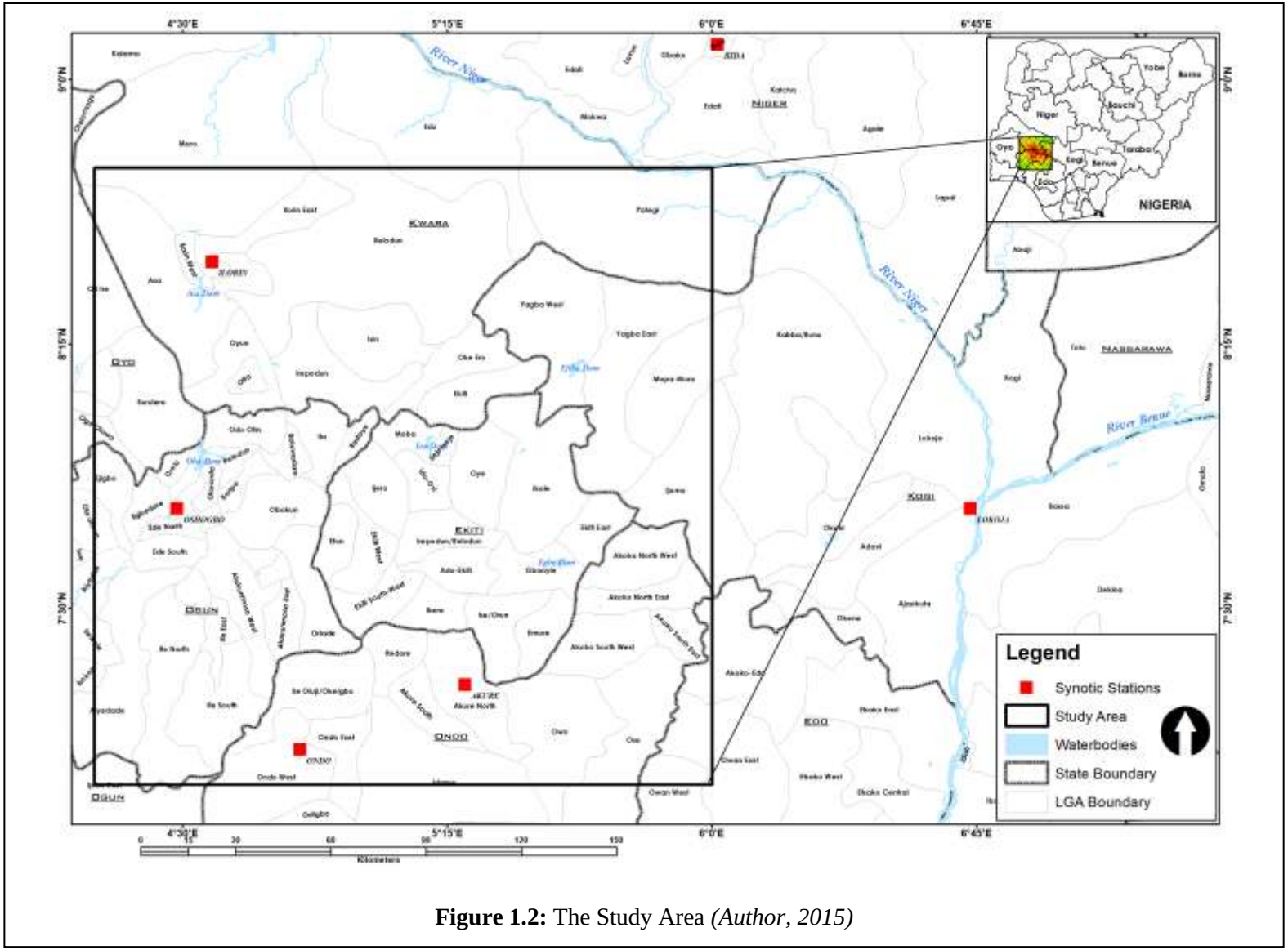

Figure 1.2: The Study Area *(Author, 2015)*

Table 1.1: Population Distribution

S/n	STATE	LGA	LGA Population	Study Area Population	Study Area (km^2)*
1	Edo	Akoko-Edo	262,110	31,191	163.14
2	Edo	Owan East	154,385	35,605	286.07
3	Edo	Owan West	97,388	22,661	170.23
4	Ekiti	Ado-Ekiti	308,621	308,074	292.89
5	Ekiti	Gbonyin	148,193	148,038	390.87
6	Ekiti	Efon	86,941	86,686	231.37
7	Ekiti	Ekiti East	137,955	137,886	320.46
8	Ekiti	Ekiti West	179,892	179,410	364.88
9	Ekiti	Ekiti South-West	165,277	164,856	344.78
10	Ekiti	Emure	93,884	93,794	300.57
11	Ekiti	Ido-Osi	159,114	158,777	231.08
12	Ekiti	Ijero	221,405	220,844	389.81
13	Ekiti	Ikere	147,355	147,058	262.12
14	Ekiti	Ikole	168,436	168,265	1,071.38
15	Ekiti	Ilejemeje	43,530	43,447	94.74
16	Ekiti	Irepodun/Ifelodun	129,149	128,899	355.53
17	Ekiti	Ise/Orun	113,754	113,596	431.34
18	Ekiti	Moba	146,496	146,166	199.02
19	Ekiti	Oye	134,210	133,998	506.24
20	Kogi	Ijumu	119,929	74,514	811.16
21	Kogi	Mopa-Muro	44,037	35,795	732.65
22	Kogi	Yagba East	149,023	143,767	1,346.90
23	Kogi	Yagba West	140,150	140,019	1,275.11
24	Kwara	Asa	126,435	122,757	1,248.57
25	Kwara	Edu	201,469	32,399	408.72
26	Kwara	Ekiti	54,850	54,764	478.95
27	Kwara	Ifelodun	206,042	179,285	2,989.09
28	Kwara	Ilorin East	204,310	203,599	484.15
29	Kwara	Ilorin South	208,691	207,902	173.81
30	Kwara	Ilorin West	364,666	363,097	104.14
31	Kwara	Irepodun	148,610	148,168	734.54
32	Kwara	Isin	59,738	59,584	631.49
33	Kwara	Moro	108,792	30,865	928.37
34	Kwara	Offa	89,674	89,336	95.04
35	Kwara	Oke Ero	57,619	57,516	436.96
36	Kwara	Oyun	94,253	93,891	474.49
37	Kwara	Pategi	112,317	72,147	1,871.35
38	Niger	Mokwa	244,937	560	9.91
39	Ogun	Ijebu East	110,196	6,937	140.64
40	Ondo	Akoko North East	175,409	175,093	371.63
41	Ondo	Akoko North West	213,792	213,775	512.40
42	Ondo	Akoko South East	82,426	82,452	225.63
43	Ondo	Akoko South West	229,486	229,382	529.77
44	Ondo	Akure North	131,587	131,368	658.95
45	Ondo	Akure South	353,211	352,486	330.77
46	Ondo	Idanre	129,024	54,160	803.27
47	Ondo	Ifedore	176,327	175,903	294.54
48	Ondo	Ile Oluji/Okeigbo	172,870	172,327	695.43
49	Ondo	Ondo East	74,758	58,206	275.55
50	Ondo	Ondo West	283,672	154,670	529.12
51	Ondo	Ose	144,901	78,323	791.82
52	Ondo	Owo	218,886	200,074	938.58
53	Osun	Aiyedade	150,392	112,619	833.50
54	Osun	Aiyedire	75,846	33,957	117.51
55	Osun	Atakunmosa East	76,197	75,938	237.22
56	Osun	Atakunmosa West	68,643	68,381	574.77
57	Osun	Boluwaduro	70,775	70,538	143.16
58	Osun	Boripe	139,358	138,830	131.43
59	Osun	Ede North	83,831	83,453	110.34
60	Osun	Ede South	76,035	75,691	217.67
61	Osun	Egbedore	74,435	74,094	269.24
62	Osun	Ejigbo	132,641	92,497	260.21
63	Osun	Ife Central	167,254	166,545	110.44
64	Osun	Ife East	188,087	187,321	171.17
65	Osun	Ife North	153,694	151,240	875.29
66	Osun	Ife South	135,338	134,789	726.98
67	Osun	Ifedayo	37,058	36,957	127.88
68	Osun	Ifelodun	96,748	96,368	113.97
69	Osun	Ila	62,049	61,858	301.82
70	Osun	Ilesha East	106,586	106,208	70.32
71	Osun	Ilesha West	103,555	103,176	62.60
72	Osun	Irepodun	119,497	118,994	63.93
73	Osun	Irewole	143,599	47,644	89.84
74	Osun	Isokan	103,177	11,083	19.25
75	Osun	Iwo	191,377	36	0.04
76	Osun	Obokun	116,511	116,104	524.94
77	Osun	Odo Otin	134,110	133,600	293.34
78	Osun	Ola oluwa	76,593	20,166	86.29
79	Osun	Olorunda	131,761	131,216	96.30
80	Osun	Oriade	148,617	148,151	463.90
81	Osun	Orolu	103,077	102,611	79.26
82	Osun	Osogbo	156,694	156,055	46.37
83	Oyo	Ogbomosho North	198,720	136,835	127.05
84	Oyo	Ogbomosho South	100,815	33,137	22.44
85	Oyo	Ogo Oluwa	65,184	18,117	102.44
86	Oyo	Ori Ire	150,628	22,405	314.78
87	Oyo	Surulere	142,070	141,411	847.08
		Total	12,211,134	**9,872,397**	37,372.79

Adapted from National Population Census, 2006; NBS & Area generated from GIS by the Author

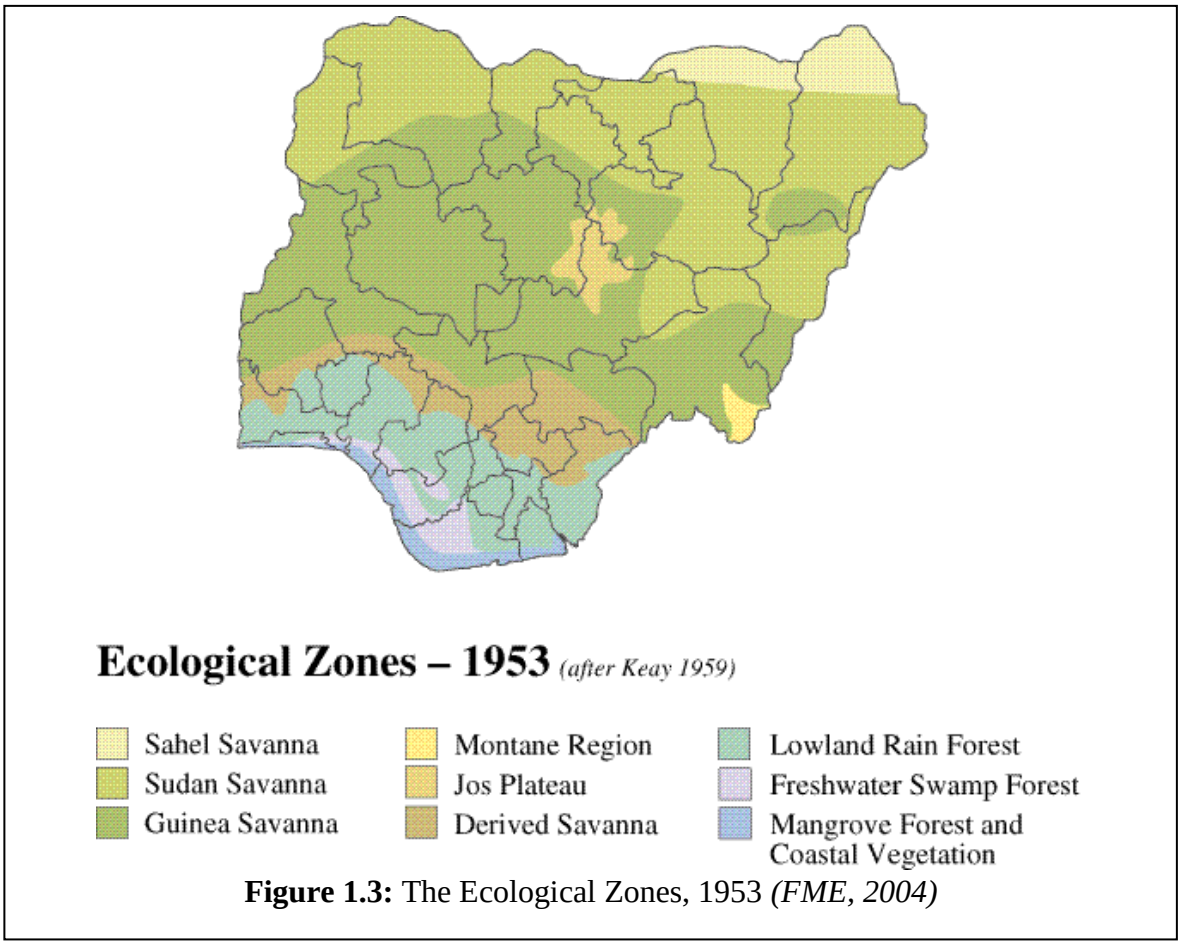

Figure 1.3: The Ecological Zones, 1953 *(FME, 2004)*

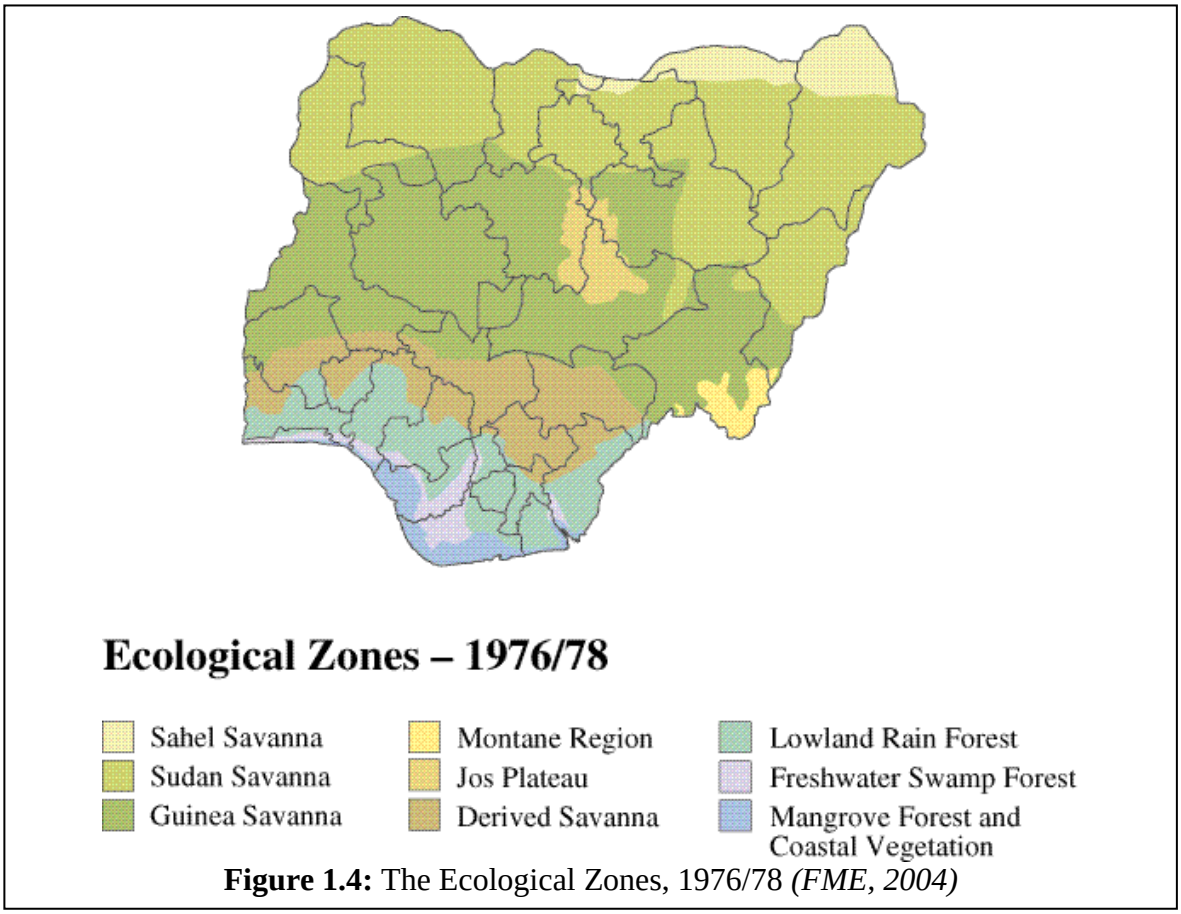

Figure 1.4: The Ecological Zones, 1976/78 *(FME, 2004)*

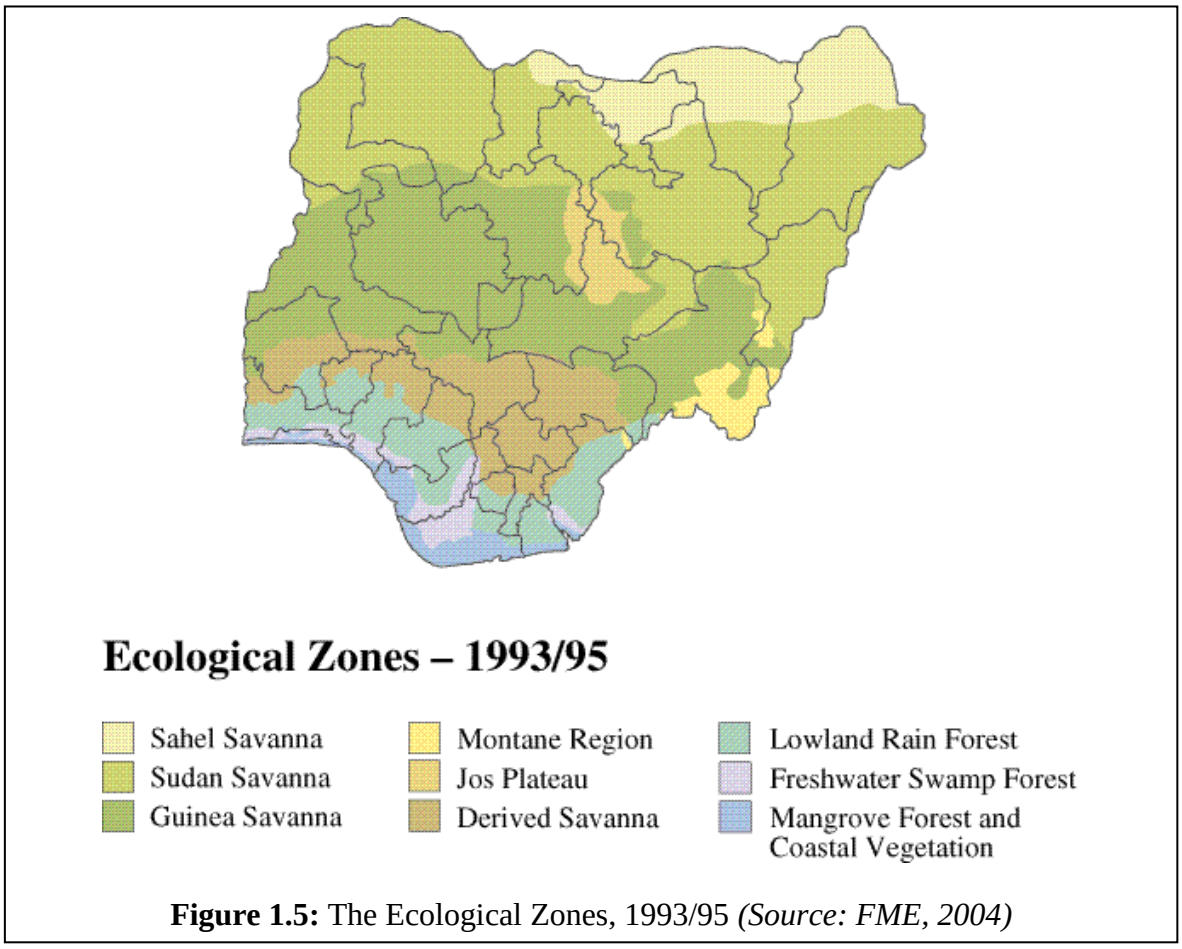

Figure 1.5: The Ecological Zones, 1993/95 *(Source: FME, 2004)*

The highest values of temperature are usually recorded in February and March as a result of the dominance of Tropical continental (cT) airmass, while the lowest is recorded in August when the tropical maritime prevails.

The relative humidity reveals a decrease in a south – north direction. The mean monthly ranges from 66% to 83% at 09:00hours and 49 to 65% at 15:00hours (Figure 1.7). Lower values are recorded in the months of January through March as against the higher value in June through September.

The study area is under the influence of the two air masses i.e. the warm and humid Tropical maritime (mT) and the dry, warm and dusty, Tropical continental (cT). The alternate rainy

and dry seasons follow the dictate by the relative positions of the Inter-tropical Convergence Zone (ITCZ).

The relief of the area is relatively flat surface, but dominated by ridge system of Fold Mountains, particularly the Efon ridge whose elevation ranges from 500 – 900m above the sea level as shown in figure 1.8. Also, the area is well drained by the Rivers Niger and its numerous tributaries, which include Rivers Asa, Osun, Oro and Awore. Some of these rivers have been dammed for irrigation and domestic water supply purposes. The dams within the study area include Ero, Ejiba, Asa, Egbe and Oba Dams as shown in figure 1.2.

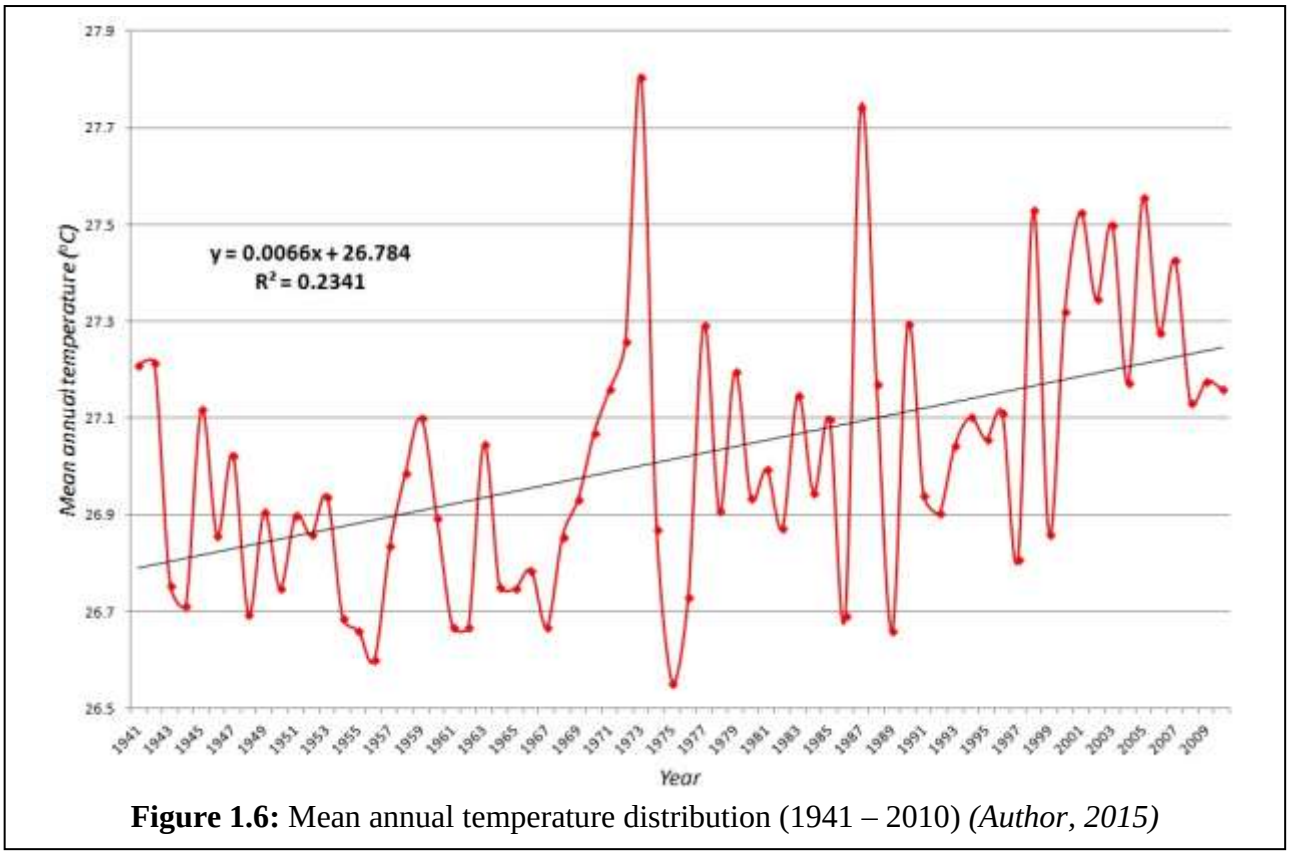

Figure 1.6: Mean annual temperature distribution (1941 – 2010) *(Author, 2015)*

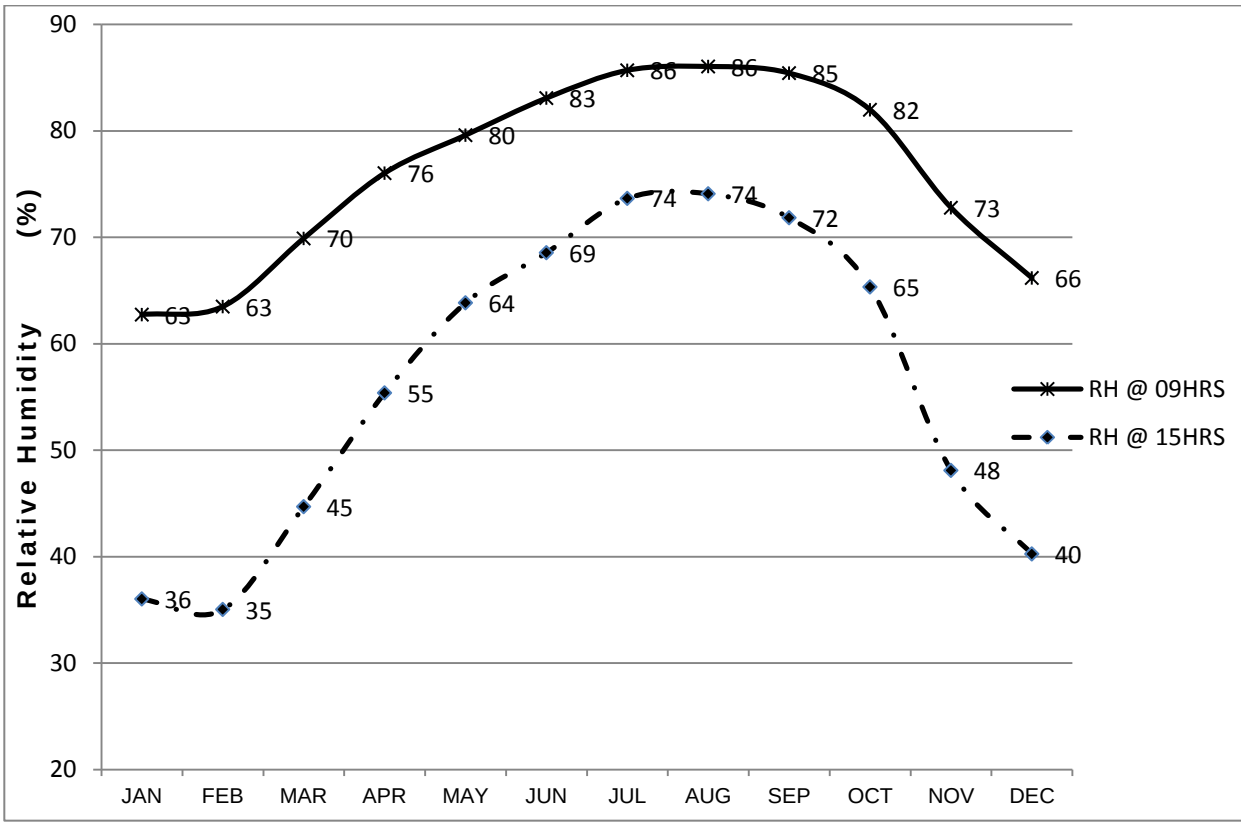

Figure 1.7: Mean monthly relative humidity distribution for 9:00hours and 15:00hours (1961 – 2010) *(Author, 2015)*

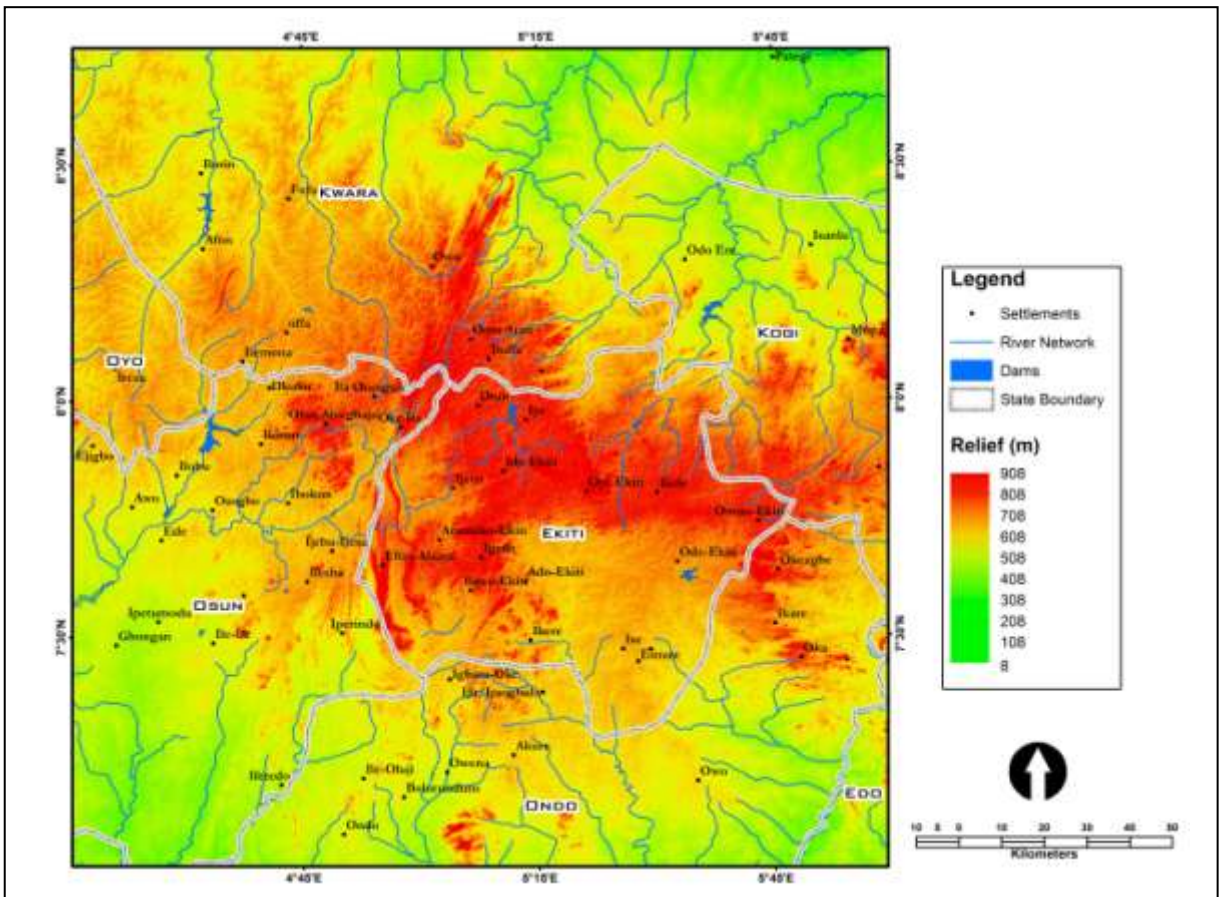

Figure 1.8: The Relief and Drainage of the Study Area *(Author, 2015)*

1.7.3.3 The Human Setting

The study area is populated mainly by the people of the Yoruba speaking tribe of Ekiti, Ondo, Osun, Kogi, Kwara, Oyo, Ogun States of Nigeria The population is estimated at about 9.8million according to the 2006 census (NBS, 2006) and is fairly distributed among the states (Figure 1.9 and Table 1.1). However, Osun State has the largest population with about 2,856,120 followed by Ekiti and Ondo States with 2,379,974 and 2,078,219 people respectively. Kwara has about 1.7million, while all the others have a total of 835,563. The average density is about 264 people per square kilometer.

The settlement patterns are both urban and rural. The urban settlement is made up of the state capitals and the LGA headquarters while the latter includes hamlets, villages and small towns. The majority of the populace engages in agricultural practices as their primary occupation with a few others in white collar jobs, trade and commerce. The southern part with forest patches (especially Ekiti, Ondo and Osun States) grow tree crops like Cocoa, Coffee, Kolanut and Citrus, sometimes mixed with dominant food crops like yam, cocoyam, plantain and maize at the subsistence level. An appreciable proportion of the people engage in large scale lumbering, logging and hunting. These activities have led to the massive deforestation of the area. More importantly, those practices involve bush burning, fallow and shifting cultivation that hardly support full vegetal regeneration.

At the northern part with tall grasses and more scattered trees are intensive animal grazing, and farming of staple food crops such as yam, cassava, maize, millets and other cereals. these are found especially around Ilorin, Pategi and Omu Aran. Also, hunting and poaching are common practice in Ipawo Itapiji, and other farming communities within the study area. In addition, the people in Oke Ogun axis engage in large scale charcoal production from

scattered cash crops trees such as mango trees (*Mangifera indica* leading to animal grazers migrating down south into the forested axis.

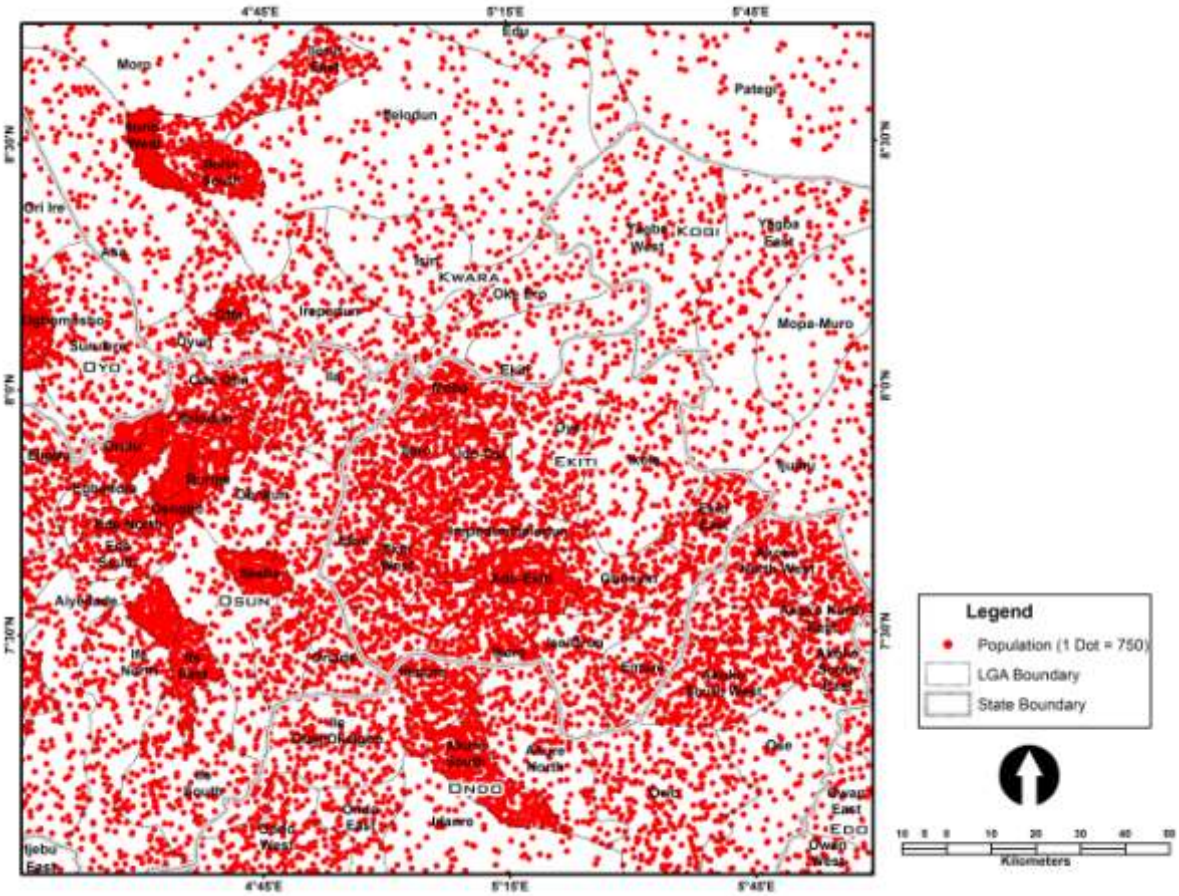

Figure 1.9: Population density of the study area *(Author, 2015)*

1.8 Thesis Layout

This thesis is presented in eight chapters as follows:

Chapter one presents the general perspective of interaction of LULC Change (LULCC) and climate variability and change. It specifically captures the introduction and background of the study. The chapter is made of eight sections, which include the statement of the problem as peculiar to the study area, aim and objectives, study area, etc.

Chapter two provides the conceptual framework and literature review of relevant works relating to the subject matter. This includes climate variability and change, downscaling in

climatology, LULC change, interaction climate variability and change as well as LULC change, and the environmental implications of the interaction.

Chapter three captures the research methodology where data sources and characteristics are discussed. Also, in the chapter, methodology framework and procedure adopted for the study are presented. Finally, data limitation is also discussed in the chapter.

Chapter four presents the result of LULC change analysis. Base maps for 1972, 1986 and 2002 with their statics and temporal characteristics are presented. The chapter also presents the discussion of LULCC of the study area.

Chapter five illustrates climate variability and change. There are five sections in the chapters, which include both temperature, while rainfall characteristics and trend for the present and future climate, temperature and rainfall distribution pattern and variability index are also discussed.

Chapter six provides the analysis of the interaction of climate and LULCC. Here, the results of modeling activities, both statistical techniques and Land Change Modeler (LCM) are presented. Also, implications of the interaction are discussed in the chapter.

Chapter seven discusses the implications of the interaction of LULC and climate change within the study area by focusing on the quantification of concentration of carbon dioxide that will be released to the atmosphere during future climate.

C**hapter eight** presents the summary of findings, policy implications and recommendations of the research.

CHAPTER TWO

LITERATURE REVIEW AND CONCEPTUAL FRAMEWORK

2.1 Literature Review

Available and current literature of the study abounds with materials in the research area – modeling of interaction between landuse/landcover (LULC) and climate change both locally and internationally. However, there are observable gaps in terms of the location, depth, extent and time covered in past studies relating to the study. Literatures are, thus, reviewed under the following sub-headings, landuse/landcover change (LULCC), climate variability and change, models and downscaling techniques in climatic studies, the interaction between climate change and landuse/landcover change and implications of the interaction. Furthermore, literature on methods and tools of analysis - Remote Sensing and Geographical Information System (GIS) and their applications to climatic variability and LULC are reviewed in this chapter.

2.1.1 Landuse/landcover Change (LULCC)

The land resources being considered in this study, include the vegetation or vegetative cover of the earth's surface and the uses into, which the land resources are put (i.e. landcover and landuse). Landcover is described as the visible evidence of landuse to include both the vegetative and non-vegetative features on the earth's surface. However, landuse is regarded as the use of land by humans with emphasis on the economic management and functions of land (Campbell, 1996, Dale, 1997). Landuse change has been described as the most significant regional anthropogenic disturbance to the environment (Roberts *et al.,* 1998). Therefore, both landuse and landcover changes are products of prevailing interaction of natural and anthropogenic processes driven by human activities. Studies have identified that landuse change is driven by both the proximate and underlying factors, which are further

driven by human activities (Geist and Lambin 2002, Fasona and Omojola, 2005). These factors of landuse change determine the controlling variables that are responsible for the quantity and magnitude and location of change.

Remote Sensing and GIS are most important and widely used techniques to monitor, assess, and evaluate landuse change and the implications of change on the global environmental (Omojola and Soneye, 1993; Adeniyi and Omojola, 1999). Consquent upon this, a number of models have been developed to evaluate and predict the trend, quantity and location of landuse. Models of landuse change are based on the known concepts of social and ecological systems due to the similarities between them and landuse (Loucks 1977, Adger 1999, Holling and Sanderson 1996). These concepts include connectivity, hierarchy and stability and resilience. Landuse change models includes the Sahelian Landuse model (SALU; Stephenne and Lambin, 2001a), the Conversion of Landuse and its Effects (CLUE; Veldkamp and Fresco, 1999a; Verburg, *et al.*, 1999a), the Cellular Automata Markov (CA_Markov), the Geomod models for predicting landuse change (Pontius and Malanson, 2005), and the Conversion of Landuse and its Effects at Small Regional extent (CLUE-S; Verburg *et al.*, 2002; Fasona, 2007). Some of these models exhibit the characteristics of the concept of social and ecological systems to analysis and simulate the rate, quantity and location of landuse change.

For instance, the CLUE model is a dynamic model, developed to capture the interaction between landuse change and the characteristics of the biophysical and socio-economic environment to simulate current LULC (Veldkamp & Fresco 1996; Verburg *et al.,* 1999; Verburg *et al.,* 2002). This model was used to stimulate landuse change in Philippines at a high resolution. In reaction to this model, however, the CLUE-S was developed to take care of some of the shortcomings of the model. Verburg *et al.,* (2002) developed clue-s model

which was specifically developed based on system theory to integrate biophysical factors with socioeconomic factors of change into the assessment of landuse change in small regions or at a fine spatial resolution. Although the model was applied in Malaysia and Philippines, Fasona (2007) has used it to assess the land degradation in the Ondo coastline of Nigeria.

In the analysis and modeling of future LULCC, the proximate and underlying drivers, which are mainly socio-cultural and economic, biophysical and ecological in nature were considered, parameterized and used for simulating the future LULCC. However, the contributions of climatic parameters to determine the nature and direction of LULCC in the future are not considered as strong factors in the models.

2.1.2 Climate System - Climate Variability and Change

Climate is often regarded as the average of weather condition (Ojo *et al.,* 2001). Thus, this has been widely accepted notion for decades to the extent that climate can be taken for granted. However, recent events have shown that the climate and environmental change have impacted significantly on the basis of human existence, this notion of climate can no longer accepted as correct (Fasona and Omojola, 2005). Climate to this end encompasses the temperatures, humidity, rainfall, wind and pressure, solar radiation, atmospheric particle count and numerous other meteorological factors in a given region over long periods of time. Climate varies in terms of space and time. Also, the climate of a location is affected by its latitude, terrain, altitude, persistent ice or snow cover, as well as nearby oceans and their currents (Ojo *et al.*, 2001, Harvey, 2000a).

In specific terms, the climate system is regarded to consist of the following components: the atmosphere, ocean, cryosphere, biosphere and lithosphere. All these components affect one another in the form of cyclic system to form a single interacting system (Harvey, 2000a). For

example, the biosphere is affected by the atmospheric conditions and influences the climate by the effect of land vegetation on surface roughness through its effect on the evaporation and the reflection or absorption of solar energy. Consquently, one of the feedbacks from the interactions of these components includes climate change induced by human activities (Le Treut *et al.*, 2007).

Climate system responds to both the external and internal radiative forcings to determine the climate of the earth's surface. The external radiative forcing arises from anthropogenic greenhouse gases, while internal radiative forcing occurs due to natural processes of variability. Variability due to long-term fluctuation in the average value of climate parameters arising from changes in oceanic circulation is called climate variability (Swanson, *et al.*, 2009). Thus, Climate change is defined as the change in climate for a comparable period of time, which may be due to external forcing or as a result of human activities. Human activities that induced climate change includes burning of fossil fuel, landuse change, deforestation, the release of aerosols into the atmosphere, and other activities that are capable of increasing the concentration of the green house gases (Langdon *et al.*, 2004, Efe, 2011, Odjugo, 2011).

Studies have established that our climate is experiencing variability and change (Folland *et al.*, (2001), Abiodun *et al.*, (2012), Oguntunde *et al.*, (2011). For instance, Folland, *et al.*, *(*2001) reported that the global surface temperature was estimated to have increased by 0.6^0C since the 19^{th} century. According to these researchers, most of the increase occurs within two periods. The first phase was 1910 and 1945 while the second period has occurred since 1976. The study further revealed that mean daily maximum and minimum land surface air temperature has increased at the rate of 0.1^0C and 0.2^0C respectively between 1950 and 1993. Similarly, precipitation is reported in the study to have continued to increase between 0.5 to

1% per decadal in the Northern hemisphere. there has also been an increase in the extreme precipitation events in places where there has been an increase in total precipitation.

The story is however different in other parts of Africa, the Southern Africa climate is experiencing variability and change in terms of warming trend. Studies have observed that the temperature of the region was increasing at the rate of 0.5^0C in the last century. This is according to IPCC, 2001 third assessment report (TAR) as indicated in Fig. 2.1. Also, the Indian Ocean, which is very close to the region, has been witnessing warming trend at the magnitude of 1^0C since 1950 with downward trend in the rainfall pattern over the same period of time (NCAR, 2005). Similarly, between 1988 and 1995, there were about 15 drought events recorded with an increase in the frequency and intensity of the extreme climate events like El Nino within the same region. For instance, in the past, it took an average of a decade or two for strong El Nino event to occur. However, according to Glantz *et al.*, (1997) the early 1980's marked the beginning of a series of strong El Nino events; 1982/1983; 1991/1992; 1994/1995; and 1997/1998 (Kandji *et al.*,2006).

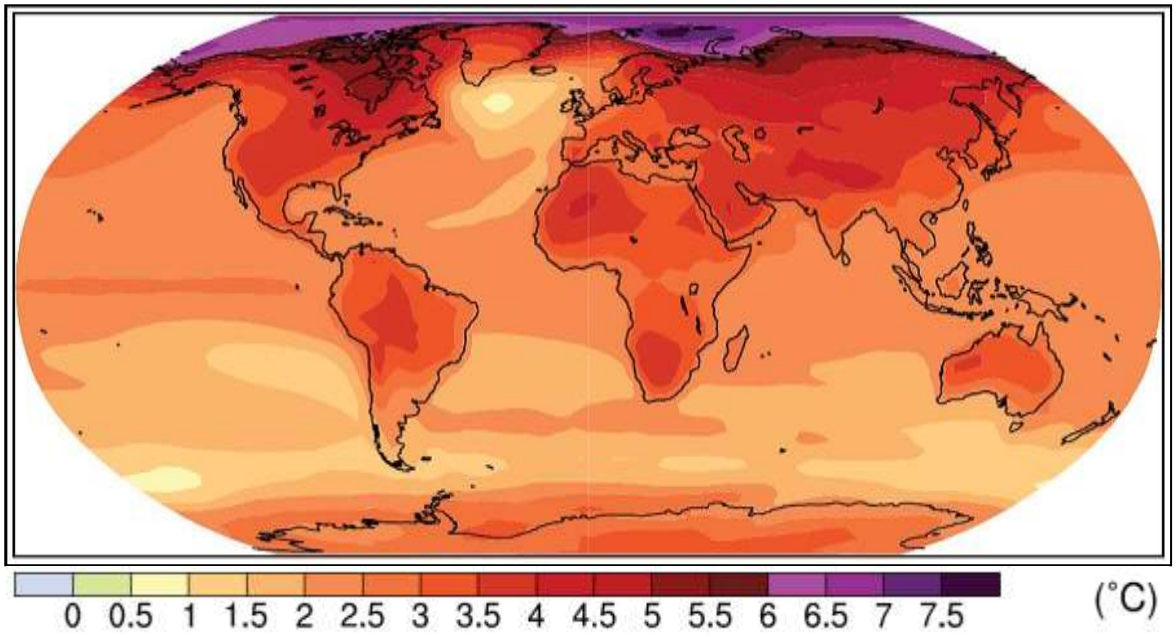

Figure.2.1: Change in mean annual temperature from 1980 – 1990 *(source: IPCC AR4 WG1)*

Furthermore, the climate of the sahelian region is not left out, which could easily be seen in the variability characteristics of the rainfall, which is the dominant climatic parameter. IPCC (2001) has further reported a reduction of about 28 – 49% in the amount of rainfall in the region between 1968 and 1997 as compared to the base period of 1931 – 1960. This report confirm other studies that reported a drastic reduction in the annual mean rainfall such as reported by Kandji *et al., (*2006). Similarly, Wang *et al.,* (2004) reported a decadal variability in the amount of the rainfall events, which resulted in drought during the last three decades of the twentieth century in the region as observed in the climate simulated studies.

Abiodun *et al.,* (2012) investigated the future impacts of global warming on climate and extreme climate events in Nigeria. In their study, nine GCMs were downscaled to stimulate past and future climates of Nigeria using two emission scenarios (B1 and A2). These researchers discovered that temperature increased significantly over all ecological Zones with the greatest of 1-4^{0}C occurring over the Sudan savannah. Similarly, Oguntunde *et al*., (2011) examined the changes in the spatial and temporal patterns of rainfall in Nigeria. Standard tests were carried out by the researchers to discover the trends in annual and monthly rainfall patterns of Nigeria over the last century. It was discovered in the study that the 1950s and 1980s were the wettest and driest decades in Nigeria having a rainfall variability index of +0.84 and -1.19 respectively. Also, the study discovered that rainfall changes varied between -3.46 and +0.76 mm/ yr^2 during the period, while 90% of Nigeria landscape exhibited negative trends but only 22% showed significant changes at 5% level. The studies have therefore shown that the Nigeria landscape is experiencing climatic variability and change.

Studies on climate variability and change had been at the global and regional extent and resolutions. However, there is the need to understand the climatic variability and change at the local levels, where localized effects of factors like landuse/landcover dynamics, burning

of biomass and others environmental factors are felt the more. Besides, spatial and temporal variability of climate are best studied using geographic techniques like GIS and remote sensing that can reveal more localized spatial differentials in climatic events over time.

2.1.3 Climate models and downscaling techniques

2.1.3.1 *Climate models*

Climate models such as energy balance models (EBMs), radiative-convective models (RCMs), statistical-dynamic models (SDMs) and general circulation models (GCMs) are developed to stimulate the behaviour of the physical, chemical and biological processes that govern the climate system (Harvey, 2013, Hewitson and Crane, 1996). These climate models are classified into four categories as mentioned above based, first, on their levels of complexity and sophistication to which they simulate the particular processes and second, on their temporal and spatial resolution. However, the focus of this research work is based on the general circulation models. This is particularly because these models since they are developed to have the highest degree of complexity and sophistication as regard how they stimulate one particular process and their resolutions (i.e. both the temporal and spatial resolution).

General Circulation Models (or GCMs) are numerical and three dimensional in nature and are developed based on the fundamental laws of Physics, laws of conservations of energy, mass and momentum and the ideal gas law (Harvey, 2000, Gates *et al.*, 1996). GCMs are mainly used to simulate or predict the response of the global climate system to increasing greenhouse gas concentrations or climate change. General Circulation Models are the most advanced tools commonly available to stimulate physical processes in the atmosphere, ocean, cryosphere and land surface.

To date, a number of the GCMs have been developed which includes atmosphere general circulation models, atmosphere general circulation models coupled to a slab ocean, ocean general circulation models and coupled atmospheric-ocean general circulation models. All of these general circulation models exhibit the same characteristics over their areas of applications and operate based on the same principles. However, they are limited in their areas of operation to certain terrains (i.e. ocean, atmosphere, cryosphere and land surfaces). Also, it is important to note that the GCMs available today are coarse in terms of resolution relative to the scale of exposure of the units. The uncertainty in their operation is that these models cannot be simulated at small scale; even though, some of the physical processes are taking place at local scales. For instance, clouds do occur at a smaller scale and their known properties must be averaged over a large area in a technique called parameterization (Harvey, 2000).

2.1.3.2 *Downscaling techniques*

The GCMs are fraught with many shortcomings. some of these shortcomings are that: they are coarse in term of resolution; used for regional and global simulation of climate and cannot simulate climate variability and change at the local level. Therefore, there is the need for downscaling some of them in order to be able to simulate and predict climate variability and change at local level. The process of downscaling involves taking model output that is average over a grid cell and deriving specific output values for specific point within the grid cell. There are, however, problems associated with downscaling, what arises from averaging climate of the grid cell without consideration for the nature of the surface and terrain characteristics (Harvey, 2013).

According to Hewitson and Crane (1996), there are two approaches to downscaling, namely the nested model and empirical approaches. The nested model is applied when regional

dynamic model at the mesoscale level or fine resolutions is needed to drive the synoptic and large scale information from GCM. However, this approach does not have a global appeal because it is computationally demanding and not easily accessible to research. Furthermore, there are difficulties in interfacing the nested model and GCM due to the need to relate coarse resolution grid cells of GCM to the fine scaled resolution of nested model of smaller grid cells. The empirical downscaling approach is computationally efficient and has more practical applicability to address the current needs of the climate change research community when compared with the model approach (Harvey, 2013; Hewitson and Crane, 1996, Abiodun *et al.,* 2012). This approach works by establishing a quantitative relationship between the GCM and local climate of the area of interest using mathematical or statistical relationship to derive transfer function from the observed data. This is similar to using the traditional statistically method to generalize for an area from the readings of the local synoptic station. This current study adopts the statistical empirical downscaling approach to generate the climate data for the parameters considered for the future climate (2011 -2050).

2.1.4 Interactions of landuse/landcover and climate change

The global environmental change is expected to have effects on the ecological, social, economic and political aspects of human society (Dale, 1997). The impacts of global environmental change include changes to biodiversity, migration, and sustainability. The climate and landuse changes are the two major implications of global environmental change taking place in the present time while, unfortunately, the causes and consequences of human induced climate change and landuse activities are largely being examined independently (Dale, 1997, Turner *et al.*, 1993).

However, landuse and climate change interact and affect each other. Landuse change contributes to climate change, and climate change also causes changes in the landcover

patterns and characteristics (Taylor *et al.,* 2002). Xue (1997)in this regard has established how anthropogenic vegetation changes have contributed to drought in the sahelian of Africa. Also, Zeng *et al.,* (1999) and Wang and Eltahir (2000a) and Anyamba *et al.,* 2002 have agreed that natural vegetation variability have played an important role in the inter-decadal climate variability in the region. In addition, the role of landscape modification in altering the convective rainfall of an area has been well documented by Pielke (2001); Pielke *et al.,* (2007) and Pitman (2003). Therefore, there is a general tendency for rainfall and evaporation to decrease with increasing land degradation and landuse change.

2.1.5 Implications of interactions of landuse/landcover and climate change

The interactions of LULC and climate change have a number of implications on both the environment and socio-economic activities. Some of these implications include desertification, flooding, windstorms, food security, water supply, air pollution, biodiversity changes and soil degradation from extreme weather, climate events, forest degradation and deforestation and climate induced resource conflicts in the savannah as revealed by Fasona and Omojola (2005). For example, forest degradation and deforestation have been fingered to contributing massively to the increase in the concentration of greenhouse gases (Betts *et al.,* 2008). According to Dale (1997), the anthropogenic release of carbon dioxide (CO_2) has increased greatly since the industrial age. In deed, approximately 61% of the anthropogenic greenhouse forcing can be attributed to CO_2 increase (Shine *et al.*, 1990). Also, landuse changes make greater contributions and accounts for the release of 90-120 PgC (Houghton and Skole, 1990). Deforestation and associated agricultural expansion induce carbon losses from the soil and vegetation. It must be noted that carbon releases from terrestrial ecosystems that result from landuse change are difficult to quantify because of the following reasons as noted by Betts *et al.,* (2008):

i. the rates of land clearing and abandonment;

ii. the estimates of the carbon stored in the vegetation and soil of managed and unmanaged ecosystems;

iii. the fate of carbon subsequent to landuse changes

Dale (1997) identifies the following as degree to which forests are protected: the political pressures within the government, population pressures within the countries, availability of other resources to sustain lives and livelihoods of that population, economic pressures from within and without the country, political stability of governments, number and ability of law enforcement agents to uphold the laws, as well as the respect the citizens have for the laws. These aforementioned factors are however, unpredictable in most developing countries (Nigeria inclusive). The amount of carbon stored in the terrestrial system affects carbon release. Yet, the amount and form of carbon stored in vegetation and soil varies by vegetative type, prevailing temperature and precipitation conditions, prior disturbances, the state of recovery, and current management. The amount of carbon in vegetation and soils declines with disturbances and recovers a portion of its value if the disturbance ceases and does not recur (Houghton *et al*, 1983).

Also, approximately 17% of the anthropogenic greenhouse forcing is methane (CH_4) (Shine *et al*, 1990). Methane is a very powerful greenhouse gas with a radiative effectiveness that is about 9 times that of CO_2 (Dale, 1997). Wetlands are the largest natural source and contribute approximately 22% of the total release of CH_4 to the atmosphere. Biomass burning also releases methane, and thus the increase in the rate of forest cutting correlates with the increase in methane release (Crutzen and Andreae, 1990). In addition, Nitrous oxide comprises approximately 4% of the anthropogenic greenhouse forcing, but their contribution has increased with the spread of human activity (Shine *et al*, 1990). Nitrous oxide is approximately 190 times more effective radiatively than CO_2. Within the biotic sphere,

human activities, particularly agriculture, have a major influence on the flux of nitrous oxides. The release of nitrous oxide to the atmosphere has increased with human activities as a result of tropical land clearing, and replacement by agriculture (Luizao *et al*, 1989) and biomass burning (Crutzen and Andreae, 1990; Cofer *et al*, 1991).

This current study assesses the implications of interaction of LULCC and climate change within the derived savannah by determining the nature, direction and magnitude of change, evaluate the climate variability and change for both the present and future climates and thereby uses the dynamic climatic parameters as drivers to simulate the present and the future LULC. The model is coupled by integrating the LULC change between 1986 and 2002 with the main drivers of change, temperature and rainfall for both the present and future climates to predict the LULC for 2010 and 2050 using the Land Change Modeler (LCM) algorithm of GIS techniques. Also, other static variables - terrain variables – elevation, slope and aspect and other anthropogenic variables like distance to urban centres, stream and disturbance were coupled with other main parameters of the model techniques. Finally, the study estimated the change in carbon stock due to the changes in LULC during the present and future climates.

2.1.6 Methods and tools of analysis

2.1.6.1.1 *Remote Sensing*

The field of remote sensing has been defined in various ways by different scholars in relation to their field study. However a close examination of each of the definitions reveals the common elements of the various definitions. Remote sensing is the science and art of obtaining information about an object, area, or phenomenon through analysis of data acquired by a device that is not in contact with the object, area, or phenomenon under investigation (Lillesand and Kieffer, 1987). It has also been defined as the science and art of acquiring information (spectral, spatial, and temporal) about material objects, area, or phenomenon,

without coming into physical contact with the objects, or area, or phenomenon under investigation (Aronoff, 1989). The science of remote sensing provides the instruments and theory to understand how objects and phenomena can be detected while the art of remote sensing is in the development and use of analysis techniques to generate useful information. Because there is no direct contact involved, some means of transferring information through space must be utilized.

Remote sensing sensors can be classified into two types, namely the optical scanners and non-optical scanners (Campbell, 2007 and Jones & Vaughan, 2010). The optical scanners are the type of sensors that operate within the visible portion of the electromagnetic spectrum (i.e. Ultraviolet rays, Visible Rays and infrared rays) as shown in the Fig.2.2. They are referred to as passive remote sensing systems because they rely or depend entirely on the energy from the sun. The optical scanners are made up of electro-optical scanners and photographic sensors – aerial photograph.

This study adopts the electro-optical spaceborne scanner of Landsat series. Landsat is one of the earth resources observation satellites specifically designed to provide data on the earth resources, including crops, forests, water bodies, landuse and minerals. They are sun synchronized orbit satellites and operate during daytime only because they depend on solar energy for their source of energy. Landsat series are used for earth resources monitoring and acquiring data. Remote sensing technique as a tool for data acquisition or collection is applied in a diverse field of research works as the main source of data. Remote sensing is applied to weather warning and forecasting, hydrological studies (i.e. assessment of drainage basin, location and extent of water bodies, etc), natural resources management, agricultural practice (assessment of crop, control of pest and disease, estimation of crop yield), geological studies, etc (Lillesand & Kiefer, 2000, Jensen, 2007, Campbell, 2007, Sabins, 2007, Jones & Vaughan, 2010).

2.1.6.1.2 *Landsat Systems*

Landsat ("land satellite") was designed in the 1960s and launched in 1972 as the first satellite tailored specifically for broad-scale observation of the Earth's land areas to accomplish land resource studies similar to what meteorological satellites had accomplished for meteorology and climatology (Campbell and Wynne, 2011). The Landsat system consists of spacecraft-borne sensors that observe the Earth and then transmit information by microwave signals to ground stations that receive and process data for dissemination to a community of data users. This current study uses all the generations of Landsat system, Landsat MSS, Landsat TM and Landsat ETM+ to generate LULC for 1972, 1986, 2002 and 2010. the reason for this is as a result of their high spatial resolution and geometric accuracy. However, they are lower spectral and radiometric details (Lillesand & Kiefer, 2000, Jensen, 2007, Campbell, 2007, Sabins, 2007, Jones & Vaughan, 2010).

In addition, the orbital characteristics of the different landsat sensors used in this study are presented in Table 2.1. The entire surface of the Earth between 81° N and 81° S latitude was subjected to coverage by Landsat sensors once every 18 days (every 9 days, if two satellites were in service) (Gao, 2009). Landsat 4 and Landsat 5 retained most of the orbital characteristics of their predecessors as presented in Table 2.1.

Table 2.1: Orbital Characteristics of Landsat Missions

Characteristics of Landsat	**Landsat (1, 2 and 3)**	**Landsat (4, 5 and 7)**
Height	915 km (880–940)	705km
Inclination	99°	98.2°
Period	103 min	98.9 min
Revolution	14 per day	233 per day
Speed	6.47 km/s	6.47 km/s
Distance between successive tracks at the equator	2,760 km	2,760 km
Distance between orbits	159.38 km	159.38 km
Repeat cycle	18 days	16 days
Overlap at the equator	14%	14%
Time of equatorial crossing	9:42 a.m.	10.00 a.m.
Total IFOV	11.56°	14.92°
Orbit type	Circular, sun-synchronous	Sun-synchronous polar

(Source: Gao, 2009)

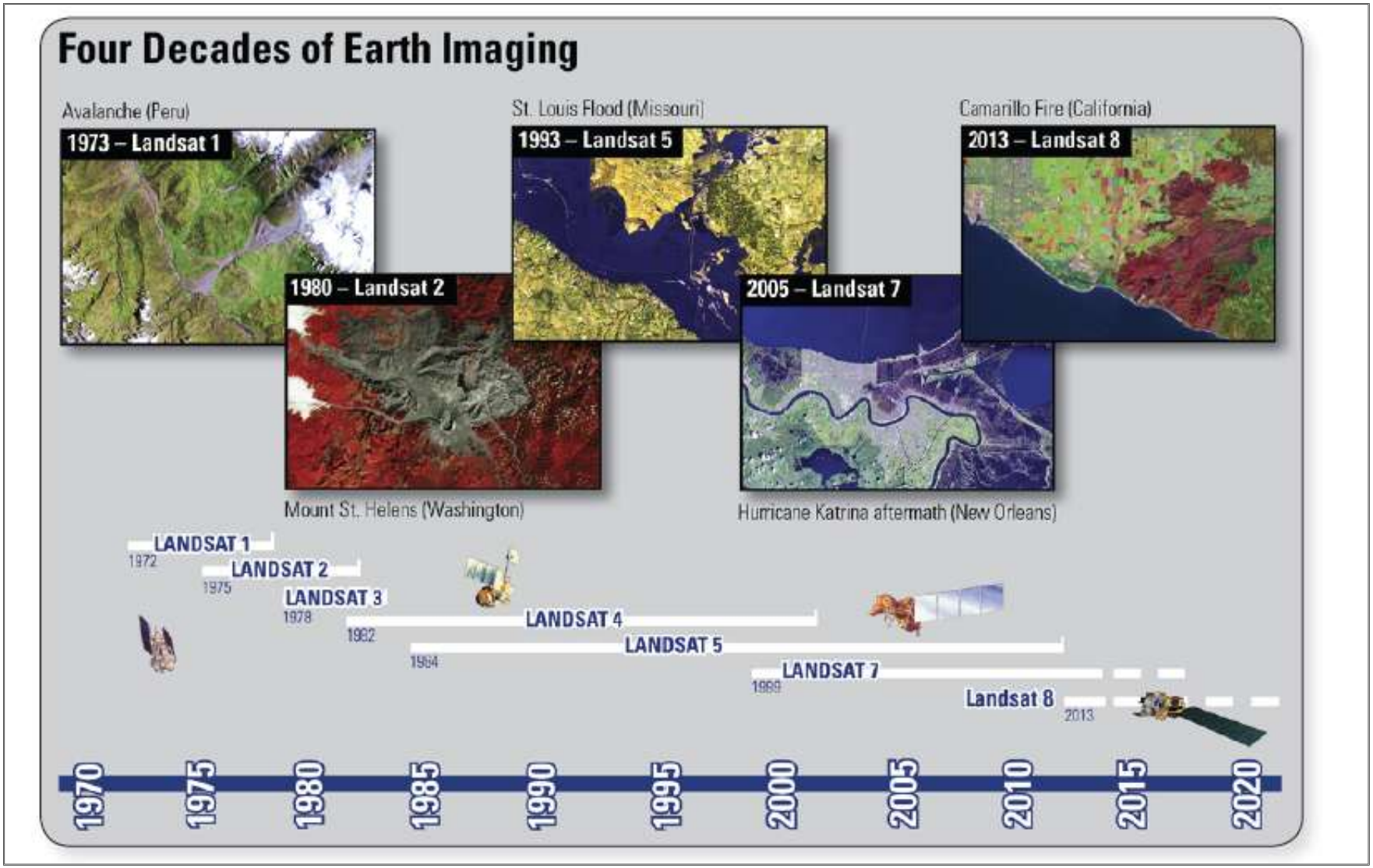

Figure 2.2: Landsat Missions *(Source: http://www.usgs.gov)*

Landsat data are used by government, commercial, industrial, civilian, military, and educational communities throughout the world. The data support a wide range of applications in such areas as global change research, agriculture, forestry, geology, resource management, geography, mapping, water quality, and coastal studies. The consistency of Landsat data acquired through the years allows for direct comparison of current specific site images with those taken months, years, or decades earlier. This comparison process can reveal land-cover changes that occur slowly and subtly, or quickly and devastatingly. The richness of the archive, combined with a no cost data policy, allows users to exploit time series of data over extensive geographic areas to establish long-term trends and monitor the rates and characteristics of land surface change for disaster response, as well as image-derived products that incorporate information on population density, elevation, and other environmental factors *(www.usgs.gov).* The research work uses data from Landsat 5 and 7 to generate LULCC for the period of study, 1972 – 2010.

2.1.6.2 Geographic Information System (GIS)

Geographic Information System (GIS) has being a major tool not only to geographic research but also to other fields of study, especially in the science related disciplines. This is because it has the ability to create and manage database, analyse, display and update of existing database for spatial phenomena. The use of GIS has grown dramatically since the 1980s. Initially it was unknown to many researchers but has become commonplace in businesses, universities and governments where they are now used for diverse applications. Consequent upon it current status, many definitions of GIS have been developed. However, each definition depends on who is giving it, and their background and view point. Also, the definitions will likely be changing as the technology and applications develop further (Pickles, 1995).

Aronoff (1989) defines GIS in the broadest sense as any manual or computer based set of procedures used to store and manipulates geographically referenced data. Due to a wide use of the computer system, many authors have restricted their definitions to only the computer system. He therefore, redefines GIS to mean a computer based system that provides the following four sets of capabilities to geo-referenced data; input, data management (data storage and retrieval), manipulation and analysis and output. In similar vein, Campbell (1996) describes GIS as a specialized system that preserves locational identities of the information it records. He explains further that 'a digital computer provides the basis for storage, manipulation, and display of large amounts of data that have been encoded in digital form'. Thus, a GIS consists of a series of overlays for specific geographic region. It is also, defined as an organized collection of computer hardware, software, geographic data and personnel designed to efficiently capture, store, update, manipulate, analyse, and display all forms of geographic referenced information (ESRI, 1990).

In general, the various definitions have revealed that GIS is a computer system that covers three main components or elements. This implies that the computer system is made up of hardware (including plotters, printers, scanners and all other physical parts of computer); software (the computer programs that run the computer) and appropriate procedures.

There is almost as much debate over what and what to be part of GIS components as there is about its definitions. Some authors have agreed in this regard that GIS is made up of three main components or elements. For example, Burrough (1986) suggests that the main components of GIS are: computer hardware, application software modules and a proper organizational context. However, Maguire (1989) stresses that data is the most important aspect or component of GIS. In general practice, however, it is soon realized that all the components mentioned are equally important, since, GIS or computer system cannot exist in

isolation. To this end, a well-designed GIS would be made up of five (5) main components or elements if all the features of the definitions are taken into consideration. These will include the computer system (hardware and operating software), application software, spatial data, data management and analysis procedures and personnel.

2.1.6.3 Applications of remote sensing and GIS to landuse/landcover studies

Landuse and landcover study is the basis of any developmental effort because before any development could take place on land, it will be necessary and important to know what exists on the ground (i.e. landcover) and the landuse pattern in the area. Landuse changes over time are in response to socio-economic and environmental forces. The practical importance of such changes for planners and administrators are obvious, as they reveal the attention an area or a community require if it is to develop in harmonious and orderly manner. Monitoring changes in landuse and landcover pattern over the earth's surface could be very difficult and complex when using the traditional methods of field survey. This is because some part of the earth's surface are inaccessible and cannot be reached or covered within a given period of time. Consequently, the use of Remote Sensing and GIS as a tool for such an exercise becomes inevitable for getting quick and accurate landuse information about the area of interest.

The applications of Remote Sensing and GIS techniques to the study of landuse and landcover are in three folds, namely, mapping, detection of change and monitoring of changes over the period of the landuse pattern. All the remote sensing systems are used to carry out studies in Landuse and landcover mapping, monitoring of change and change detection. However, the type of remote sensing system to be used in any particular context would depend on the level of details of information required and terrain or location of the study area. For instance, landuse/landcover mapping can be interpreted more or directly from

evidence visible on aerial images. However, for mapping of rural areas or where a generalized mapping is required other remote sensing systems images are used because they have a wider coverage and are less expensive to use. Landuse maps are generally produced at a variety of scales, ranging from 1:12,500 to 1:250,000 and smaller. Some examples can be cited in this respect. Omojola and Soneye (1993) used Remote Sensing and GIS techniques to assess the landuse/ landcover off the middle Sokoto River of the northwestern Nigeria. In the study, imagery acquired from Landsat satellite system was used to generate landuse/ landcover information of the study area. In the study, Landsat MSS was used because the study area was a rural area where agricultural land was the basis for landuse, thus the information required was highly generalized. Also, a small scale (1:125,000) and coarse resolution imagery were required for the mapping, therefore, Landsat MSS was used in the study because it has the characteristics that fit into the requirement i.e. it has a coarse spatial resolution of 79m by 82m, five spectral bands two in the visible, two near infrared and one thermal infrared. Also, the climate of the study area made Landsat MSS suitable for the mapping.

Similarly, Adeniyi and Omojola (1999) used archived remotely sensed data to evaluate landuse/ landcover change in Sokoto – Rima basin of the NW Nigeria. The objectives of the study were to make an inventory of landuse/ landcover, determine the trend, rate, nature, location and magnitude of landuse/ landcover change and evaluate the environmental and socio economic implications of the changes within the study area using multisource archival and multidate remote sensing and GIS techniques. In other to achieve these objectives, Adeniyi and Omojola (1999), used aerial photographs of scales 1:40,000 and 1:25,000 for 1962 and 1977 respectively; SPOT (P, XS) and Landsat (MSS) of 1986. Maps of 1:50,000 scales were generated from these remotely sensed data. These remotely sensed data were

used basically because of their scales, coarse resolutions and the level of detail of the final product (i.e. maps of scales 1:50,000).

Furthermore, in Alabama satellite Remote Sensing and GIS techniques were used to assess and monitor landuse/landcover change. Madison County, Alabama was said to be developing at an observed annual rate of 1% for the last 16 years. But by 2000 developed land covered about 30% of the county. At this rate, by 2020 nearly 50% of the county will be developed and this becomes a major source of concern for policy makers and researchers. Subsequently, Laymon (2003) carried out landuse change study for the county in order to ascertain the level of development that had taken place between 1984 and 2000. The objectives of the study were to develop a land resource plan for Madison County and to assess the change in landuse over the 16-year period from 1984 to 2000. Landsat TM images were acquired for 1984 and 1990 while Landsat ETM+ images were acquired for 2000. Landcover/landuse classes were aggregated into "developed" and "undeveloped" superclasses. The difference between these maps reflects changes in the distribution of Developed and Undeveloped land that had occurred during the intervening periods. In this study, Landsat TM images were used for 1984 and 1990 because of its coarse resolution and the classification scheme adopted. However, in 2000 a better resolution image from Landsat-7 ETM+, which has 15m and 30m spatial resolution at pan band and 1-5,7 bands respectively, was used because more area had turned to developed area. It thus required more information to come out with the master plan and to ascertain the actual growth rate of the county. He finally found out that the development in the area was about 1.1% per year. In other areas, remotely sensed data were used to monitor and analyse vegetation response patterns to environmental change.

This study adopted Remote Sensing and GIS techniques for the modeling of the interaction between LULCC and climate change in the derived savannah region of Nigeria. The remote sensing techniques, which are made of different scales and resolutions, are used to generate

the base data for the LULC for 1972, 1986, 2002 and 2010. Additionally, the GIS techniques provide the environment for the integration of all the data, the climatic data, static factors such as elevation, slope, distance to stream, road and disturbance of LULC variables and other spatial data used for the analysis and modeling. It also provides the software for the manipulation, analysis, overlying and modeling operations for the simplification of modeling candidates and cartographic designs for the generation of statistics and virtual display of results.

2.1.7. Emissions scenarios

Emissions scenarios were developed by IPCC between 1990 and 1992 for long term projection climate change and variability and its impacts and possible options for adaptations and mitigations. However, emission scenarios were revised in a Special Report on Emission Scenarios released in 2000 by the IPCC working group after much evaluation due to changes in the understanding of driving forces of emissions and methodologies since 1992 (IPCC, 2000 & Nakicenovic *et al.*, 2000).

There are four major narrative storylines developed for the future greenhouse gas emissions. This is based on the complex system generated by driving forces such as demographic development, socio-economic development, and technological change in order to yield four sets of scenarios called families. These families are **A1, A2, B1** and **B2**. These four families were further grouped into six scenarios, containing one group family each of **A2, B1** and **B2**. Furthermore, the A1 family was regrouped into three scenarios (**A1F, A1B** and **A1T**). However, the scenarios assume that:

- The **A1** family has alternative developments of energy technologies and describes future world that is characterized by very rapid economic growth, global population that peaks in mid-century and declines thereafter, and the rapid introduction of new

and more efficient technologies and energies. **A1FI** - fossil fuel intensive, **A1B** - balanced, and **A1T** - predominantly non-fossil fuel.

- The **A2** scenario family explains a future world that is heterogeneous, self reliance and preservation of local identities. A world with increasing global population, regionally oriented economic development and per capita economic growth and technological change are more fragmented and slower than in other narratives.
- The **B1** scenario family depicts a world that has similar global population that peaks in midcentury and declines thereafter, as in the A1 storyline, but with rapid changes in economic structures toward a service and information oriented economy, with emphasis on material intensity reductions, clean and resource-efficient technologies. It further emphasises on global solutions to economic, social, and environmental sustainability, including improved equity, but without additional climate initiatives.
- The **B2** scenario family illustrates a world in which the emphasis is on local solutions to economic, social, and environmental sustainability. It characterized by continuously increasing global population at a rate lower than the A2, intermediate levels of economic development, and less rapid and more diverse technological change than in the B1 and A1 storylines. Moreover, the scenario is also oriented toward environmental protection and social equity, it focuses on local and regional levels.

The Climate special report emission scenario A2 family storyline was adopted for this current study. This is because the study area is witnessing continuous changes in population dynamics and environmental change, increase in per capita income and an economy geared towards regional development. It is used to generate the future climatic parameters used for this study.

2.2 Conceptual Framework

Conceptual framework is the organisational devices used to identify variables. It clarifies the relationship among variables involved in a research in order to understand and resolve the research problem. In the field of resource analysis and management, theories and laws formulation are always difficult (Mitchell, 1989), since theories involve statements that have explanatory and predictive power. Although, these attributes are demanding, yet, they help to explain why there are as yet little of geographical theories of resource management that can be identified. The stocks and flow approach concept has been identified to be the most appropriate for this current study is and used to clarify the relationship among the research variables.

The stocks and flows is an integrated assessment framework approach adopted by IPCC (2001) and Le Treut *et al.*, (2007). It presents the earth's system as an interacting system, which is made up of four subsystems representing the stocks, society and the economy, atmospheric concentrations, climate system and natural systems. Meanwhile, the arrows in the Fig.2.3 show the flow from one system as it affects another. **Society and the Economy** with their socio-economic development paths, with the main drivers including population growth, energy use, economic growth, technological change and land-use change. Also included are: anthropogenic emissions from the society and economy which includes expansion of industries, technological development and burning of fossil fuel hat leads to the increase in the **atmospheric concentrations** of the greenhouse gases and aerosols. In addition, the **climate system** is affected by the increase in the atmospheric concentrations leading to increase or decrease in solar radiation that reaches or leaves the earth's surface thereby disturbing the natural processes of the climate system and causing an increase in the average air temperature and increase in the sea level.

Finally, the **natural systems** (i.e. landuse, food and water systems, ecosystems and biodiversity and animal and plant health) is stressed due to the long-term effect of the rise in air temperature and sea level and these, in turn, cause climate change stresses on natural systems. These add to the effects of air pollution and to non-climate change-related stresses leading to loss of land through sea level rise, more floods and droughts, stress on food and fresh-water provision, loss of biodiversity and changes in animal and plant health. The interactions and feedbacks between the systems are complex and with possibilities of leading to extreme events such as climate change, critical thresholds and shocks. For instance, there are three feedbacks and interactions between these systems. There is a feedback from the sea temperature rise to atmospheric concentrations, which is because the sea absorbs less carbon dioxide (CO_2) at higher temperature (Barker, 2003). There is also a possibility of some feedbacks from the changes in the natural systems to the climate system, such as albedo effects from changing landuse, and other perhaps larger interactions between the natural systems and atmospheric concentrations**.**

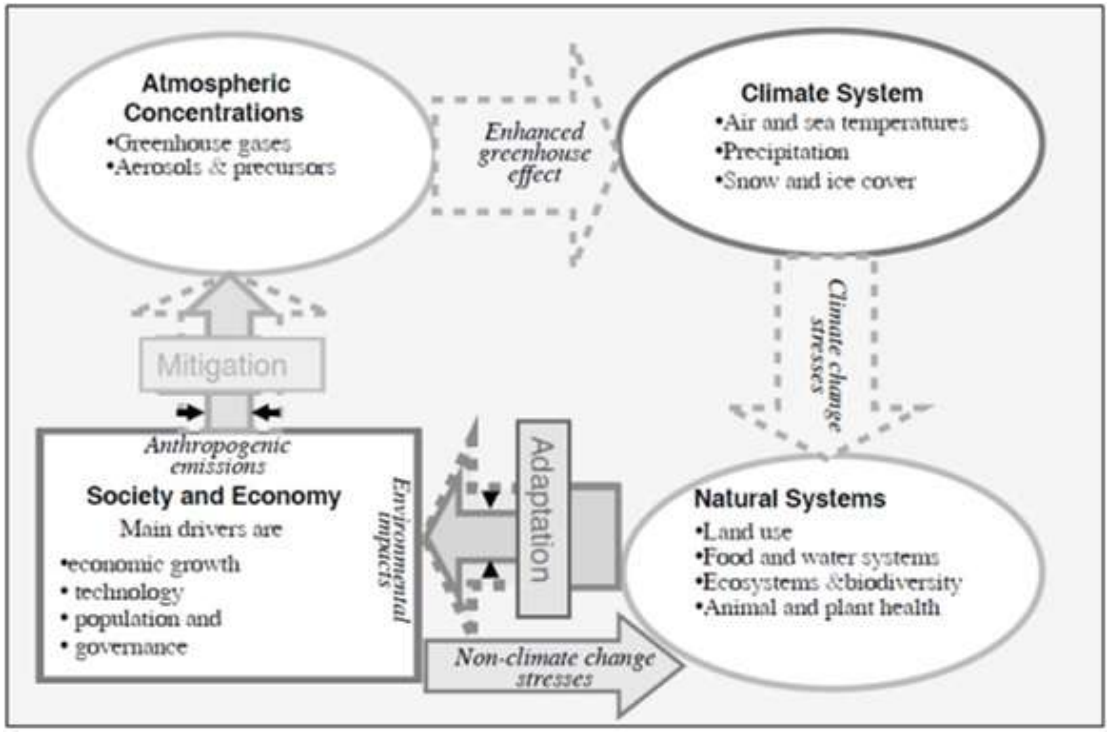

Fig. 2.3: The Stocks and Flows Approach as an integrated assessment framework for climate change. *(Source: Barker, 2003)*

In this study, the natural system represents the land surface characteristics of landuse/landcover change (LULCC), while the climate system adapts the parameters of the local climate including rainfall and temperature. These are considered to be the stocks while the flows are the drivers of landuse/landcover changes i.e. mainly the climatic variables for both present and future climates that kick-start the process.

CHAPTER THREE

METHODOLOGY

3.1 Introduction

This chapter presents the materials and methods adopted for the study and it is documented in five sections. The characteristics and sources of data used in the research work are presented in the first section, while the subsequent sections serially provide an insight into the methods and procedures adopted in order to achieve the specific objectives of the study.

3.2 Data, Data Sources and Characteristics

The method adopted for this research involves the collection, collation and use of both spatial and non-spatial data. Data were sourced through reconnaissance and field survey, interaction with the inhabitants and ground truthing (ground information). The sources and characteristics of spatial data used are presented in Table 3.1.

3.2.1 Satellite remotely sensed data

The sources and characteristics of the satellite data are presented in Table 3.1. Specifically, archived series of Landsat data (MSS, TM and ETM+ satellites) and ASTER DEM covering the study area are sourced from internet portals of various data vendors. The specific bands of Landsat data series are documented to follow the extent of advancement in earth-resource data collection. Landsat is reputed as the first earth-resource data collection satellite with rich inventory hence, its choice for this study. In addition, ASTER DEM data are sourced from the online portal of ERSDAC (Earth Remote Sensing Data Analysis Centre) and used as elevation data. It provides a better spatial resolution (30m), when compared to vertical interval (50 ft) from topographic map sheets.

Table 3.1: Sources and characteristics of data

Data	Identification/Coverage	Scale Resolution/Units	Date	Sources
Landsat 7 ETM+ Satellite Imagery (SLC – off)	Paths 190 and Rows 54 – 55	Spatial Resolution - 15 (P), 30m (B- IR), 60m (TIR); Spectral Resolution - 8bands (0.45 – 2.35µm, 10.4 -12.5µm)	Jan., 2010	USGS Earth explorer *http://earthexplorer.usgs.gov/*
Landsat 7 ETM+ Satellite Imagery (SLC – on)	Paths 190 and Rows 54 – 55	Spatial Resolution - 15 (P), 30m (B- IR), 60m (TIR); Spectral Resolution - 8bands (0.45 – 2.35µm, 10.4 -12.5µm)	Feb., 2003	USGS Earth explorer *http://earthexplorer.usgs.gov/*
Landsat 7 ETM+ Satellite Imagery	Paths 190 and Rows 54 – 55	Spatial Resolution - 15 (P), 30m (B- IR), 60m (TIR); Spectral Resolution - 8bands (0.45 – 2.35µm, 10.4 -12.5µm)	Nov., 2002	Global Landcover Facility (GCLF) - *www.landcover.org*
Landsat TM Satellite Imagery	Paths 190 and Rows 54 – 55	Spatial Resolution - 15 (P), 28.5m (B- IR), 120m (TIR); Spectral Resolution - 7bands (0.45 – 2.35µm, 10.4 -12.5µm);	Nov., 1986	Global Landcover Facility (GCLF) - *www.landcover.org*
Landsat1 MSS Satellite Imagery	Paths 204 - 205 and Rows 54 – 55	Spatial Resolution - 15 (P), 79m (G - NIR); Spectral Resolution - 4bands (0.5 – 1.1µm);	Nov., 1972	Global Landcover Facility (GCLF) - *www.landcover.org*
Elevation Data - ASTER GDEM (Version 2)	ASTGTM2 – (N06E004 – N06E006, N07E004 –N07006 & N08E006) – 9 scenes	Spatial Resolution – 30m or 1 arc second	2011	Earth Remote Sensing Data Analysis Centre *www.gds.aster.ersdac.or.jp*
Population	Study Area	LGA Population Figure	2006	National Bureau of Statistic (NBS) *www.nigerianstat.gov.ng*
Future climatic data	Stations – Ilorin, Bida, Lokoja, Akure, Ondo and Oshogbo	0.5 Degree latitude by longitude	2011 - 2050	Intercomparison Project phase 3 (CMIP3) *(www.engr.scu.edu /~emaurer/global_data/)*
Present climatic Data -Temperature and Rainfall	Meteorological Stations – Ilorin, Bida, Lokoja, Akure, Ondo and Oshogbo	Temperature (Monthly Tmax and Tmin) - degree centigrade (^{0}C), Rainfall (monthly Rainfall) - Millimeters (mm)	1941 - 2010	Nigerian Meteorological Agency (NIMET), Lagos

Source: Author, 2015

The Landsat (land satellite) system is a suite of development in earth resources data collection. The three suites developments (i.e. Landsat MSS, TM and ETM+) are used in this study. The focal characteristics of these sensor systems are detailed in Table 3.2, which provides a synoptic view of the resolution and other key traits. The Landsat data series were downloaded using the WRS (World Reference System) platform with path 204–205 and row 54–55 for MSS (1972), and path 190 and row 54–55 for TM and ETM+ (1986 and 2002) from the Global Land Cover Facility (GLCF) of Department of Geography, University of Maryland. The Landsat 7 ETM+ for 2003 and 2010 were downloaded from the Scan Line Corrector (SLC) on and off archives of US Geological Survey earth explorer portal. The ETM+ series were stored in two separate archives since the sensor developed 'SLC error' on May 31, 2003, which resulted in gaps or stripes on the images of some sections of the earth's surface. SLC-off and SLC-on was used to differentiate the archives.

The Multispectral Scanner (MSS) was used despite its low spatial, spectral and radiometric resolution when compared to the subsequent sensors. It provided a base for understanding the ground conditions of the study area. The Landsat MSS is made up of four spectral resolutions; however, bands 2, 3 and 4 were used to generate false colour composite imagery used for 1972. The bands were used because they provide clarity and distinguish the natural vegetation features better than the combination of other bands (Campbell & Wynne, 2011; Gao, 2009).

The Thematic Mapper (TM) and (Enhanced Thematic Mapper plus) ETM+ with its improved spatial, spectral and radiometric details provided a platform on which the earth-based changes in the study area can be assessed. As stated in Table 3.2, there are seven bands of TM, however, three bands were selected for this study (2, 4 and 7) to generate false colour

Table 3.2: Focal characteristics of the Landsat sensor typologies used

Focal characteristics	Sensor systems		
	Multispectral Scanner (MSS)	**Thematic Mapper (TM)**	**Enhanced Thematic Mapper plus (ETM+)**
Spatial resolution (metres)	80 (Pan – 40; thermal 237)	30 (thermal – 120)	30 (Pan-15; thermal 60)
Spectral resolution	4 bands (visible and near infrared)	7 bands (visible, near IR, mid IR and thermal IR)	8 bands (visible, near IR, mid IR and thermal IR)
Dynamic range	7 bits	8 bits	8 bits
Repeated cycle	16days (14 orbits/day)	16days (14.56 orbits/day)	16days (14.56 orbits/day)
Swath width	180 km	185 km	185 km
Satellite vehicle	Landsat 1-4	Landsat 5	Landsat 7
Year launched	July 23, 1972	March 1, 1984	April 15, 1999
Orbit altitude	917 km	705 km	705 km

Sources: Campbell & Wynne, 2011; Gao, 2009)

composite. These bands were used mainly to enhance interpretation and reveal the conditions of vegetation. However, the Landsat 7 ETM+ of 2010 has scan line error or gaps/stripes and the necessary gap-filling process was carried out using the Landsat 7 ETM+ of 2003 of the same path and row to fill the gaps/stripes with the aid of 'frame_and_fill_win32' software developed and provided free by the National Aeronautical and Space Administration (NASA). During the filing process, 2010 and 2003 images were used as the 'anchor' and 'fill_scene_1' folders. The filling operation failed for the band 7 of 2010 image, therefore, bands 3, 4 and 5 were selected for the study.

3.2.2 Climatic data

The climatic data (monthly rainfall and temperature–maximum and minimum) for the period between 1941 and 2010 were acquired from the Nigerian Meteorological Services (NIMET), Lagos for six stations (i.e. Ilorin, Bida, Lokoja, Akure, Ondo and Oshogbo) within and around the study area. However, there were data gaps in the time series data from NIMET. For instance, there are no data recorded for the Ilorin station between 1941 and 1945 for both temperature minimum and maximum while temperature maximum records for 1961, 1963–64

and 1966–69 were not alos available. In addition, there were no records for Bida (temperature maximum) in 1996, in Oshogbo station for temperature (max (1948–1956)) and rainfall (1948–1957), in Ondo for 1941 for all parameters, Lokoja for temperature variables and Akure between 1941 and 1979 for all parameters. The Akure station actually started operations in 1980. The period between 1941 and 2010 was adopted for this study in order to account and accommodate for the standard climatic period, which simply defines climate as the average weather or atmospheric conditions of a place for a period between 35 and 40 years (Ojo *et al.,* 2001). Nevertheless, the issue of data gaps was resolved by statistically regressing the years with gap against the data of the same period from the nearest station having a similar correlation with the stations with the data gaps. Consequently, the missing years were determined using the trend line equations.

The future climate data for monthly average precipitation and temperature (2011 – 2050) were obtained from the World Climate Research Programme's (WCRP's) Coupled Model Intercomparison Project phase 3 (CMIP3) multi-model dataset (Meehl *et al*., 2007). They were projected for 32 different climates under two emission scenarios (SRES A2 and B1 for 16 GCMs). The data were downloaded for six stations within and around the study area from the archive of the Civil Engineering Department of Santa Clara University, Santa Clara, CA, US. This study adopted the data from one of the GCMs, the MRI-CGCM2.3.2 model under emission scenarios, SRES A2 using statistically downscale techniques, to a 0.5 degree grid, based on observed 1950-1999 gridded data of Adam and Lettenmaier (2003) and later adapted for use in studies as described in Maurer *et al.*, 2009. MRI-CGCM2.3.2 data was adopted for this study because it is the most reliable of all the eighteen GCMs evaluated to accurately capture and stimulate the climatology and variability of the West African Monsoon System for both the present and future climates under various emission scenarios

(Vizy & Cook, 2006, and Abiodun *et al.*, 2013). It is also used to maintain stable control run without using surface flux corrections (Dia, 2006).

3.2.3 Terrain Data

The elevation data covering this study were generated from nine scenes of one arc second (30m), 1^0 *x* 1^0 grid ASTER GDEM2 (Advanced Spaceborne Thermal Emission and Reflection Radiometer Global Digital Elevation Model Version 2). The study area was clipped out of the mosaicked nine scenes of ASTER GDEM2. However, other terrain variables (i.e. aspect and slope) were generated from the elevation data.

3.2.4 Population density

Population density is the ratio of population to the area covered in square kilometer by a place. The population density map for this study was produced from the Local Government Area (LGA) population figure for 2006 downloaded from the archive of the National Bureau of Statistics (NBS). Population density figures were calculated and attached to the polygon attribute table of LGAs and then interpolated to generate the surface density map.

3.2.5 Other datasets

Other datasets used for the study for the purpose of modeling the interaction between climate and landuse/landcover change (LUCC) include NDVI (Normalized Difference Vegetation Index), distance from the urban, distance from road, distance from disturbance and distance from the stream are all derivatives of generating landuse/landcover from satellite imageries. The Normalized Difference Vegetation Index (NDVI) is a mode designed to provide a quantitative measurement of green vegetation biomass and can also be used as a proxy for environmental change (Thiam & Eastman, 2009). The Normalized Difference Vegetation

Index is expressed as the difference between the near infrared (NIR) and red bands (RED) normalized by the sum of these bands:

$$NDVI = \frac{NIR-RED}{NIR+RED} \qquad \text{---------- (Eqn. 3.1)}$$

It is commonly used because it retains the ability to minimize topographic effects while producing a linear measurement scale. The measurement scale has the desirable property ranging from 1 to -1 with 0 representing the approximate value of no vegetation; thus negative value represents non-vegetated surfaces. For this study, bands 4 and 3 (near infrared and red) of the Landsat 7 ETM+ satellite imagery were used to generate NDVI for the 2002.

3.3 Methods and Procedures

There are four main methods and procedures adopted for this research as illustrated in the methodological flowchart in figure 3.1. The methods and procedures include remote sensing and GIS, multivariate statistical analysis, modeling, validation and prediction of implications. Remote sensing and GIS techniques are adopted to achieve the first of the objectives of the study. The second objective was achieved by using the multivariate statistical analysis, while the third objective was achieved through the combination of the results of the analysis done in the first and second objectives with other driving forces of environmental change as shown in the methodological flowchart illustrated in Fig.3.1. This is to model the future landuse/landcover patterns within the Derived Savannah region of Nigeria. Finally, objective four assesses the future implications of the landuse/landcover patterns obtained from the modelling of landuse/landcover and climate change in the third objective, which resulted in the determination of the quantity of carbon dioxide that would be emitted during the future climate.

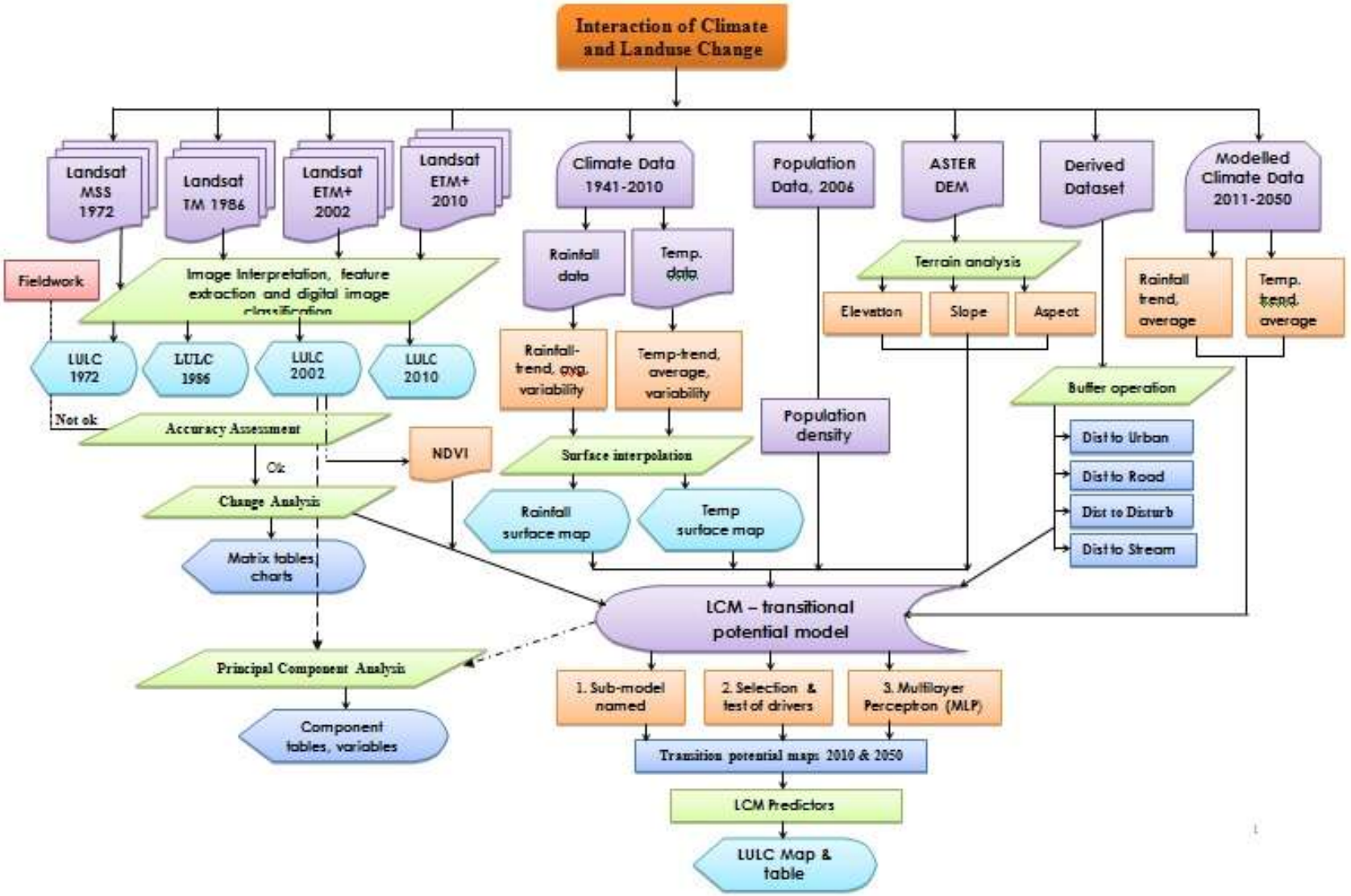

Figure 3.1: Methodological Flowchart *(Source: Author, 2015)*

3.3.1 Assessment of landuse/landcover change

(i) Image inspection and interpretation

Remote sensing and GIS techniques are used to interpret and classify the satellite images (Landsat MSS, Landsat TM and ETM+). This is in order to generate the spatial characteristics of LULC for 1972, 1986, 2002 and 2010. The first step taken was the inspection and examination of the Landsat images with respect to resolutions and the minimum mapping unit (MMU) in order to determine the bands that are suitable for the analysis. Consequent upon this, for 1972, Landsat MSS bands 2, 3 and 4 were used to generate the false colour composite image that was interpreted and classified into LULC classes. In addition, bands 2, 4 and 7 of Landsat (TM & ETM+) were used to generate the false colour composite images for 1986 and 2002, while bands 3, 4 and 5 were used to generate 2010 image from Landsat ETM+.

(ii) Image classification technique

A systematic image classification scheme was adapted from the modified US Geological Survey Classification System (Campbell, 1997). Thus, ten classes were generated as presented in Table 3.3. Training data, which correlates with the number of classes generated, were carefully selected and delineated, signature files were developed using the Idrisi selva software. Thus, the supervised classification technique was used based on the level of accessibility to the study area. Subsequently, the maximum likelihood classifier was used to classify the images to generate the base maps for 1972, 1986, 2002 and 2010, which formed the result for the first objective.

Maximum likelihood supervised algorithm (defined as MAXLIKE in IDRISI) was used for two key reasons:

1. the selected sample sizes were large enough to permit a clear definition of the training data (Strahler, 1980 and Eastman, 2009); and
2. the statistical qualities of MAXLIKE, which is based on the Bayesian probability theory permit the use of information from a set of pre-selected training through the combination of the mean and variance/co-variance data of the signatures to estimate the posterior probability that a pixel belongs to definite class (Eastman, 2012).

Consequent upon this, the LULC base maps for 1972, 1986, 2002 and 2010 were generated.

Table 3.3: The LULC Classification Scheme

ID	LULC Classes	Description of Classes
1	Urban	This covers the built areas, roads and surfaces with appreciable human constructions
2	Waterbody	This includes all streams, ponds, lakes, dams and rivers within the study area
3	Forest	Areas covered by broadleaved evergreen and deciduous forest areas of height between 3 and 5m. It includes wetlands, plantation and light and heavy , gallery, palm and montane forests
4	Woodland	This covers areas that were left to fallow after harvesting of forest without any plan to re-grow and where that are littered with deadwood
5	Grassland	This covers area with high to low grasses, shrub and stunted woods and used for extensive grazing.
6	Farmland	This includes area covered by all forms of agricultural practices involving tillage including both plots with regular and irregular shapes
7	Fire Scar	This covers area with black spots or dots on the imageries that were recognised as bush burning sites for new farmlands
8	Degraded Surfaces	This is area that cannot support plant growth or plant cultivation. Its includes exposed surfaces, bare surfaces and rock outcrops

Source: Modified from USGS Classification system (Campbell & Wynne, 2011)

(iii) Accuracy Assessment

Assessing the accuracy of the classification of satellite imageries for 1972, 1986 and 2002 was difficult because of the time gap (i.e. there were about 10 to 40 years time difference in the acquisition of the satellite imageries and the actual field exercise). However, the landuse/landcover data for 2002 was used for the accuracy assessment and validation of the LULC map. The field exercise was carried out with hardcopy of predicted LULC map 2010, handheld Global Positioning System (GPS - Garmin 76X), Digital camera (Canon PowerShot A3400 IS, 16megapixels) and field note. A sample size of 300 locations/points was selected and sampled using the stratified systemic techniques, which was established by using GPS

coordinates and the landuse/landcover patterns were recorded. In order to determine the ideal number of locations (pixels) for the accuracy assessment for landuse/landcover classification, binominal probability was used; and expressed is as follows:

$$N = \frac{Z^2 pq}{E^2} \ldots\ldots\ldots\ldots \text{ Eqn. (3.2)}$$

where, N = numbers of locations or points
p = expected percentage accuracy and q = 100 – p
E = maximum allowable error
Z = 2 based on bimodal distribution (i.e. Confidence level set at 1.96 for the 95 percent two-tailed from standard normal deviation data set (Fitzpatrick-Lins, 1981; Gao, 2009).

The samples collected for the accuracy assessment was far more than the required sample size of 204 to achieve 85% accuracy for the study. However, in order to guide against some landuse/landcover classes being overemphasised, the sample size of 300 was used.

In addition, the study employed confusion or error matrix (a two-dimensional matrix) to evaluate the errors of omission and commission in other to determine the overall accuracy of the classification exercise. The omission error was determined by the percentage of the ratio of all the figures in a column, except the main diagonal ones to the total sum of all the figures in the column; while the percentage of the ratio of all the figures in the row, except the main diagonal ones to the total sum of all the figures in the row was used to calculate the commission error. Consequently, the LULC classification was further subjected to the overall accuracy assessment by evaluating the user's and producer's accuracies. The user's and producer's accuracies were calculated from the ratio of the main diagonal cell value of a row to the total sum of all the figures in the same row and ratio of the main diagonal cell value of a column to the total sum of all the figures in the same column respectively. These accuracies pertain to the individual LULC classes, thus, they could be misleading when high accuracies

values are obtained. In order to ensure that the user's and producer's accuracies are not cosmetic, therefore, the overall accuracy was determined. Overall accuracy of classification was calculated from the ratio of the sum of all the figures in the main diagonal cells to the total sum of all the evaluated pixels. Finally, the confidence interval for the overall accuracy of classification was provided, which was derived from:

$$P\left(-b\left(<\frac{X-\mu}{\frac{\sigma}{\sqrt{N}}}\right)<b\right)=1 \quad \ldots\ldots\ldots\ldots\ldots \text{Eqn. (3.3)}$$

Where, P = probability of correctly labelling pixels in a classification

N = total number of samples

α = significance level

μ = population mean derived from the sum of the population elements divided by the number of observations or population size

X = sample mean

σ = standard deviation

b = confidence limit

(Source: Gao, 2009).

(iii) Change Analysis

Change analysis is usually carried out using two methods in Remote Sensing and GIS techniques; pre-classification and post-classification methods. The method adopted for change analyses is the one sequel to Lu, *et al*., (2004); which asserts that good change detection must take cognizance of the following points; (1) area change and change rate; (2) spatial distribution of changed types; (3) change trajectories of land-cover types; and (4) accuracy assessment of change detection results. The post-classification method is well implemented in the Land Change Modeler (LCM) extension of Idrisi software. Firstly, it was ensured that the base maps of 1972, 1986 2002 and 2010 had the same spatial extents; that number of columns and rows were equal and were then combined (i.e. 1972 and 1986, 1986 and 2002, 2002 and 2010 and 1972 and 2010) to generate change maps for the periods. Secondly, the area extents were generated for the periods and exported to Microsoft Excel

software pivot table where they were sorted into rows and column to form contingency or squared matrix table. Thirdly, the sum for each of the rows and columns and grand sum were generated. Finally, the gains and loss were evaluated and their percentages obtained. In conclusion, the change analysis was carried out by comparing the area covered by each of LULC classes and so matrix tables were generated with validation of final results.

3.3.2 Evaluation of climate variability and change

(i) Statistical techniques - The climatic data (monthly Rainfall and Temperature - maximum and minimum (1941–2010)) and model data (average temperature and rainfall (2011–2050)) were summarized using the statistical tools of measures of central tendency and dispersion. The monthly mean, annual mean and standard deviation were computed for the parameters considered in all the stations and standardized using a combination of standard deviation and mean. Percentages of coefficient of variation for each of the stations were computed from the standard deviation of annual mean divided by the mean of annual mean and multiplied by 100. The temporal variability index was determined from the standardize departure of the parameters in order to separate climate into wet and dry climatic periods and warm and cold climatic periods for the rainfall and temperature parameters respectively.

Consequently, the anomalies and variability indices for the climatic variables were determined using the following formulae:

$$\boldsymbol{Z = \frac{X-\mu}{\sigma}} \qquad \text{---------- (eqn. 3.4)}$$

$$\boldsymbol{CV = \frac{\sigma}{\mu} * 100} \qquad \text{---------- (eqn. 3.5)}$$

$$\boldsymbol{\delta i = (Pi - \mu)/\sigma} \qquad \text{--------- (eqn. 3.6)}$$

$$\sigma = \sqrt{\frac{\Sigma(xi-\mu)}{n-1}}$$ ---------- (eqn. 3.7)

Where, Z = Anomalies (standardization)

CV = Coefficient of Variation

X = Value of climatic variables

δ_i *= Variability index for year (i)*

p_i *= annual value of the climate parameter for year (i)*

σ *= Standard deviation*

μ *= Mean*

(Sources: Akinsanola & Ogunjobi, 2014; Oguntunde et al., (2011))

Single figures were derived for each of the stations and used to create surface maps. These figures were interpolated using the Inverse Distance Weighted (IDW) tool of spatial analyst extension in ArcGIS 10 to generate surface maps so as to reveal the spatial patterns, trend and coefficient of variability index and temporal variability.

(iii) Interpolation Technique – This research adopts the Inverse Distance Weighted (IDW) model to create the surface maps for the rainfall and temperature parameters. The IDW model was used because of the coarse nature or distance between synoptic stations within the study area. The IDW predicted very well in a situation where the influences of phenomena or observations diminish in their contributions with distances. The IDW is simple, effective and well implemented in the Spatial Analyst tool of ArcGIS software. Also, the IDW model always interpolates values of observations within the range of data values, so that the approximate values may not contain peaks and valleys. Therefore, the IDW involves dividing each of the observations by its distance from the target point raised to a power (α) (Smith *et al.,* 2007). Thus:

$$\boldsymbol{Z}j = kj \sum_{i=1}^{n} \left(\frac{\mathbf{1}}{\boldsymbol{d}ij^{\alpha}}\right) zi$$ ……. (Eqn. 3.8)

Where, Zj = Predicted Value

$\boldsymbol{d}_{ij}$ *=distance between the known value and predicted value*

$\boldsymbol{z}_i$ *= the known value*

$\boldsymbol{k}_j$ *= an adjustment to ensure that the weights add up to 1(Smith et al., 2007)*

3.3.3 Modelling interaction between climate change and LULC

Two methods (statistical – Principal Component Analysis (PCA) and modeling – Land Change Modeler (LCM) techniques were adopted in this research to model the interaction between the climate and landuse/landcover change. The methods required identification and parameterization of the underlying and proximate drivers of the landuse/land cover change and climate parameters in order to identify the controlling variables and to generate transition potential maps of the interaction. The drivers used and parameterized in this study include population density, normalized deferential vegetative index (NDVI), distance from the stream, road, urban and disturbance (anthropogenic factors) and nature of terrain (elevation, aspect, slope, etc.).

These factors have been identified to aid rapid transformation of LULC change from one class to another. For example, Giest and Labmin (2001) identify demographic factor or population pressure, which was represented with population density in this study, as one of the underlying driving forces which underpin the proximate causes of LULC change. Also, biophysical factors such as nature of terrain (i.e. elevation, aspect, slope, etc), distance from stream, road and urban centres do act as catalysts or obstacles to LULC change in certain locations (Verburg *et al.,* 2002). However, these factors were considered as static variables in this study.

The climate components, which include mean monthly rainfall and temperature parameters for observed and model data, were also used to model and predict the interaction in the present and future climate. These drivers and parameters (elevation, slope, aspect, temperature, and rainfall) were turned into map layers, rasterized and resampled into a cell size of 28.5m, so that the data layers would have the same cell size and resolution with the

LULC data. The digital values from the continuous variables (distance to stream, distance to road and cover, elevation, slope, aspect, temperature, rainfall and population) and the discrete variables (distance to stream, distance to road and cover) were weighted (from 0 to 100) in order of their susceptibility to deforestation and forest degradation process (i.e. the nearer to road, stream, urban and disturbance places with forest cover are the more susceptible to degradation) and rasterized as presented in Tables 3.4 and 3.5 before they were extracted and imported into the class code of LULC of 2002.

Table 3.4: Parameterisation of road and stream

Distance from Road (m)	Weight	Distance from Stream (m)	Weight	Distance from Urban (m)	Weight	Distance from disturbance (m)	Weight
0 - 1000	100	0 – 2500	60	0 – 4000	60	0 - 2000	100
1001 - 2000	75	2501 - 5000	50	4001 – 8000	50	2001 - 4000	75
2001 - 3000	50	5001 - 7500	40	8001 – 12000	40	4001 - 6000	50
3001 - 4000	25	7501 - 10000	30	12001 – 16000	30	6001 - 8000	25
4001 - 5000	5	10001 - 12500	20	16001 – 20000	20	8001 - 10000	5
5001 – 6000	0	12501 – 15000	10	20001 – 24000	10	> 10000	0
		>15000	0	>24000	0		

Source: Author, 2015

Table 3.5: Assigning weights to LULC

LULC	Weight	LULC	Weight
Urban	0	Degraded surface	5
Waterbody	10	Fire scar	10
Forest	100	Cloud cover	0
Woodland	70	Grassland	50
Farmland	30	No Data	Not Applicable

Source: Author, 2015

In addition, the extracted data were fed into principal component analysis to assess the controlling variables of the interaction. Finally, raster maps of the drivers (see appendix I) and climate parameters were combined with LULCC map (1986 – 2002) input into Land Change Modeler (LCM) of Idrisi Selva software to predict the interaction between climate and LULC in 2010 and 2050 for present and future climates respectively. The land change prediction in LCM involves three major steps (change analysis, transition potential modeling and change prediction) as shown in Fig.3.2. The change analysis was to assess the transition between LULC classes of 1986 and 2002 and change map was produced.

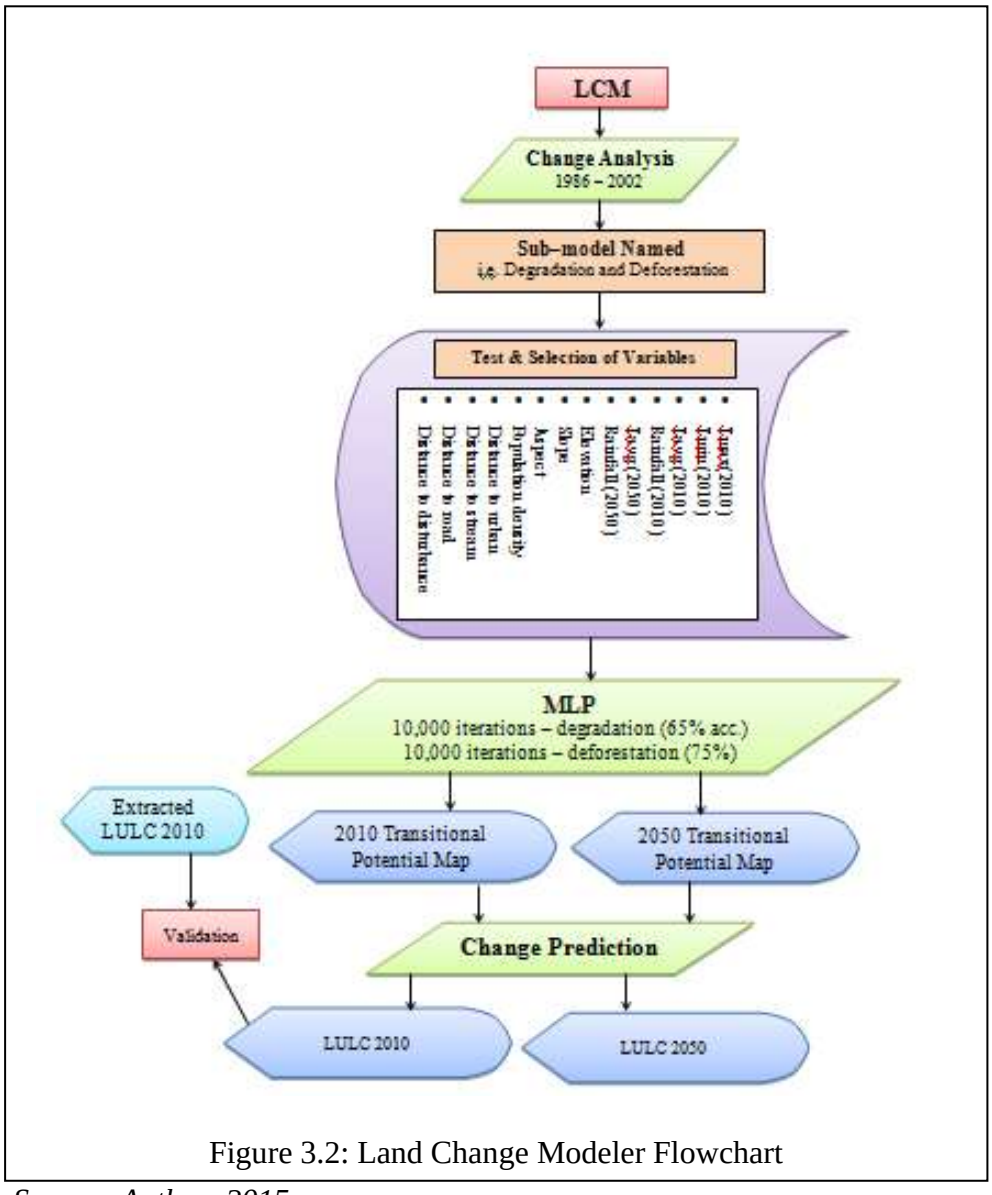

Figure 3.2: Land Change Modeler Flowchart

Source: Author, 2015

The next step taken was the transition potential modeling where transition potential maps (i.e. suitability maps) were created. In the change map produced, a large number of transitions were involved. However, the dominant transitions were used and grouped into sub model named either as forest degradation or deforestation according to the direction of LULC change. Thus, there were eight land transitions named as forest degradation and deforestation in each of the sub models. The forest degradation and deforestation sub models were modeled using Multi-Layer Perceptron (MLP) to generate about 18 transition potential maps or images. Change prediction is the final step of the land change prediction in LCM. Here, the Markov transition probabilities generated from step 2 were viewed and edited where necessary. Finally, the specific years (2010 & 2050) of interest were specified to create both the soft and hard predicted maps. However, for the interaction during the future climate, the present climatic parameters were replaced with future climatic parameters (i.e. Rainfall (2005). In conclusion, the steps involved in the prediction of LULC are summarized below:

Stage 1: Change analysis

- Change analysis was performed between LULC maps for 2002 and 1986 to determine the nature, magnitude and direction of transition between the LULC classes within the period.

Stage 2: Transition potentials modelling

- Sub-model named – this was done to indicate the direction of transition either as forest degradation or deforestation;
- Test and selection of variables – the variables as indicated in Fig.3.2 were tested and selected based on their level of association and importance by considering their Cramer's V (i.e. a measure of association between the variables and sub-model named that ranges from 0 – 1). Variables are selected based on the decision rule that states values greater than 0.15 are suitable and most suitable at 0.4, while variables with

values less than 0.15 rejected and considered not suitable. The Cramer's V values for the variables used for this work are presented in Table 3.6. All variables were suitable, but aspect and distance to stream rejected due to their low Cramer's V values;

- Multi-layer Perceptron (MLP) – MLP is a dynamic process used to run the sub-model named deforestation and forest degradation at 10,000 iterations each). It is used to predict the potential for transition based on the values at any location for the variables. The process will first of all create a random sample of cells that are experienced for each of eight transitions we are modelling and an additional set of random samples for each of the cases of pixels that could have, but did not go through the transition;
- Transition potential maps were generated after the iterations;
- Note – the same process was repeated for 2050. All variables were considered as static expect the climatic data of present climate that were interchanged with the future climate data.

Table 3.6: Cramers' V values for the variables

S/n	Explanatory Variables (Drivers)	Cramers' V Values
1	Distance to disturbance	0.1895
2	Evidence likelihood	0.337
3	Elevation (Elev31)	0.0992
4	Rainfall (Rain31)	0.2622
5	Temperature (Temp31)	0.2229
6	Population (Pop31)	0.1816
7	NDVI (NDVI31)	0.4066
8	Distance to Stream	0.0547
9	Distance to urban centres	0.1147
10	Distance to Road	0.144
11	Slope (Slope31)	0.0553
12	Aspect (Aspect31)	0.0316
13	Ravg50 (Future Rainfall)	0.2785
14	Tavg50 (Future Temperature)	0.265

Source: Author, 2015

Stage 3: Change prediction

- Transition Markov probabilities were generated based on the transition potential maps
- Year of prediction was specified (i.e. 2010 and 2050)

(i) Model Validation

The model was validated using the real LULC map for 2010 generated from Landsat 7 ETM+ and predicted 2010 LULC map. The Kappa index (Kno) was calculated using *validate algorithm* in Idrisi software to compare and check for level of agreement in terms of quantity that was good between the LULC classes in real and predicted maps.

3.3.4 Estimation of carbon stock

The implication of the interaction was assessed in order to determine the amount of Greenhouse Gases (GHGs) especially, carbon dioxide (CO_2) that would be emitted by 2050, considering the present rate of deforestation and degradation within the study area. The study adopts the BioCarbon Fund (BioCF) methodology of the World Bank (https://unfccc.int/files/methods/redd/submissions/application/pdf/redd_20090425_biocarbon_fund.pdf) for estimating reductions of GHG emissions for mosaic deforestation, the Reductions of Emissions from Deforestation and forest Degradation (REDD) method implemented in the Land Change Modeler (LCM) of Idrisi Selva software.

The method adopted assumes that deforestation and forest degradation are major impacts of the LULC change within the future climate. Therefore, LULC maps of 2002 and 2010 were reclassified into four classes as presented in Table 3.7. This is to allow the researcher to determine emissions due to deforestation and forest degradation. All other LULC classes were lumped together to form a class (non-forest). These basemaps for 1986 and 2010 were fed into the land change modeler (LCM) and transition potentials were generated for the

transition between the forests and non- forest classes used for the drivers of LULCC within the study area. The suitability, relevance and selection of the drivers were done using the SimWeight model approach. It, thus, allows, the generation of a transition potential image. Thereafter, a prediction panel or tab was run to predict the LULC 2050 at about five stages and to generate the statistics of GHG concentration that will be emitted during the period. Other parameters, using estimating the concentration of GHGs emitted, are presented in the tables 3.8 to 3.10. Table 3.8 presents the assumed quantities of carbon dioxide within a hectare of forest and non forest areas both below and above the ground. Therefore, the sum of below and above the ground quantities of carbon dioxide per hectare, multiplied by hectares of forest area lost or gain and non forest area gain or lost due to degradation and deforestation activities, determines the quantity of carbon dioxide emitted or absorbed. Meanwhile, Tables 3.9 and 3.10 present the parameters that were included or excluded in the quantification.

Table 3.7: LULC classification scheme for assessment of implication

ID	Old LULC Classes	New Classes (2010 and 2050)
1	Waterbody	Waterbody
2	Forest	Forest
3	Urban, Woodland, Grassland, Farmland, Fire Scar and Degraded Surfaces	Non Forest
4	Cloud cover and No data	No Data

Sources: Modified from table 3.3 (Campbell & Wynne, 2011, Author 2015)

Table 3.8: Carbon density per LULC classes

LULC Classes	Above-Ground	Below-Ground	Dead wood	Harvested wood products	Litter	Soil organic carbon
Forest	458.75	102.32	0.00	0.00	0.00	0.00
Non-forest	37.03	9.96	0.00	0.00	0.00	0.00

Average Carbon Density +-95% CI (tCO2e ha-1) (Source: Modified from Eastman, 2012)

Table 3.9: Carbon pools included or excluded in the study

Carbon Pool	Include/Exclude	Justification/Explanation of Choice
Above-ground	Included	Estimated from Tree canopies using RS data
Below-ground	Included	Estimated from Tree canopies using RS data
Dead wood	Excluded	Data not Available
Harvested wood products	Excluded	Data not Available
Litter	Excluded	Data not Available
Biomass Burning	Included	Fire Scar and bush burning during land preparation
Soil organic carbon	Excluded	Data not Available

(Source: Modified from Eastman, 2012)

Table 3.10: Sources and GHG included or excluded in the study

Sources	Gas	Include/Exclude	Justification/Explanation of Choice
Biomass Burning	CO2	Included	Counted as Carbon Stock Change
Biomass Burning	CH4	Included	Counted as GHGs stock Change
Biomass Burning	N2O	Included	Counted as GHGs stock Change

(Source: Modified from Eastman, 2012)

3.4 Data Limitations

The quality of the result of the interpretation and analysis of Landsat 7 ETM+ of 2010 was affected by SLC off error and acquisition date. The imagery and result were not used for further analysis other than the validation and calibration of the model. Also, the gaps identified in the climatic data were filled by using the regression equation station against a close station without gaps and positive correlation. Hence, the result of the filling did not affect the quality of analysis.

CHAPTER FOUR

ASSESSMENT OF LANDUSE/LANDCOVER CHANGE

4.1 Introduction

This chapter presents the result of the assessment of the dynamic nature of Landuse/Landcover (LULC) within the study area between 1972 and 2010. The chapter is divided into three sections. Section one presents the result of the inventory of the LULC for the static (base) years 1972, 1986, 2002 and 2010. Section two presents the multi-temporal analysis of the LULC between 1972 and 1986, 1986 and 2002, 2002 and 2010, and finally, 1972 and 2010; while section three discusses the nature, magnitude, direction and location of change within the study area as revealed from the contingency matrix of change analysis.

4.2 The Static Landuse/Landcover Characteristics

The static characteristics of the landuse/landcover generated from satellite imageries for the years 1972, 1986, 20002 and 2010 for the study area of about 37,751.91km^2 are shown respectively in figures. 4.1 to 4.4. The statistics are provided in Tables 4.1 to 4.4.

4.2.1 The Landuse/landcover (LULC) in 1972

The study revealed that in 1972, there were seven classes of LULC classes within the study area. Farmland covered an area of 293.86km^2, which represents about 0.8% of the total land resources of 37,751.91km^2. Degraded surfaces and forest covered an area of 5,430.48km^2 and 21,021.99km^2 respectively, which accounts for about 14.4% and 55.7% of the area; while grassland and urban areas occupied about 5,440km^2 (14.4%) and 88.07km^2 (0.2%) respectively. In addition, the waterbody and woodland occupied 10.53km^2 (which is less than 0.0%), and 1,929.73km^2 (5.1%) respectively (Figure 4.1 and Table 4.1).

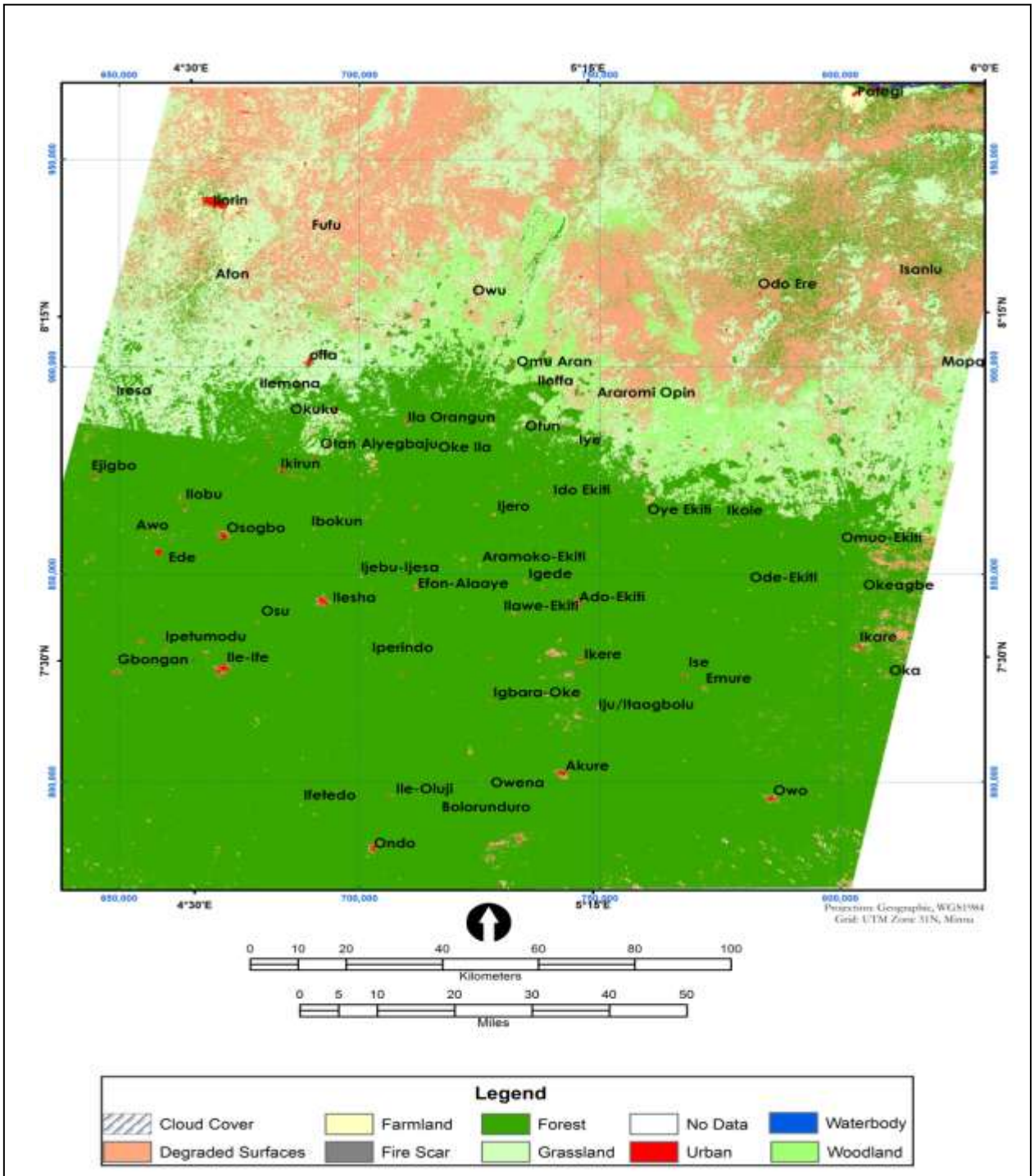

Figure 4.1: Spatial distribution of LULC patterns in 1972

Source: Author, 2015

Table 4.1: Areal extent of static characteristics of the LULC for 1972

S/n	LULC Class	Area (Km^2)	Area (Ha)	%
1	Cloud Cover	8.66	865.53	0
2	Farmland	293.86	29,386.39	0.8
3	Degraded Surface	5,430.48	543,047.85	14.4
4	Fire Scar	0	0	0
5	Forest	21,021.99	2,102,198.85	55.7
6	Grassland	5,440.10	544,009.96	14.4
7	Area without Data	3,528.50	352,849.68	9.3
8	Urban	88.07	8,806.90	0.2
9	Waterbody	10.53	1,052.92	0
10	Woodland	1,929.73	192,973.38	5.1
Total (1972)		**37,751.91**	**3,775,191.46**	**100.0**

Source: Author, 2015

4.2.2 The Landuse/landcover (LULC) in 1986

In 1986, LULC classes increased to eight with an addition of fire scar. Table 4.2 illustrated the statistics of the area occupied by the individual LULC classes, while figure 4.2 shows the spatial distribution patterns of the LULC, forest, farmland, grassland and woodland, which covered about 15,984.09km^2 (42.3%), 7,419.34km^2 (19.7%), 5,861.25km^2 (15.5%) and 3,459.83km^2 (9.2%) respectively.

Table 4.2: Areal extent of static characteristics of the LULC for 1986

S/n	LULC Class	Area (Km^2)	Area (Ha)	%
1	Cloud cover	0.09	8.93	0.0
2	Farmland	7,419.34	741,933.84	19.7
3	Degraded Surfaces	345.07	34,506.82	0.9
4	Fire Scar	976.05	97,605.24	2.6
5	Forest	15,984.09	1,598,408.82	42.3
6	Grassland	5,861.25	586,125.29	15.5
7	Area without data	3,444.08	344,408.38	9.1
8	Urban	229.12	22,912.03	0.6
9	Waterbody	32.99	3,298.63	0.1
10	Woodland	3,459.83	345,983.49	9.2
Total (1986)		**37,751.91**	**3,775,191.47**	100.0

Source: Author, 2015

In addition, the remaining 13.3% of the area was covered by degraded surfaces, fire scar, urban, waterbody and area without data in the following proportions 345km^2 (0.9%),

976.05km^2 (2.6%), 229.12km^2 (0.6%), 32.97km^2 (0.1%) and 3,444.08km^2 (9.2%) respectively.

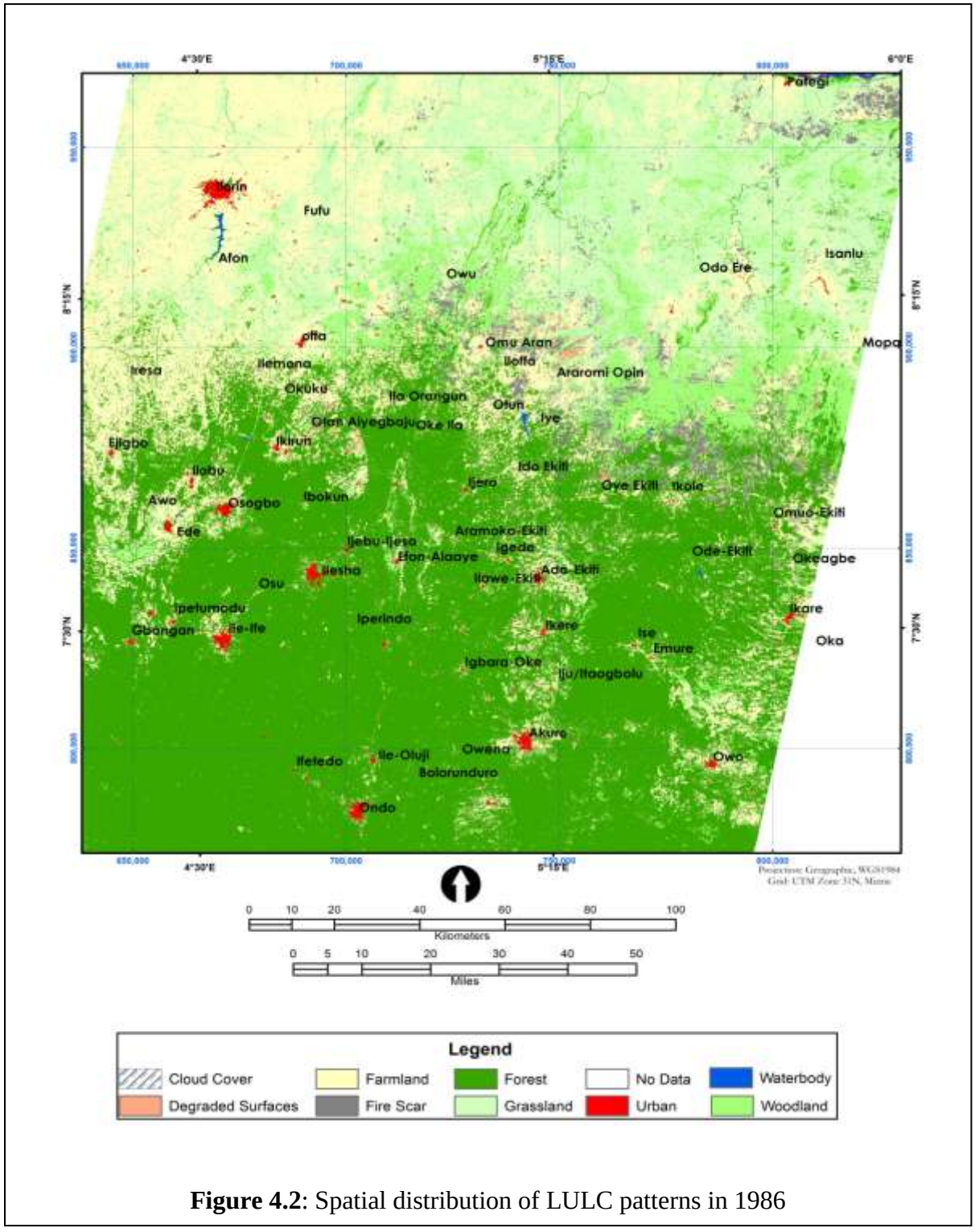

Figure 4.2: Spatial distribution of LULC patterns in 1986

Source: Author, 2015

4.2.3 The Landuse/Landcover (LULC) in 2002

The static characteristics of LULC in 2002 are shown in figure 4.3 and presented statistically in Table 4.3. The statistics reveal that the study area was covered with 16,959.53km^2 (44.9%) of forest, 5,559.40km^2 (14.7%) of woodland, 5,437.46km^2 (14.4%) of grassland and 3,828.59km^2 (10.1%). During the same year, the table also shows that waterbody, urban, degraded surfaces and fire scar occupied 77.02km^2, 1,087.38km^2, 1479.06km^2 and 539.82km^2 respectively, which constitute 0.2%, 2.9%, 3.9% and 1.4% of the study area. In addition, 2,783.65km^2 (7.4%) comprised area without data or satellite imagery coverage and zero cloud cover was recorded in 2002.

Table 4.3: Areal extent of static characteristics of the LULC for 2002

S/n	LULC Class	Area (Km^2)	Area (Ha)	%
1	Cloud cover	0.00	0.00	0.0
2	Farmland	3,828.59	382,859.15	10.1
3	Degraded Surfaces	1,479.06	147,905.77	3.9
4	Fire Scar	539.82	53,981.97	1.4
5	Forest	16,959.53	1,695,952.74	44.9
6	Grassland	5,437.46	543,745.90	14.4
7	Area without data	2,783.65	278,365.47	7.4
8	Urban	1,087.38	108,737.94	2.9
9	Waterbody	77.02	7,702.24	0.2
10	Woodland	5,559.40	555,940.29	14.7
	Total (2002)	**37,751.91**	**3,775,191.47**	100.0

Source: Author, 2015

4.2.4 The Landuse/landcover (LULC) in 2010

Farmland and grassland occupied 32.4% (12,223km^2) and 27.8% (138,656km^2) of the study area respectively. Also, forest, degraded surfaces and urban covered 17.8% (6,716km^2), 4.35% (1,643 km^2) and 2.5% (942km^2) of the study area respectively as illustrated in Table 4.4 and figure 4.4.

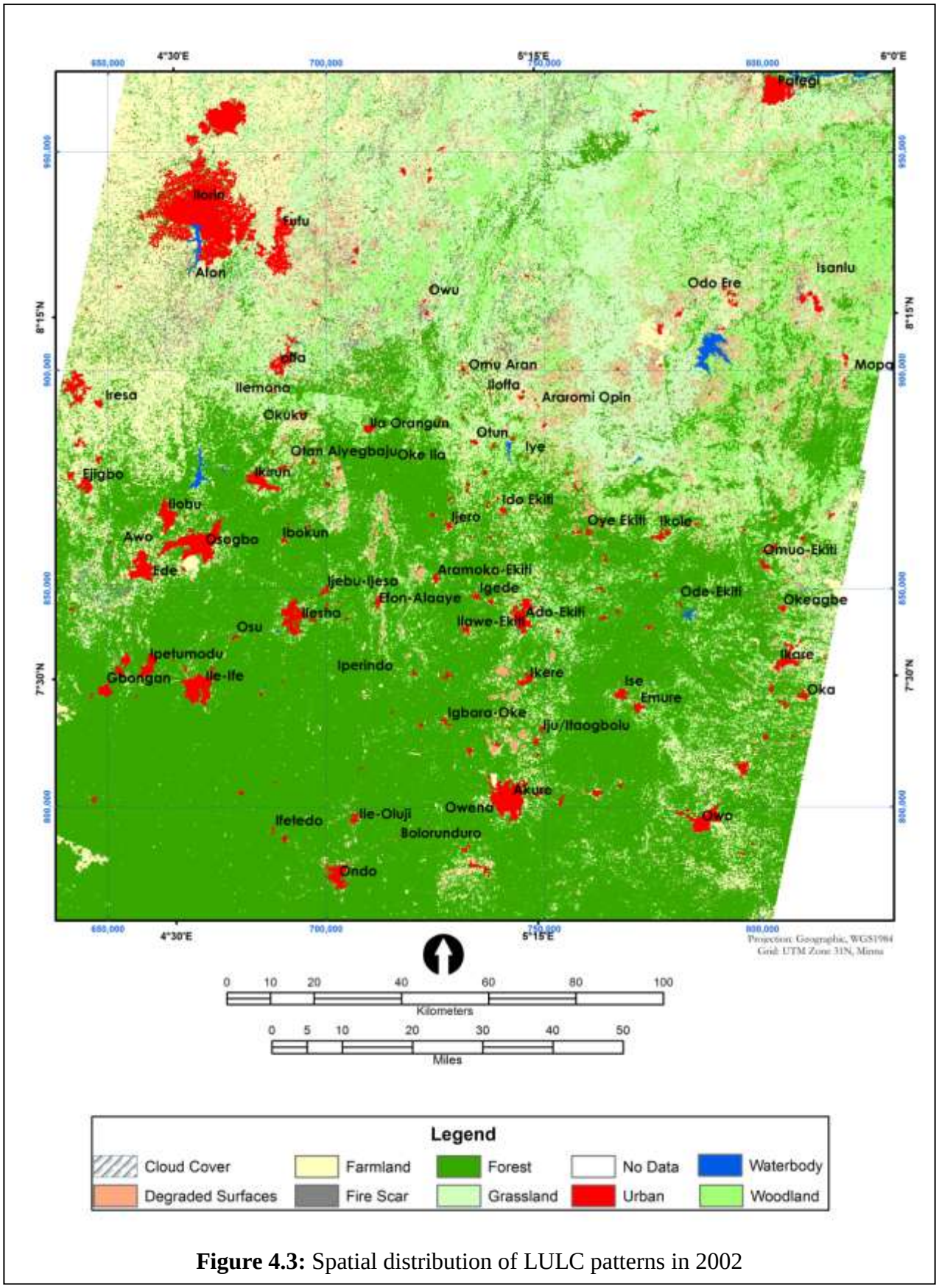

Figure 4.3: Spatial distribution of LULC patterns in 2002

Source: Author, 2015

Table 4.4: Areal extent of static characteristics of the LULC for 2010

S/n	LULC Class	Area (Km^2)	Area (Ha)	%
1	Cloud cover	0.03	2.68	0.00
2	Farmland	12,223.37	1,222,336.51	32.38
3	Degraded Surfaces	1,643.66	164,365.69	4.35
4	Fire Scar	26.49	2,648.75	0.07
5	Forest	6,716.87	671,687.38	17.79
6	Grassland	10,504.49	1,050,448.97	27.83
7	Area without data	1,386.56	138,655.62	3.67
8	Urban	942.13	94,213.12	2.50
9	Waterbody	88.13	8,813.32	0.23
10	Woodland	4,220.19	422,019.43	11.18
	Total (2010)	**37,751.91**	**3,775,191.47**	100.0

Source: Author, 2015

4.3 Temporal Characteristics of the Landuse/Landcover

The magnitude and nature of change in the static and temporal characteristics of landuse/ landcover within the study area are presented in Table 4.5. The study revealed that urban area and waterbody gained about 1,135% and 635% of net change in 2002 and increased from 8.8km^2 and 10.53km^2 in 1972 to 1,087.37km^2 and 77.02km^2 in 2002. Also, the woodland and farmland gained 188% and 1,202% between 1972 and 2002, from 1,929.73km^2 to 5,559.40km^2 and 293.86km^2 to 3,828.59km^2 respectively. However, farmland decreased from 7,419.34km^2 to 3,828.59km^2 between 1986 and 2002 by losing about 48.4% of its total area coverage, while the woodland gained 79.29% between 1972 and 1986 and had its gain decreased to 60.68% between 1986 and 2002.

However, the study revealed that forest lost 19.32% by reducing its holding from 21, 022km^2 to 16,960km^2 between 1972 and 2002. In similar trend, grassland lost 7.23% between 1986 and 2002 by reducing from 5,861.25km^2 to 5,437.46km^2 which was almost equivalent to the area extent (i.e. 421.15km^2) gained between 1972 and 1986, which represented 7.74%.

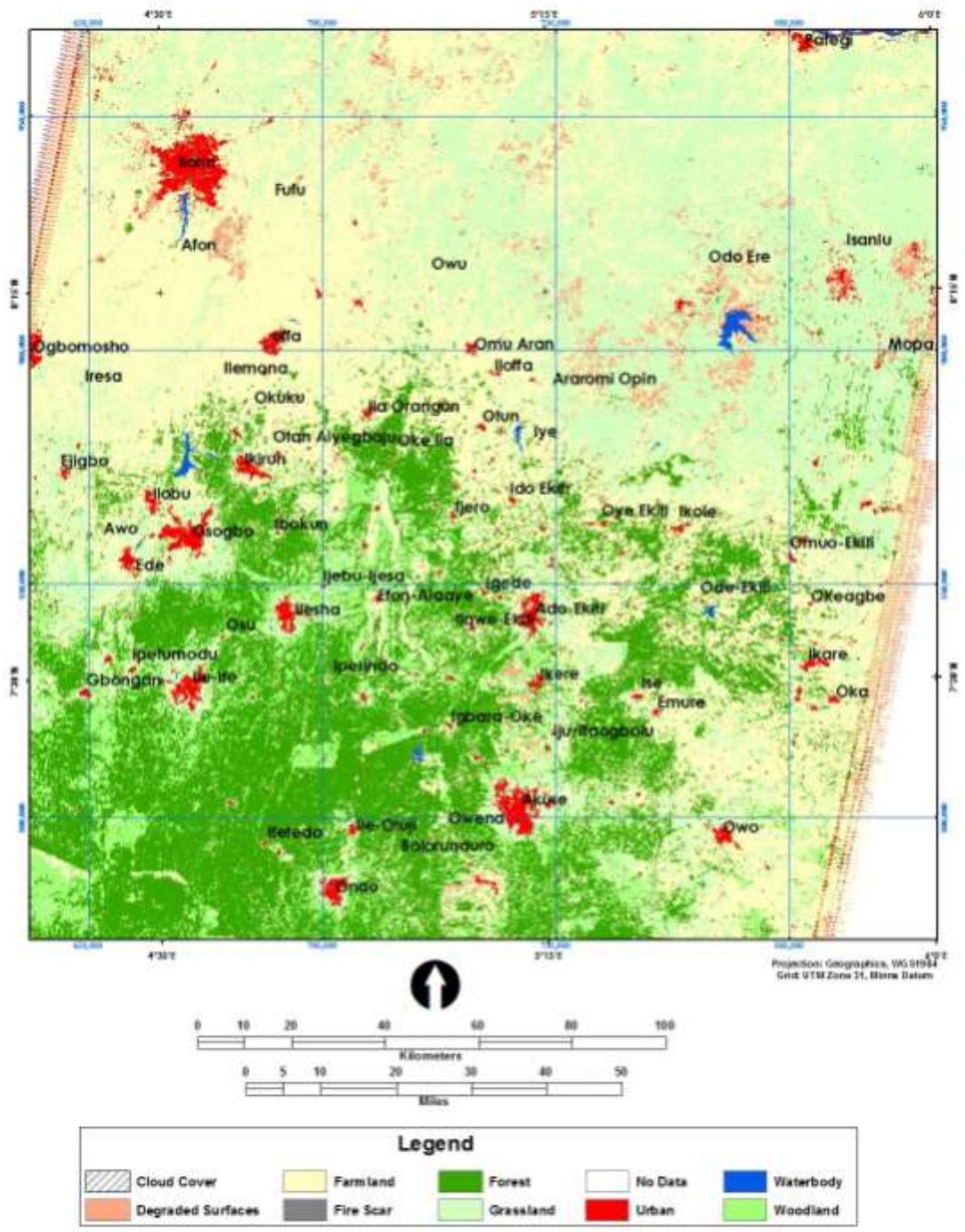

Figure 4.4: Spatial distribution of LULC patterns in 2010

Source: Author, 2015

Table 4.5: Net change in the landuse/landcover (1972 – 2002)

S/n	LULC Class	LULC 1972 (ha)	LULC 1986 (ha)	LULC 2002 (ha)	1972 - 1986 (ha)	%	1986 - 2002 (ha)	%	1972 - 2002 (ha)	%
1	Cloud Cover	865.5	8.9	0.0	-856.6	-99	-8.9	-100	-865.5	-100
2	Farmland	29,386.4	741,933.8	382,859.2	712,547.5	2,425	-359,074.7	-48	353,472.8	1,203
3	Degraded Surface	543,047.9	34,506.8	147,905.8	-508,541.0	-94	113,399.0	329	-395,142.1	-73
4	Fire Scar	0.0	97,605.2	53,982.0	97,605.2	100	-43,623.3	-45	53,982.0	100
5	Forest	2,102,198.9	1,598,408.8	1,695,952.7	-503,790.0	-24	97,543.9	6	-406,246.1	-19
6	Grassland	544,010.0	586,125.3	543,745.9	42,115.3	8	-42,379.4	-7	-264.1	0
7	Area without Data	352,849.7	344,408.4	278,365.5	-8,441.3	-2	-66,042.9	-19	-74,484.2	-21
8	Urban	8,806.9	22,912.0	108,737.9	14,105.1	160	85,825.9	375	99,931.0	1,135
9	Waterbody	1,052.9	3,298.6	7,702.2	2,245.7	213	4,403.6	133	6,649.3	632
10	Woodland	192,973.4	345,983.5	555,940.3	153,010.1	79	209,956.8	61	362,966.9	188

Source: Author, 2015

However, all together, grassland lost about 0.05% between 1972 and 2002. Furthermore, incidences of bush burning were recorded within the study area due to bad method of farming and gaming, between 1986 and 2002.

4.4 The Landuse/Landcover Change Matrix

Tables 4.6, 4.7 and 4.8 present the contingency matrices of LULC change for the periods 1972 - 1986, 1986-2002 and 1972-2002. On the matrix tables, the figures in the rows indicate the loss to the row headers from other LULC categories, while the figures in the columns indicate the gain by the column header resulting from competition with other LULC categories. The diagonal figures indicate the unchanged areas or the static LULC. The figures in the columns LULC 1972 and 1986 indicate the total areal extent for each of the LULC classes in the rows for years 1972 and 1986 respectively. Also, the rows LULC 1986 and 2002 figures reveal the total area coverage of each of the LULC classes for these years in columns. While, the gain rows and loss columns indicate the percentage gain and lost by the individual LULC classes. In addition, other figures within the rows and columns show the direction and magnitude of transition from one class to another.

Table 4.6: Net change in the landuse/landcover in ha, 1972 – 1986

LULC Class	Cloud cover	Degraded Surface	Farmland	Fire Scar	Forest	Grassland	Area without Data	Urban	Waterbody	Woodland	LULC1972 (ha)	Loss (1972)	%(Loss)	Rate
Cloud Cover	0.0	0.2	52.1	0.2	630.1	5.8	149.2	1.8		26.2	**865.5**	865.5	100.0	
Degraded Surfaces	0.2	13,661.7	173,398.4	29,950.1	23,453.2	232,176.0	17,852.4	4,464.0	430.6	47,661.3	**543,047.9**	529,386.1	97.5	7.0
Farmland	0.1	921.7	23,278.8	112.2	661.3	2,544.5	36.6	1,666.4	64.3	100.6	**29,386.4**	6,107.6	20.8	1.5
Fire Scar	0.0	0.0	0.0	0.0	0.0	0.0	0.0		0.0	0.0	**0.0**	0.0	0.0	0.0
Forest	8.4	5,471.3	294,445.8	24,199.9	1,493,127.5	122,220.2	55,736.4	10,431.6	1,019.0	95,538.6	**2,102,198.8**	609,071.3	29.0	2.1
Grassland	0.3	6,933.9	169,879.2	15,629.8	53,122.9	161,451.3	11,512.3	1,462.9	581.1	123,436.3	**544,010.0**	382,558.6	70.3	5.0
Area without Data	0.0	3,379.7	56,605.1	968.0	13,695.5	23,484.6	249,419.9	438.0	99.7	4,759.2	**352,849.7**	103,429.8	29.3	2.1
Urban	0.0	273.8	3,100.1	184.1	250.5	388.3	46.9	4,276.8	262.2	24.2	**8,806.9**	4,530.1	51.4	3.7
Waterbody	0.0	30.0	24.4	2.8	31.8	8.9		136.7	815.6	2.7	**1,052.9**	237.3	22.5	1.6
Woodland	0.0	3,834.6	21,149.9	26,558.1	13,435.9	43,845.7	9,654.9	33.7	26.1	74,434.4	**192,973.4**	118,539.0	61.4	4.4
LULC1986 (ha)	**8.9**	**34,506.8**	**741,933.8**	**97,605.2**	**1,598,408.8**	**586,125.3**	**344,408.4**	**22,912.0**	**3,298.6**	**345,983.5**	**3,775,191.5**	1,754,725.4		
Gain (1986)	8.9	20,845.1	718,655.0	97,605.2	105,281.3	424,673.9	94,988.5	18,635.2	2,483.0	271,549.1	1,754,725.4			
%(Gain)	100.0	60.4	96.9	100.0	6.6	72.5	27.6	81.3	75.3	78.5				

Source: Author, 2015

Table 4.7: Net change in the landuse/landcover in ha, 1986 – 2002

LU Class	Degraded Surface	Farmland	Fire Scar	Forest	Grassland	Area without Data	Urban	Waterbody	Woodland	**LU1986 (ha)**	Loss (1986)	%(Loss)	Rate
Cloud Clover	0.1	3.1		1.7	0.2		2.8	0.1	1.0	**8.9**	8.9	100.0	6.3
Degraded Surfaces	8,744.9	9,373.1	1,133.8	2,419.8	6,481.6	1,284.2	2,070.8	53.1	2,945.4	**34,506.8**	25,761.9	74.7	4.7
Farmland	53,335.1	212,298.8	14,561.3	147,069.2	144,452.8	18,830.0	62,521.6	652.3	88,212.8	**741,933.8**	529,635.0	71.4	4.5
Fire Scar	14,344.4	7,455.4	4,462.6	10,709.3	32,146.6	35.7	434.5	333.6	27,683.2	**97,605.2**	93,142.7	95.4	6.0
Forest	11,157.2	61,159.9	3,716.4	1,341,169.4	30,822.3	1,716.8	16,832.1	1,611.7	130,222.9	**1,598,408.8**	257,239.4	16.1	1.0
Grassland	42,909.5	61,670.1	20,962.2	52,917.0	232,761.2	8,512.6	7,301.7	1,666.9	157,424.0	**586,125.3**	353,364.1	60.3	3.8
Area without Data	3,866.0	10,532.0	1,601.8	43,140.6	8,967.8	246,144.5	644.9	0.0	29,510.7	**344,408.4**	98,263.9	28.5	1.8
Urban	236.6	2,568.3	61.7	1,847.5	397.7	269.7	17,057.7	214.0	258.9	**22,912.0**	5,854.4	25.6	1.6
Waterbody	67.7	143.3	93.0	454.7	60.8	3.2	22.0	2,356.5	97.4	**3,298.6**	942.1	28.6	1.8
Woodland	13,244.2	17,655.1	7,389.1	96,223.6	87,654.9	1,568.7	1,849.8	814.0	119,584.0	**345,983.5**	226,399.5	65.4	4.1
LU 2002 (ha)	**147,905.8**	**382,859.2**	**53,982.0**	**1,695,952.7**	**543,745.9**	**278,365.5**	**108,737.9**	**7,702.2**	**555,940.3**	**3,775,191.5**			
Gain 2002 (ha)	139,160.8	170,560.3	49,519.4	354,783.3	310,984.7	32,221.0	91,680.3	5,345.7	436,356.3				
% (Gain)	94.1	44.5	91.7	20.9	57.2	11.6	84.3	69.4	78.5				

Source: Author, 2015

Table 4.8: Net change in the landuse/landcover in ha, 1972 – 2002

LU Class	Cloud cover	Degraded Surface	Farmland	Fire Scar	Forest	Grassland	No Data	Urban	Waterbody	Woodland	**LU1972 (ha)**	Loss (1972)	%(Loss)	Rate
Cloud Cover	0.0	0.0	84.1	0.0	754.6	1.0	0.0	1.1	0.0	24.9	**865.5**	865.5	100.0	3.3
Degraded Surfaces	0.0	60,372.6	82,202.1	20,479.5	42,732.5	196,465.0	0.0	22,188.6	1,936.5	116,671.1	**543,047.9**	482,675.3	88.9	3.0
Farmland	0.0	1,493.6	11,829.7	484.3	1,434.8	3,032.4	0.0	10,667.6	90.3	353.7	**29,386.4**	17,556.7	59.7	2.0
Fire Scar	0.0	0.0	0.0	0.0	0.0	0.0	0.0	0.0	0.0	0.0	**0.0**	0.0	0.0	0.0
Forest	0.0	37,005.9	149,085.9	11,884.4	1,517,136.1	98,887.1	0.0	49,380.5	3,412.7	235,406.2	**2,102,198.8**	585,062.7	27.8	0.9
Grassland	0.0	30,734.8	94,598.4	12,265.3	89,390.4	159,427.0	0.0	18,844.4	1,007.8	137,741.8	**544,010.0**	384,583.0	70.7	2.4
No Data	0.0	2,960.4	33,682.2	943.3	17,485.7	10,942.8	278,365.5	2,002.0	114.6	6,353.1	**352,849.7**	74,484.2	21.1	0.7
Urban	0.0	457.3	1,492.1	126.8	559.9	699.0	0.0	4,971.4	315.5	184.9	**8,806.9**	3,835.5	43.6	1.5
Waterbody	0.0	18.4	67.5	1.9	167.3	5.8	0.0	2.0	784.8	5.3	**1,052.9**	268.1	25.5	0.8
Woodland	0.0	14,862.8	9,817.3	7,796.5	26,291.4	74,285.9	0.0	680.3	40.0	59,199.3	**192,973.4**	133,774.1	69.3	2.3
LU2002 (ha)	**0.0**	**147,905.8**	**382,859.2**	**53,982.0**	**1,695,952.7**	**543,745.9**	**278,365.5**	**108,737.9**	**7,702.2**	**555,940.3**	**3,775,191.5**			
Gain (2002)	0.0	87533.2	371029.5	53982.0	178816.6	384318.9	0.0	103766.6	6917.4	496741.0				
%(Gain)	0.0	59.2	96.9	100.0	10.5	70.7	0.0	95.4	89.8	89.4				

Source: Author, 2015

4.4.1 Changes in the landuse/landcover, 1972 - 1986

The study revealed that degraded surfaces, urban and waterbody lost 97.48%, 51.44% and 22.54% respectively from their previous locations and area extents to other LULC classes between 1972 and 1986 as presented in table 4.6, figures 4.5 and 4.6. In addition, grassland, woodland, forest and farmland lost 70.32%, 61.43%, 28.97% and 20%, respectively to other LULC classes between 1972 and 1986. During the same period, degraded surfaces, waterbody and urban area gained more locations and area amounting to 60.41%, 75.28% and 81.33% respectively. Furthermore, there were about 6.59%, 96.86%, 72.45%, and 78.49% of forest, farmland grassland and woodland spread to other LULC classes between 1972 and 1986.

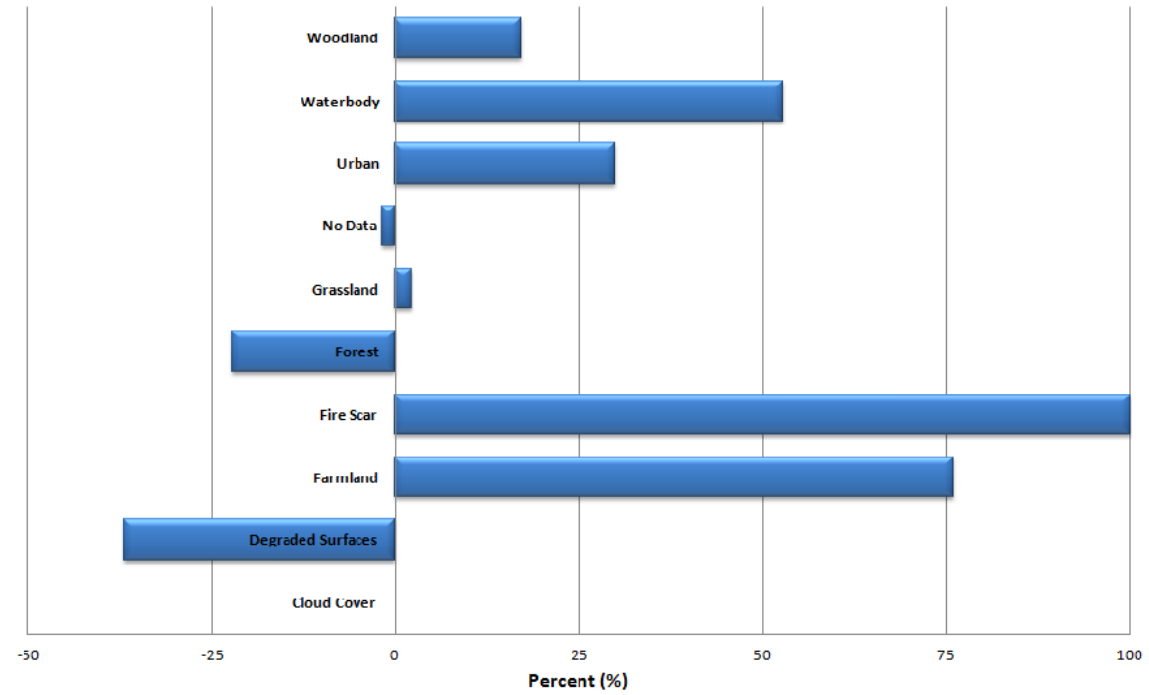

Figure 4.5: The LULC Changes, 1972 - 1986

Source: Author, 2015

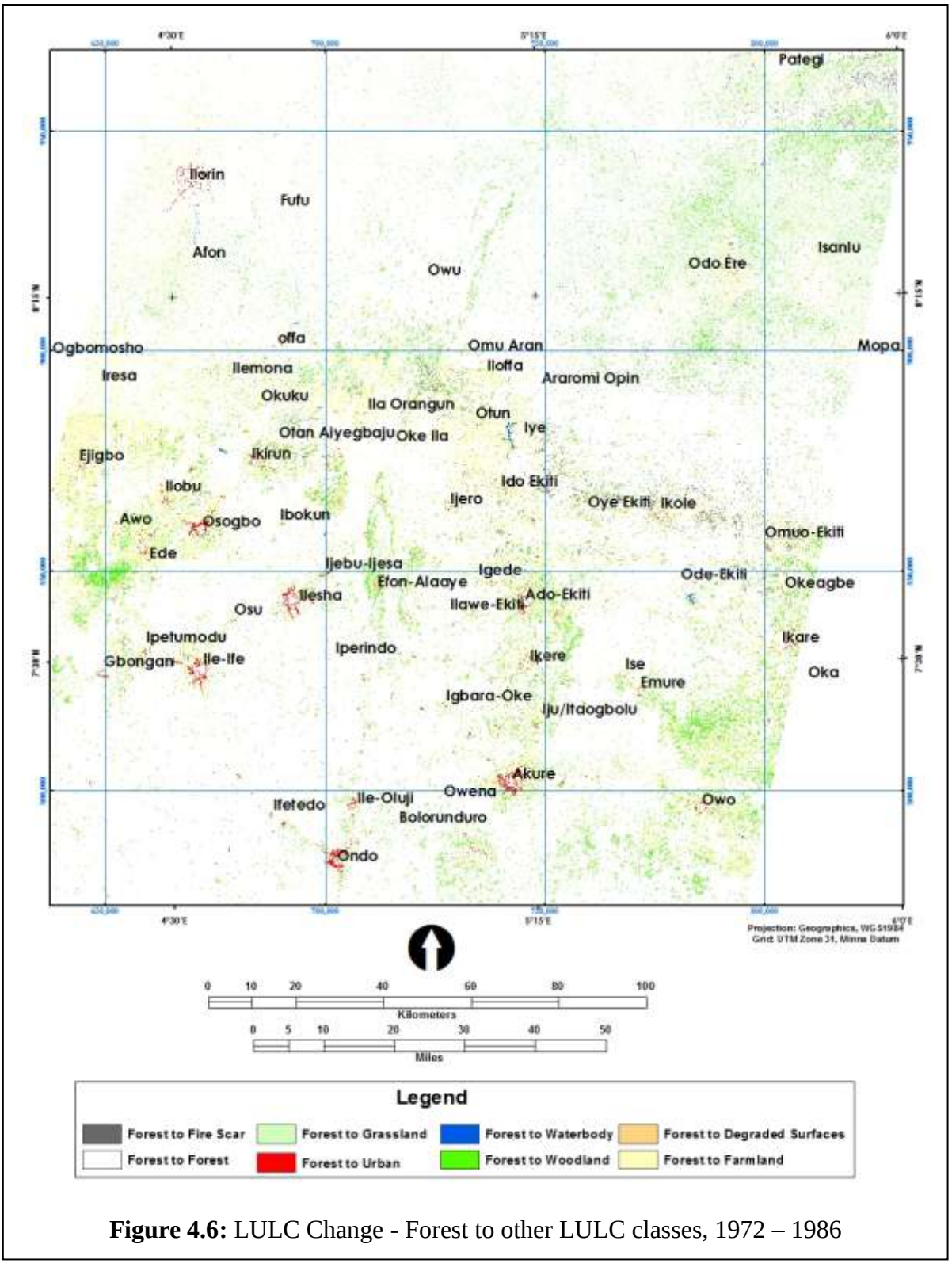

Figure 4.6: LULC Change - Forest to other LULC classes, 1972 – 1986

Source: Author, 2015

4.4.2 Changes in landuse/landcover between 1986 and 2002

The Table 4.7, figures 4.7 and 4.8 illustrated the location, direction and magnitude of change in the static characteristics of LULC during the period (i.e. 1986 – 2002). During the period between 1986 and 2002, the study revealed 74.66%, 95.43%, 16.09%, 60.29%, 65.44% and 71.39% of degraded surfaces, fire scar, forest, grassland, woodland and farmland recorded were lost to other classes respectively, while, woodland and farmland expanded more to other spatial location and LULC classes by 78.49% and 44.55%.

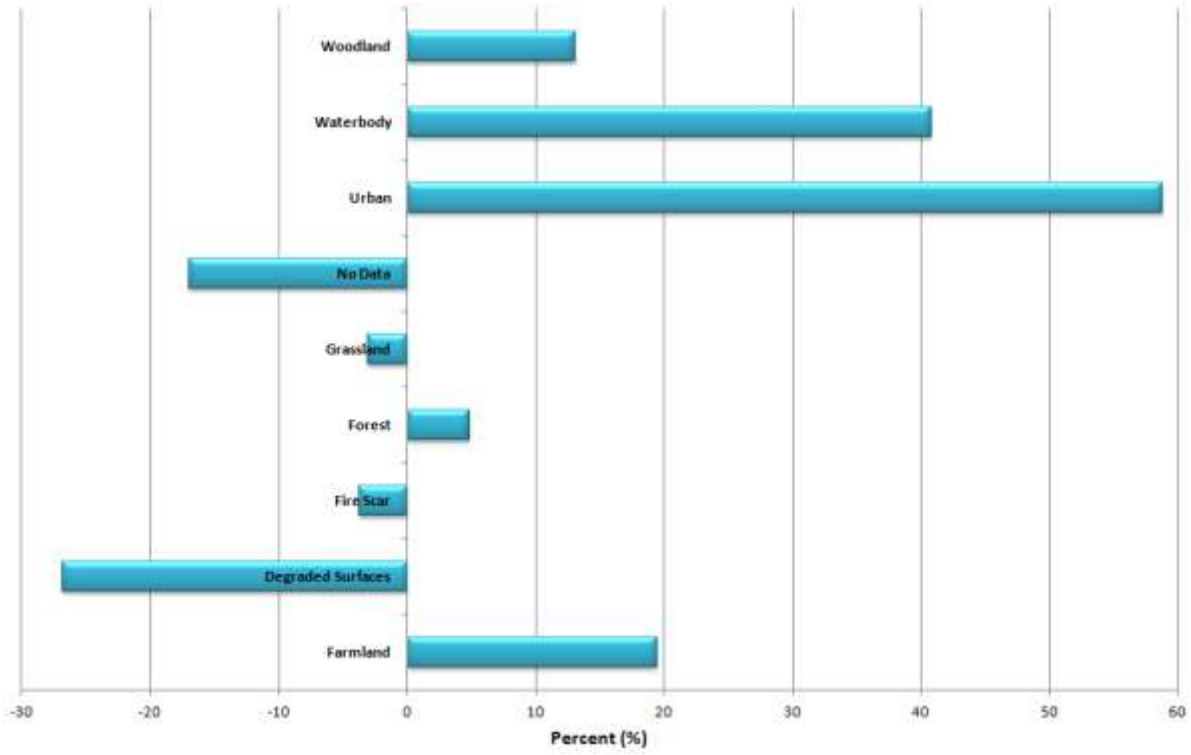

Figure 4.7: The LULC changes, 1986 - 2002

Source: Author, 2015

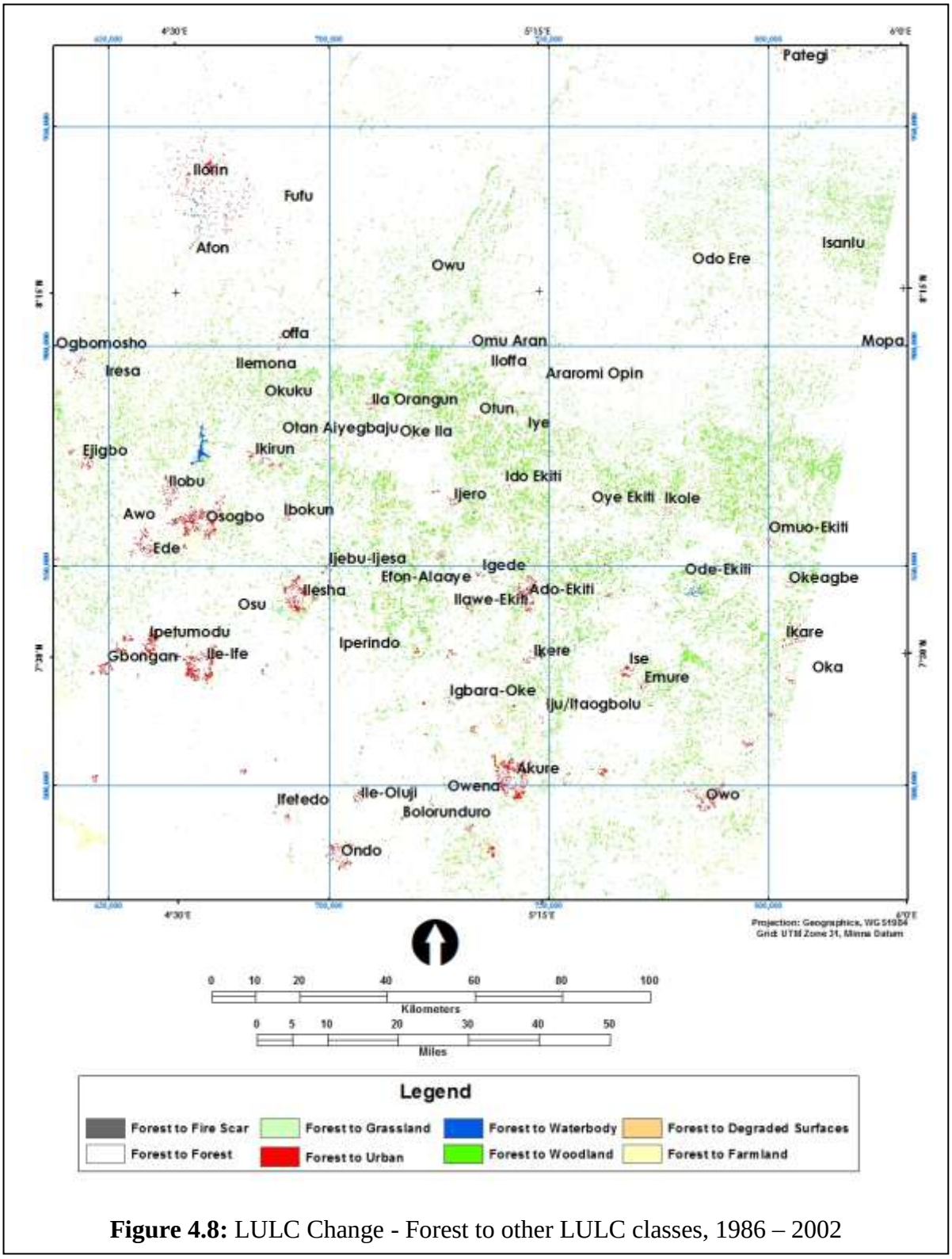

Figure 4.8: LULC Change - Forest to other LULC classes, 1986 – 2002

Source: Author, 2015

4.4.3 Changes in Landuse/landcover between 1972 and 2002

Table 4.8, figures 4.9 and 4.10 presented the statistics and overall net change in the spatio-temporal distribution LULC patterns within the study area during the period of study (i.e. 1972 and 2002). The study revealed that farmland, woodland and grassland expanded more into other LULC classes by proportions of 97.9%, 89.4% and 70.7% respectively. Also, other LULC classes like forest and degraded surface recorded marginal gains of 10.5% and 59.2% respectively.

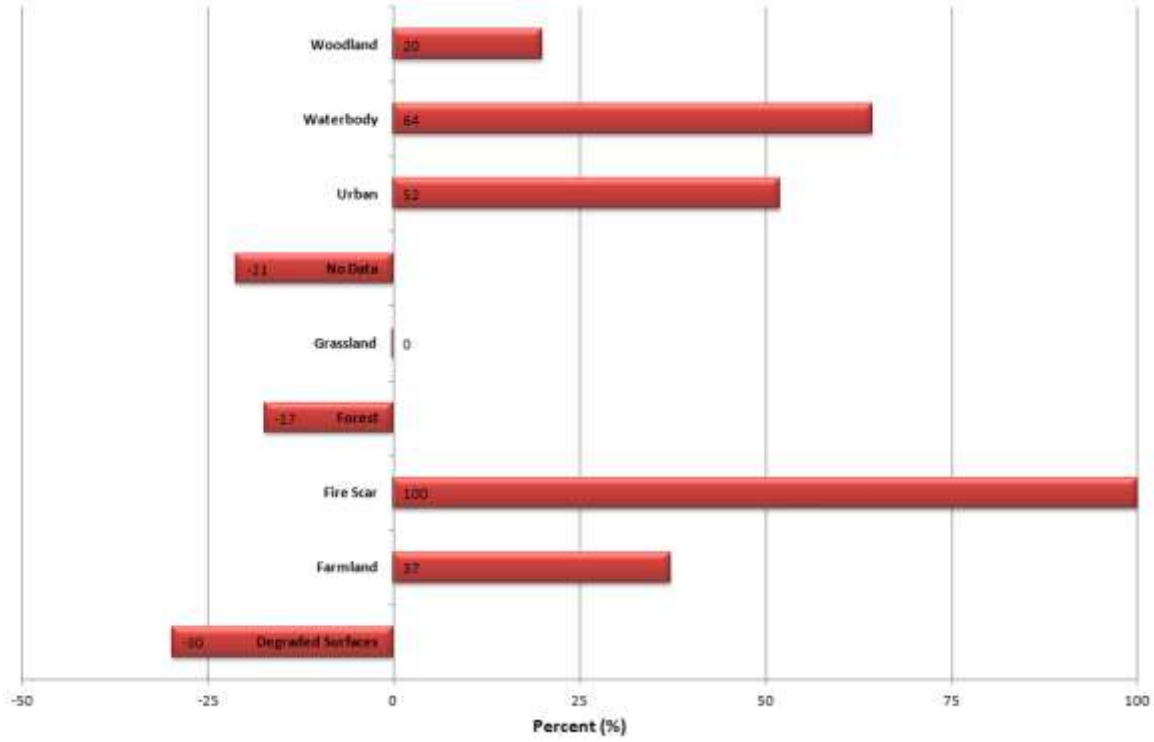

Figure 4.9: The LULC Changes, 1972 - 2002

Source: Author, 2015

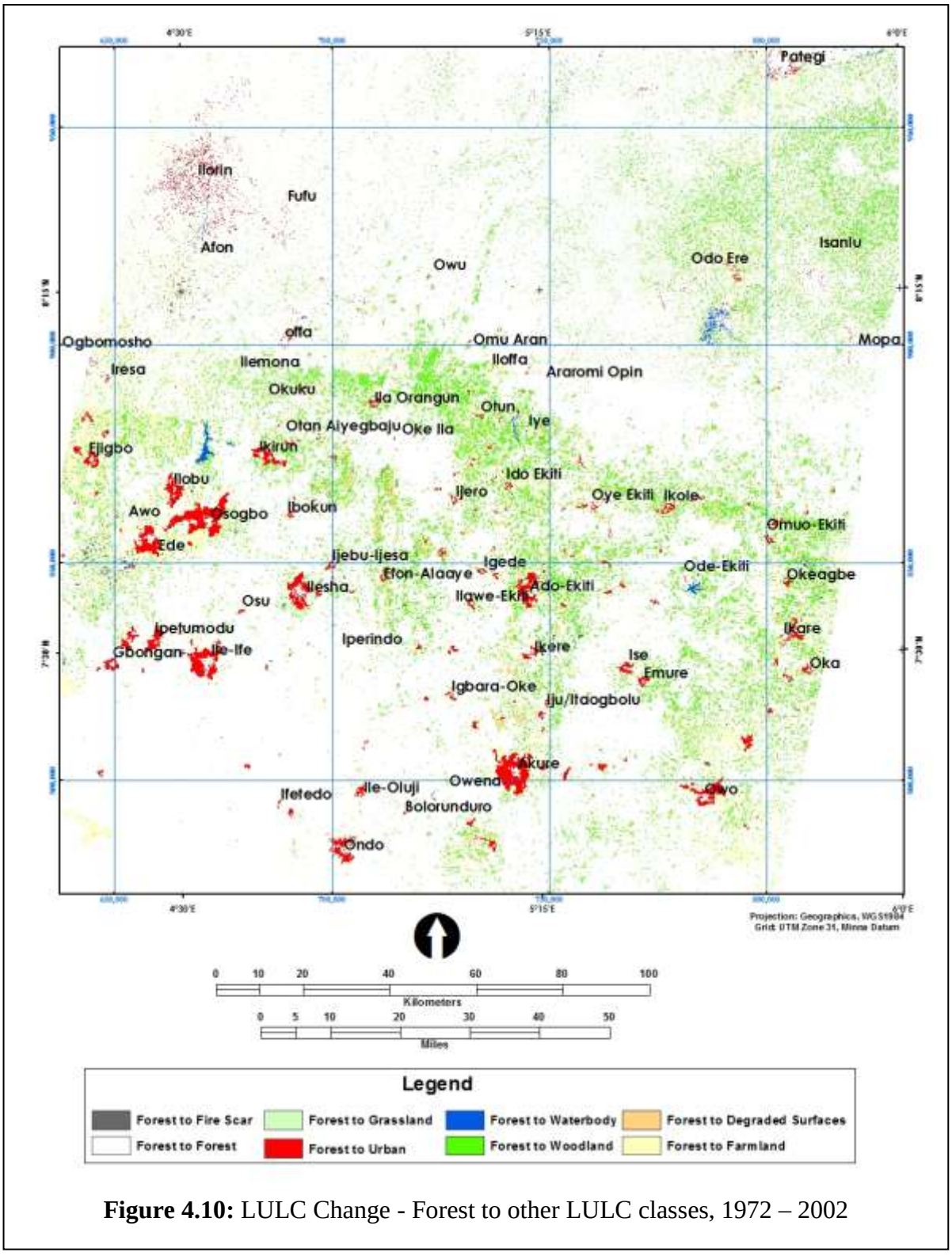

Figure 4.10: LULC Change - Forest to other LULC classes, 1972 – 2002

Source: Author, 2015

4.5 Landuse/Landcover Classification Accuracy Assessment

300 field points were randomly sampled and collated for confusion or error matrix (Table 4.10) that was employed to validate classification for the 2002 LULC data**.** The errors of omission and commission were determined before the determination of the overall accuracy of the classification exercise as presented in Table 4.9. As presented in Table 4.9, the overall LULC accuracy was 86.67%. The average omission and commission errors were 18.51% and 9.92%, respectively. Therefore, the average producer's and user's accuracies were 90% and 81%, respectively. Some of the LULC classes like waterbody and cloud cover were not difficult to detect and identify on images, while others, including degraded surface, forest, grassland, urban and woodland as shown with producer's accuracy greater than 85%. However, the highest confusion occurred between fire scar and farmland having 23% and 18% of the producer's and user's accuracies. This was due to the farmland method (bush burning) employed for farm land clearing within the study area.

Furthermore, In order to determine whether the overall accuracy of 86.67% is within the acceptable limit, the tested overall accuracy was determined and found to be within 83% and 91% for lower and upper limit for two tail test at 95% confidence interval and 0.05 significant level. Therefore, this level of accuracy for the LULC classification is acceptable and within the required limit for exploratory studies of forest degradation, deforestation and in general for environmental changes (Fasona, 2007).

Table 4.9: Confusion matrix statistics

Variables	Percent (%)
Average omission error	18.51
Average commission error	9.92
Average user accuracy	81
Average producer accuracy	90.08
Overall accuracy	86.67
Tested overall accuracy (two tail)	82.98 - 91.02

Source: Author, 2015

Table 4.10: Confusion matrix for the LULC classification accuracy

LULC	Cloud cover	Degraded Surface	Farmland	Fire scar	Forest	Grassland	Area without Data	Urban	Waterbody	Woodland	Total	Error	Omission	User's accuracy
Cloud cover	0	0	1	0	1	0	0	0	0	1	3	3	100.00	0.00
Degraded Surface	0	30	0	0	1	0	0	1	0	1	33	3	9.09	90.91
Farmland	0	0	40	2	2	1	0	1	0	1	47	7	14.89	85.11
Fire scar	0	0	0	20	1	0	0	0	0	0	21	1	4.76	95.24
Forest	0	0	5	1	55	2	0	0	0	2	65	10	15.38	84.62
Grassland	0	0	1	1	1	30	0	0	0	1	34	4	11.76	88.24
Area without Data	0	0	0	0	0	0	0	0	0	0	0	0	0.00	100.00
Urban	0	5	1	2	0	0	0	30	0	0	38	8	21.05	78.95
Waterbody	0	0	0	0	0	0	0	0	10	0	10	0	0.00	100.00
Woodland	0	1	1	0	1	1	0	0	0	45	49	4	8.16	91.84
Total	0	36	49	26	62	34	0	32	10	51	300		18.51	81.49
Error	0	6	9	6	7	4	0	2	0	6				
Commission error	0.00	16.67	18.37	23.08	11.29	11.76	0.00	6.25	0.00	11.76	9.92			
Producer's Accuracy	100.00	83.33	81.63	76.92	88.71	88.24	100.00	93.75	100.00	88.24	90.08			

Source: Author, 2015

CHAPTER FIVE

CLIMATIC VARIABILITY AND CHANGE

5.1 Rainfall Characteristics and Trend

The rainfall characteristics and trends for the Derived Savannah during the present climate (1940 - 2010) and future climate (2011 – 2050) are presented in figures 5.1, 5.2, 5.3, 5.4 and 5.5 respectively. The figure 5.1 shows that the mean annual rainfall increases at the rate of 1.20mm annually with a long term mean of 1,316mm for the present climate; while figure 5.2 reveals that the future climate (2011 – 2050) has a long term mean of 1,393mm and will be increasing annually at a rate of 3.13mm.

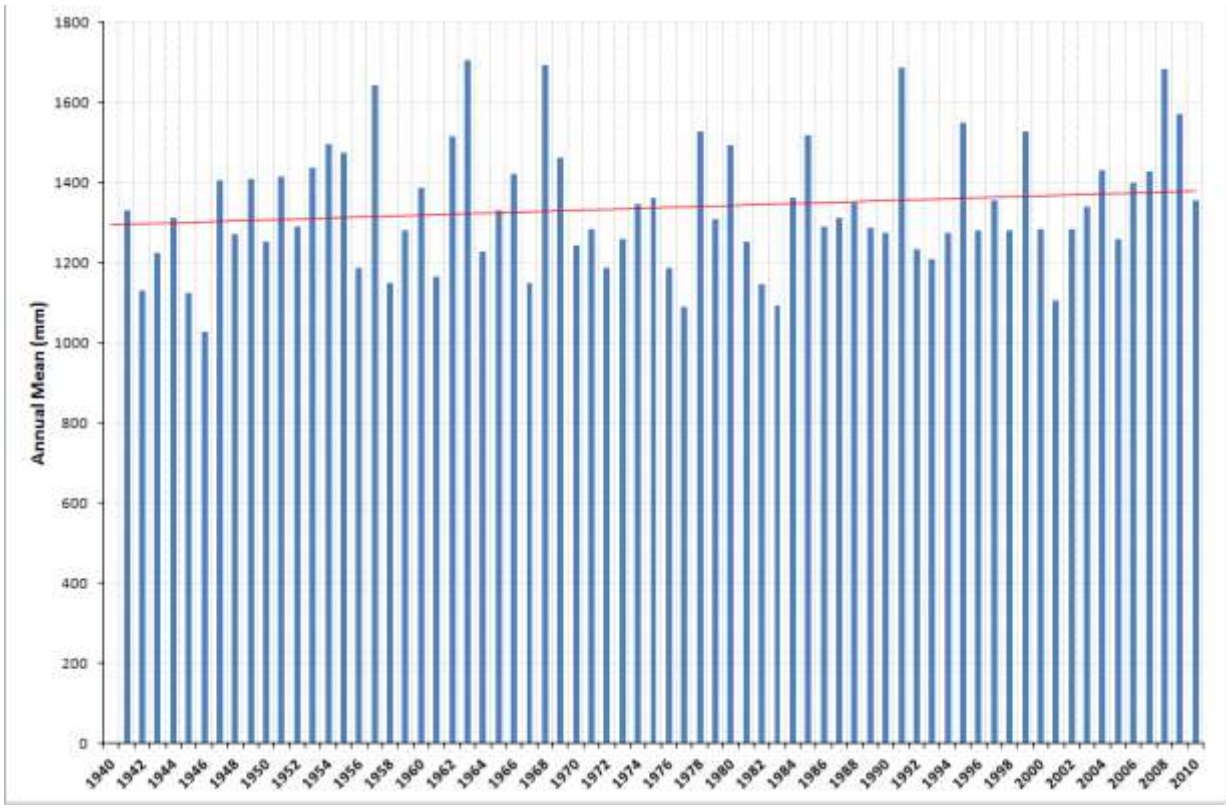

Figure 5.1: Rainfall characteristics and trend for the present climate (1941 – 2010)

Source: Author, 2015

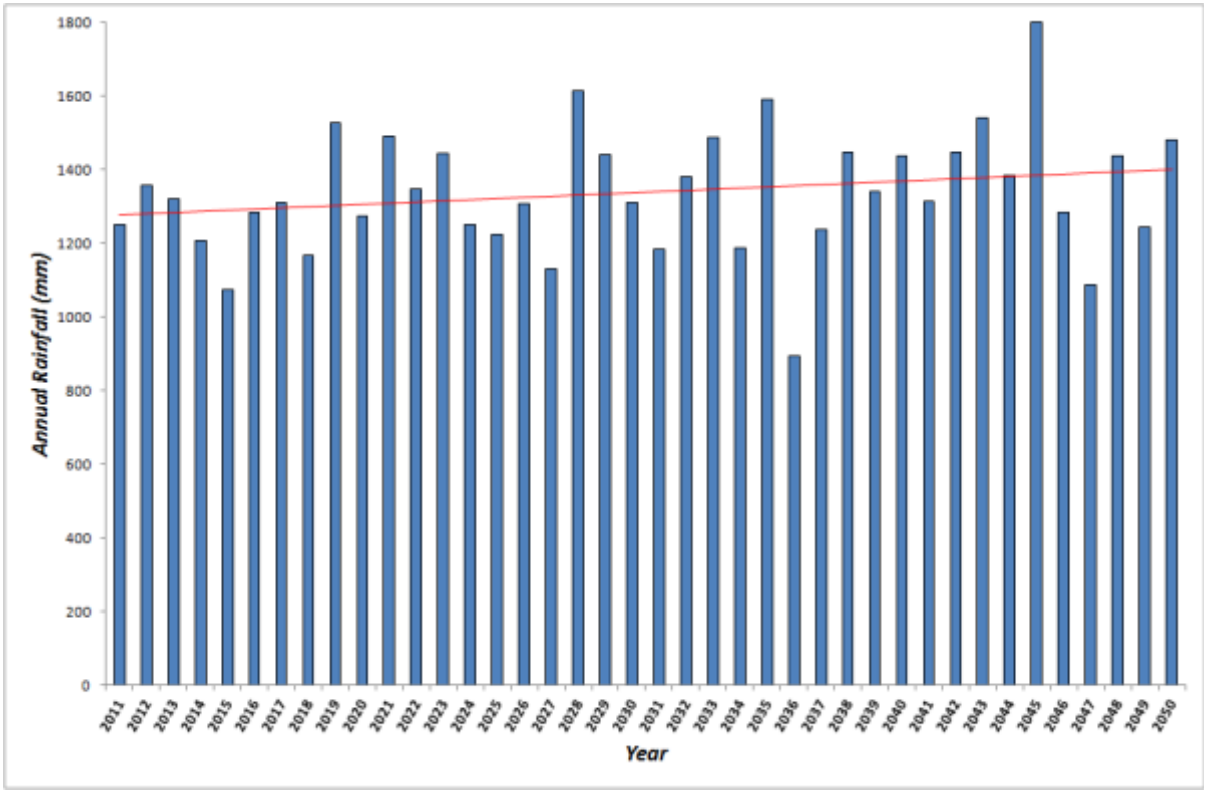

Figure 5.2: Rainfall characteristics and trend for the future climate (2011 – 2050)

Source: Author, 2015

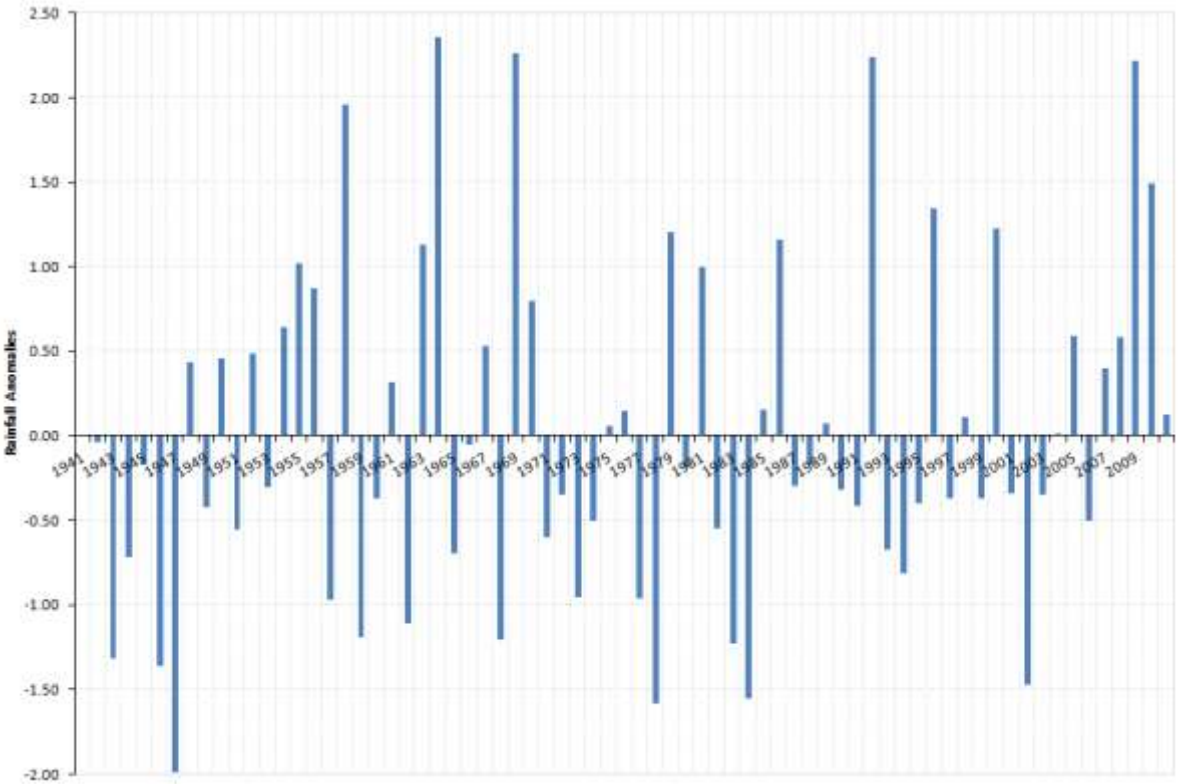

Figure 5.3: Rainfall anomaly characteristics and trend for present climate (1941 – 2010)

Source: Author, 2015

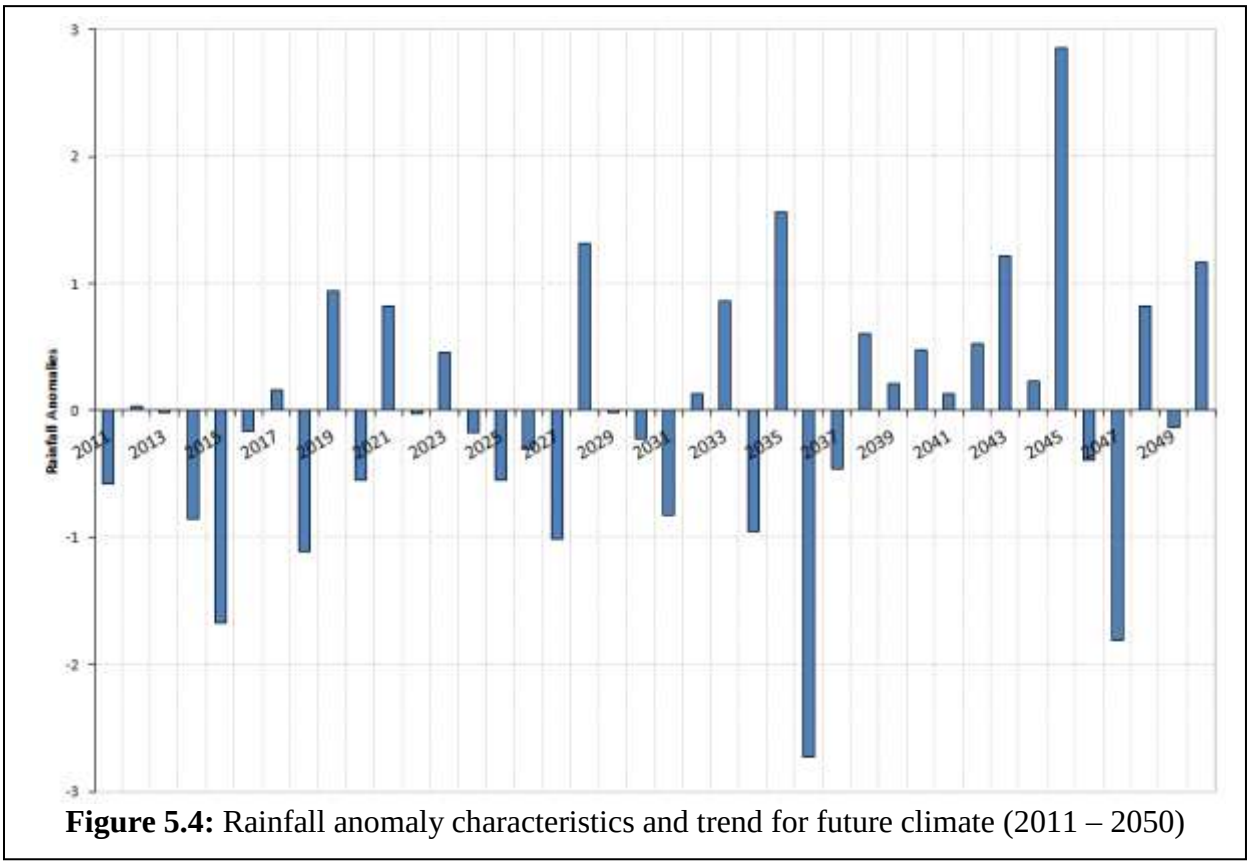

Figure 5.4: Rainfall anomaly characteristics and trend for future climate (2011 – 2050)

Source: Author, 2015

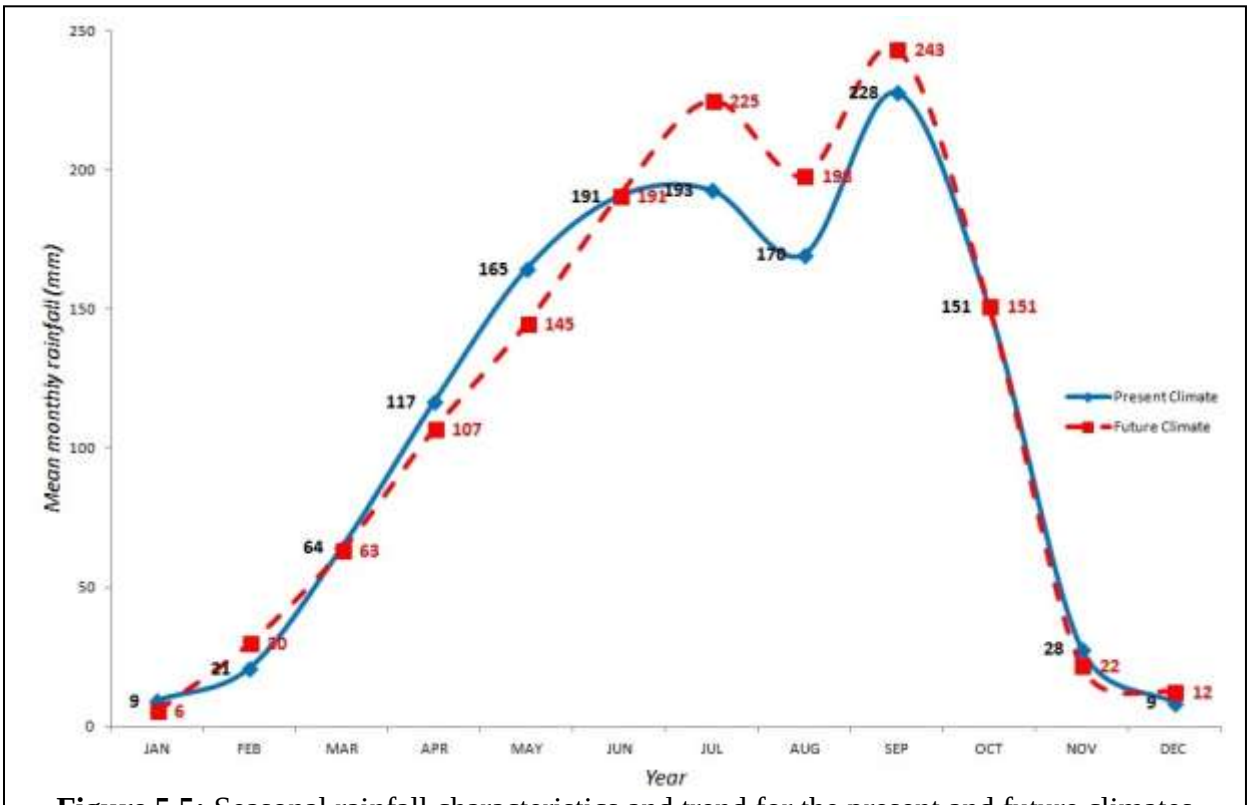

Figure 5.5: Seasonal rainfall characteristics and trend for the present and future climates

Source: Author, 2015

The rainfall anomalies for both the present and future climates are shown in figures 5.3 and 5.4. During the present climate, the study area records positive trend of rainfall anomaly, increasing annually at a rate of 0.007mm. The study area receives lowest and highest of 951mm and 1,688mm in 1946 and 1991 respectively, which represent about 28% and 28% below and above the mean annual rainfall respectively. However, during future climate, the positive trend of rainfall anomaly will continue, even though, it will be increasing at a rate of 0.23mm per annum as shown in figure 5.4.

The seasonal rainfall pattern within the study area as presented in figure 5.5 exhibits double maxima in both climates with the highest rainfall of 228mm and 243mm recorded in the month of September during the present and future climates. Furthermore, the second peak rainfall was recorded in July, measuring 193mm and 225mm for both present and future climates respectively.

5.2 Temperature Characteristics and Trend

The temperature characteristics within the study area are presented in figures 5.6, 5.7, 5.8 and 5.9 for both the present and future climates. The mean annual temperature characteristics of the derived savannah for the period of study are shown in figures 5.6 and 5.7. The mean temperature pattern reveals positive trend during both the present and future climates, which were increasing annually at a rate of 0.009^{o}C and 0.014^{o}C, respectively.

Furthermore, the annual temperature anomalies are shown for the present and future climates in figures 5.8 and 5.9 respectively. The temperature anomalies show a positive trend for both climates. In the present climate, annual temperature anomaly increases at the rate of 0.03, while it will be increasing at a rate of 0.04 per annum during future climate. The lowest and highest temperature of 26.6^{o}C and 27.8^{o}C were recorded during the present climate in 1973

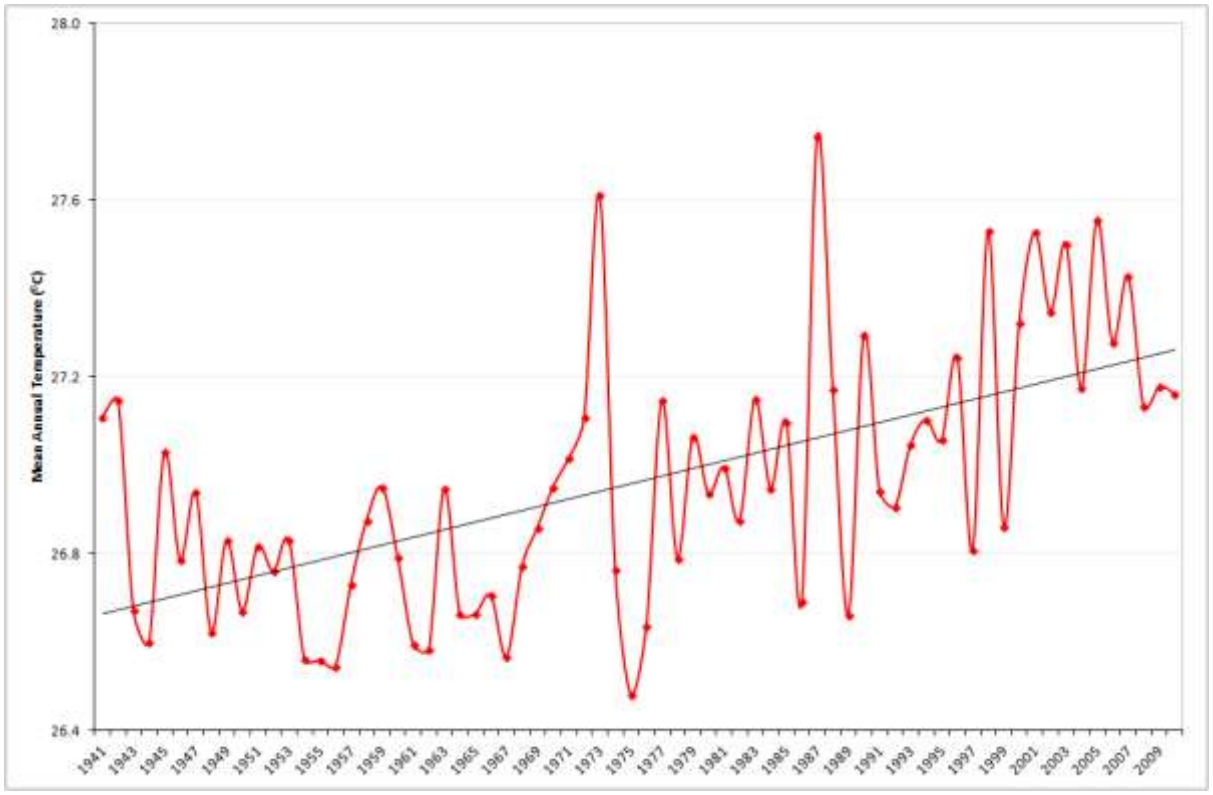

Figure 5.6: Temperature characteristics and trend for present climate (1941 – 2010)

Source: Author, 2015

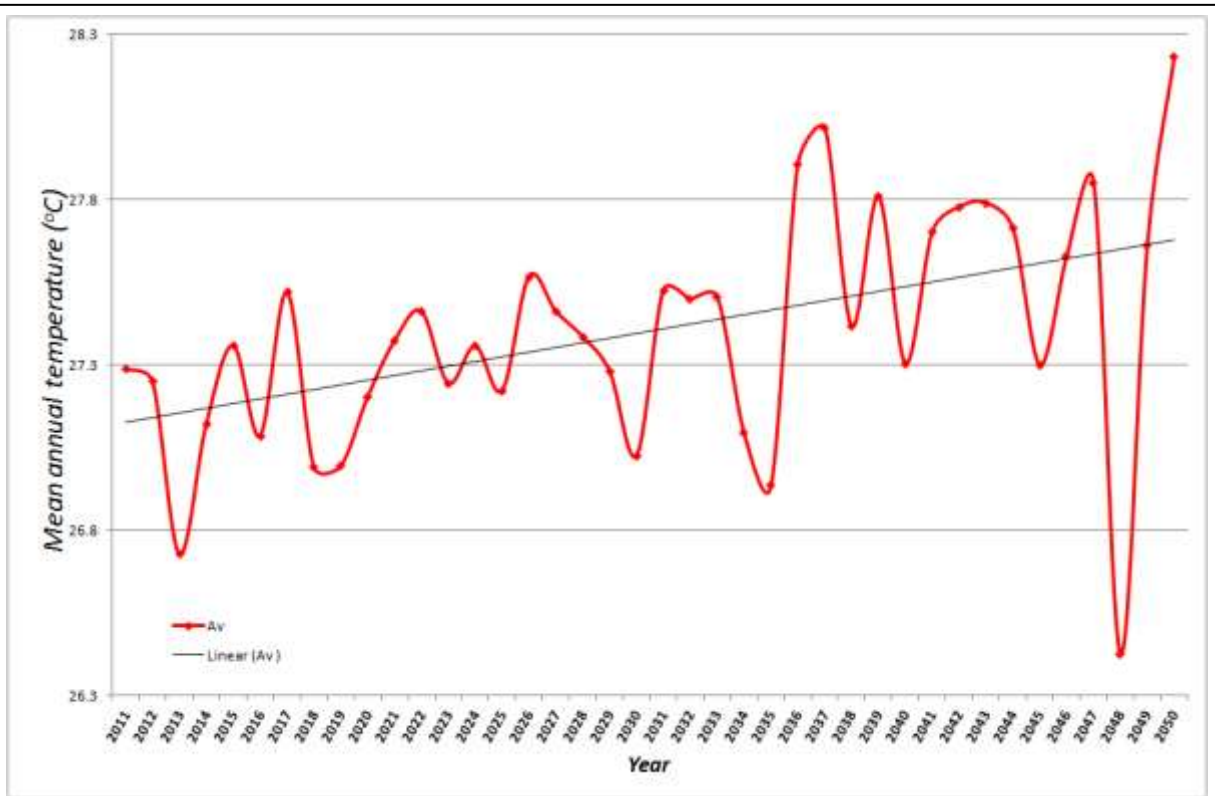

Figure 5.7: Temperature characteristics and trend for future climate (2011 – 2050)

Source: Author, 2015

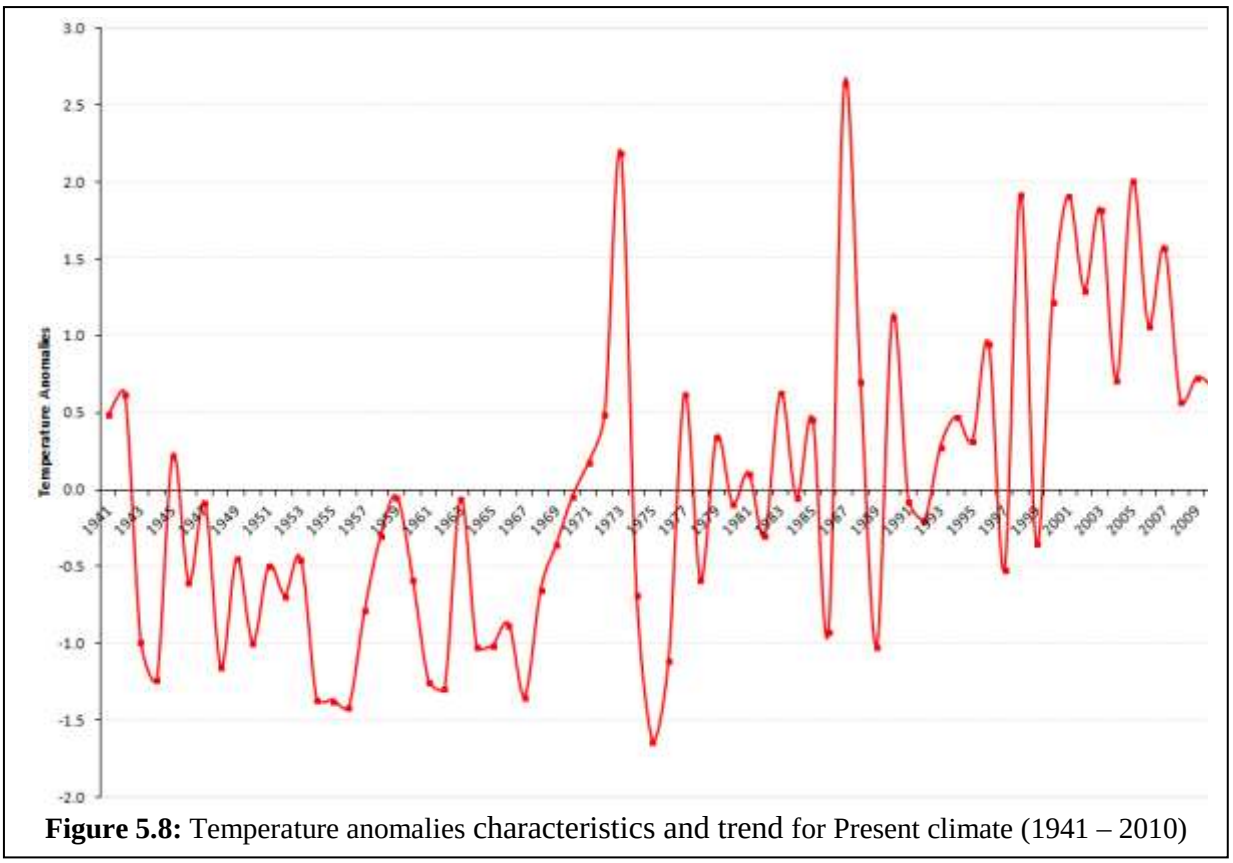

Figure 5.8: Temperature anomalies characteristics and trend for Present climate (1941 – 2010)

Source: Author, 2015

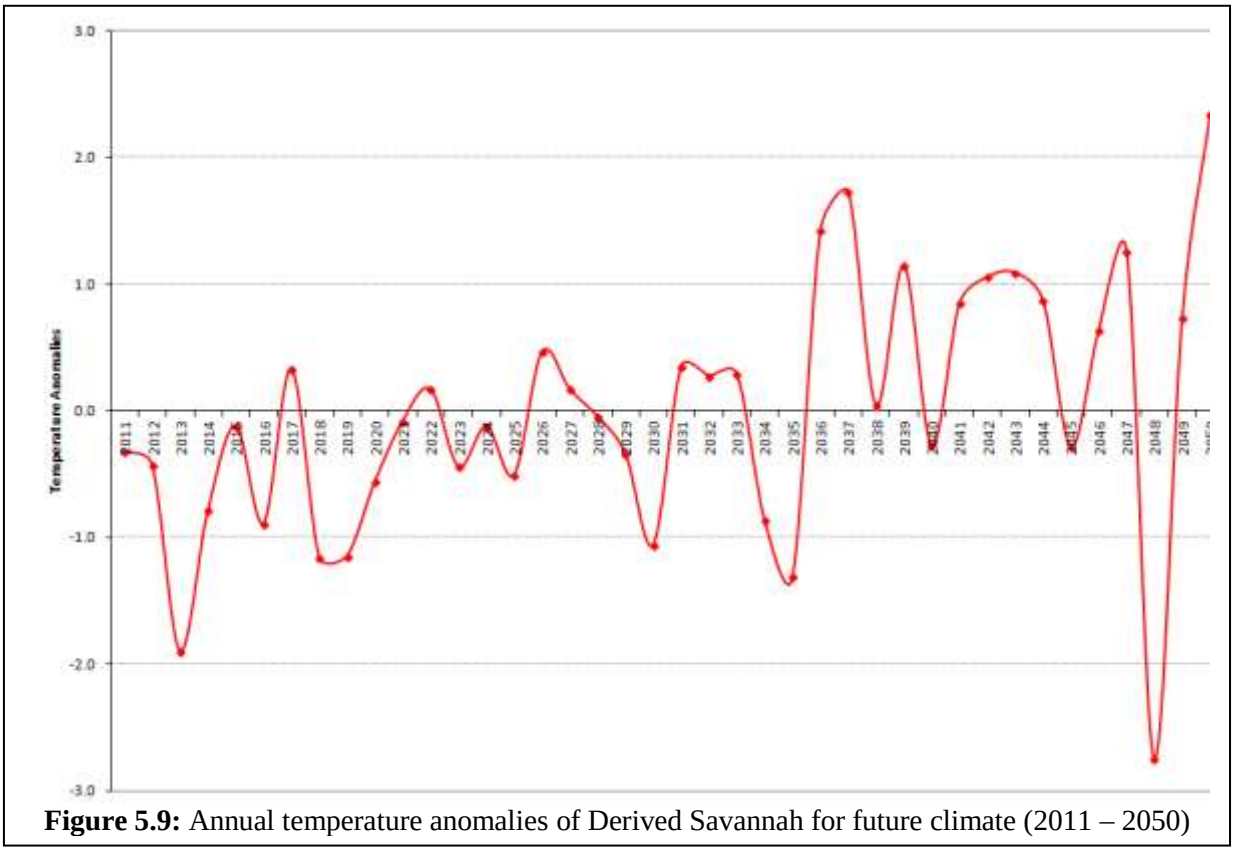

Figure 5.9: Annual temperature anomalies of Derived Savannah for future climate (2011 – 2050)

Source: Author, 2015

and 1975, respectively, which were 1.7% and 3% below and above the normal mean annual temperature as illustrated in figure 5.8.In addition, 28.2^{o}C and 26.4^{o}C will be received as the highest and lowest annual temperature in the future climate, which represent about 3.0% and 3.5% above and below mean annual temperature respectively as depicted in figure 5.9.

5.3 Spatial Patterns of the Present Rainfall and Temperature Variability, 1941-2010

5.3.1 Spatial pattern of Rainfall variability

The spatial pattern exhibits an increasing trend in the mean annual rainfall towards the southern (i.e. north to south direction) part of the study area during the present climate (1941-2010). The spatial pattern of annual mean rainfall is shown in figure 5.10. The mean annual rainfall ranges between 1,191mm and 1,628mm and these extremes were recorded in Ondo and Pategi areas respectively. Related studies in Nigeria have also predicted similar trend and direction of increasing rainfall (Oguntunde *et al.,* (2012), Odjugo, 2011).

The spatial distribution and pattern of annual rainfall anomaly for the Derived Savannah is shown in figure 5.11 during present climate. The annual rainfall anomaly recorded during the present climate range between -0.77 and 1.54 which were about 9.50% and 23.71% below and above mean annual rainfall received in the area as illustrated in figure 5.11. Places like Oshogbo, Ilorin, Ogbomosho, Offa, Ede, Isanlu, Pategi, etc recorded negative rainfall anomaly during the present climate, while Ejigbo, Osu, Ondo, Ado-Ekiti, etc recorded positive anomaly as illustrated in the figure 5.11

The annual rainfall variability indices range from 15% to 23% for the study area during the present climate as illustrated in figure 5.12. In figure 5.12, Pategi and Akure recorded least and highest rainfall variability during the present climate. Also, annual rainfall was more stable in areas like Oshogbo, Ondo and Ilorin which recorded 17%, 18% and 19% of rainfall variability index respectively than 23% recorded in Akure.

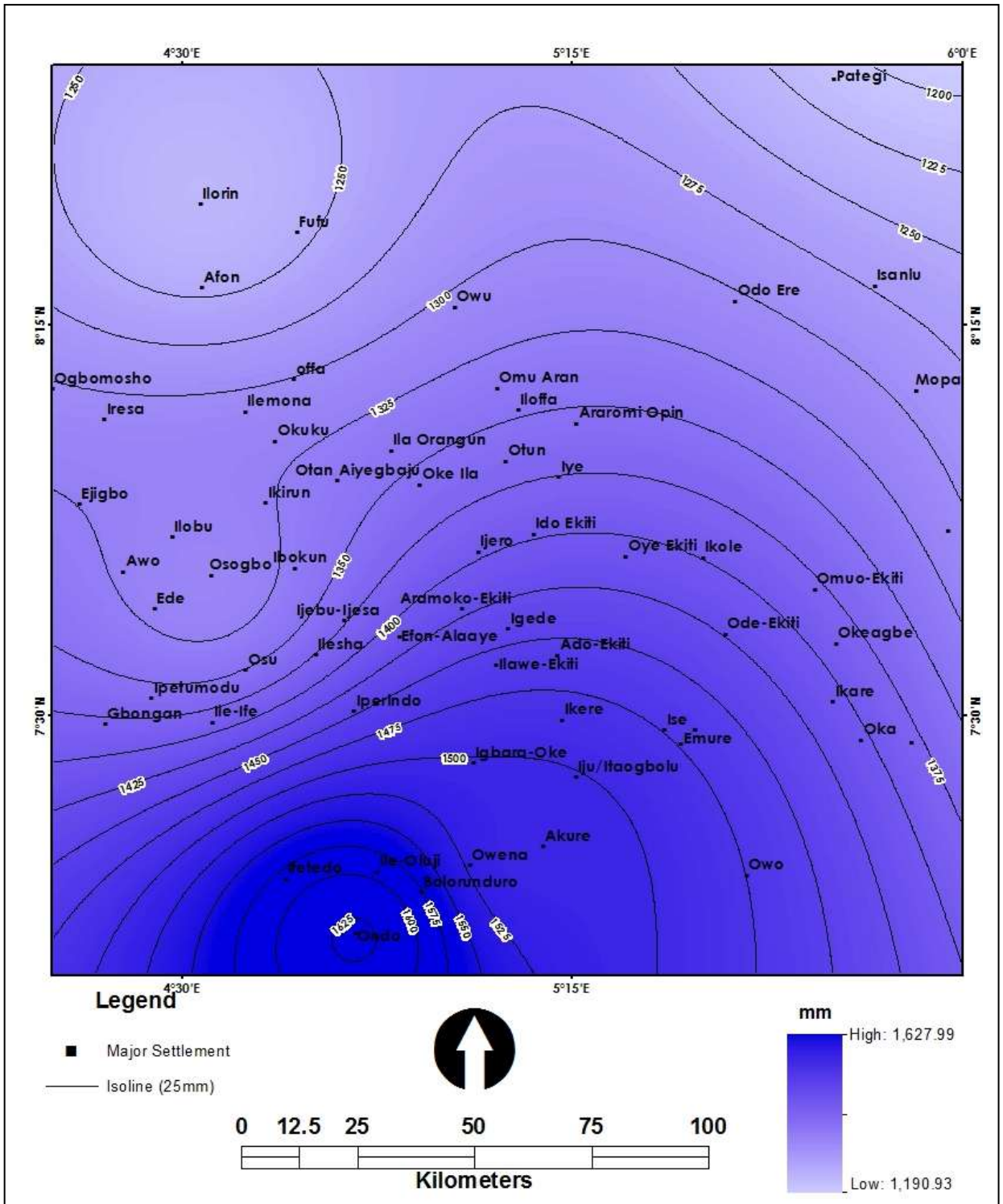

Figure 5.10: The spatial pattern of mean annual rainfall for the present climate (1941 – 2010)

(Author, 2015)

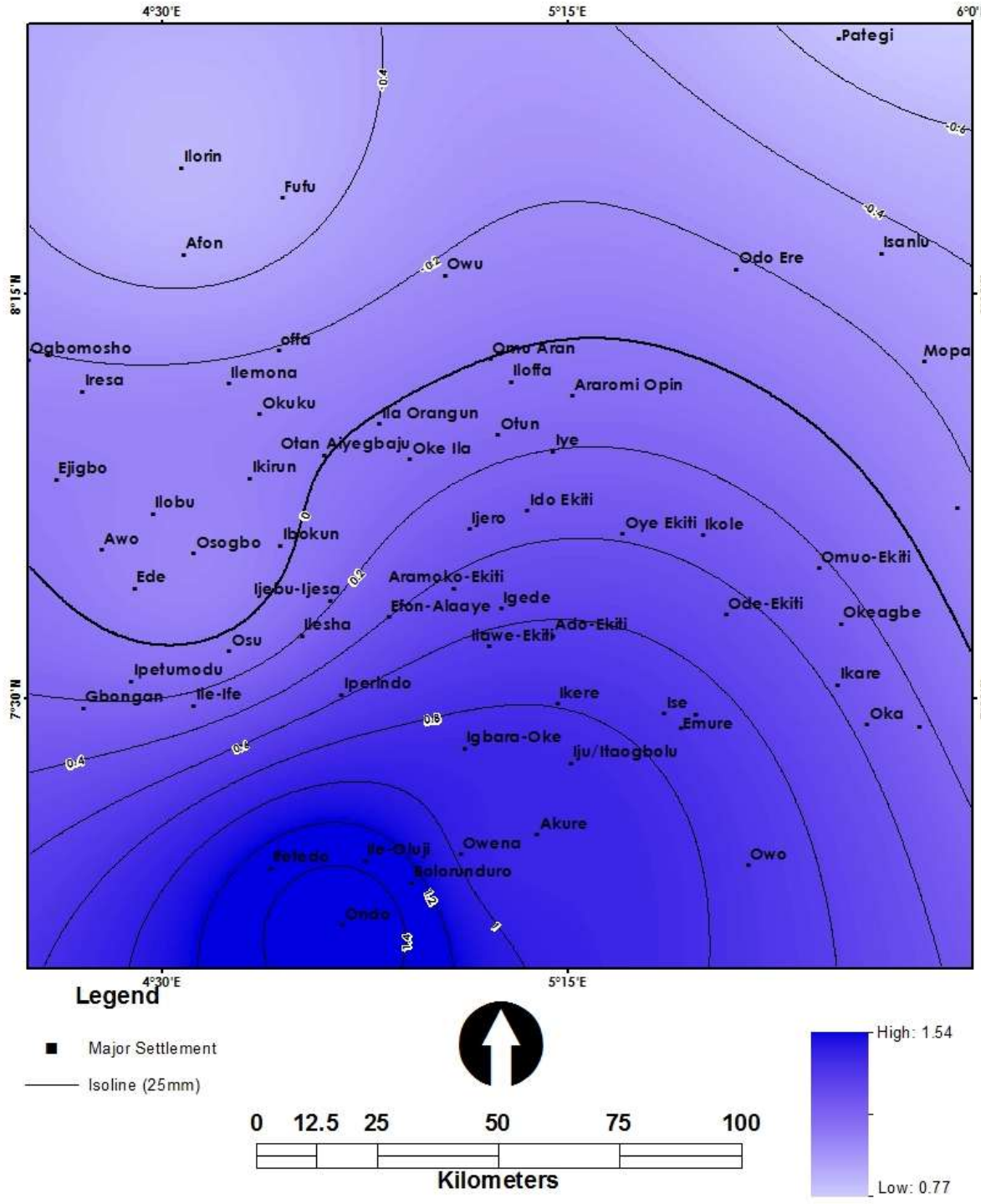

Figure 5.11: The spatial pattern of annual rainfall anomalies for the present climate (1941 – 2010)

(Author, 2015)

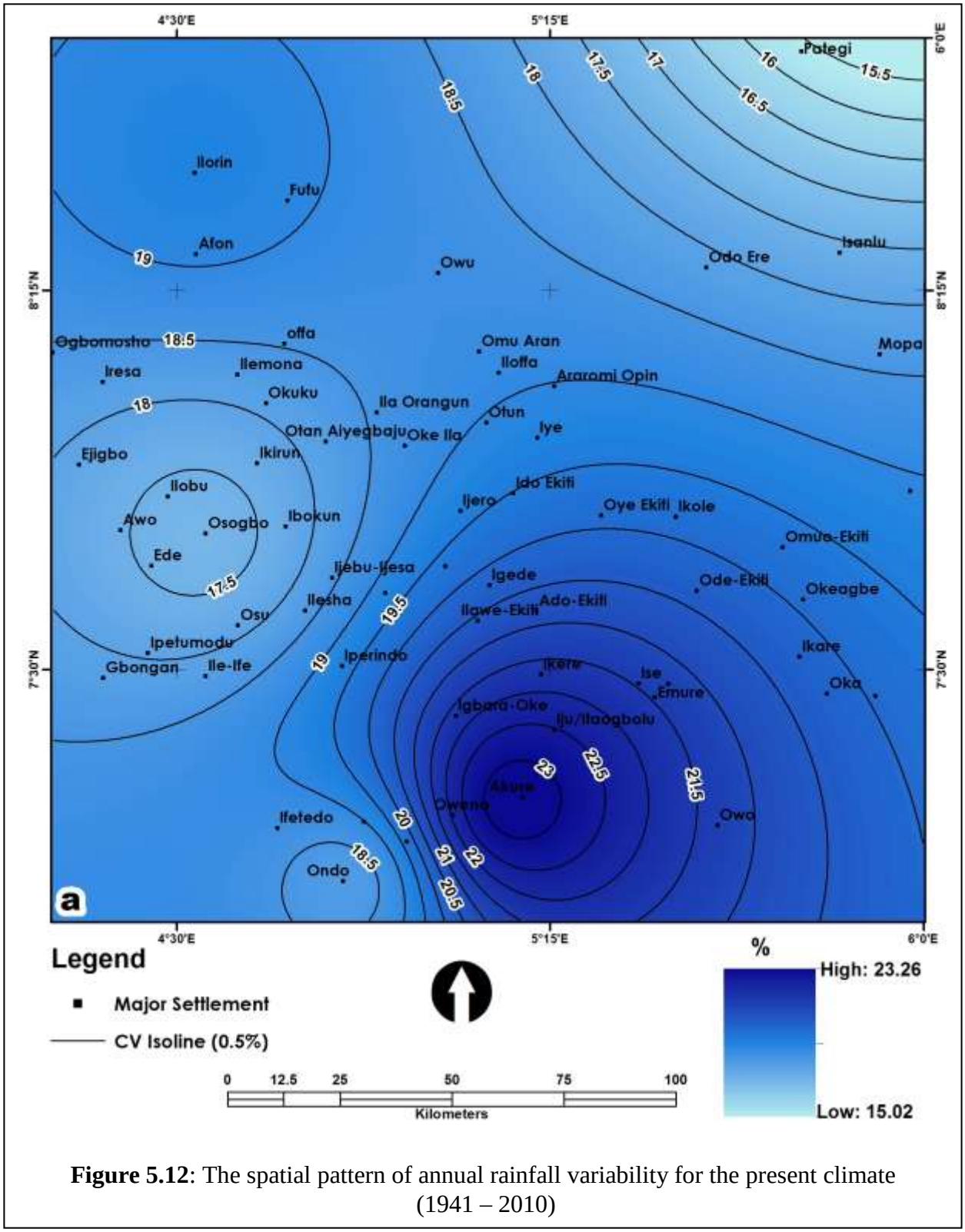

Figure 5.12: The spatial pattern of annual rainfall variability for the present climate (1941 – 2010)

Source: Author, 2015

5.3.2 Spatial pattern of Temperature variability

The spatial distribution pattern of the mean annual temperature, temperature anomaly and temperature variability index within the study area are shown in figures 5.13, 5.14 and 5.15 respectively for the present climate. Figure 5.13 reveals that mean annual temperature ranges from 26.3^{o}C to 27.9^{o}C for the study area during the present climate, which were recorded in Ondo and Pategi areas.

The spatial patterns of temperature anomalies were totally different in terms of distribution and extent during the present climate within the study area. Figure 5.14 shows the spatial pattern of temperature anomaly during the same period and it reveals that there were increasing trends of anomaly. Furthermore, during the present climate, temperature anomalies ranging from -2.6 to 3.4 in Ondo and Pategi areas recorded the lowest and highest anomalies respectively as can be seen in figure 5.14. Places to the south west and north east ends of zero anomalies in the figure 5.14 received temperature below and above the longtime mean annual temperature during the present climate.

The distribution patterns of climate variability indices for temperature variables are shown in figure 5.15 with indices ranging from 1.42 to 2.41% for present climate. This also shows that Ilorin and Oshogbo have lowest and highest temperature variability during the present climate.

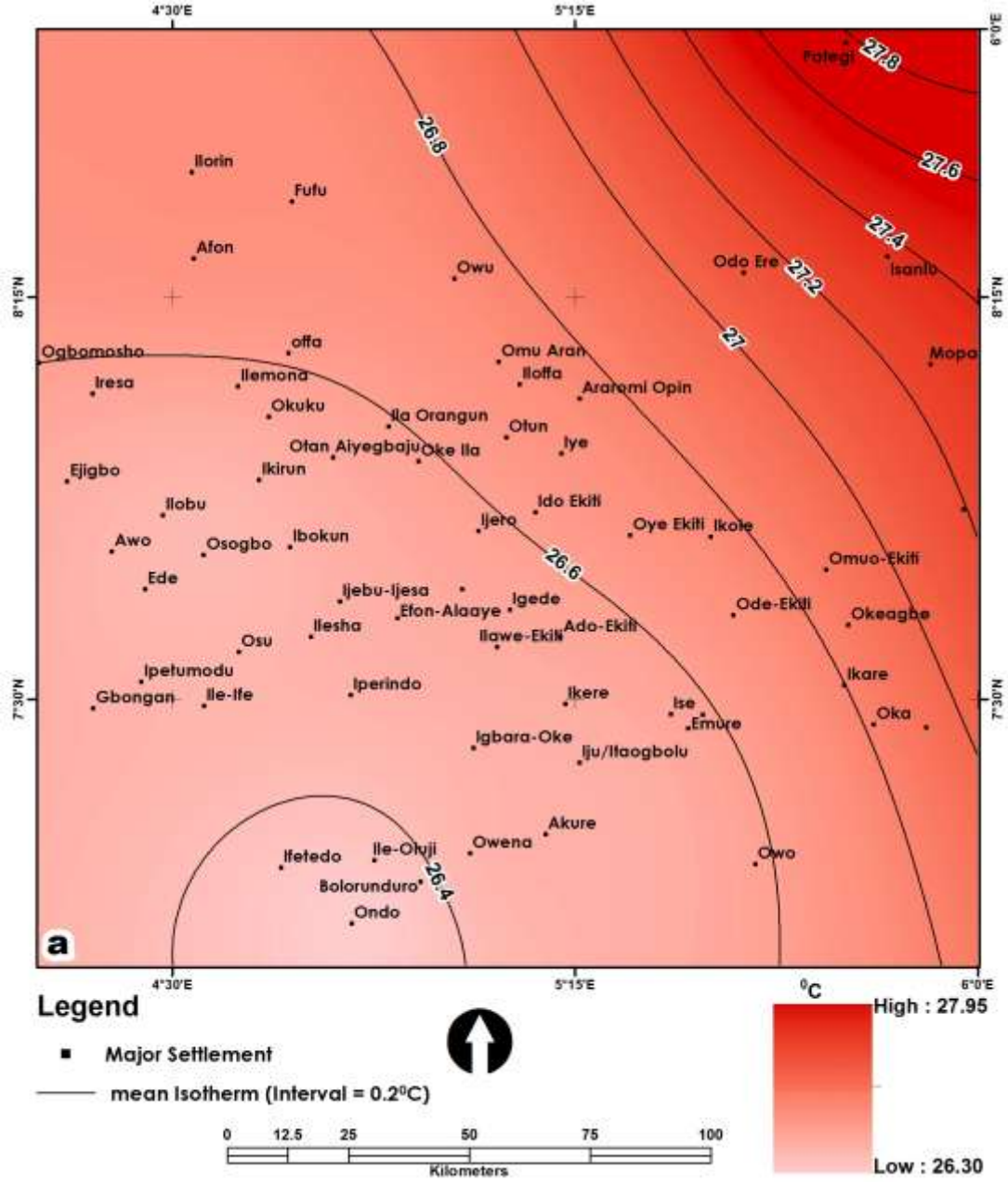

Figure 5.13: The spatial pattern of mean annual temperature for the present climate (1941 – 2010) *(source: Author, 2015)*

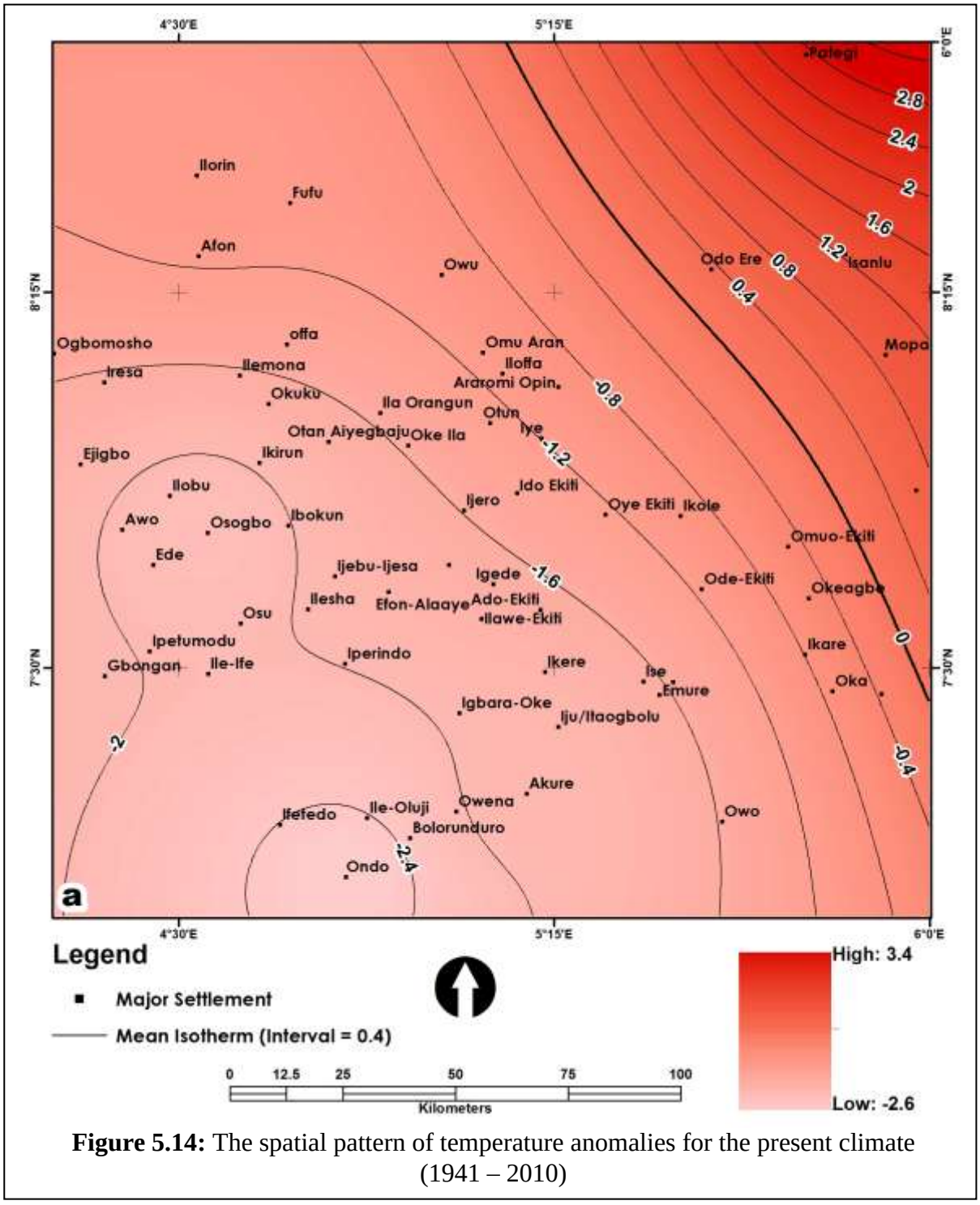

Figure 5.14: The spatial pattern of temperature anomalies for the present climate (1941 – 2010)

(Author, 2015)

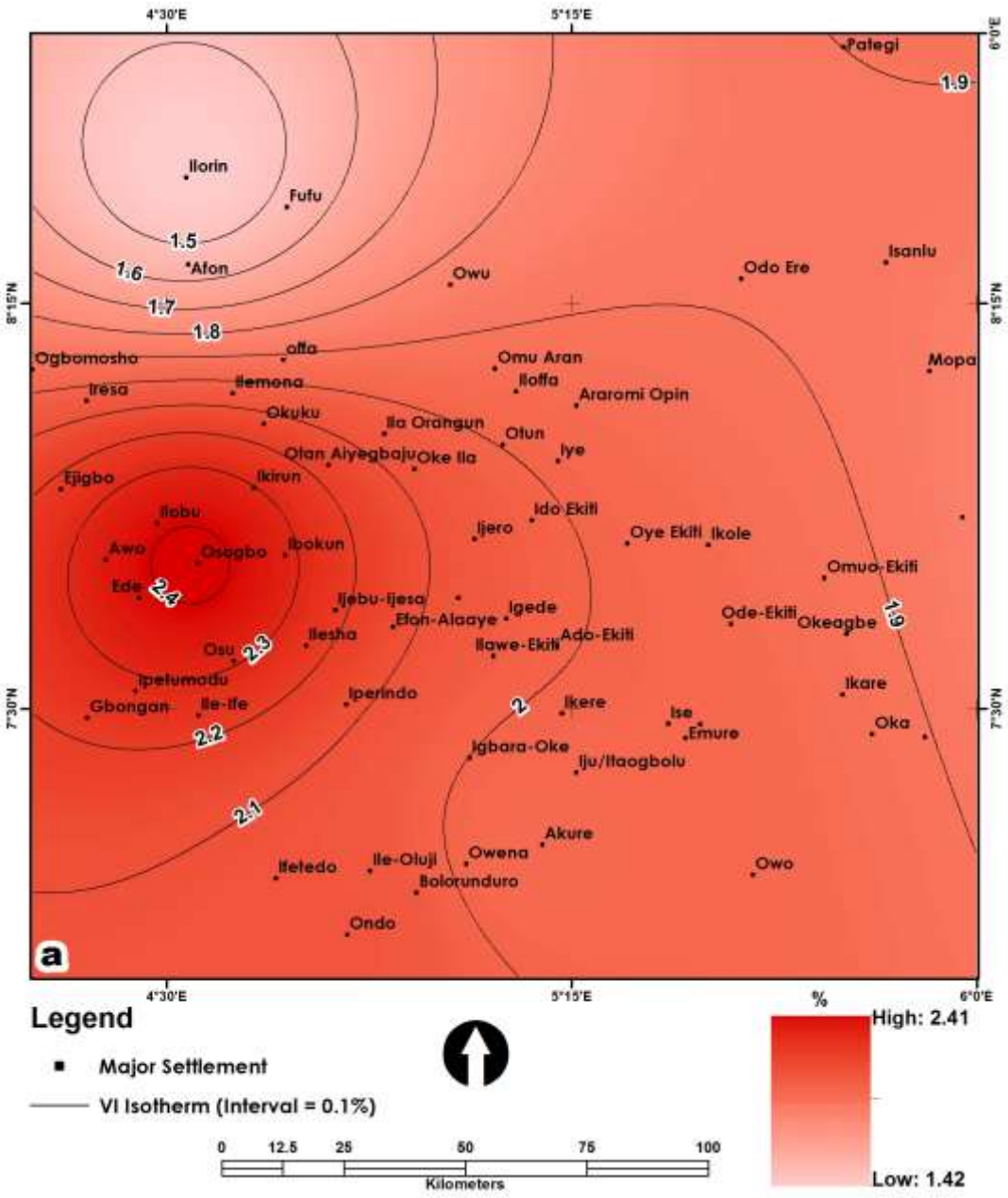

Figure 5.15: The spatial pattern of temperature variability for the present climate (1941 – 2010)

Source: Author, 2015

5.4 Spatial Patterns of the Future Rainfall and Temperature Variability, 2011 - 2050

5.4.1 Spatial pattern of Rainfall variability

The spatial pattern exhibits an increasing trend in the mean annual rainfall towards the southern (i.e. north to south direction) part of the study area during the future climate (2011 – 2050) as illustrated in figure 5.16. The mean annual rainfall ranges between 1,210mm and 1,690mm in the future climate. Pategi and Ondo areas will receive highest and lowest mean annual rainfall of 1,210mm and 1,690mm respectively during the future climate, which are slightly higher than the values during present climate.

The study revealed that Derived savannah will record annual anomalies ranging from -0.68 to 1.11, which represent about 13.13% and 21.32% below and above normal or mean annual rainfall to be received during the future climate as illustrated in figure 5.17. The latitudinal positions of isolines have shifted southward, bringing more places to below normal or mean annual rainfall during the future climate. For instance, places like Ibokun, Otan Aiyebaju, Ila Oragungun, Omu Aran and Ilofa will be receive below their longtime mean annual rainfall.

The annual rainfall variability indices range from 9% to 13% for the study area during the future climate as shown in figure 5.18. Furthermore, there will be a total shift in the distribution of rainfall variability indices in the future climate as captured in figure 5.18; Ondo and Oshogbo will record highest rainfall variability index of 12.5% and 12.25% respectively and Pategi will receive 9%.

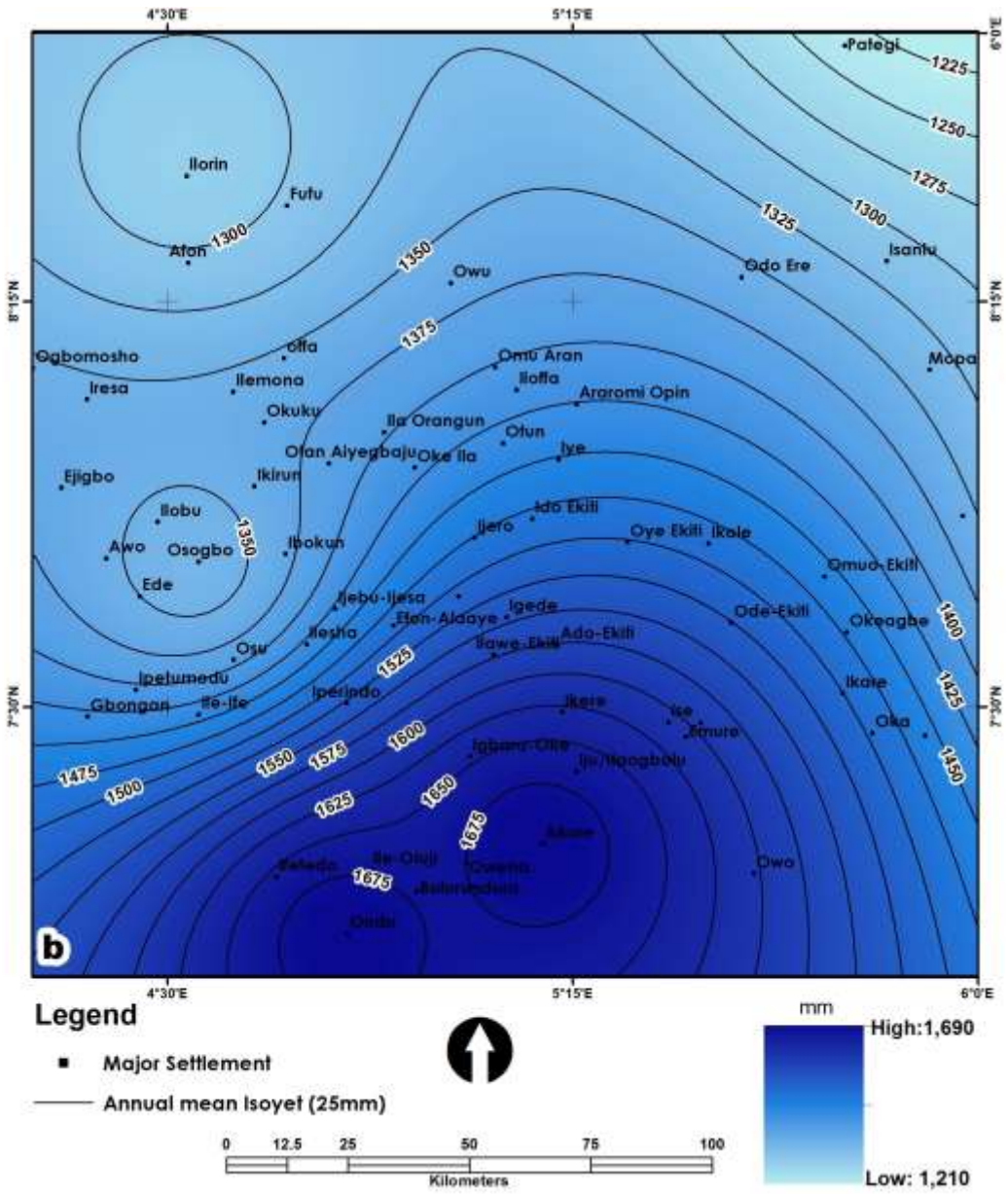

Figure 5.16: The spatial pattern of mean annual rainfall for the future climate (2011 – 2050) *(Author, 2015)*

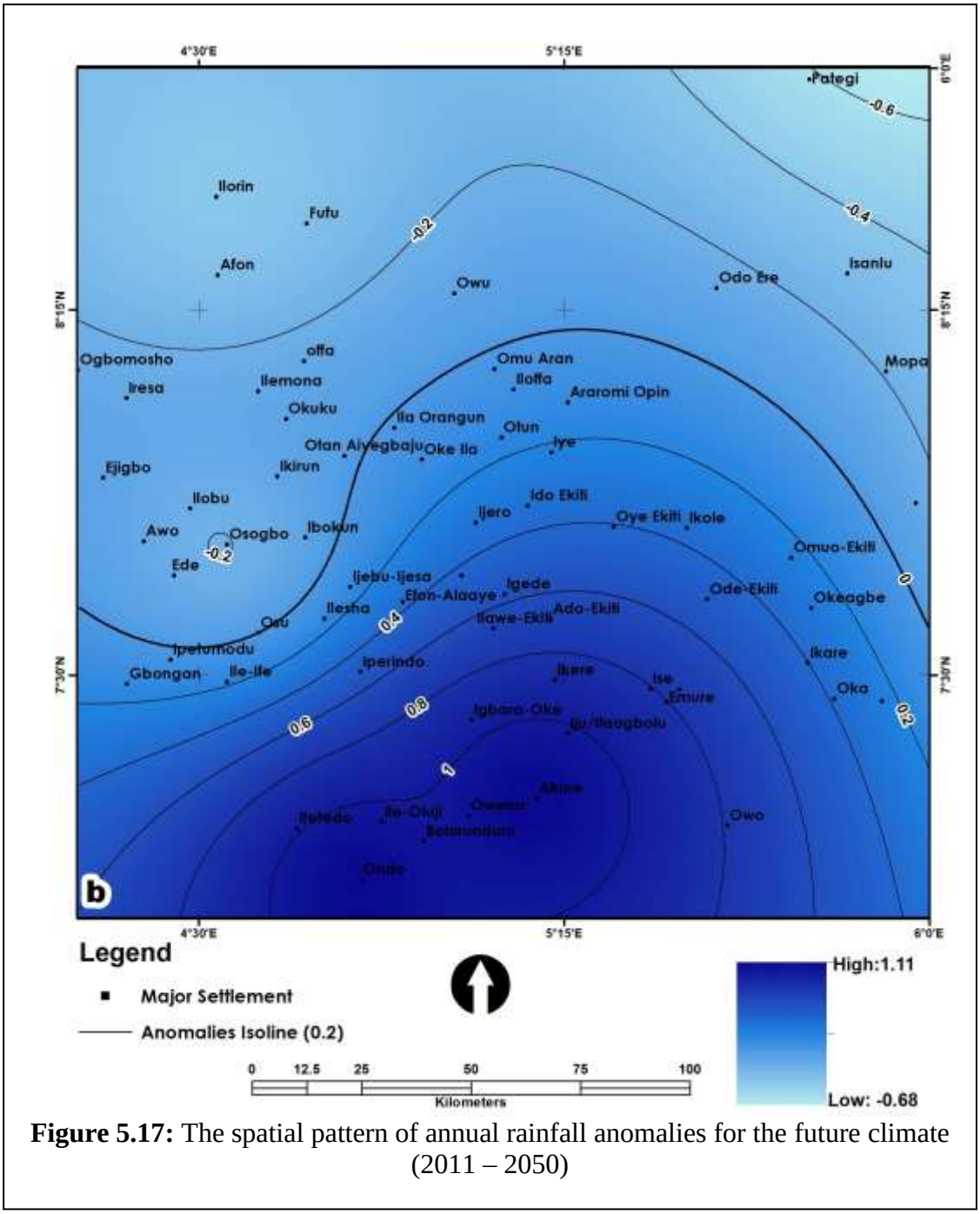

Figure 5.17: The spatial pattern of annual rainfall anomalies for the future climate (2011 – 2050)

Source: Author, 2015

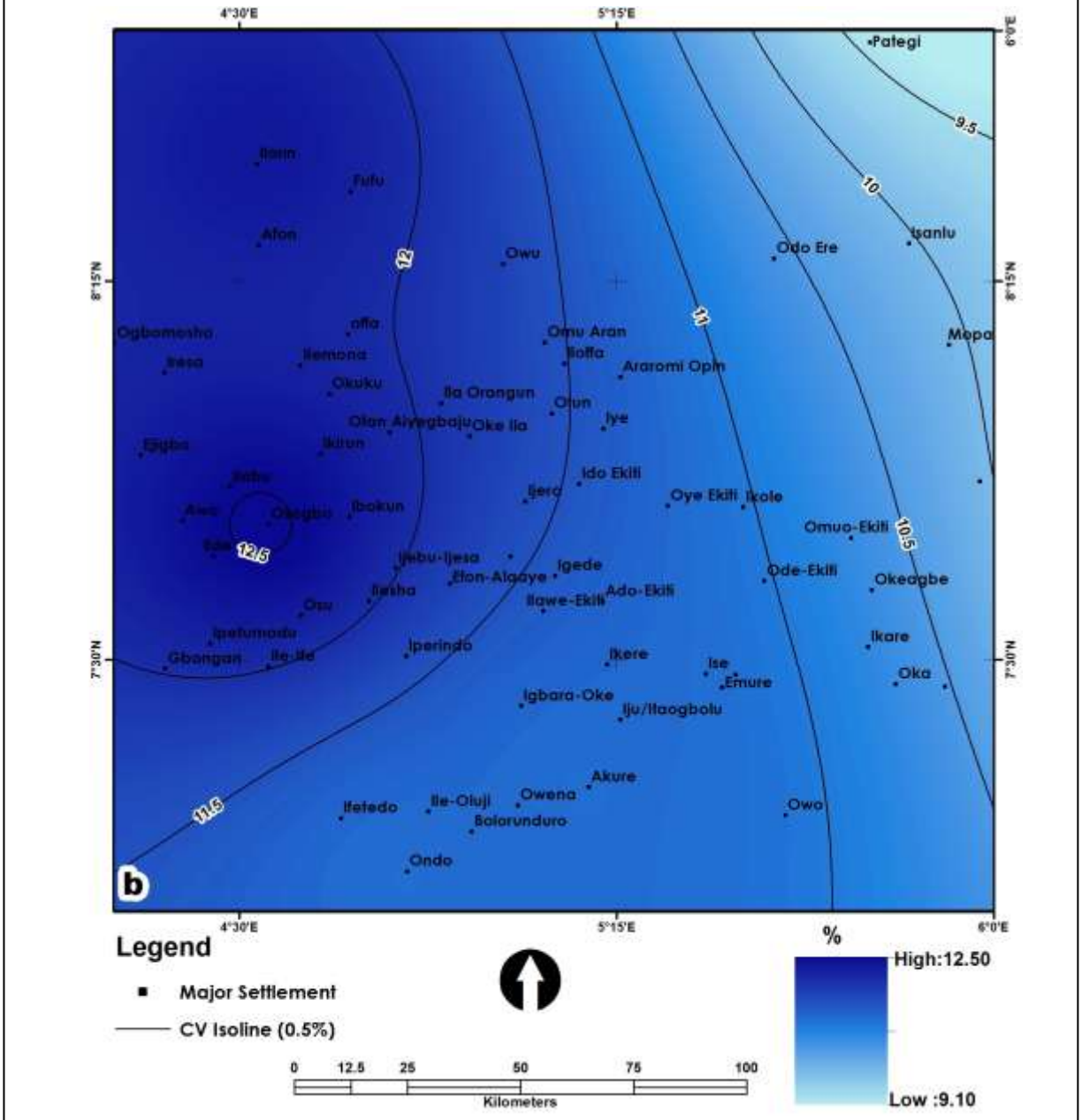

Figure 5.18: The spatial pattern of annual rainfall variability for the future climate (2011 – 2050)

Source: *Author, 2015*

5.4.2 Spatial pattern of Temperature variability

The spatial pattern of the mean annual temperature, annual temperature anomaly and temperature variability index during future climate within the study area are shown in figures 5.19, 5.20 and 5.21 respectively. The mean annual temperature ranges from 27.0^{o}C to 27.9^{o}C for the study area future climate as shown in figure 5.19. The annual temperature will be about 1.3% higher in the future climate than present climate. Temperature will increase in the south – north direction across the study area during the future climate. Oshogbo and Pategi areas will receive the least and most temperature of about 27^{o}C and 27.9^{0}C during the future climate respectively.

Furthermore, during the future climate, temperature anomalies ranging from -0.9 to 1.8 and Oshogbo and pategi will receive the least and most temperature anomalies during the period as shown in figure 5.20. As shown in figure 5.20, the extent and coverage of the anomalies have been narrowed down during future climate to places like Ondo, Akure, Ado-Ekiti, Ikole, Ikare, Owo, etc, which will now be receive temperature above their normal longtime mean.

The distribution pattern of climate variability indices for temperature variables are shown in figure 5.21 with indices ranging from 1.27 to 1.33% for future climate. Furthermore, Temperature will be more stable but higher than in the present climate; Pategi and Oshogbo will receive lowest and highest temperature variability during the future climate as revealed in figure 5.21.

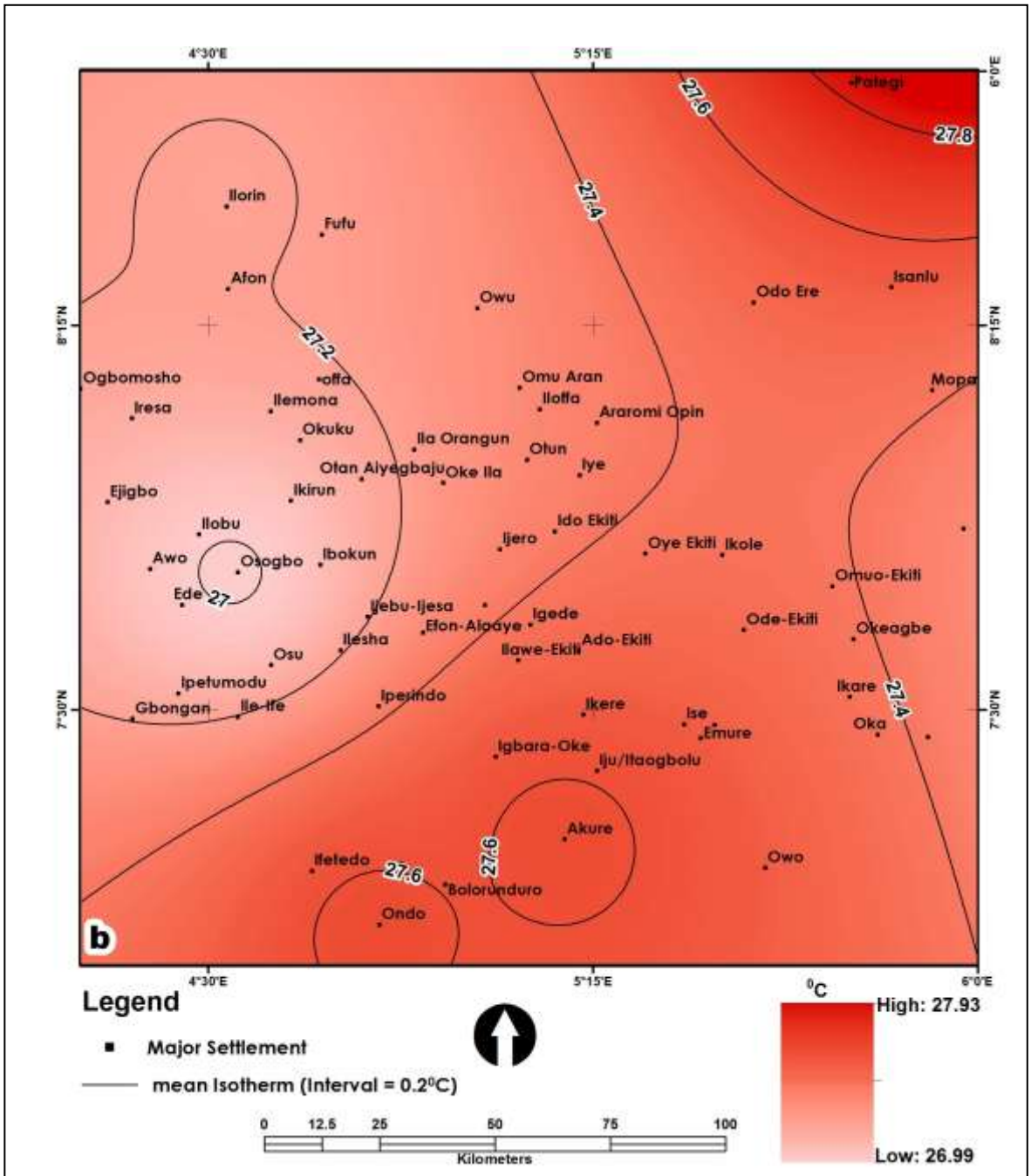

Figure 5.19: The spatial pattern of mean annual temperature for the future climate (2011 – 2050)

Source: Author, 2015

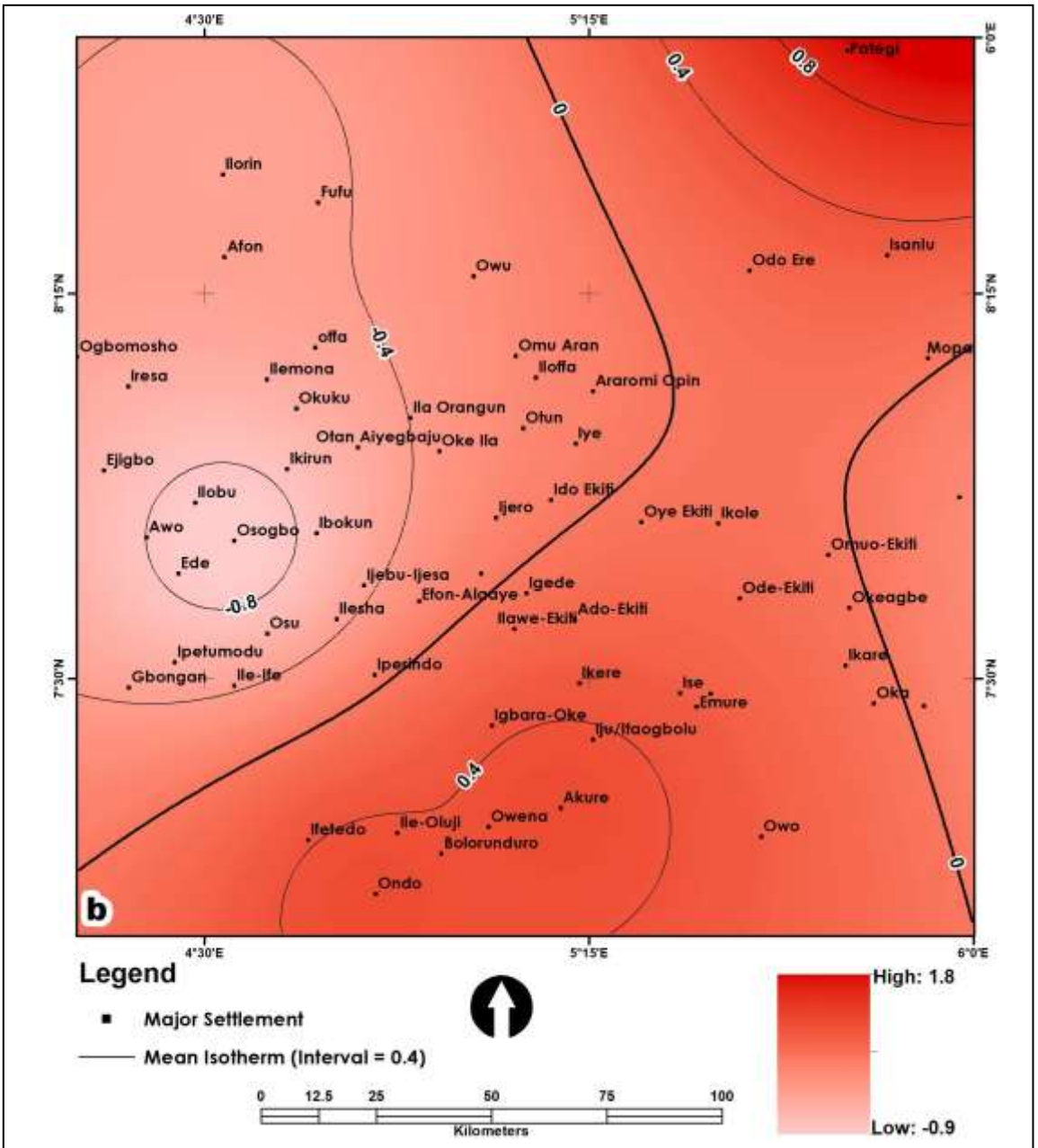

Figure 5.20: The spatial pattern of annual temperature anomalies for the future climate (2011 -2050)

Source: Author, 2015

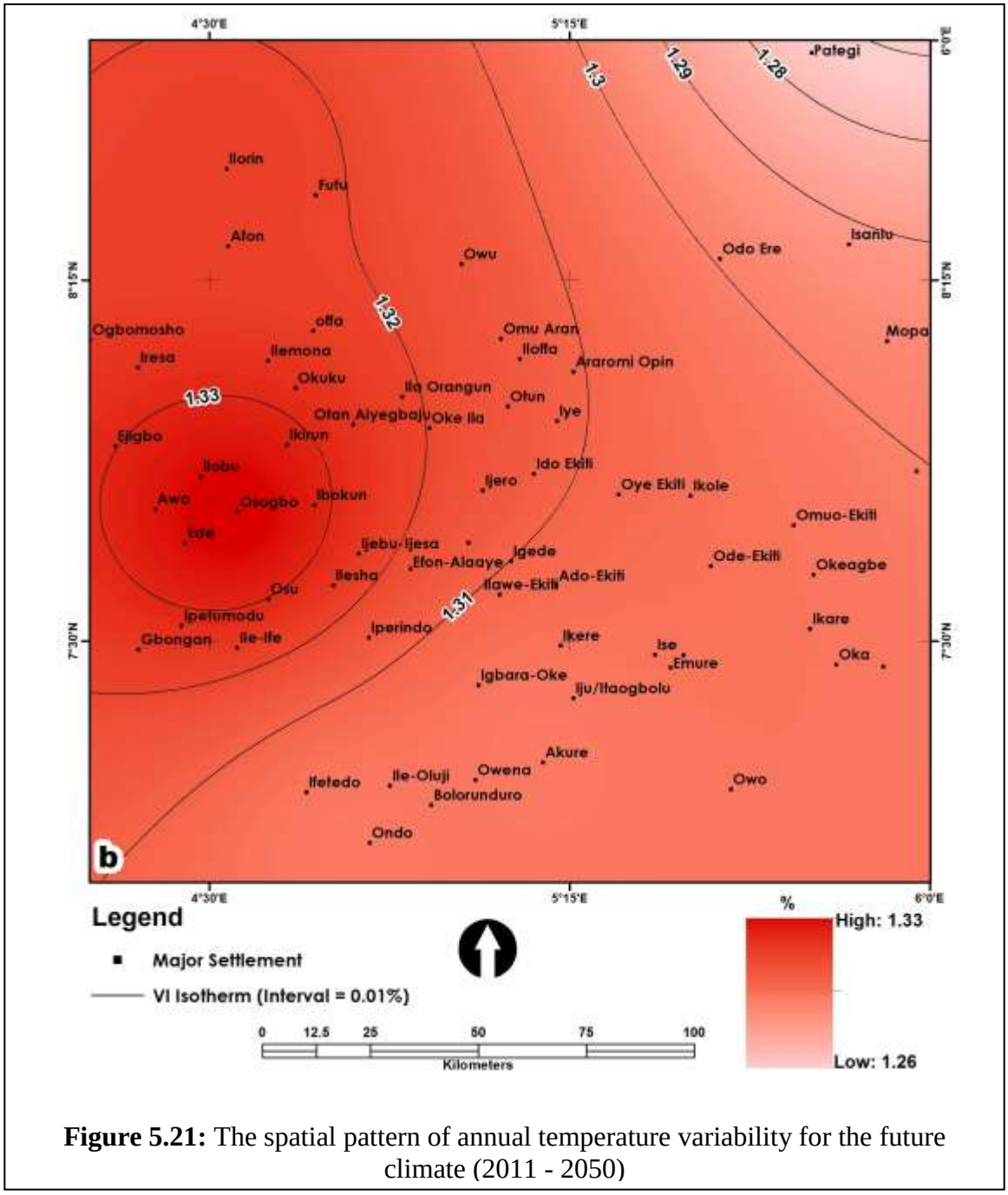

Figure 5.21: The spatial pattern of annual temperature variability for the future climate (2011 - 2050)

Source: Author, 2015

5.5 Temporal Patterns of the Present Rainfall and Temperature Variability

5.5.1 Temporal patterns of rainfall variability

The patterns of annual and decadal rainfall variability indices of the derived savannah for the present climate are shown in figures 5.22 and 5.23 respectively. Annual rainfall variability indices during the present climate range from -2.00 and 2.38 (i.e. severely dry and extremely wet) as shown in figure 5.22. During the period, 23 wet years, 33 dry years and nine (9) normal climatic years were identified. This is consistent with the findings of Oguntunde *et al.* (2011). The present climate is further divided into two periods (i.e. 1941 – 1975 and 1976 – 2010) in order to understand the temporal variability pattern. The z-test for the two periods reveals that there is change since the **z** calculated of -0.3267 is less than the tabulated, 1.9599 at 5% significant. Also, the cumulative probability curve in figure 5.23 shows the change in the temporal distribution patterns of rainfall for the first period and rainfall is slightly higher in the second period (1976 – 2010).

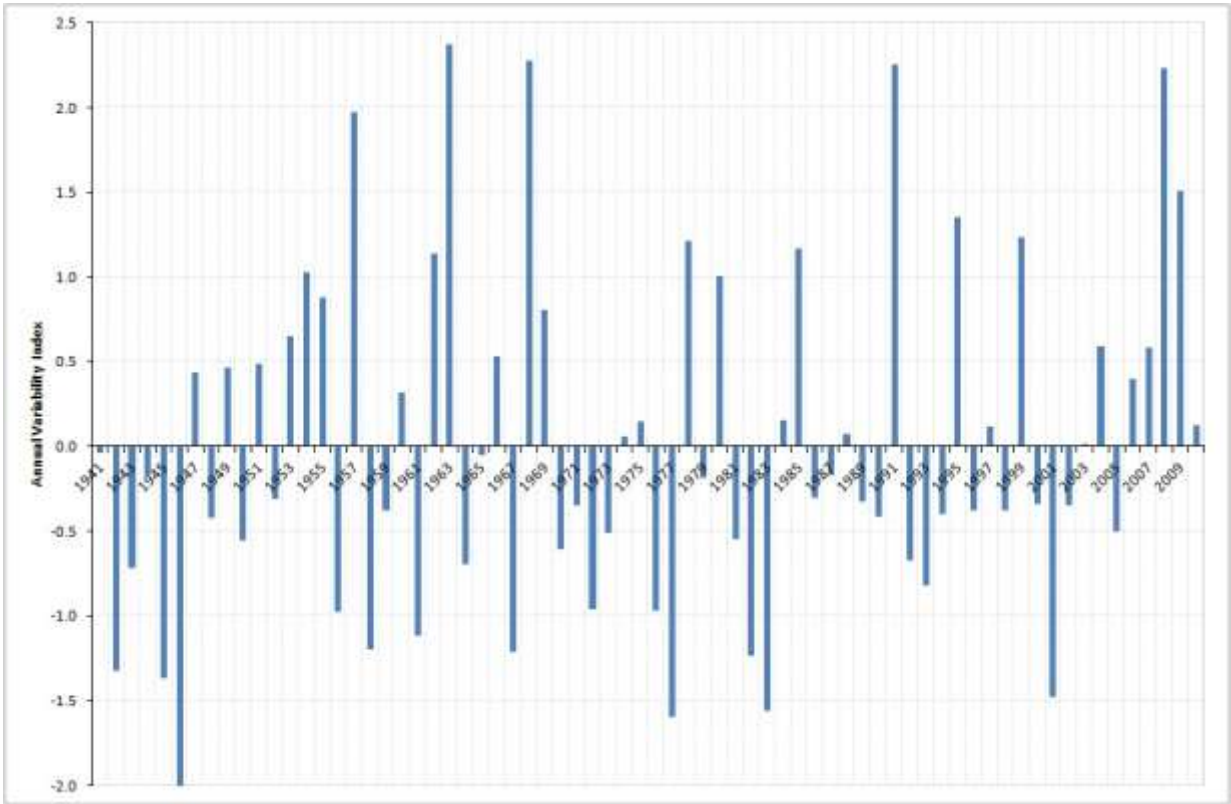

Figure 5.22: Annual Rainfall variability index for present climate (1941 – 2010) *(Author, 2015)*

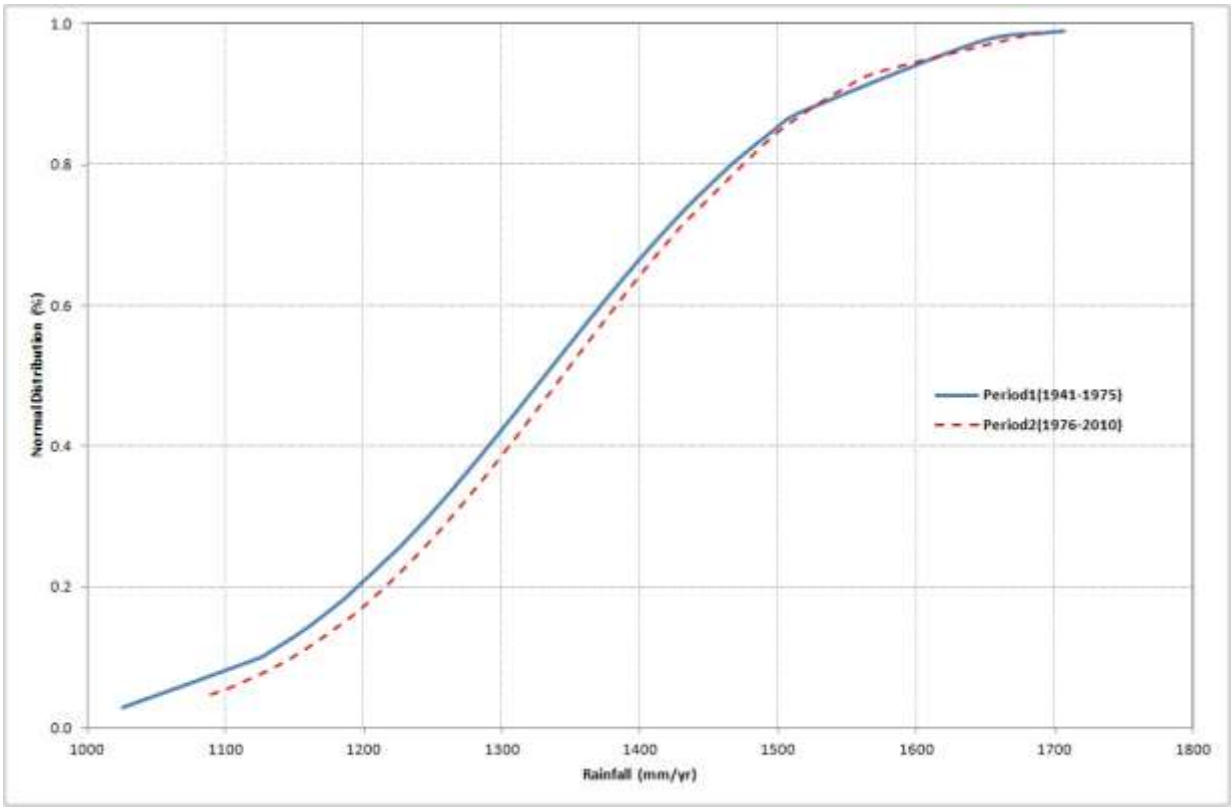

Figure 5.23: Temporal variability change in Rainfall for present climate (1941 – 2010) *(Author,*

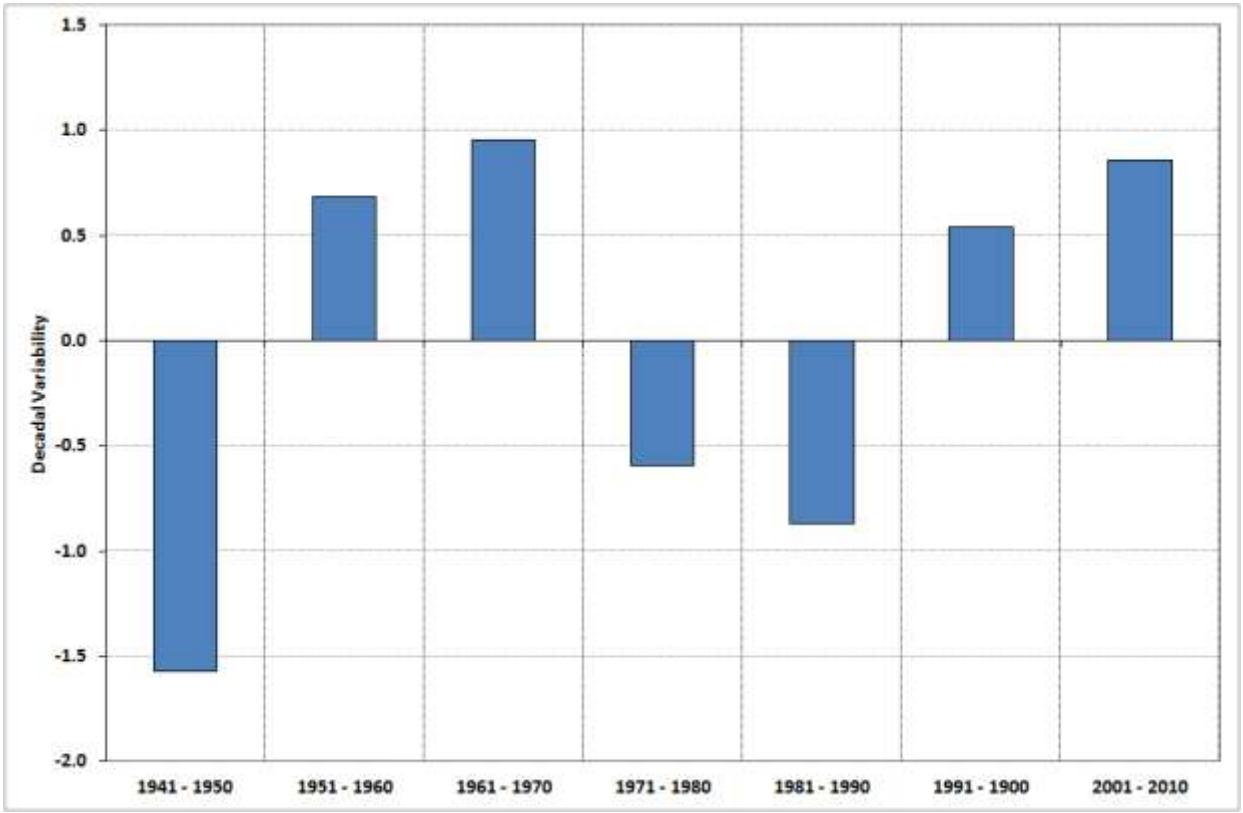

Figure 5.24: Decadal Rainfall variability index for present climate (1941 – 2010) *(Author, 2015)*

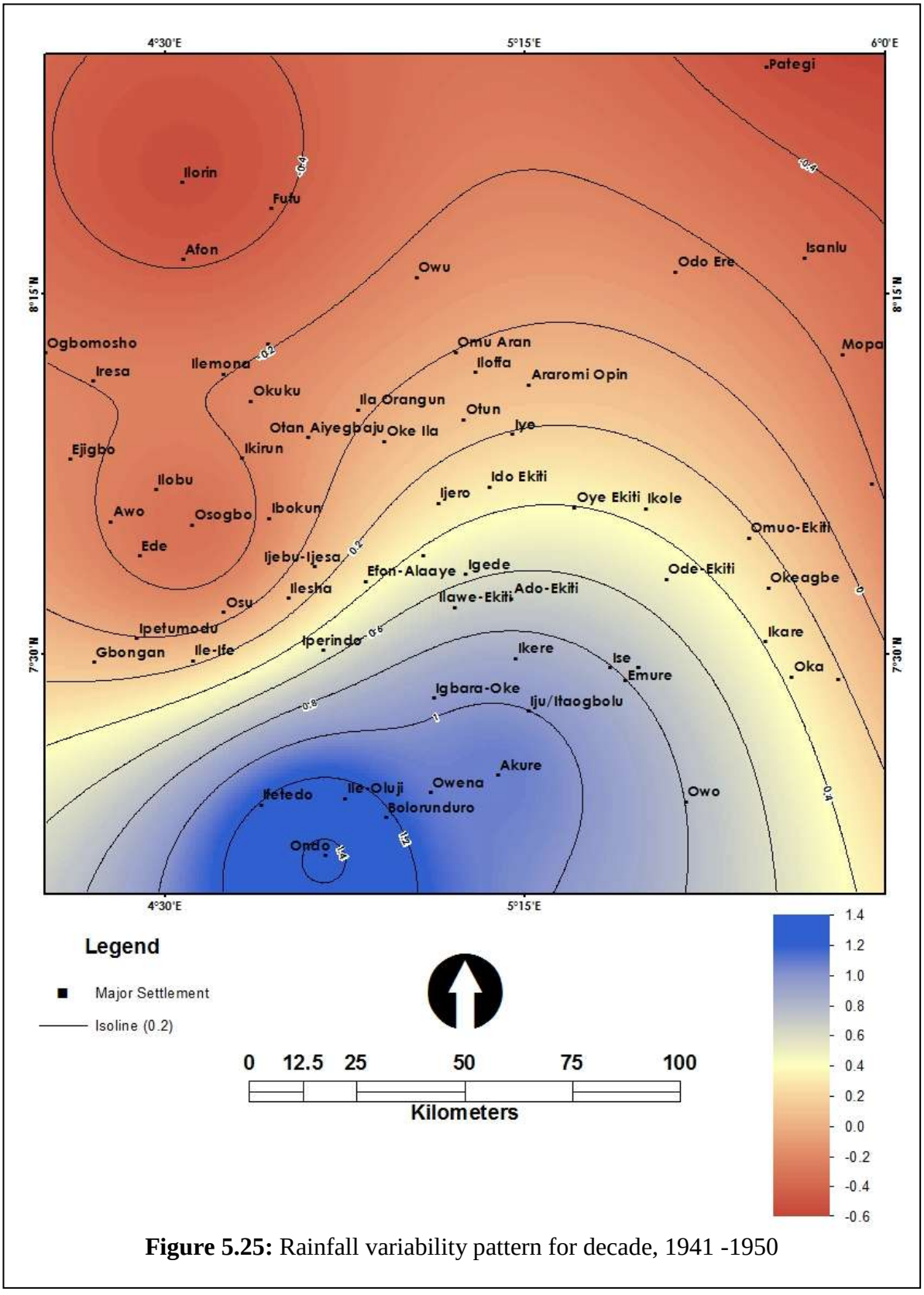

Figure 5.25: Rainfall variability pattern for decade, 1941 -1950

Source: Author, 2015

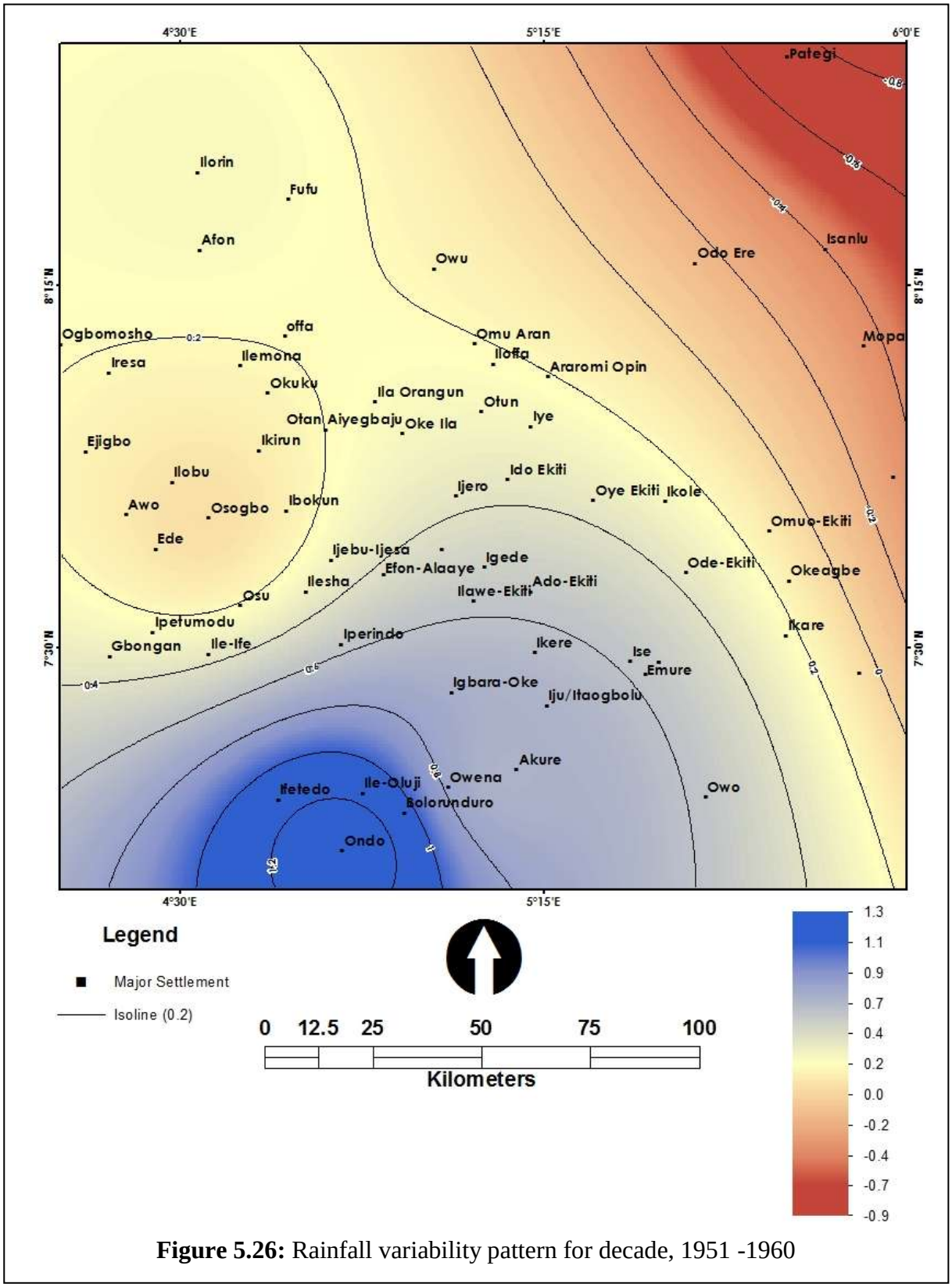

Figure 5.26: Rainfall variability pattern for decade, 1951 -1960

Source: Author, 2015

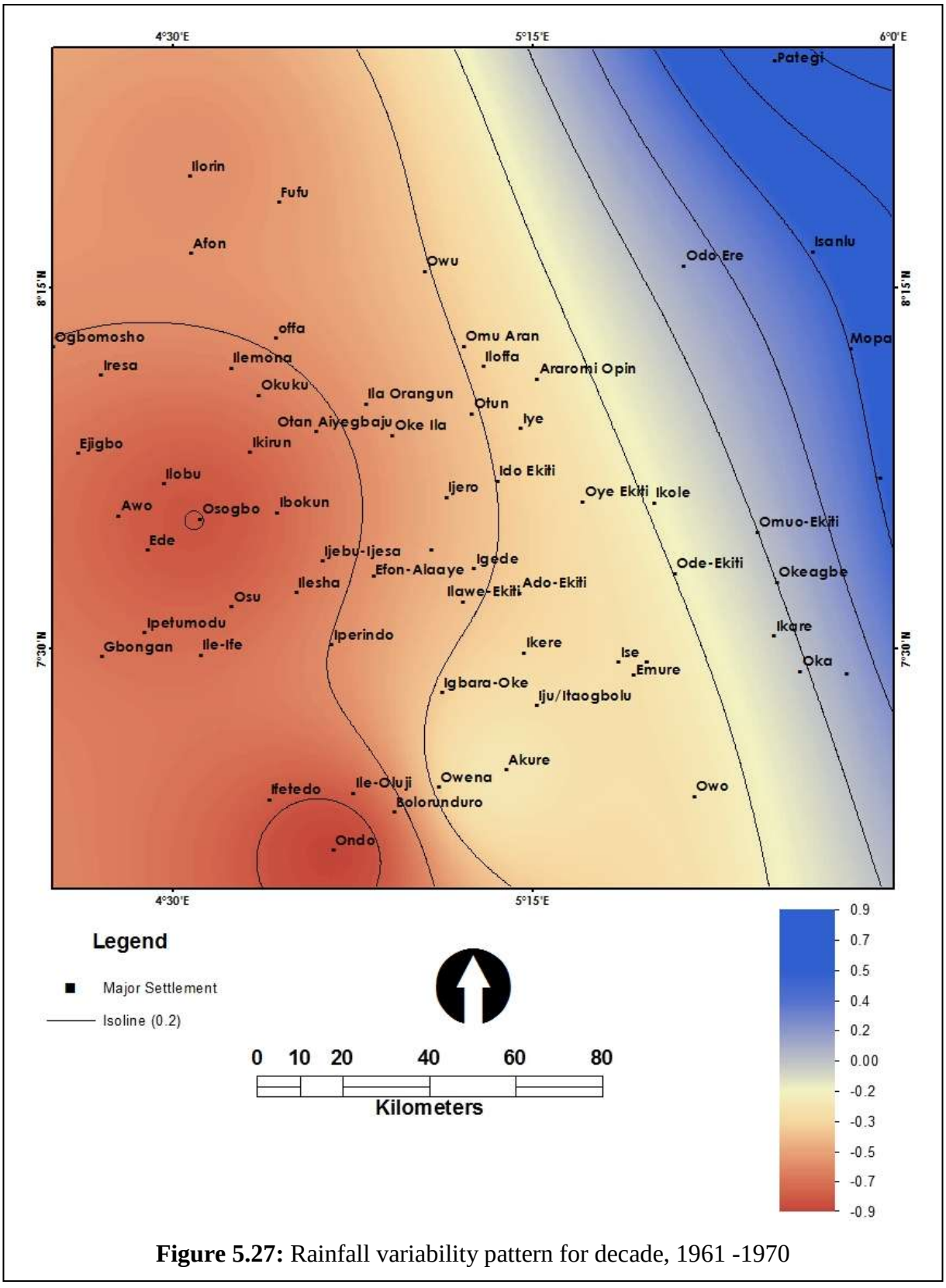

Figure 5.27: Rainfall variability pattern for decade, 1961 -1970

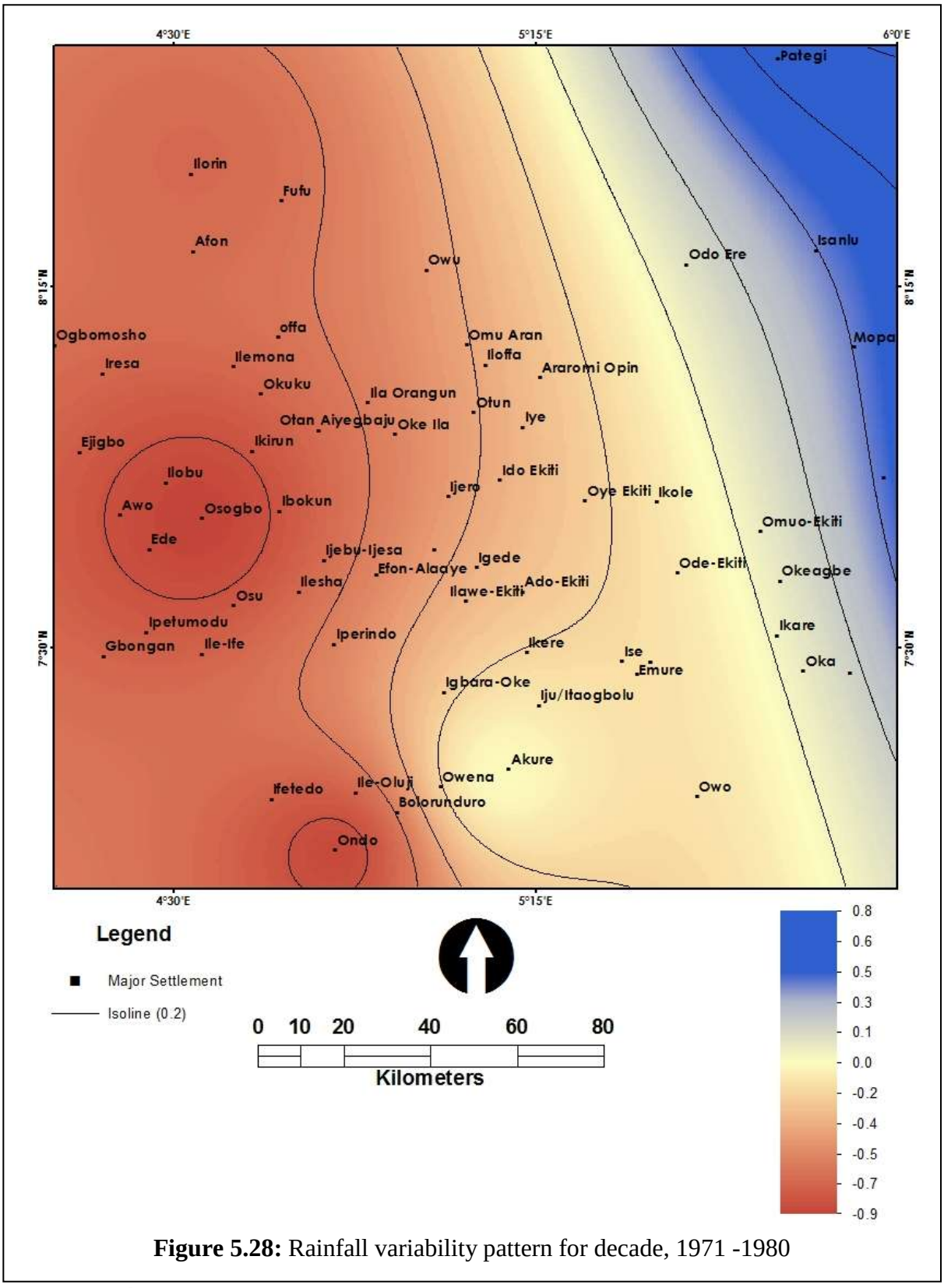

Figure 5.28: Rainfall variability pattern for decade, 1971 -1980

Source: Author, 2015

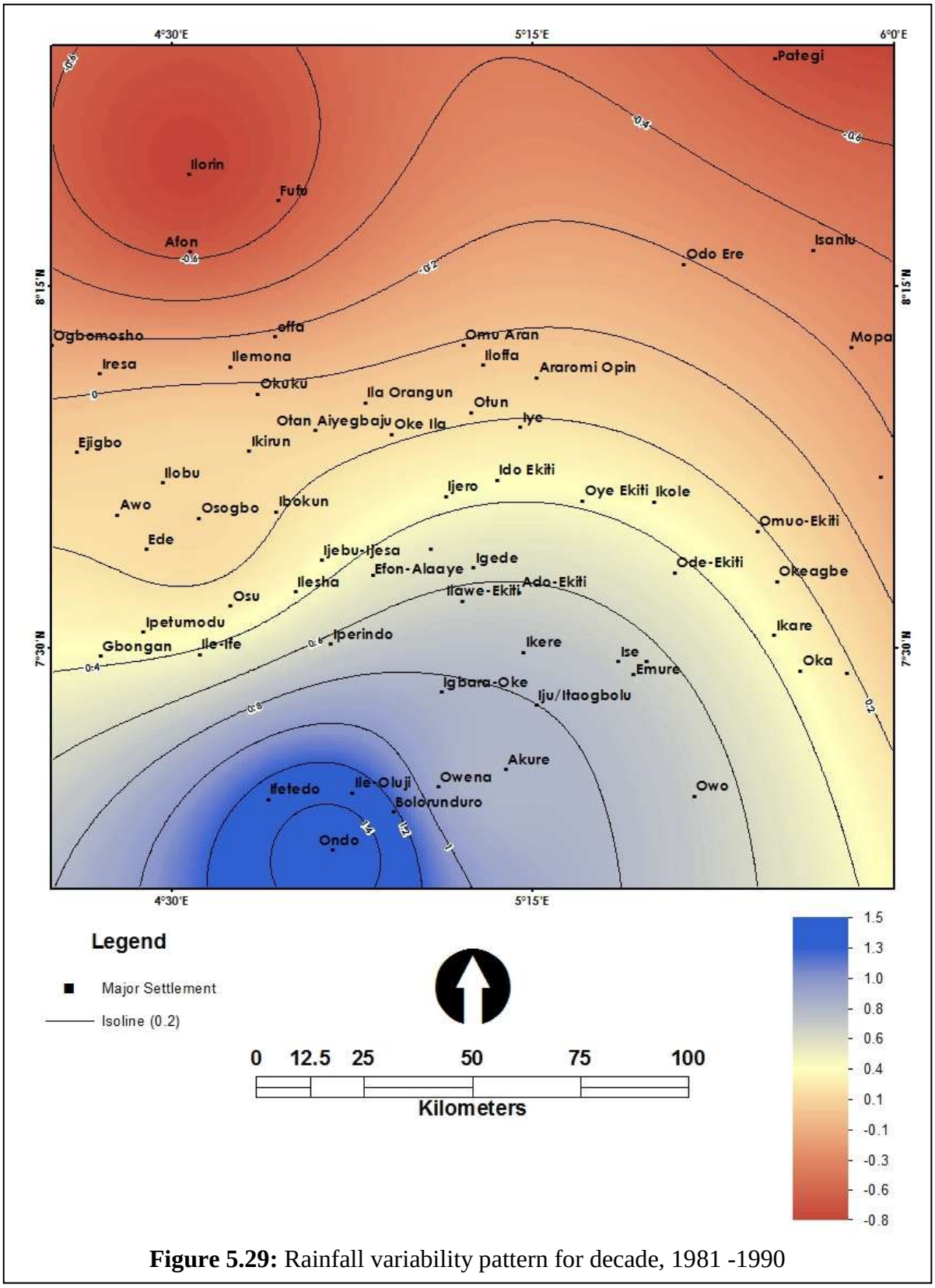

Figure 5.29: Rainfall variability pattern for decade, 1981 -1990

Source: Author, 2015

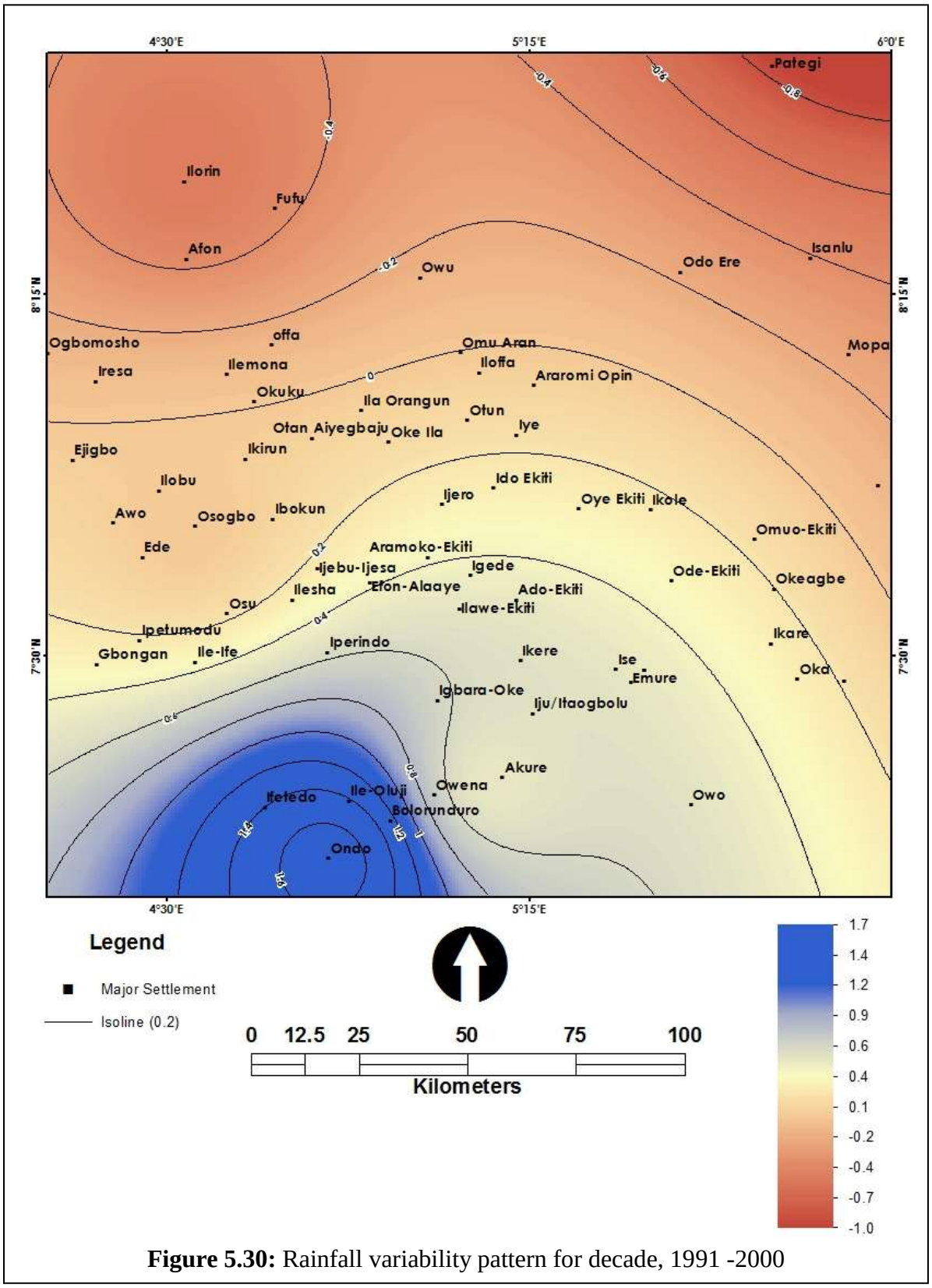

Figure 5.30: Rainfall variability pattern for decade, 1991 -2000

(Author, 2015)

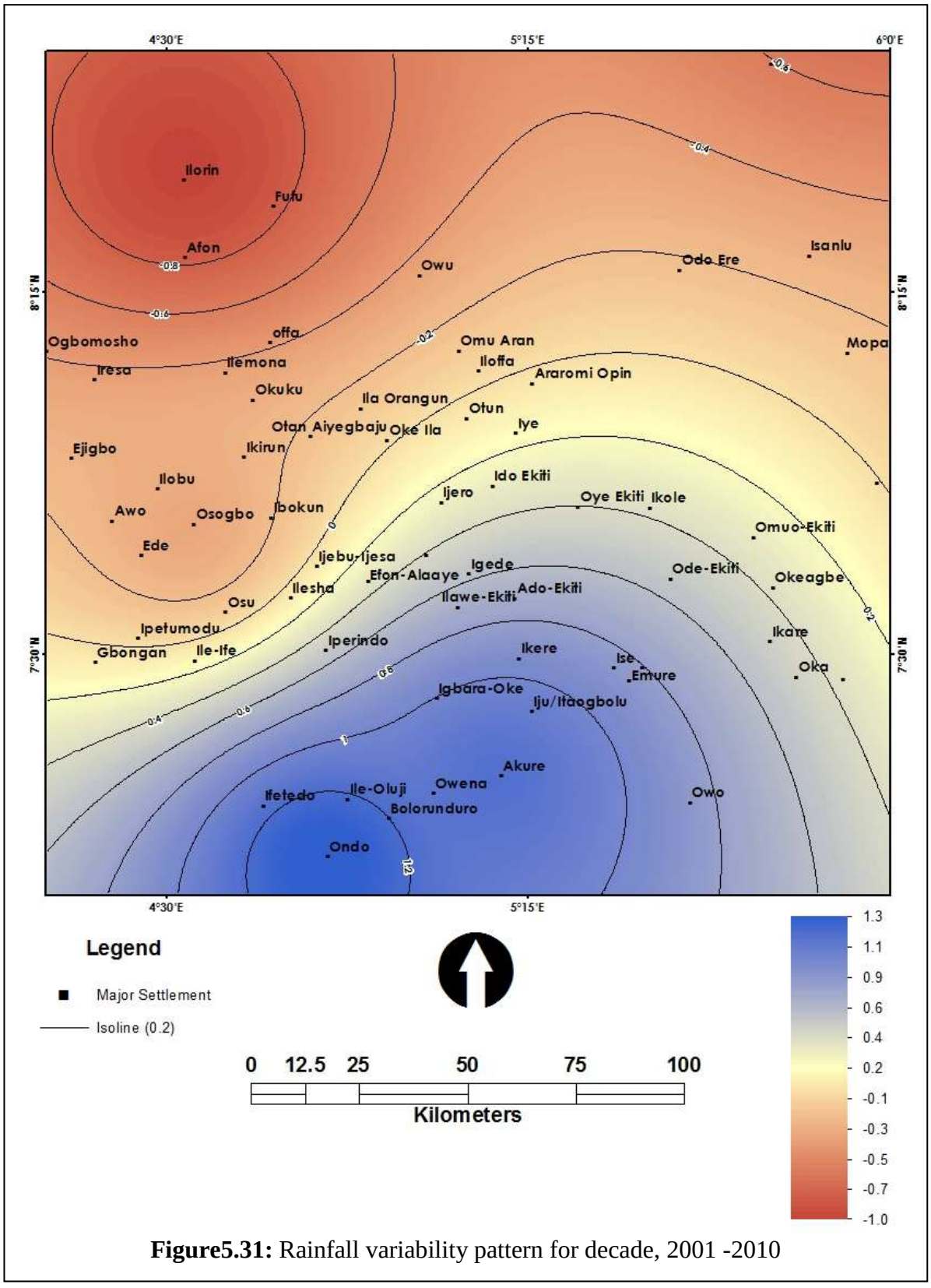

Figure5.31: Rainfall variability pattern for decade, 2001 -2010

Source: Author, 2015

The decadal rainfall variability shows a positive trend and increase at a rate of 0.19% per decade as presented in figure 5.24. The driest and wettest decade for the study area were recorded in the 1941 - 1950 and 1961 – 1970. However, there are differences in the spatio-temporal patterns, looking at the variability indices on the decadal basis as in Figure5.25 to 5.31. These show that the study area experienced moderately wet period in the southern part for most of the decade except in the decades 1961 – 1970 and 1971 – 1980 when the entire area experienced moderately dry periods.

5.5.2 Temporal patterns of temperature Variability

Figures 5.32 and 5.33 present the annual and decadal temperature variability indices pattern of the derived savannah for the present climate respectively. The range of annual temperature variability indices is from -1.64 and 2.64 and positive trend for the present climate as shown in Figure5.33. Similar to the findings of Akinsanola and Ogunjobi (2014), the study area experienced a continuous cold and sporadic warm period or low and high temperature variability between 1945 and 1970 and 1971 and 2010 respectively.

Similarly, there are some noticeable differences in the spatial patterns of the temperature variability within the decades as shown in figure 5.33. Also, decadal variability reveals that the study area experienced cold and warm periods during the first four and last three decades of the present climate. This result is in agreement with the findings of Abiodun *et al.*, (2012), Oguntunde *et al.* (2011), and Akinsanola & Ogunjobi (2014). In addition, the spatial patterns of the decadal temperature variability show that the study area experienced colder and warmer periods for most of the decades as depicted in figure 5.34 to 5.40. For decades of 40s, 50s 60s and 70s, Oshogbo experienced colder periods and recorded variability index ranges of -0.9 to -1.3, while Ondo recorded lowest temperature variability index of -1 for 80s

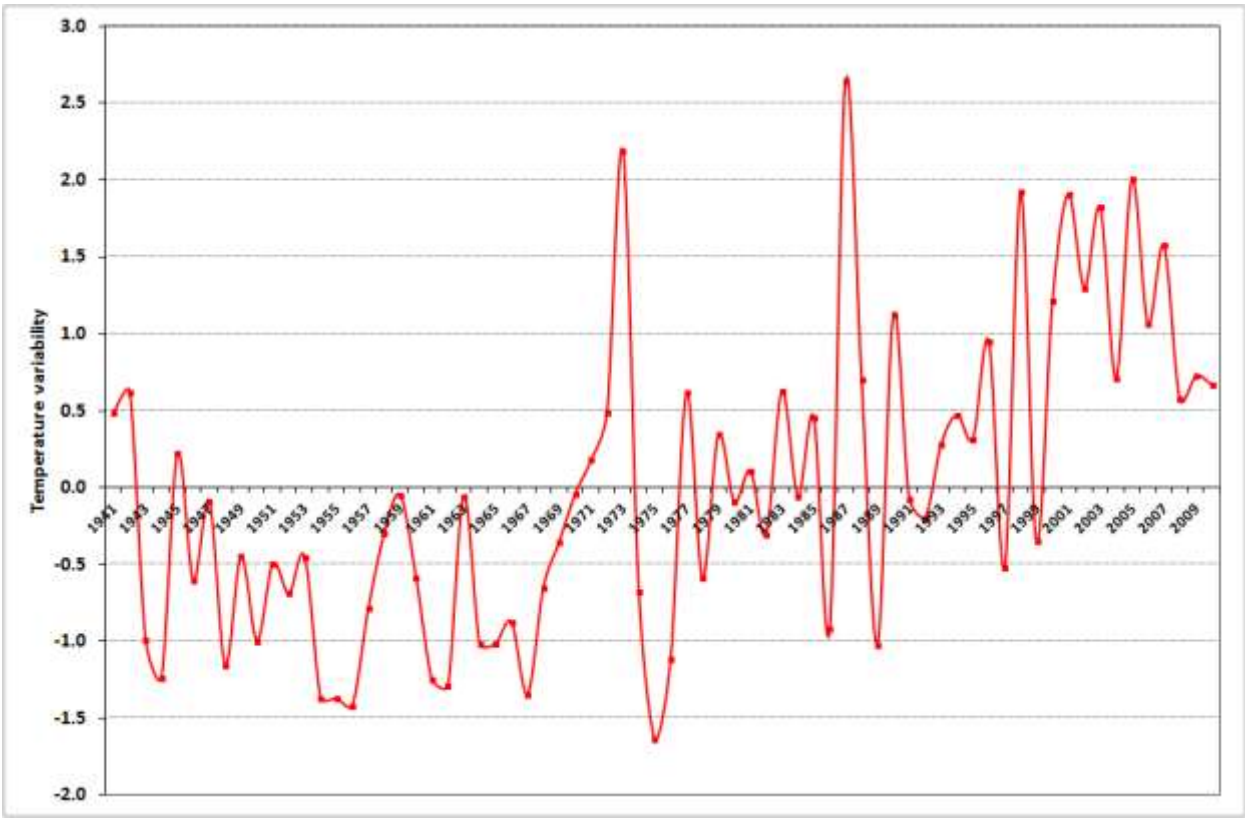

Figure 5.32: Annual temperature variability index for present climate (1941 – 2010) *(Author, 2015)*

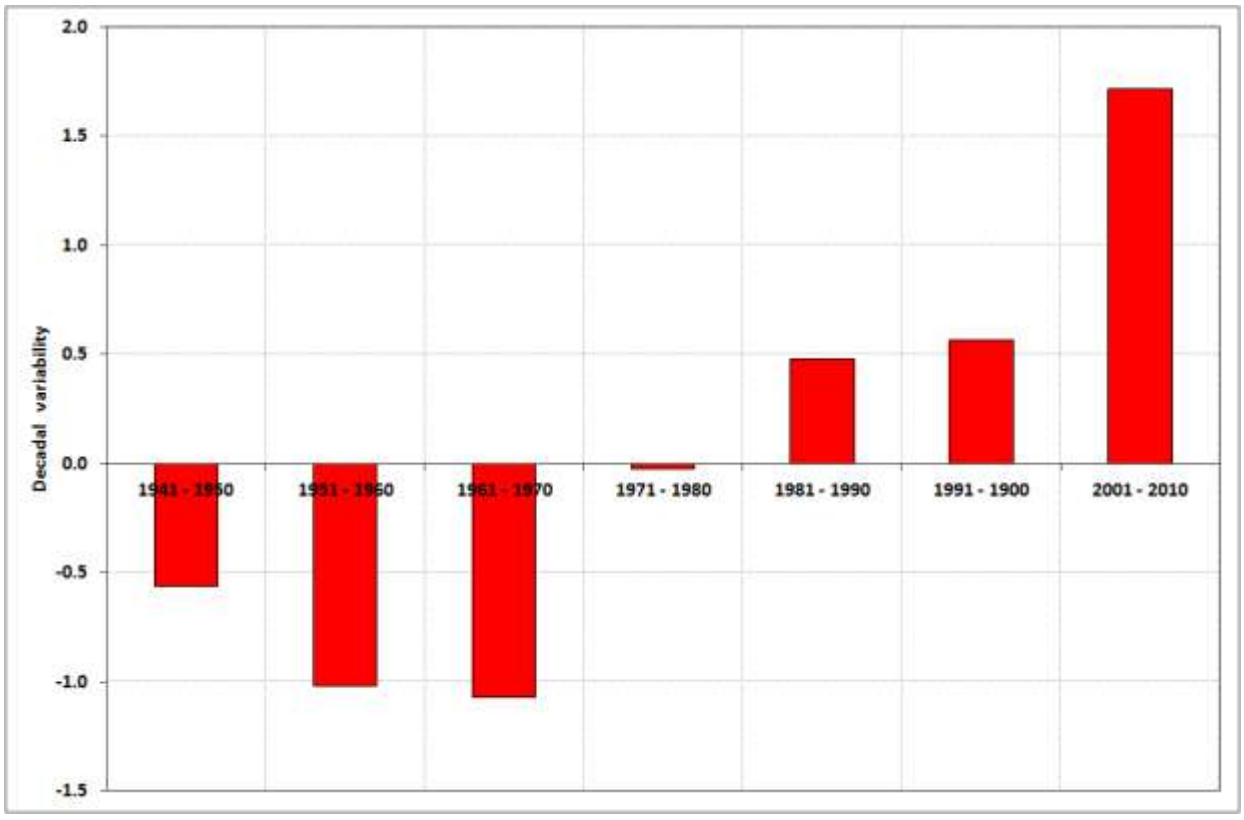

Figure 5.33: Decadal temperature variability index for present climate (1941 – 2010) *(Author, 2015)*

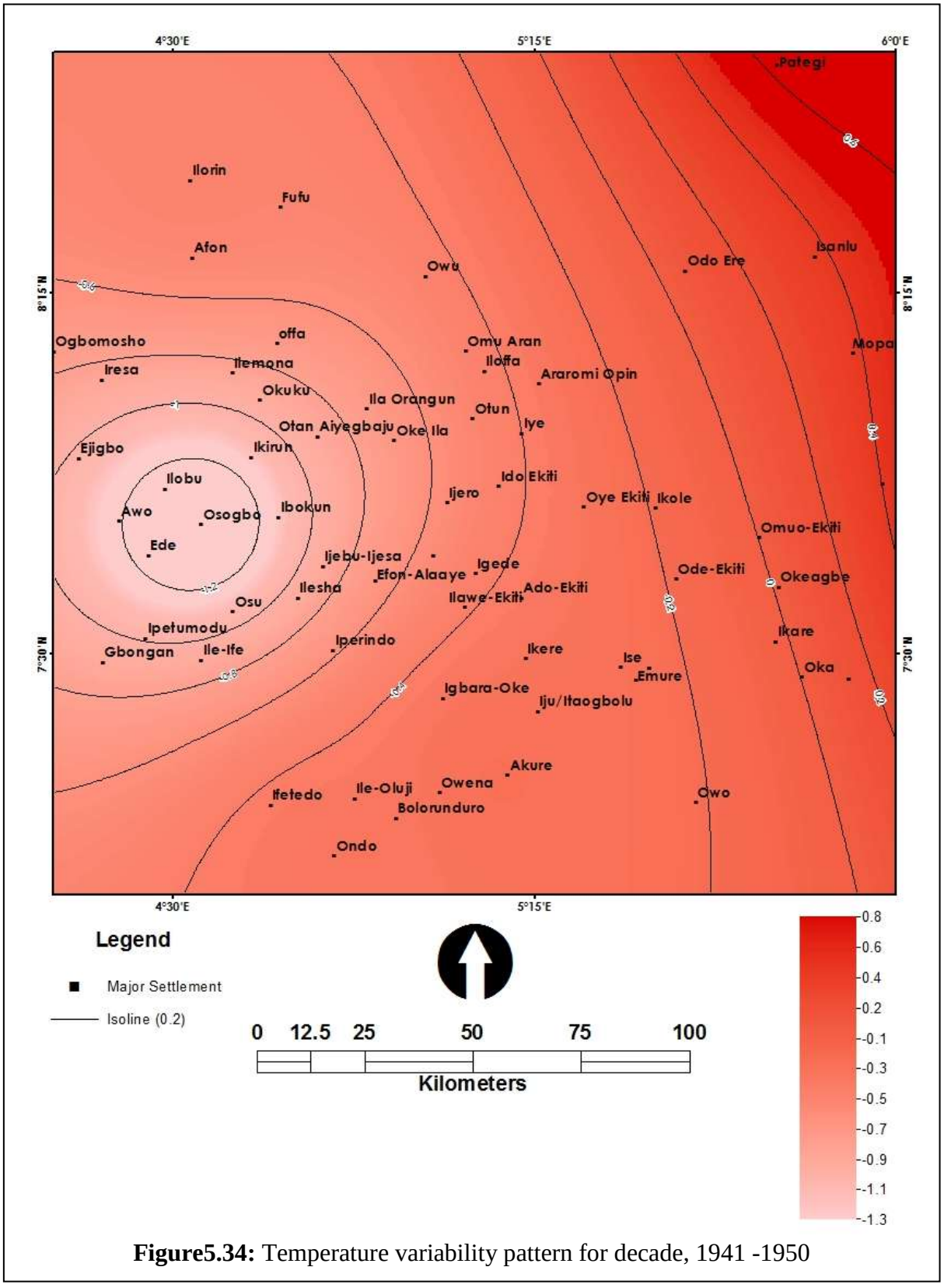

Figure5.34: Temperature variability pattern for decade, 1941 -1950

Source: Author, 2015

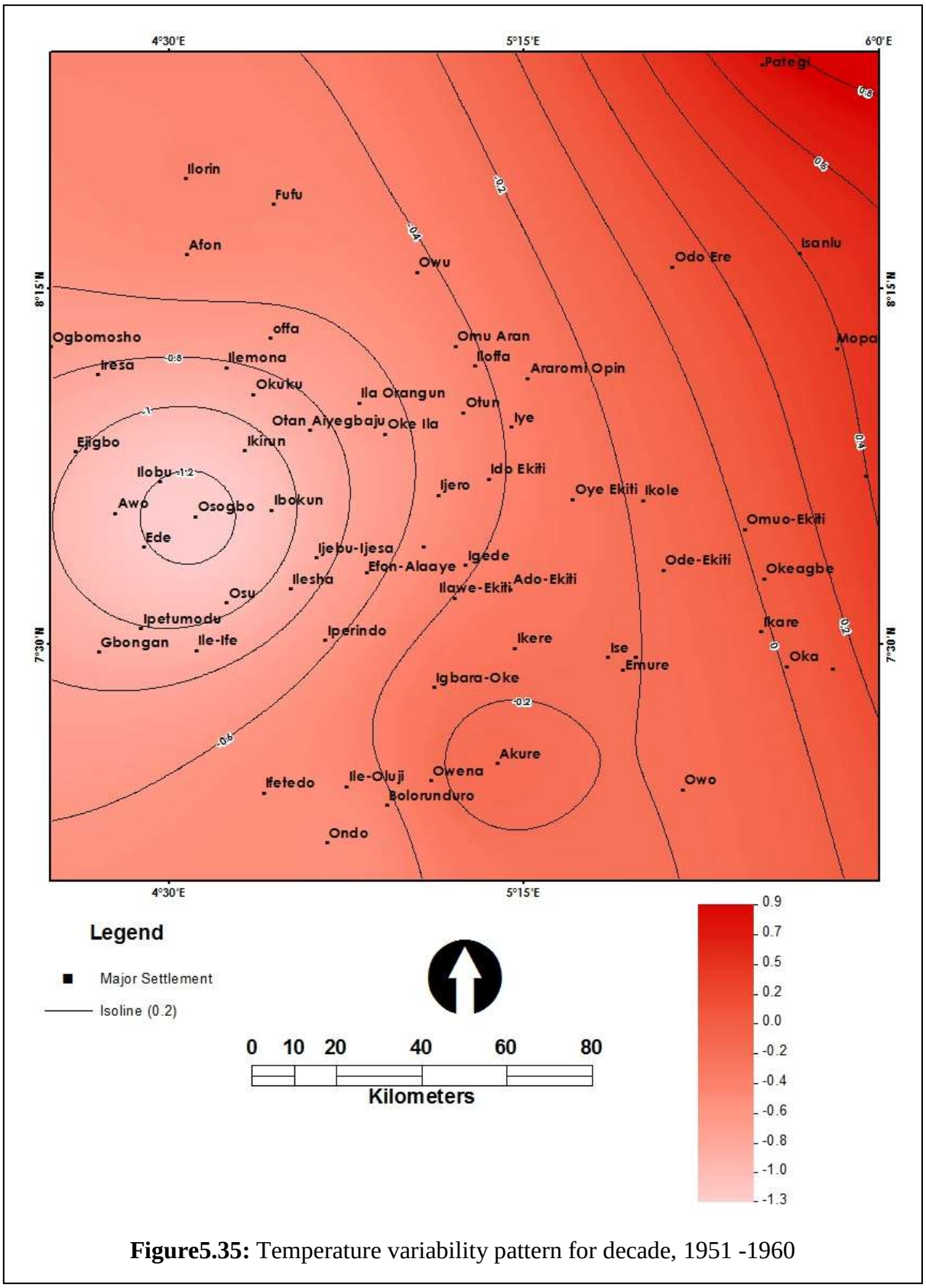

Figure5.35: Temperature variability pattern for decade, 1951 -1960

Source: Author, 2015

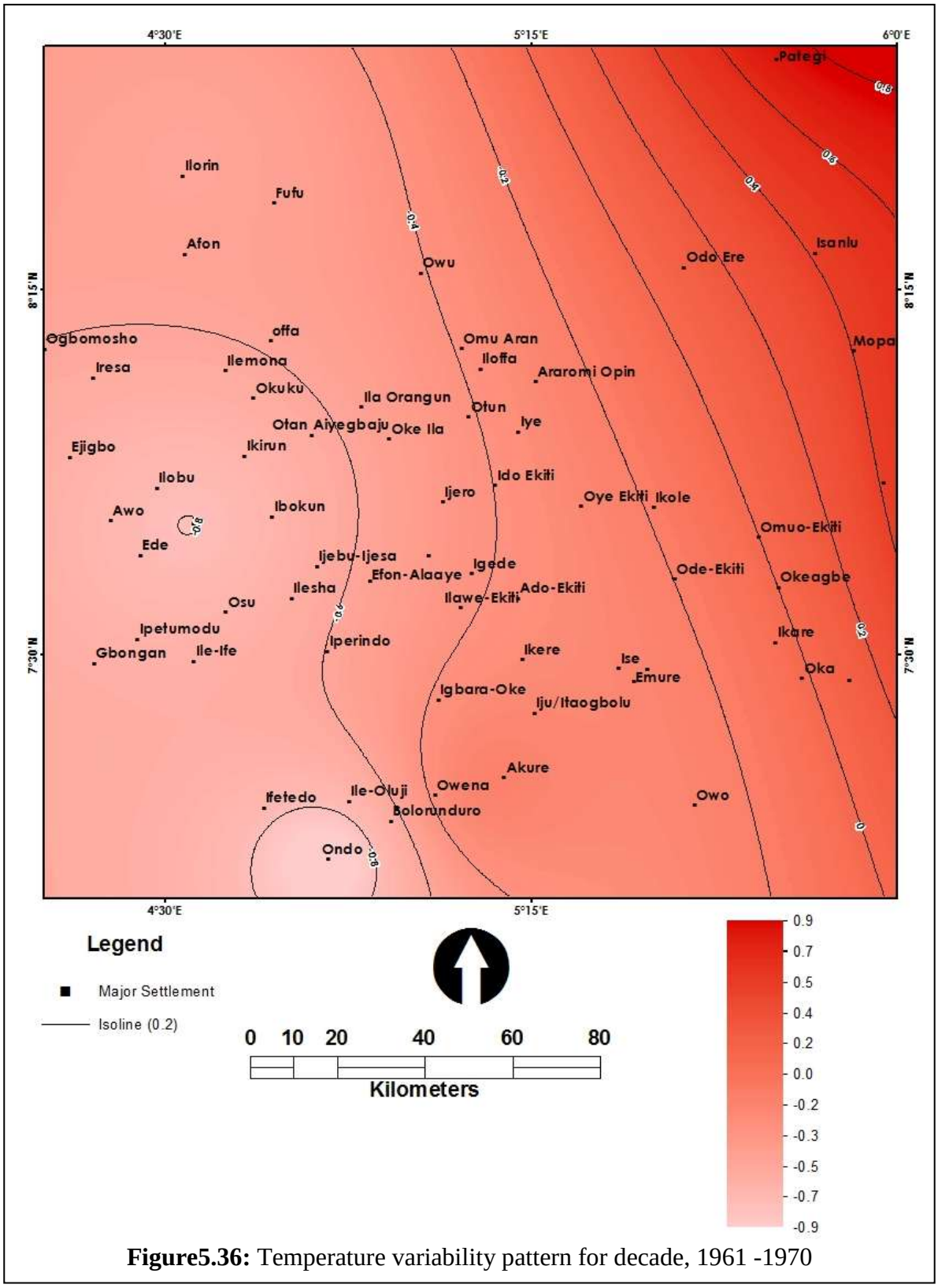

Figure5.36: Temperature variability pattern for decade, 1961 -1970

Source: Author, 2015

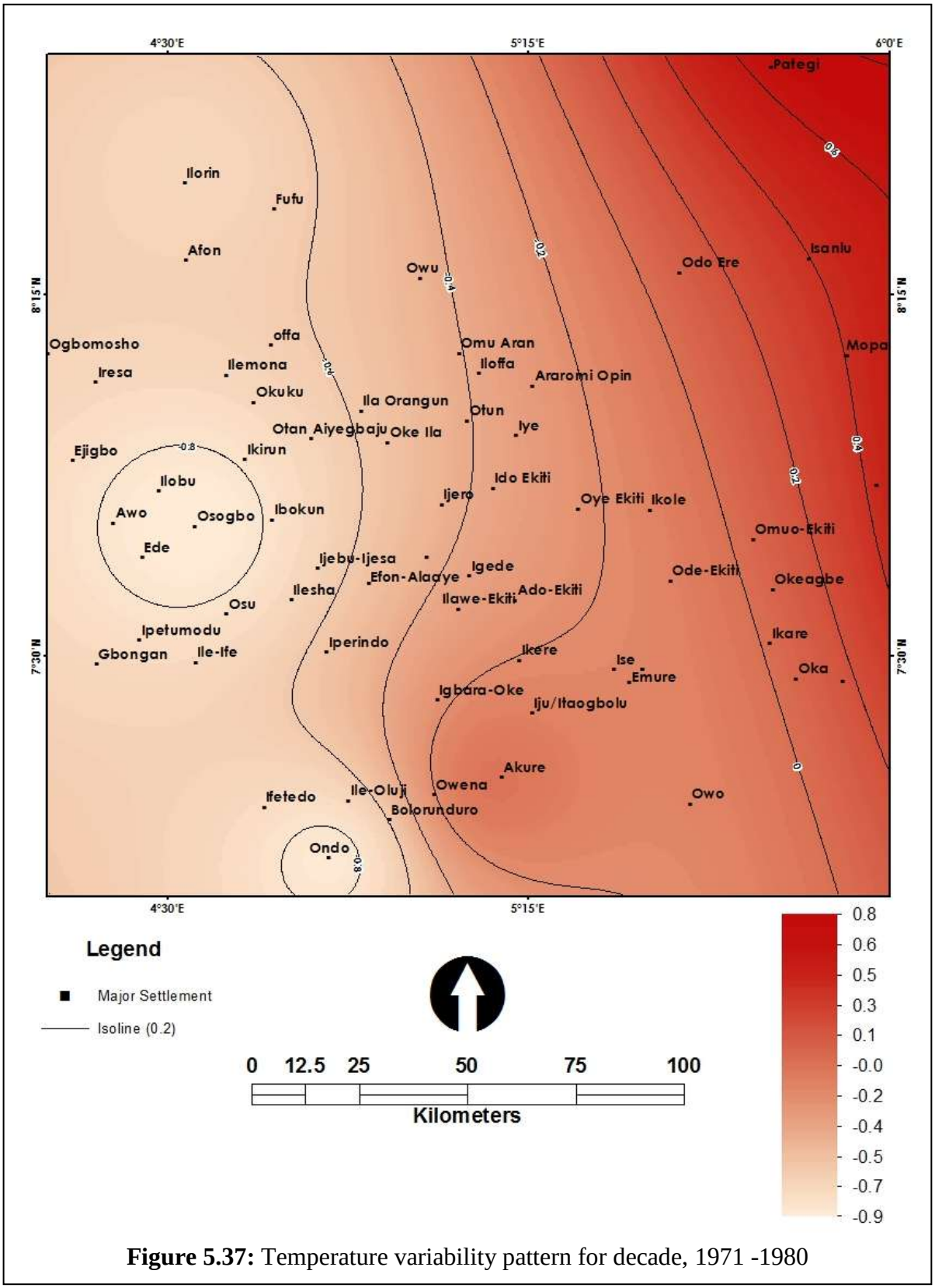

Figure 5.37: Temperature variability pattern for decade, 1971 -1980

Source: Author, 2015

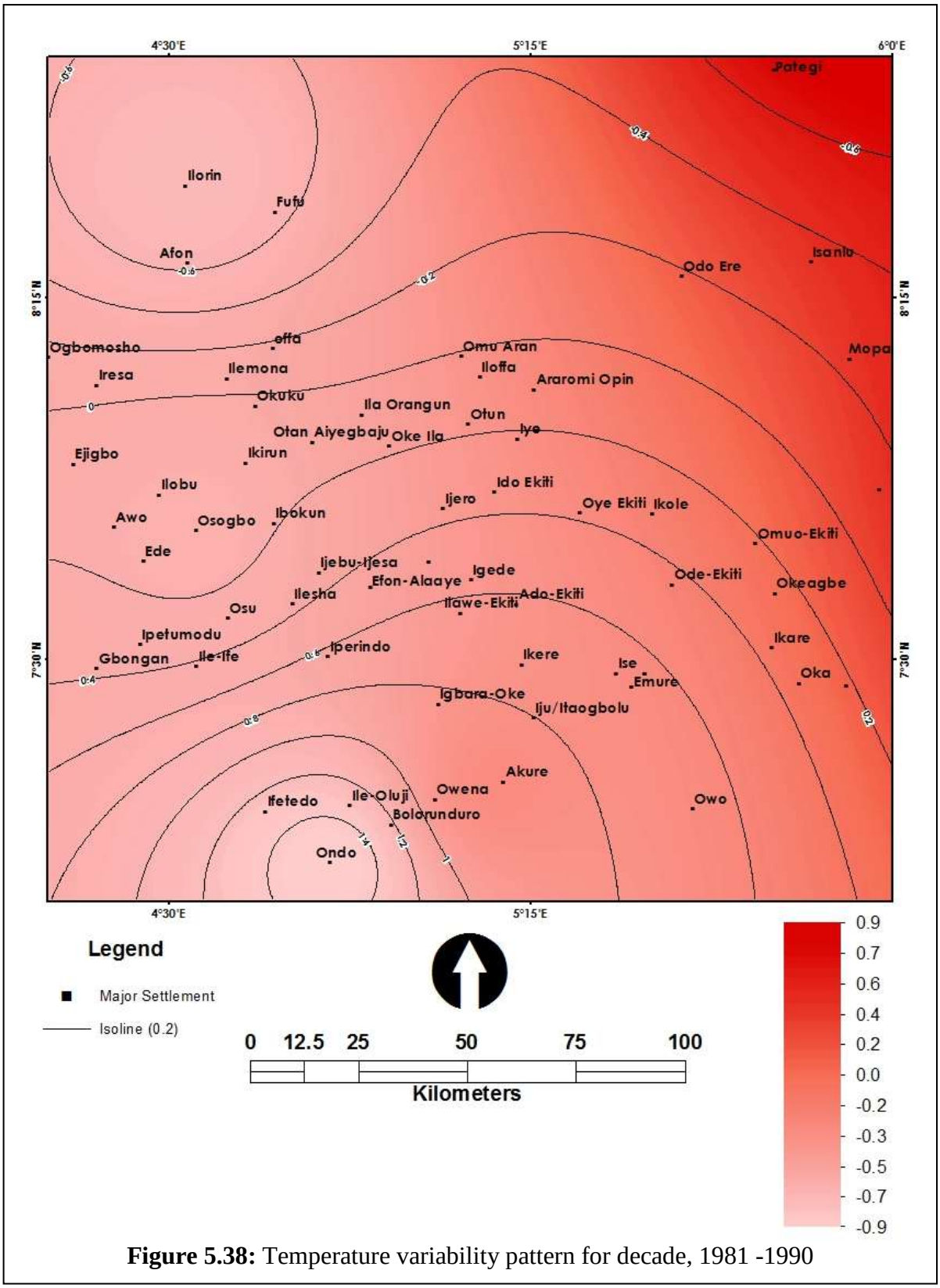

Figure 5.38: Temperature variability pattern for decade, 1981 -1990

Source: Author, 2015

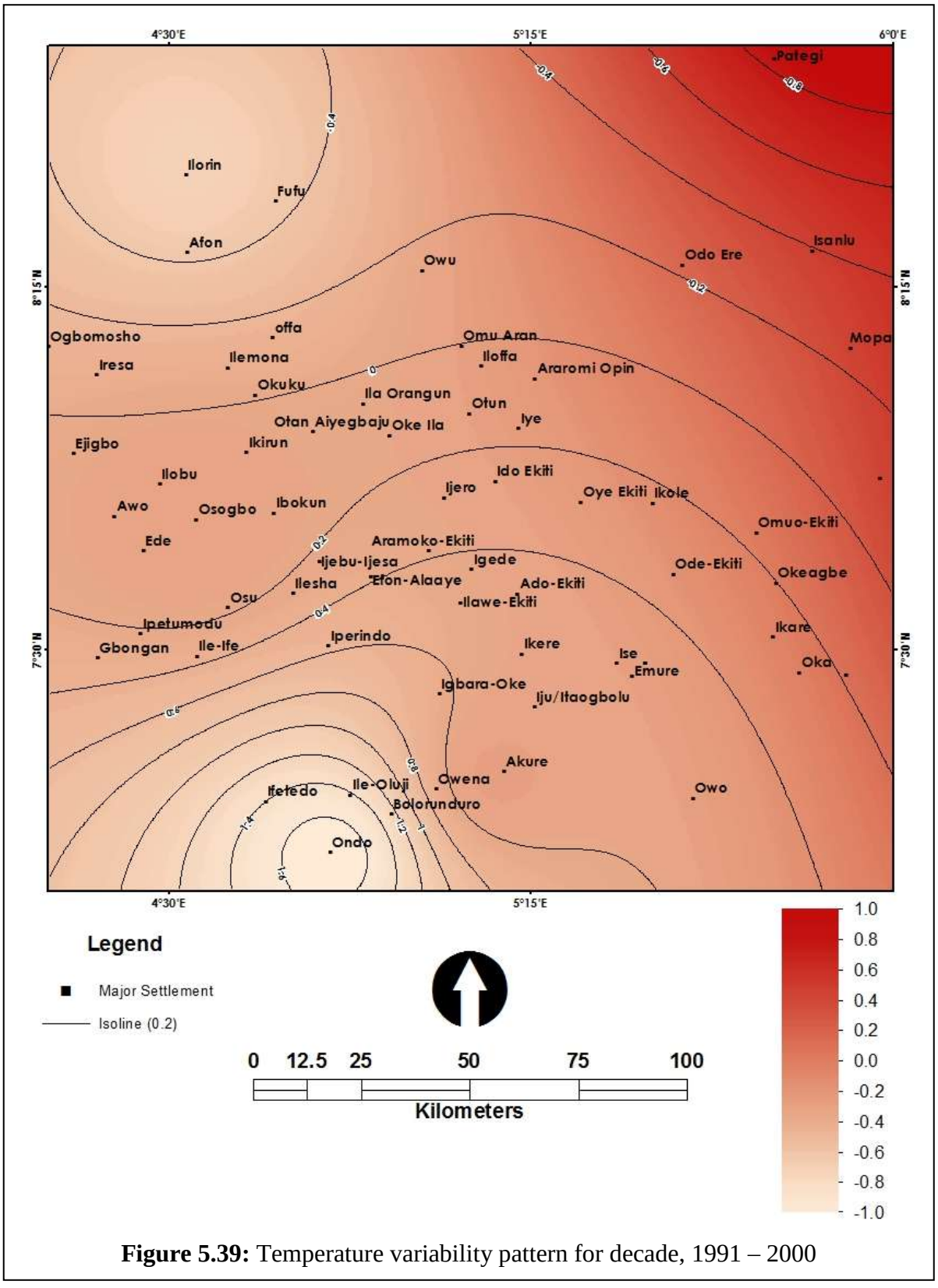

Figure 5.39: Temperature variability pattern for decade, 1991 – 2000

Source: Author, 2015

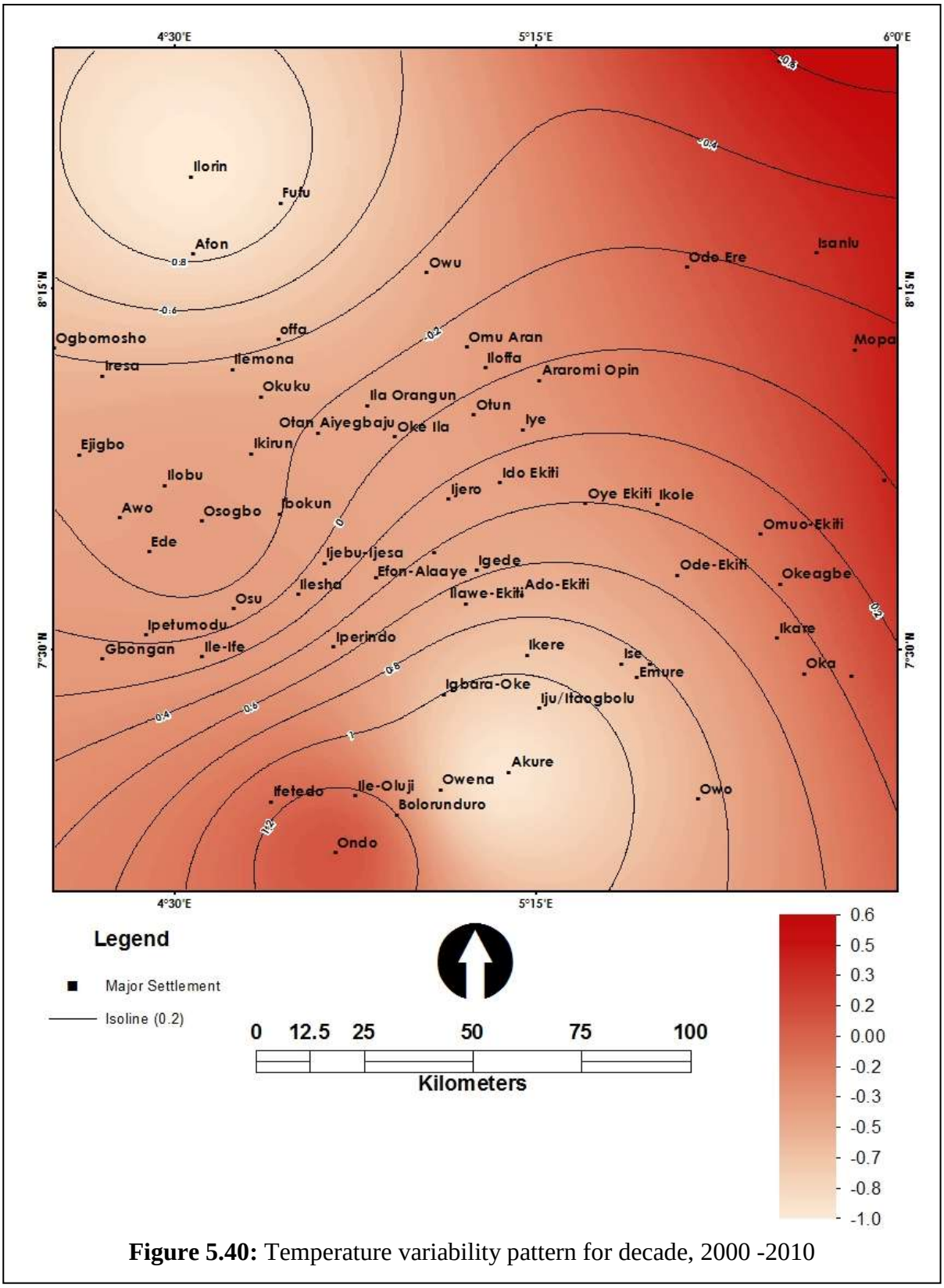

Figure 5.40: Temperature variability pattern for decade, 2000 -2010

Source: Author, 2015

and 90s decades. However, the north eastern end of the area records the highest temperature variability index throughout during present climate.

5.6 Temporal Patterns of the Future Rainfall and Temperature Variability

5.6.1 Temporal patterns of rainfall variability

Annual and decadal rainfall variability indices pattern of the study area for the future climate are shown in figures 5.42 and 5.42 respectively. Annual rainfall variability indices during the future climate (2011 – 2050) will vary between -2.73 and 2.85 meaning that the area will experience extremely wet and dry respectively. For about 52.5% of the period, the area will record low rainfall variability. However, decadal variability index of rainfall will be slightly different, varying between -1.1 and 1.3. Moderate wet and dry will be recorded in the decades of 2010s and 2040s respectively as shown in figure 5.42

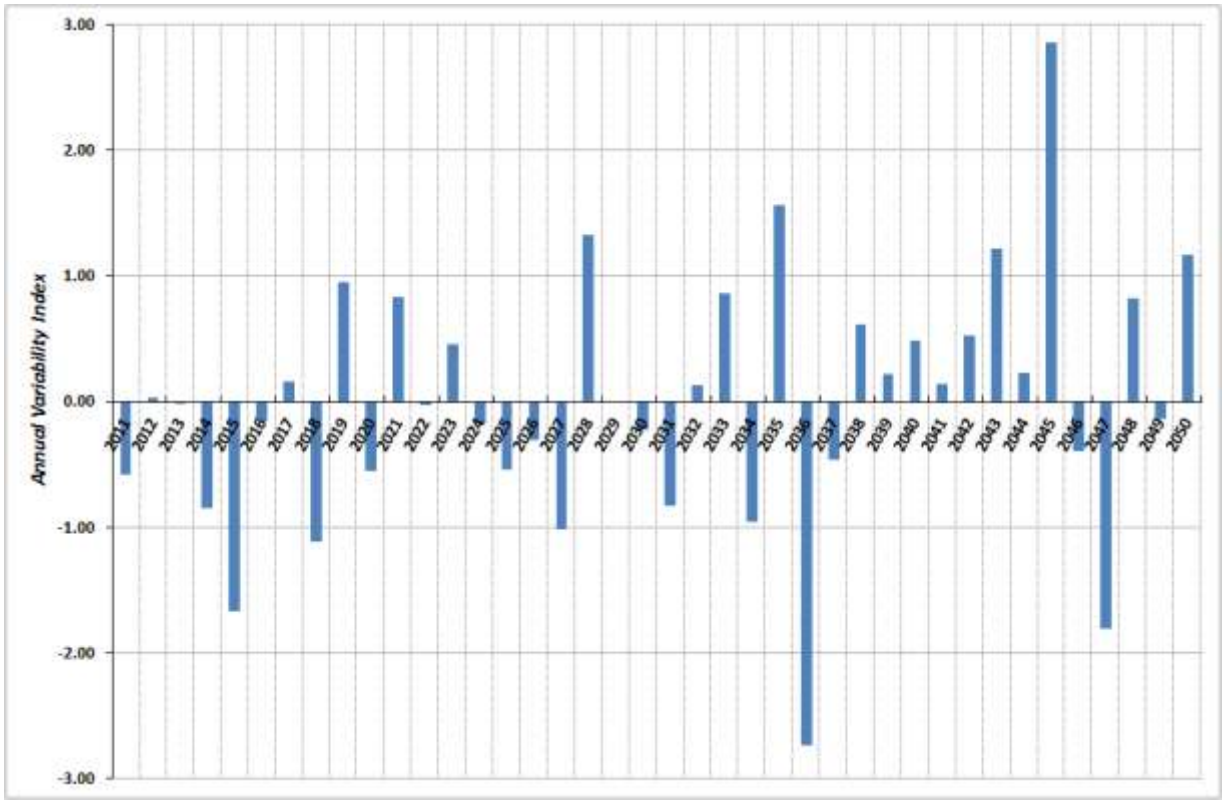

Figure 5.41: Annual rainfall variability index for future climate (2011 – 2050) *(Author, 2015)*

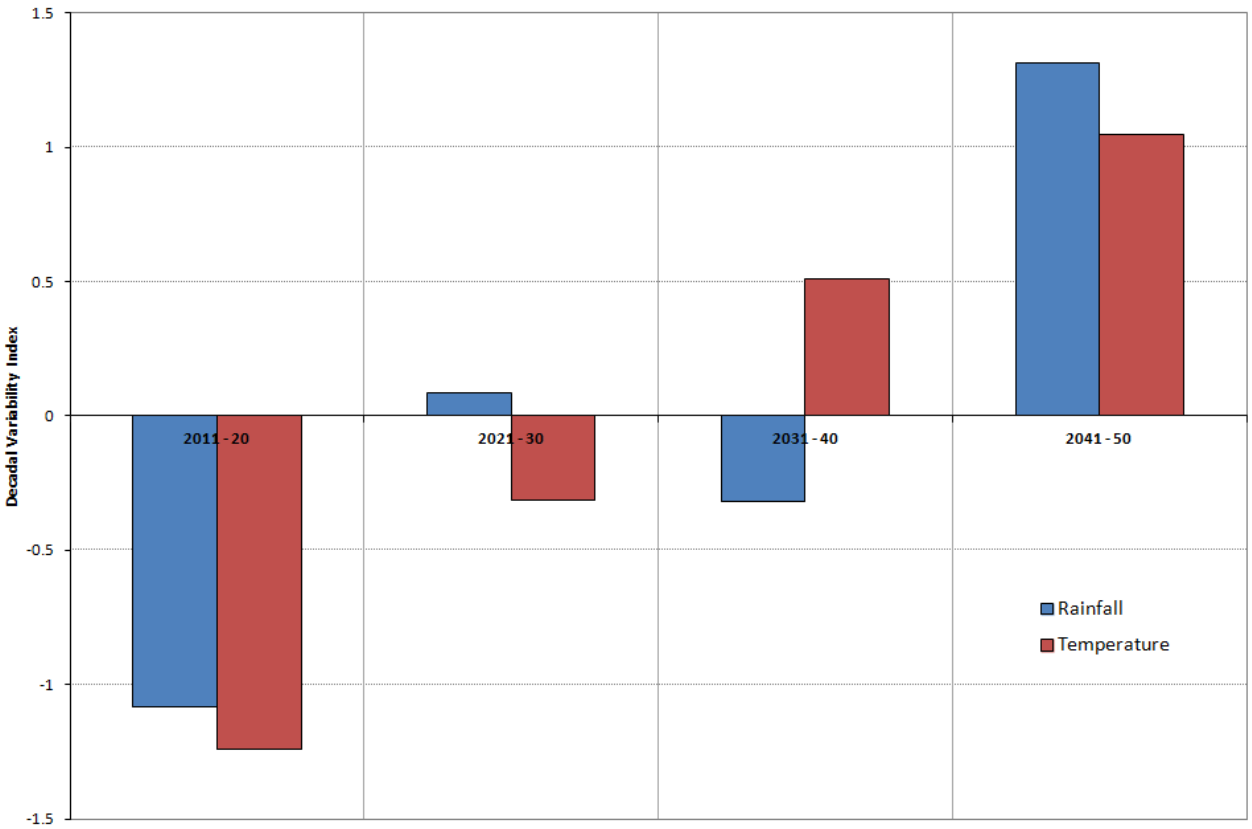

Figure 5.42: Decadal rainfall and temperature variability index for the future climate (2011 – 2050) *(Author, 2015)*

The spatial pattern of the decadal rainfall variability paints a different picture as in figures 5.43 to 5.46. Figure 5.43 shows that the decade of 2011 – 20 will record -0.7 and 1.3 of spatial rainfall variability index, while the spatial rainfall variability index for the decade of 2021 – 30 will vary between -0.8 and 1.2, and so will experience normal and moderately wet period for the decade as shown in Figure5.44. Throughout all the decades, Akure and Ondo will experience moderately wet periods with variability indices ranging between 1.2 and 1.3, while the least variability index of 0.8 will be recorded in Pategi in all the decades.

5.6.2 Temporal patterns of temperature variability

Figures 5.42 and 5.47 show the decadal and annual variability indices of temperature during the future climate. As shown in figure 5.47, the study area will record a positive annual variability trend of temperature in the future with variability indices ranging -2.75 and 2.34.

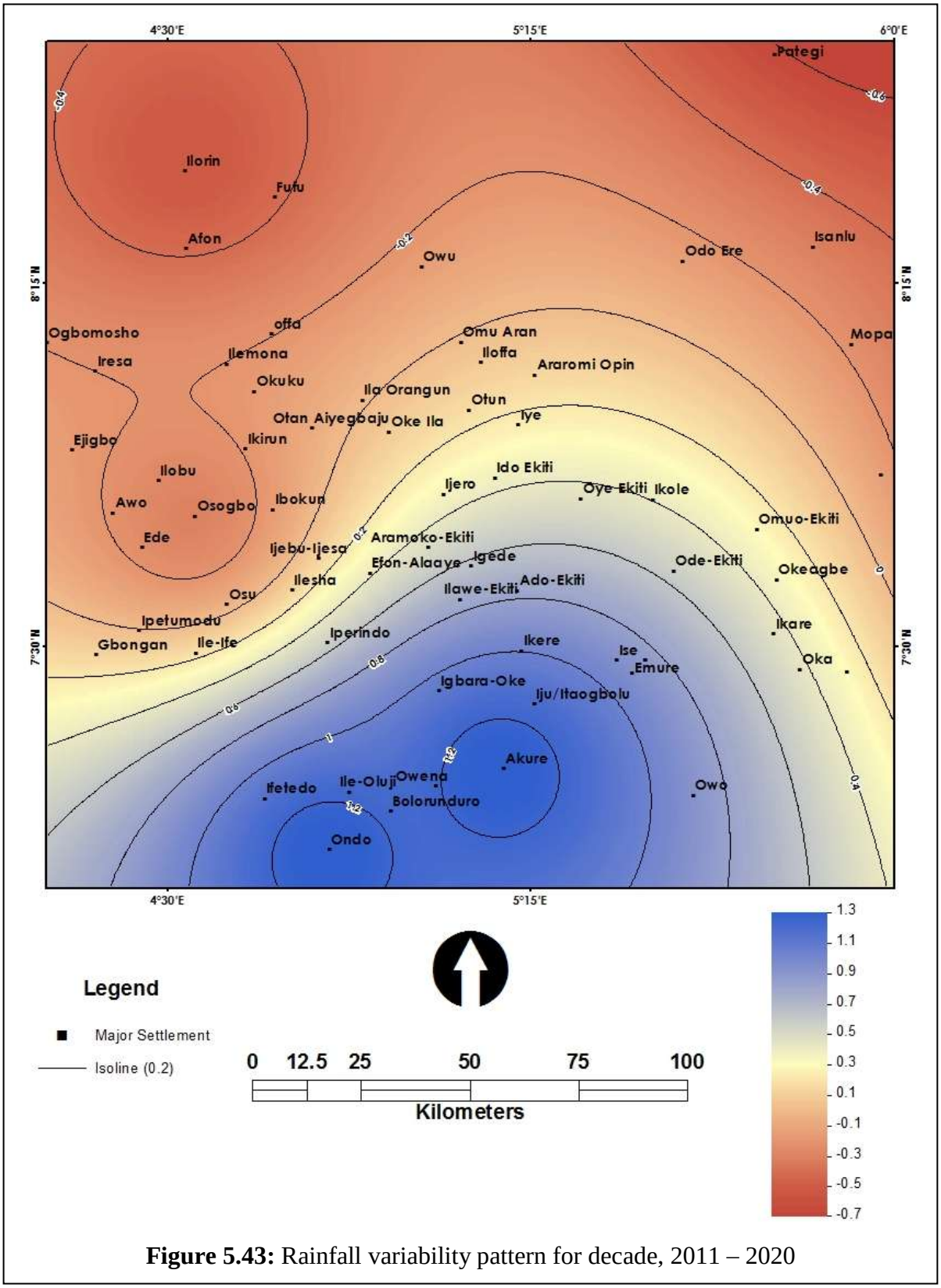

Figure 5.43: Rainfall variability pattern for decade, 2011 – 2020

Source: Author, 2015

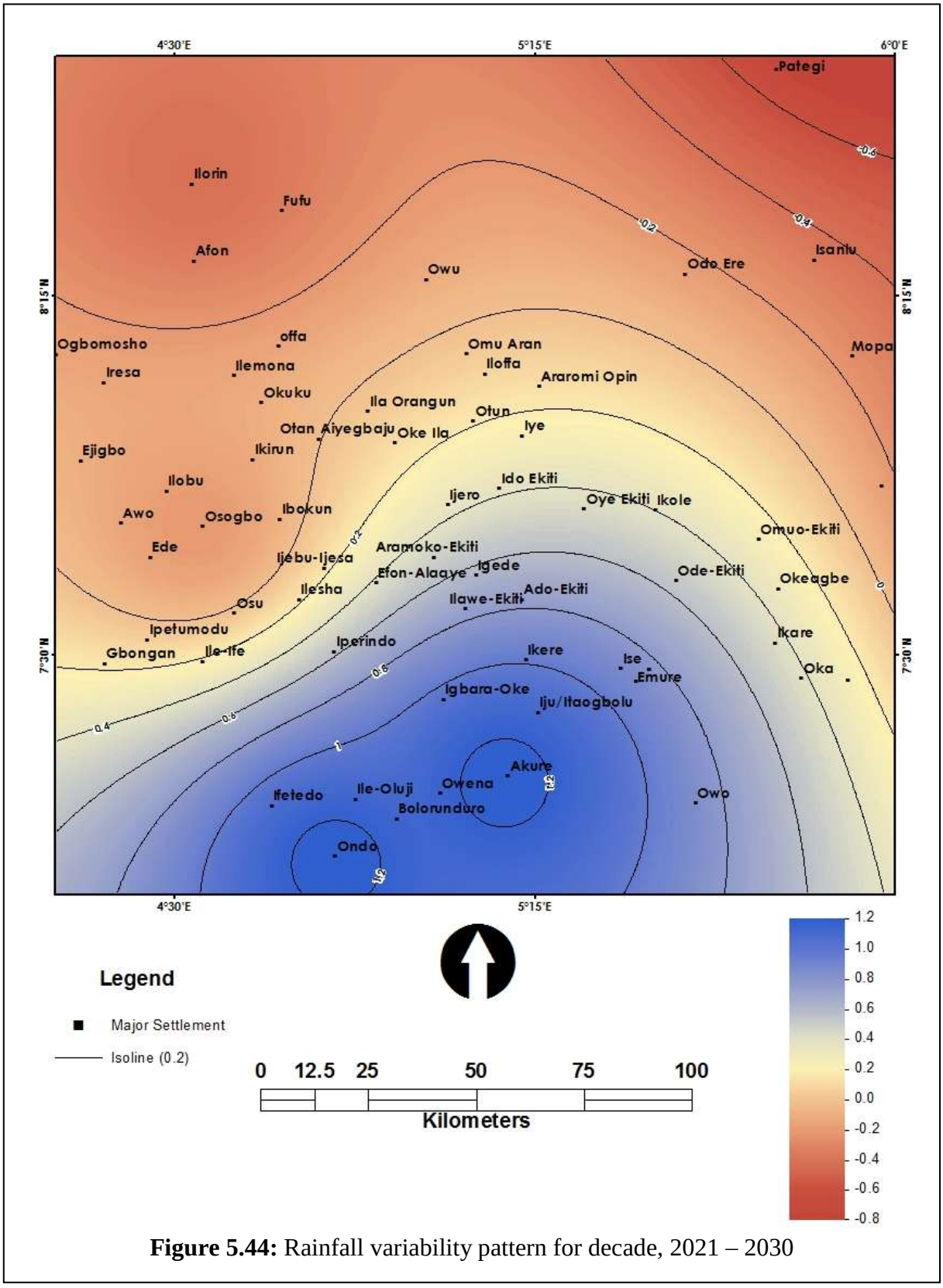

Figure 5.44: Rainfall variability pattern for decade, 2021 – 2030

Source: Author, 2015

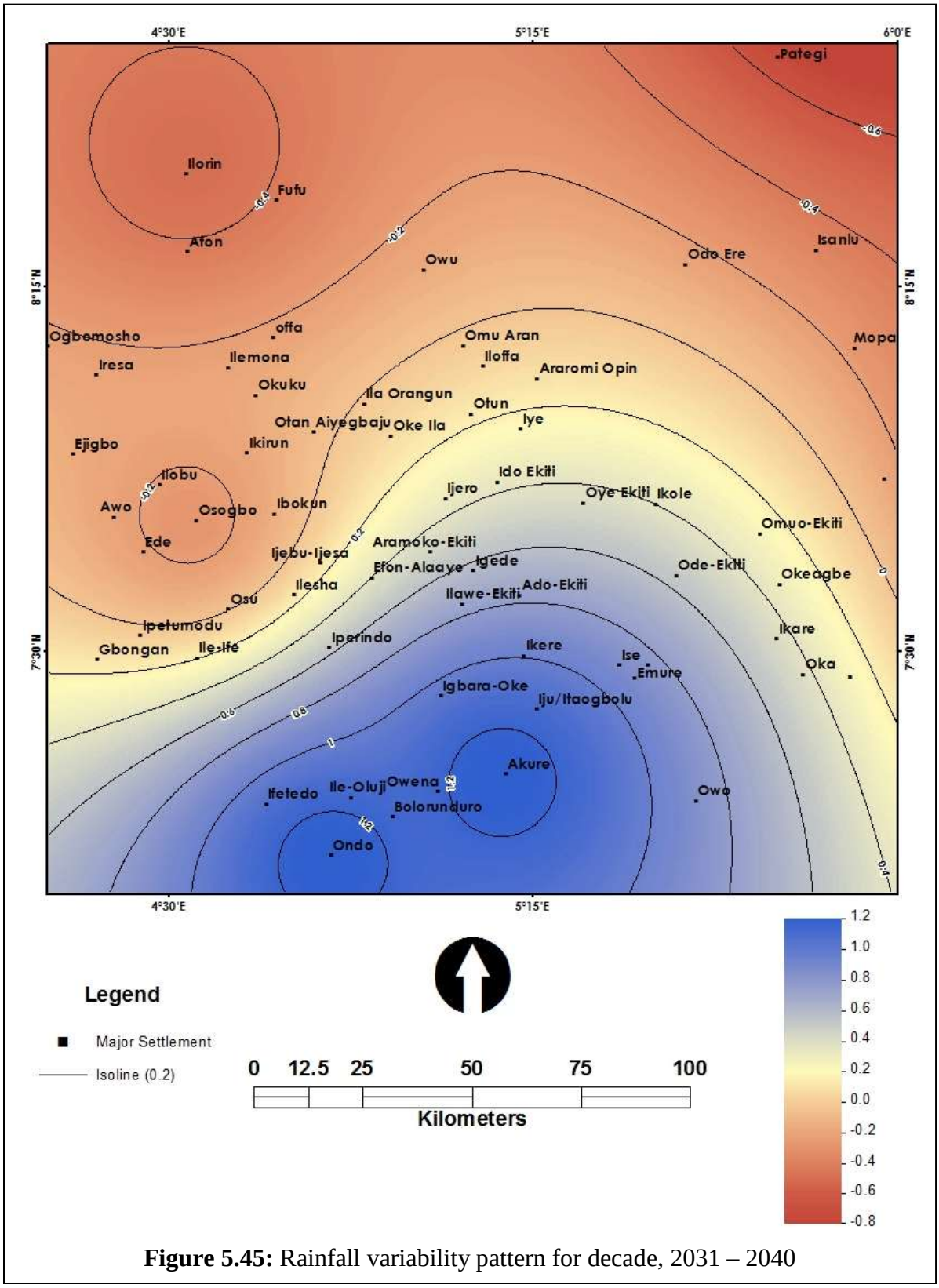

Figure 5.45: Rainfall variability pattern for decade, 2031 – 2040

Source: Author, 2015

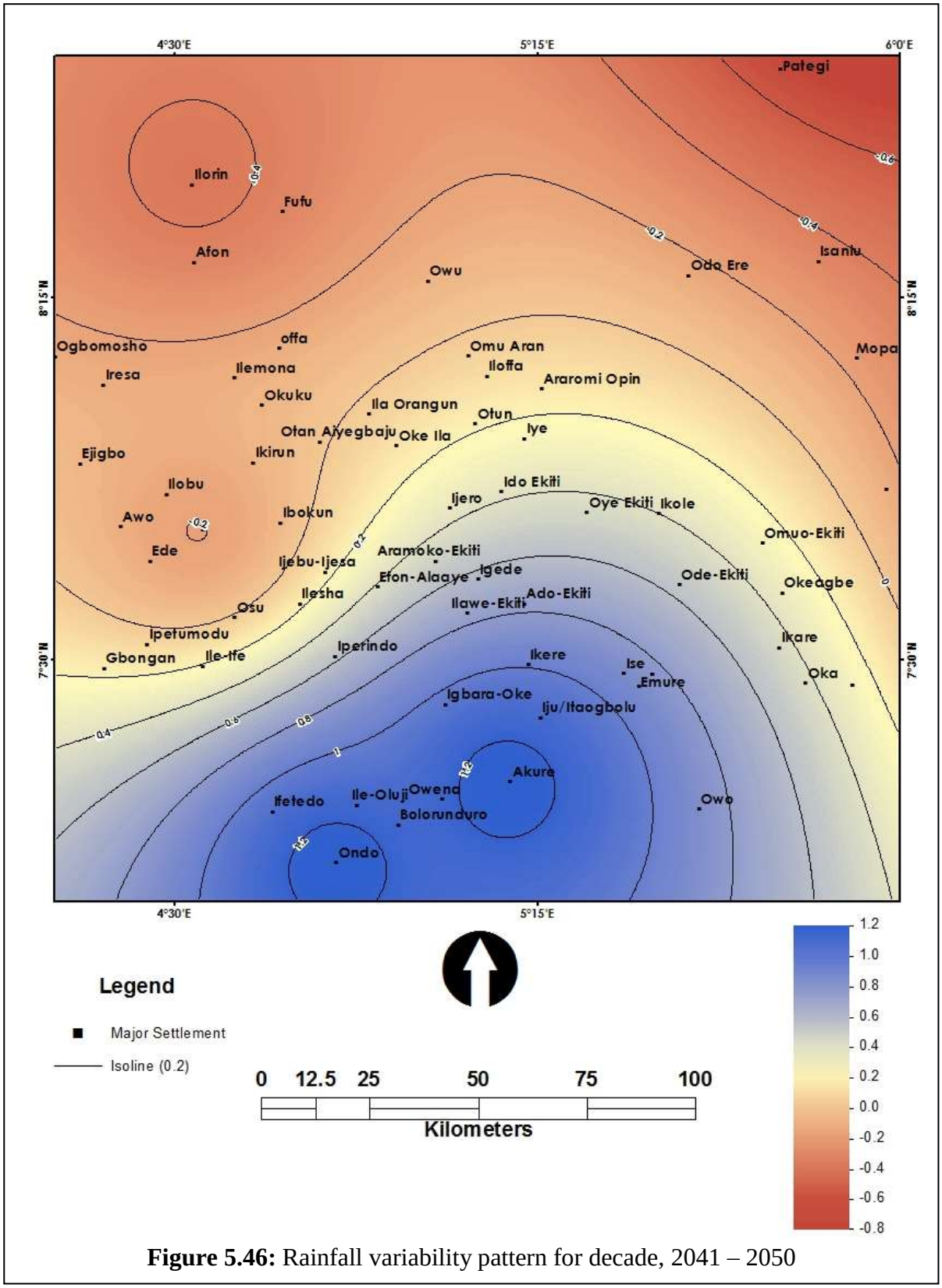

Figure 5.46: Rainfall variability pattern for decade, 2041 – 2050

Source: Author, 2015

The decadal variability pattern of temperature shows that the area will record varied indices between -1.2 and 1.0. Therefore, the area will experience colder and warmer periods than the normal period during the first two and last decades of the future climate respectively.

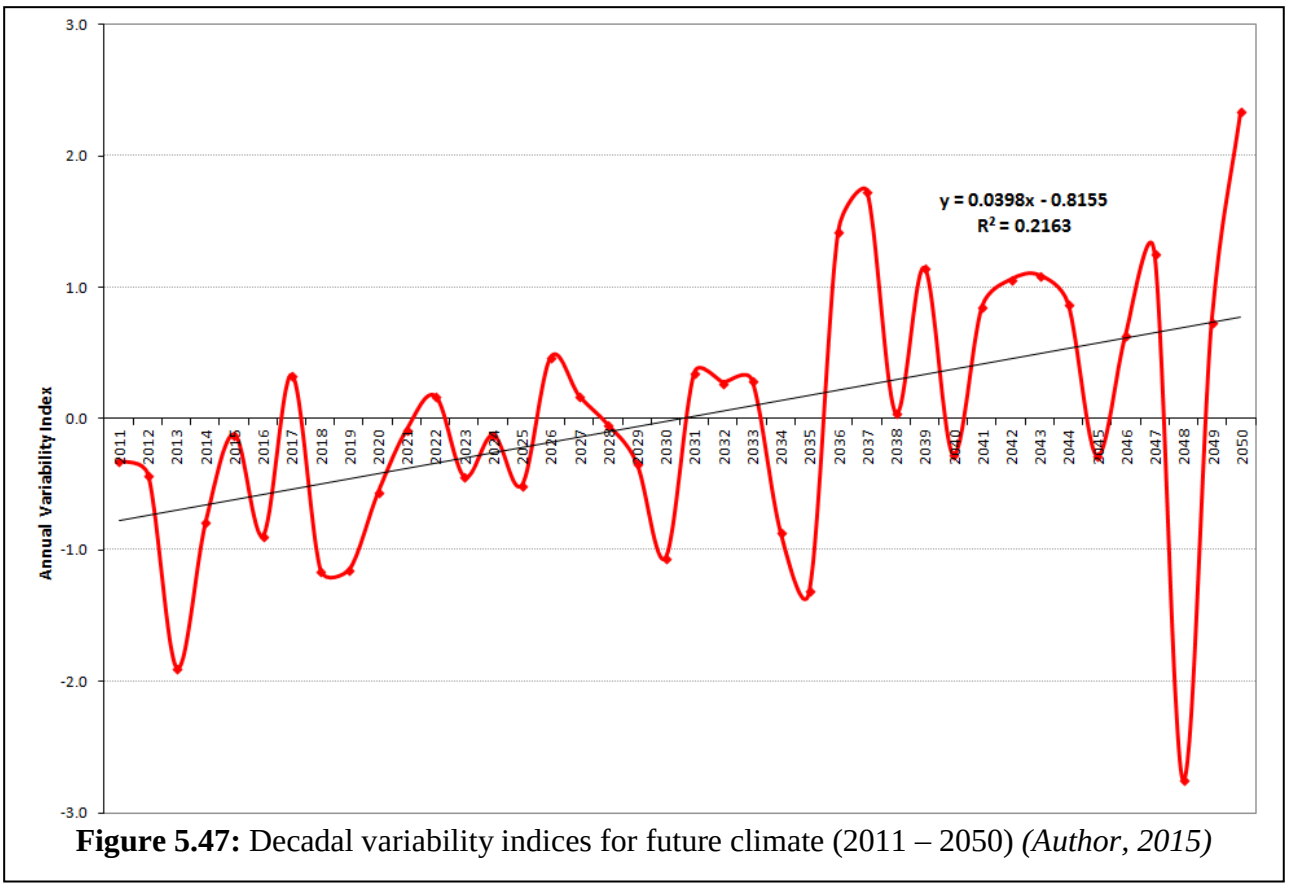

Figure 5.47: Decadal variability indices for future climate (2011 – 2050) *(Author, 2015)*

However, the spatial distribution of the decadal temperature variability indices are slightly different as presented in figure 5.48 and 5.51. The temperature variability indices will vary from -0.9 to 1.1 (2011-2020 and 2021-2030) and -0.9 and 1.2 (2031-2040 and 2041-2050) spatially. In all the decades, Oshogbo will record the lowest variability indices, while the highest indices will be recorded in Pategi area during the future climate.

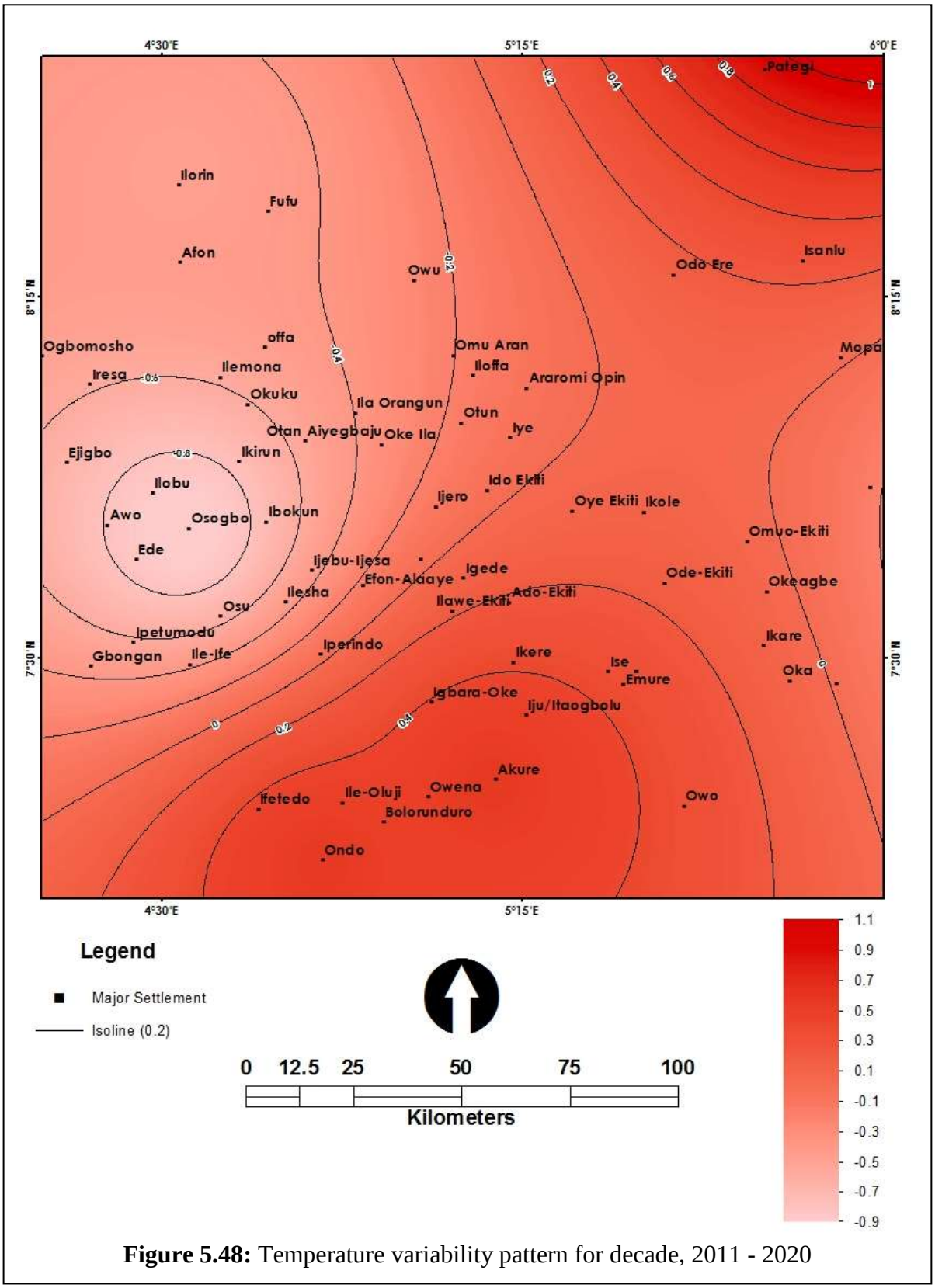

Figure 5.48: Temperature variability pattern for decade, 2011 - 2020

Source: Author, 2015

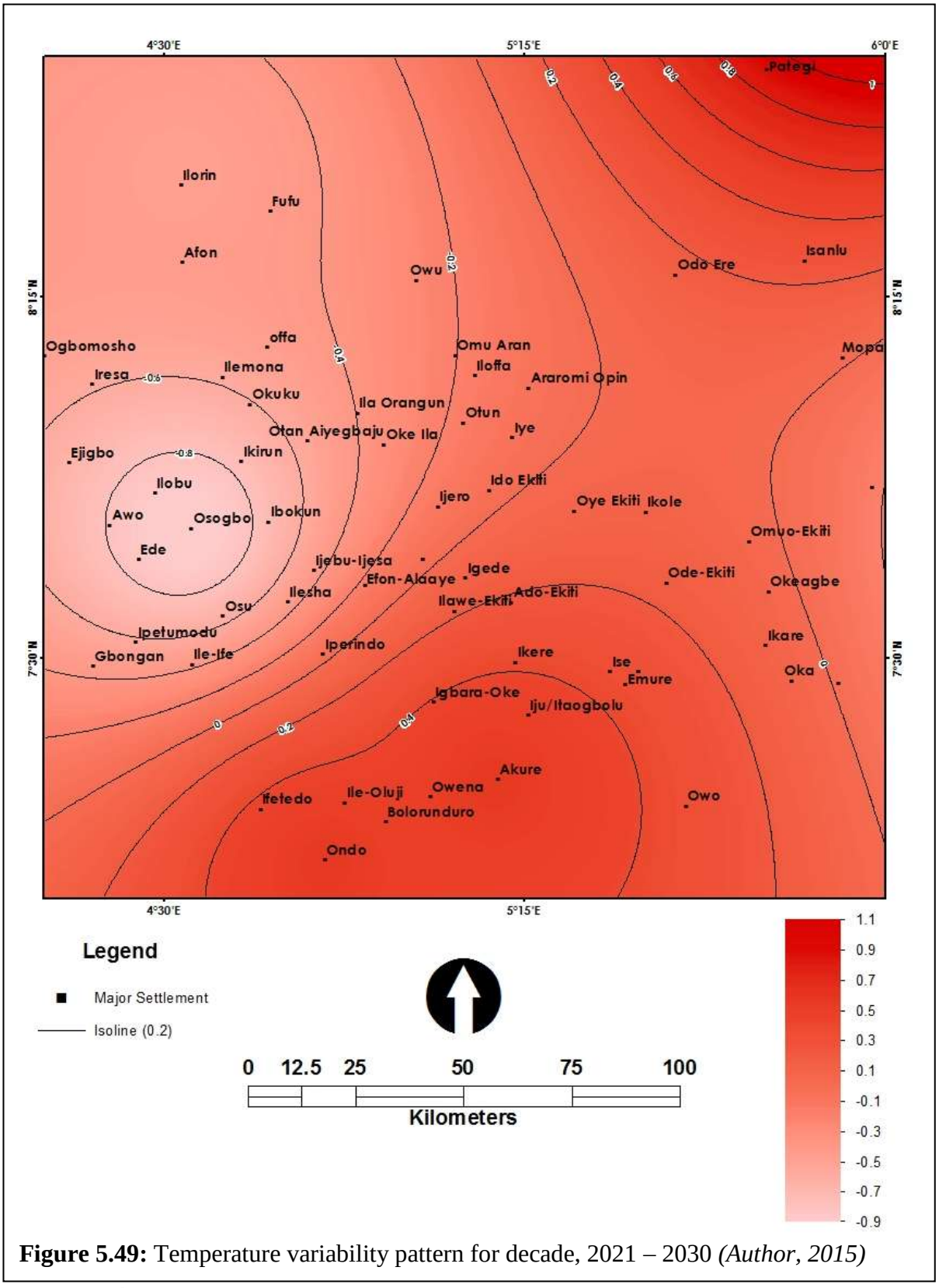

Figure 5.49: Temperature variability pattern for decade, 2021 – 2030 *(Author, 2015)*

Source: Author, 2015

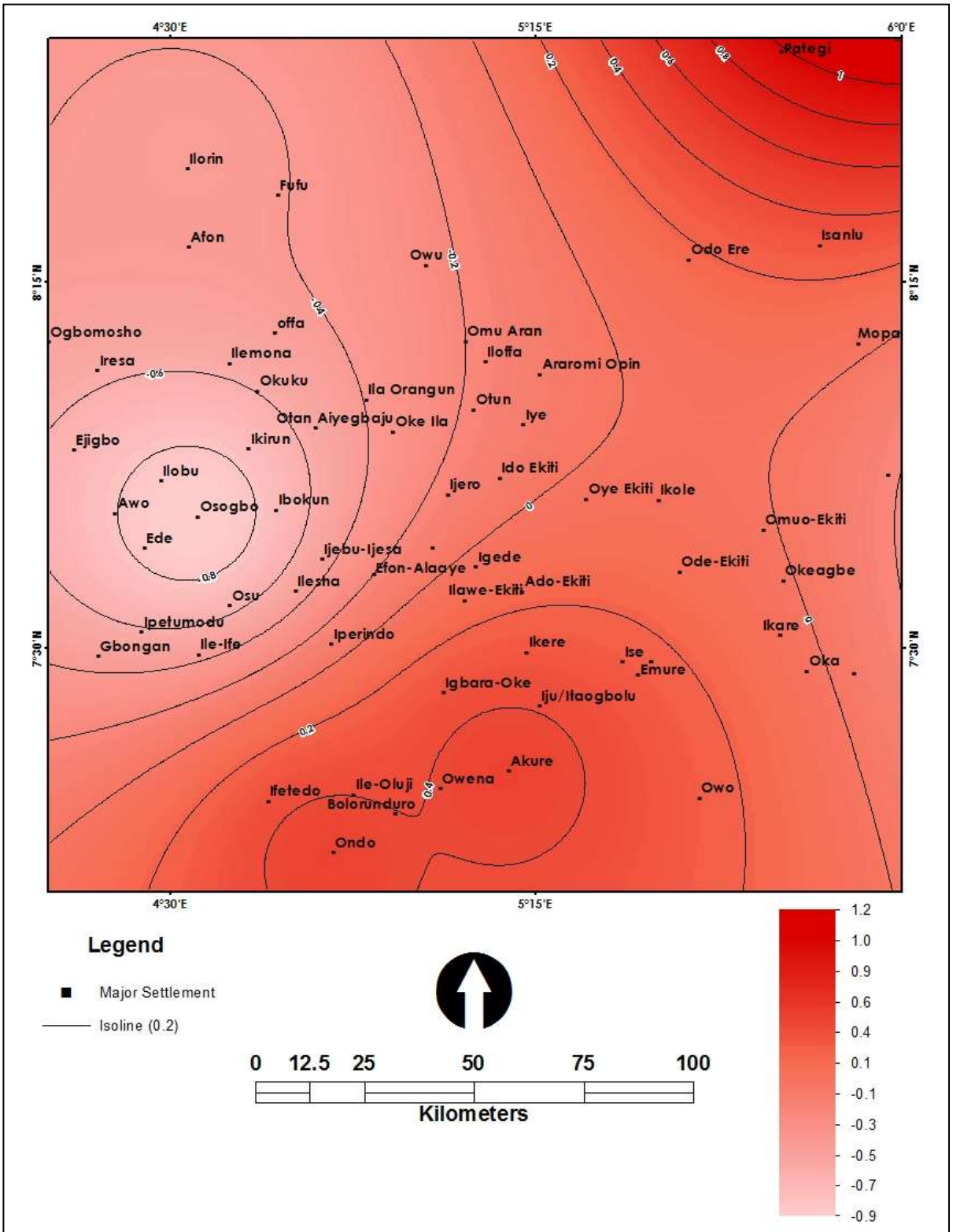

Figure 5.50: Temperature variability pattern for decade, 2031 – 2040 *(Author, 2015)*

Source: Author, 2015

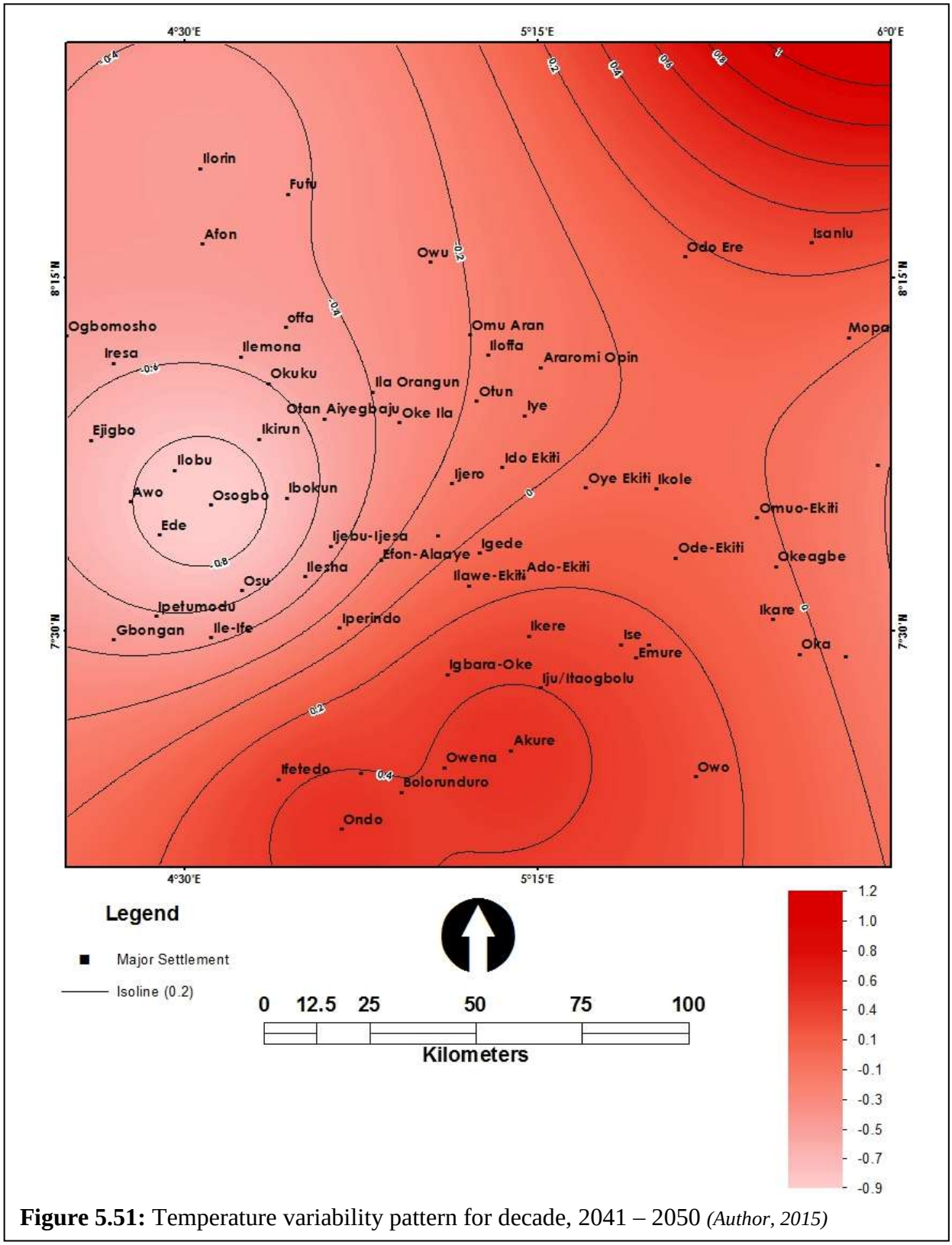

Figure 5.51: Temperature variability pattern for decade, 2041 – 2050 *(Author, 2015)*

Source: Author, 2015

CHAPTER SIX

THE LANDUSE/LANDCOVER AND CLIMATE CHANGE INTERACTION OVER THE STUDY AREA

6.1 Introduction

This chapter presents the results of the analyses carried out in order to achieve the objective three of this research. This objective three was achieved by integrating the results of the analyses of climate variability and change obtained in chapter five with the assessment of landuse/landcover change presented in chapter four to generate LULC pattern for the present and future climates of the Derived Savannah. The chapter is divided into five sections; section one presents the result of statistical modelling of the LULC and climate change interaction, section two presents the result of the modelling of the interaction using the Land Change Modeler (LCM) techniques of Idrisi Selva software to predict the nature of interaction of LULC and climate change of the Derived Savannah for the present climate. The third section discusses the LCM techniques result to generate LULC pattern for the future climate, while section four presents the spatio-temporal analysis of LULC during the present and future climate. Lastly, section five discusses the model validation and calibration.

6.2 Statistical Modelling of Interaction of LULC and Climate Change

Tables 6.1 and 6.4 show the four and three components extracted for both the present and future climates, which were the dominant controlling variables of the interaction between the LULC and climate change within the Derived Savannah. Also, Tables 6.2 and 6.3 the present variance of extraction and rotation sums of squared loading for both climates. In the present climate, four components extracted have extraction sums of squared loadings of 92.97%; while during the future climate three components were extracted to arrive at the extraction

sums of squared loadings of 85.21%. During the present climate as presented in Table 6.2, components 1 and 2 accounting for 43.35% and 23.75% of the total variances, and components 3 and 4 accounts for 17.16 and 8.72%, respectively. In addition, component 1 indicates that climate (especially the rainfall) and topography have strong or dominant influence and control on the landcover. It also show a close interaction between the variables of landcover, topography and climate which accounts for the highest percentage of variance loadings. However, components 2, 3 and 4 were dominated by other variables which are anthropogenic in nature.

Similar situation will continue during the future climate (2011 – 2050) as presented in Table 6.4; component 1 has explanatory power of about 40.97%, which explains the importance of climate (especially rainfall), topography and anthropogenic (distance from disturbance) influence on the landcover. Components 2 and 3 have an extracted sum of squared of loading of 22.70% and 21.54%, respectively as shown in Table 6.3. These indicate the dominance of increased population, distances from disturbance and urban centre, which constitute anthropogenic activities, will be on the increase in the future. Detailed results of the Principal Component Analysis (PCA) for both climates are presented in appendix II.

Table 6.1: Rotated component matrix for interaction between LULC and climate change (present climate)

Variables/Drivers	Component			
	1	2	3	4
Forest Cover	.704	.185	.081	.552
Aspect	.172	.916	.147	-.223
Distance to disturbance	.635	.156	-.575	.461
Elevation	.169	.913	-.004	.030
NDVI31	.592	.766	.097	.152
Population Density	-.039	-.347	-.899	-.142
Average Rainfall	.979	.098	-.127	-.096
Distance to road	-.057	-.215	-.010	.955
Slope	.760	.373	.346	.058
Distance to river	.413	.735	-.381	-.240
Average Temperature	-.226	-.530	.781	.102
Distance to Urban centre	-.159	.163	.888	-.212

Table 6.2: Explanatory Variance of components for interaction between LULC and climate Change (present climate)

Component	Initial Eigenvalues			Extraction Sums of Squared Loadings			Rotation Sums of Squared Loadings		
	Total	% of Variance	Cumulative %	Total	% of Variance	Cumulative %	Total	% of Variance	Cumulative %
1	6.070	43.355	43.355	6.070	43.355	43.355	3.880	27.716	27.716
2	3.325	23.750	67.105	3.325	23.750	67.105	3.852	27.512	55.227
3	2.402	17.155	84.260	2.402	17.155	84.260	3.608	25.768	80.996
4	1.220	8.715	92.974	1.220	8.715	92.974	1.677	11.979	92.974

Source: Author, 2013

Table 6.3: Explanatory Variance of components for interaction between LULC and climate Change (future climate)

Component	Initial Eigenvalues			Extraction Sums of Squared Loadings			Rotation Sums of Squared Loadings		
	Total	% of Variance	Cumulative %	Total	% of Variance	Cumulative %	Total	% of Variance	Cumulative %
1	4.916	40.970	40.970	4.916	40.970	40.970	4.602	38.351	38.351
2	2.724	22.701	63.672	2.724	22.701	63.672	2.944	24.531	62.881
3	2.585	21.538	85.210	2.585	21.538	85.210	2.679	22.328	85.210

Source: Author, 2013

Table 6.4: Rotated component matrix for interaction between LULC and climate change (Future climate)

Variables	Component		
	1	2	3
Forest Cover	.810	-.409	.049
Aspect	.584	.655	-.357
Distance to disturbance	.700	-.186	.653
Future Rainfall	.784	.086	.251
Future Temperature	.063	-.911	-.282
Elevation	.652	.540	-.155
NDVI31	.934	.245	-.162
Population Density	-.280	.129	.929
Distance to road	.111	-.805	.141
Slope	.832	-.038	-.285
Distance to river	.638	.675	.220
Distance to Urban centre	-.083	.037	-.957

Source: Author, 2013

6.3 LCM Modelling of Interaction of LULC and Climate Change in the Present Climate

6.3.1 Transition potential maps

The transition potential maps to determine the nature and spatial distribution of interaction between LULC and climate change during the present climate (2010) are shown in figures

6.1 to 6.6. Table 6.5 presents the Markov probabilities for the transition between classes of LULC within the period between 2002 and 2010. Figure 6.1 shows the transition potential from degraded surfaces to farmland, fire scar, forest, grassland, waterbody and woodland classes of LULC. This further shows that they have transition potential ranging from 0 to 1. For instances, the transition between degraded surface to farmland, fire scar, forest, grassland and woodland have 0 – 0.89, 0 – 0.61, 0- 0.90, 0 – 0.966, 0 – 0.266 and 0 – 0.0011 suitability respectively. There is almost zero or impossible chance for waterbody to transit to forest area within the study area during the present climate. The suitability of forest to transit to degraded surfaces, farmland, fire scar, grassland, urban, waterbody and woodland are shown in figure 6.2 (a – g) with suitability ranging from 0 – 0.938, 0 – 0.989, 0 – 0.999, 0 – 0.009, 0 – 0.999, 0 – 0.021 and 0 – 1.0 respectively. Figure 6.2*d* reveals that the least suitability (0 – 0.009) is recorded between the interaction of forest and grassland and concentrated within the southern end of the study area during the present climate. Furthermore, woodland records the highest transition potential of 1 from forest during the present climate as shown in Fig.6.2*g*.

The transition potentials from grassland to degraded surfaces, farmland, fire scar, forest, urban, waterbody and woodland with suitability probabilities ranging from 0 to 0.013, 0 to 0.009, 0 to 0.999, 0 to 0.0016, 0 to 0.953, 0 to 0.013 and 0 to 0.0022 as shown in Fig.6.3*(a – g)* respectively. In addition, figure 6.3c and 6.3g reveal that the highest and least interactions occur between grassland and fire scar and grassland and forest which have 0 – 99.9% and 0 – 1.6% chance of changing from grassland to fire scar and forest. Also, figure 6.4 shows the transition potential from waterbody to forest which reveals that waterbody has 0 to 83.3% chance of changing to forest but with the highest concentration of low percentages.

Similarly, figure 6.5 shows the potential of woodland to transition during the present climate. The sensitivity of woodland to transit to degraded surfaces, farmland, fire scar, forest,

grassland and urban land are shown in figure 6.5 *(a - f)* as having transition potentials ranging from 0 – 0.999, 0 – 0.686, 0 – 0.999, 0 – 0.846, 0 – 0.009 and 0 – 0.996 respectively.

Table 6.5: Markov transition probabilities of LULC for present climate

LULC Class	Cloud cover	Degraded Surfaces	Farmland	Fire Scar	Forest	Grassland	No Data	Urban	Waterbody	Woodland
Cloud cover	0.0000	0.4566	0.0000	0.0000	0.1142	0.0000	0.0000	0.3127	0.0076	0.1089
Degraded Surfaces	0.0000	0.3943	0.0757	0.0192	0.1404	0.1925	0.0196	0.0728	0.0000	0.0855
Farmland	0.0000	0.3290	0.3667	0.0388	0.0045	0.1608	0.0289	0.0388	0.0006	0.0318
Fire Scar	0.0000	0.0352	0.1896	0.0605	0.0349	0.3640	0.0000	0.0000	0.0026	0.3133
Forest	0.0000	0.0285	0.0021	0.0004	0.9016	0.0000	0.0000	0.0046	0.0005	0.0623
Grassland	0.0000	0.0956	0.0707	0.0421	0.0117	0.4839	0.0088	0.0021	0.0019	0.2832
No Data	0.0000	0.0209	0.0059	0.0028	0.0636	0.0030	0.8378	0.0000	0.0000	0.0659
Urban	0.0000	0.0959	0.0030	0.0006	0.0365	0.0000	0.0058	0.8523	0.0058	0.0000
Waterbody	0.0000	0.0312	0.0128	0.0298	0.0766	0.0000	0.0000	0.0016	0.8381	0.0098
Woodland	0.0000	0.0264	0.0272	0.0212	0.2165	0.2709	0.0004	0.0000	0.0015	0.4359

Source: Author, 2015

The higher suitability recorded for the woodland within the northern part of the study area, apart from the grassland which has less than 1% and is localized. Furthermore, figure 6.6a shows the transition potentials from farmland to forest which has 0 – 69.4% chance to change, while figure 6.6 *(a & b)* shows the modeled transition potentials from fire scar to the forest and urban areas, which has a 0 - 0.989 and a 0 – 0.999 respectively. The combined transition potential maps with Markov probability statistics are presented in Table 6.5. The figures at the main diagonal cells reveal the probabilities of each LULC class to remain in the same location during the present climate, while the figures on the right cells of the main diagonal show the chances of other LULC classes to transit to the LULC class from the main diagonal. In addition, the figures on the left cells of the main diagonal of Table 6.5 present the probabilities of the LULC classes to transit from LULC class in the main diagonal cells.

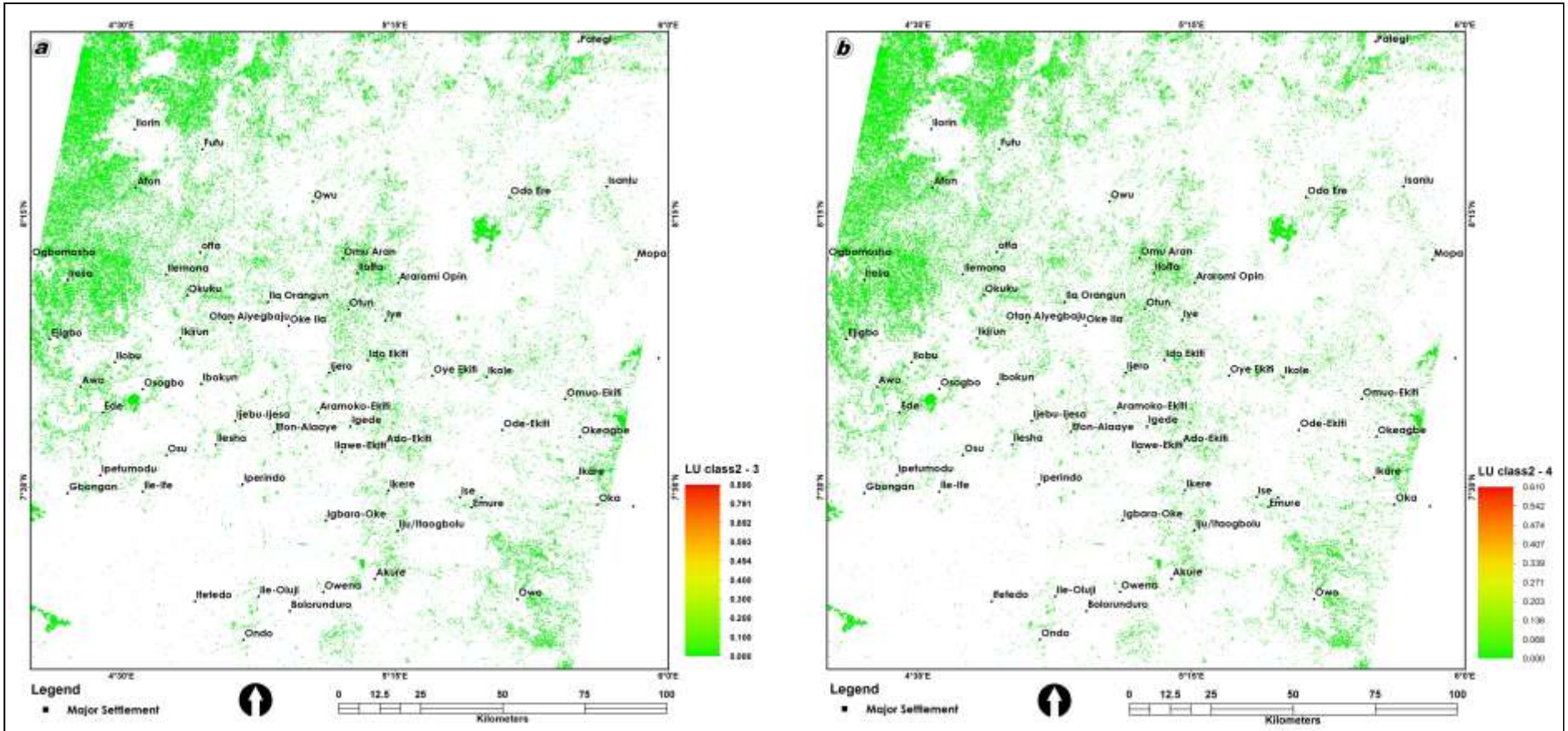

Figure 6.1: Transition potential from degraded surfaces to (a) farmland and (b) fire scar *(Source: Author, 2015)*

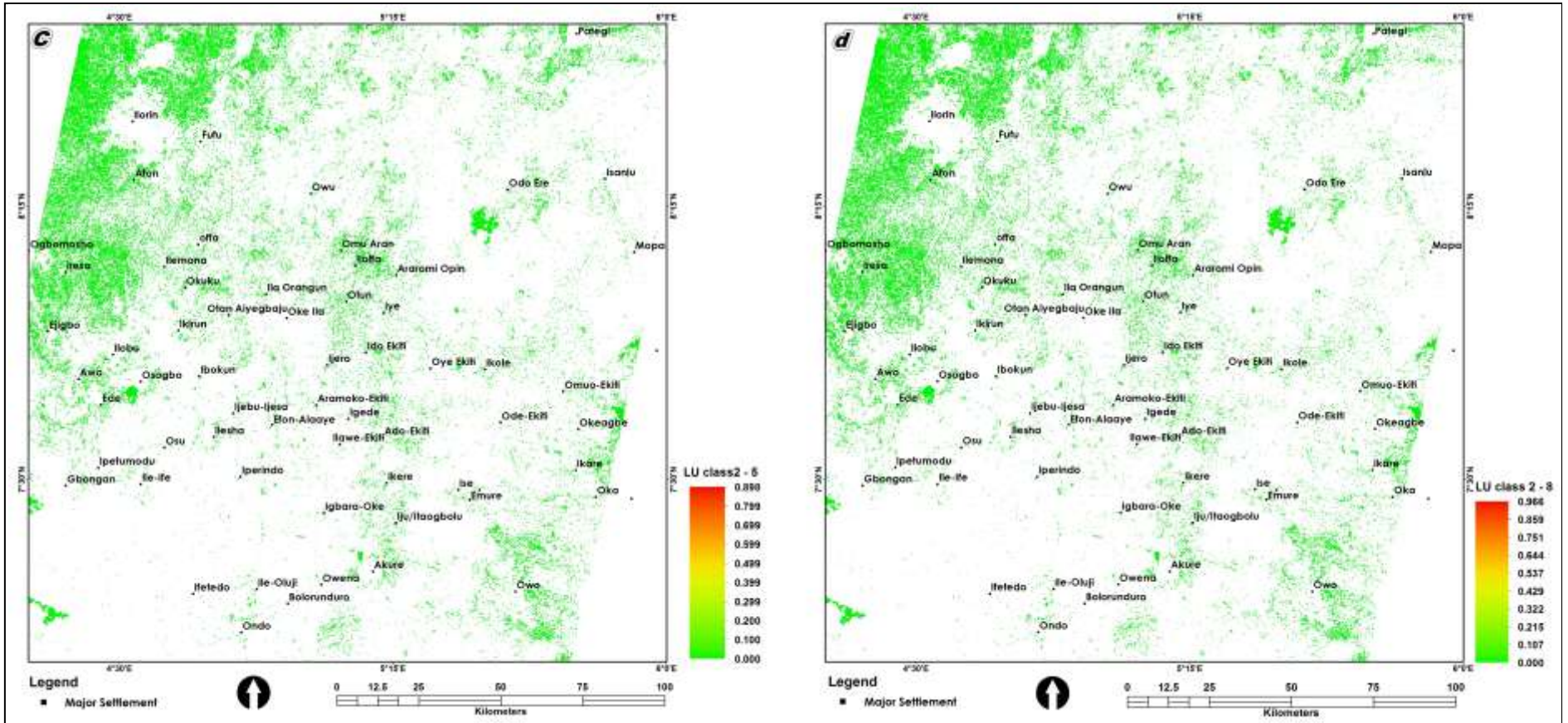

Figure 6.1: Transition potential from degraded surfaces to (c) forest and (d) urban *(Source: Author, 2015)*

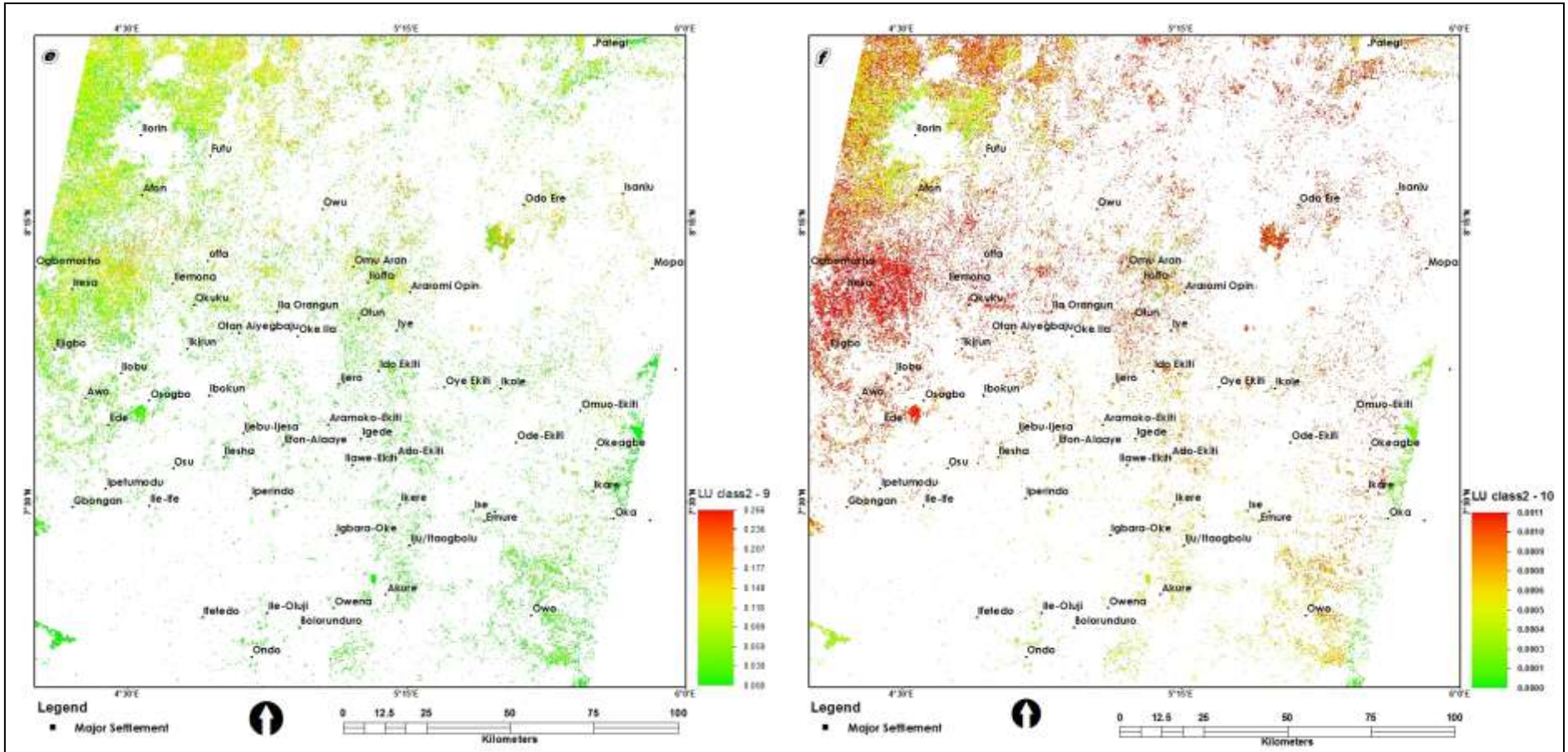

Figure 6.1: Transition potential from degraded surfaces to (e) waterbody and (f) woodland *(Source: Author, 2015)*

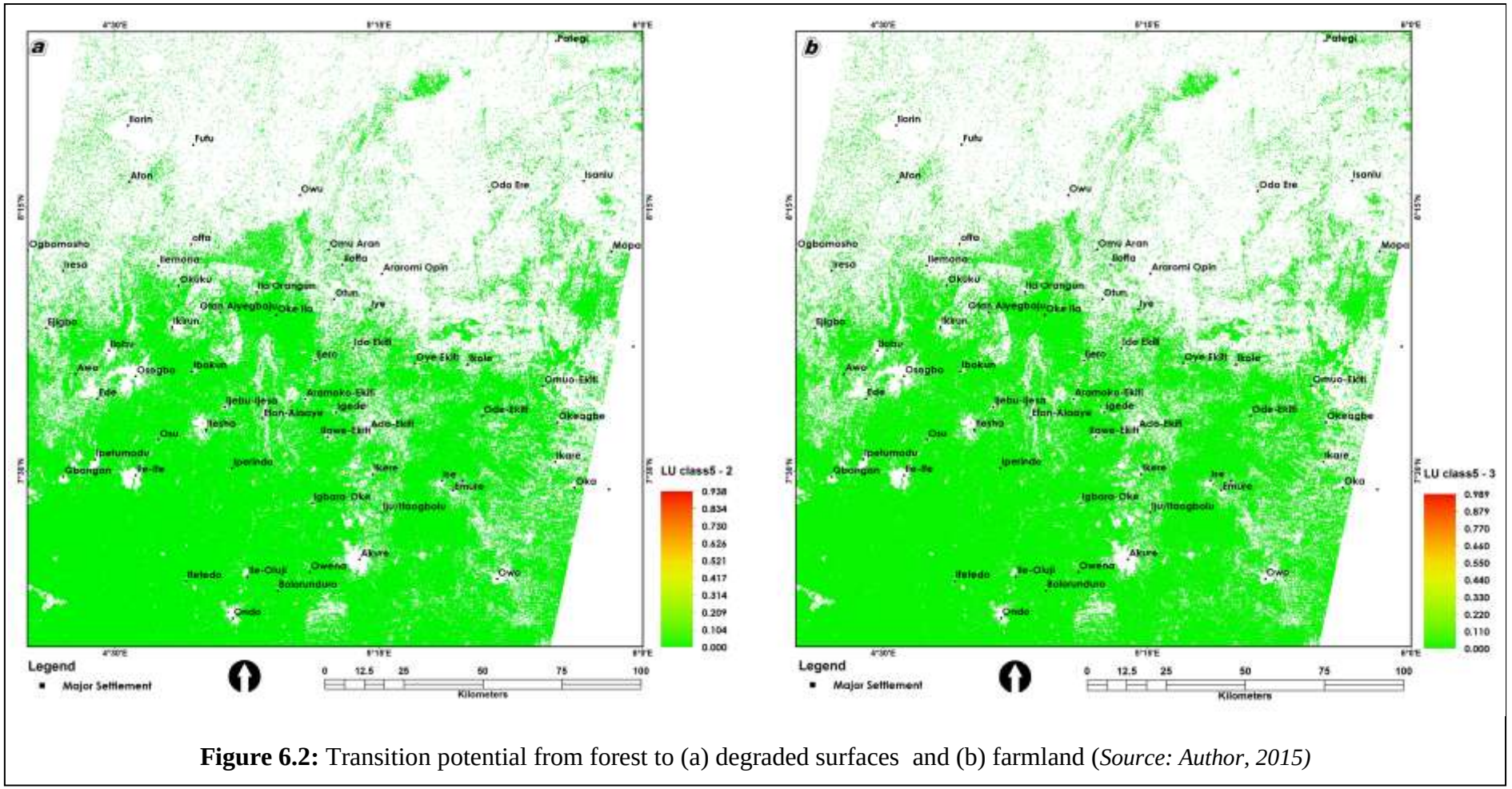

Figure 6.2: Transition potential from forest to (a) degraded surfaces and (b) farmland (*Source: Author, 2015)*

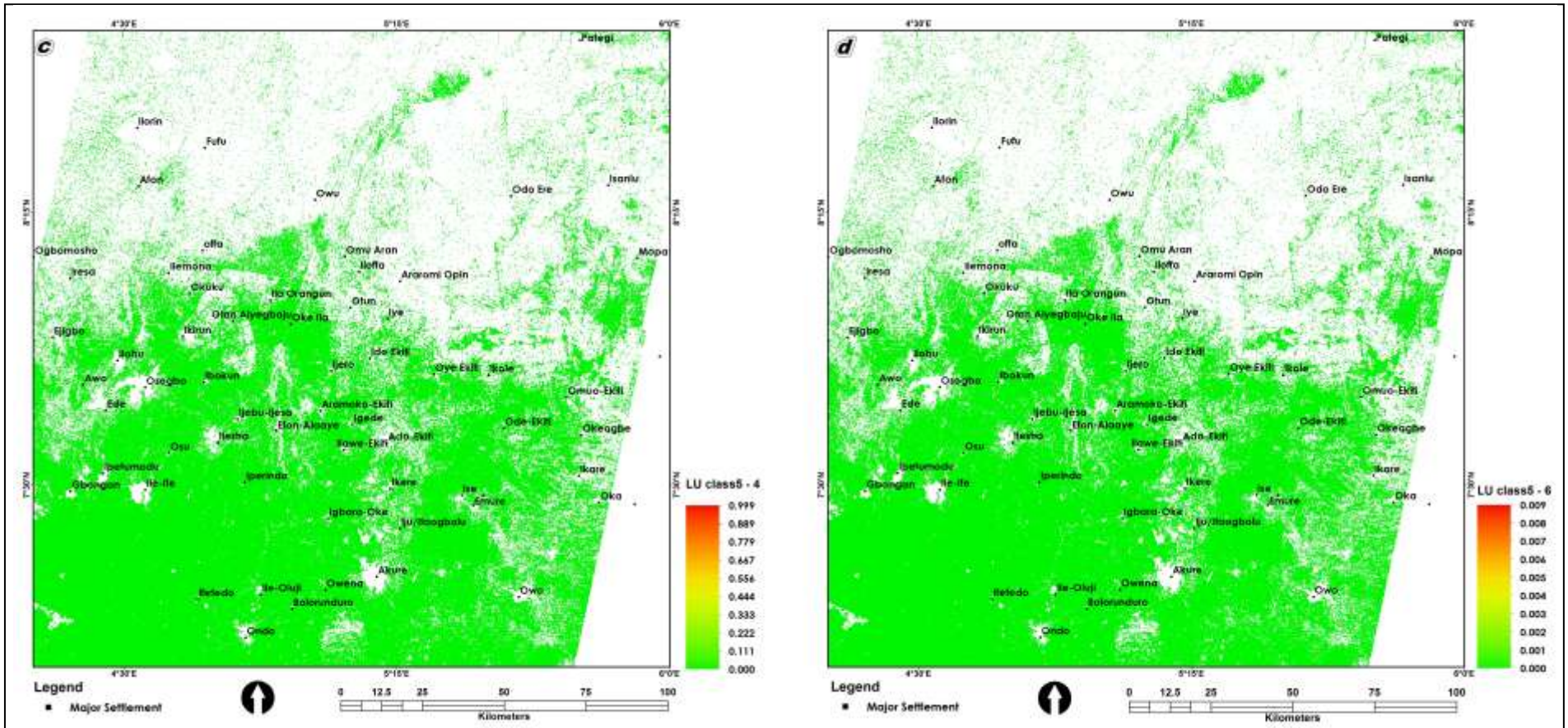

Figure 6.2: Transition potential from forest to (c) fire scar and (d) grassland (*Source: Author, 2015)*

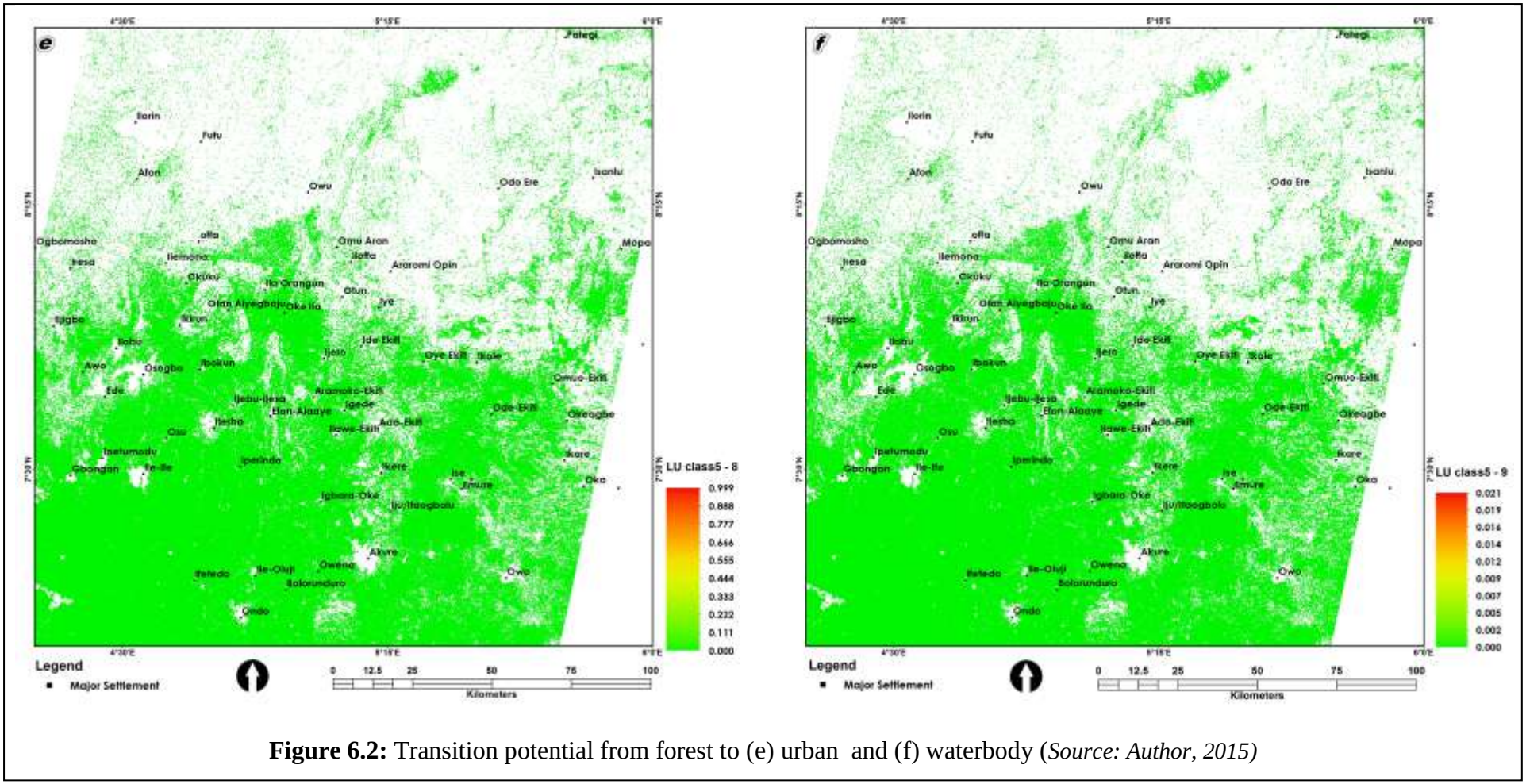

Figure 6.2: Transition potential from forest to (e) urban and (f) waterbody (*Source: Author, 2015)*

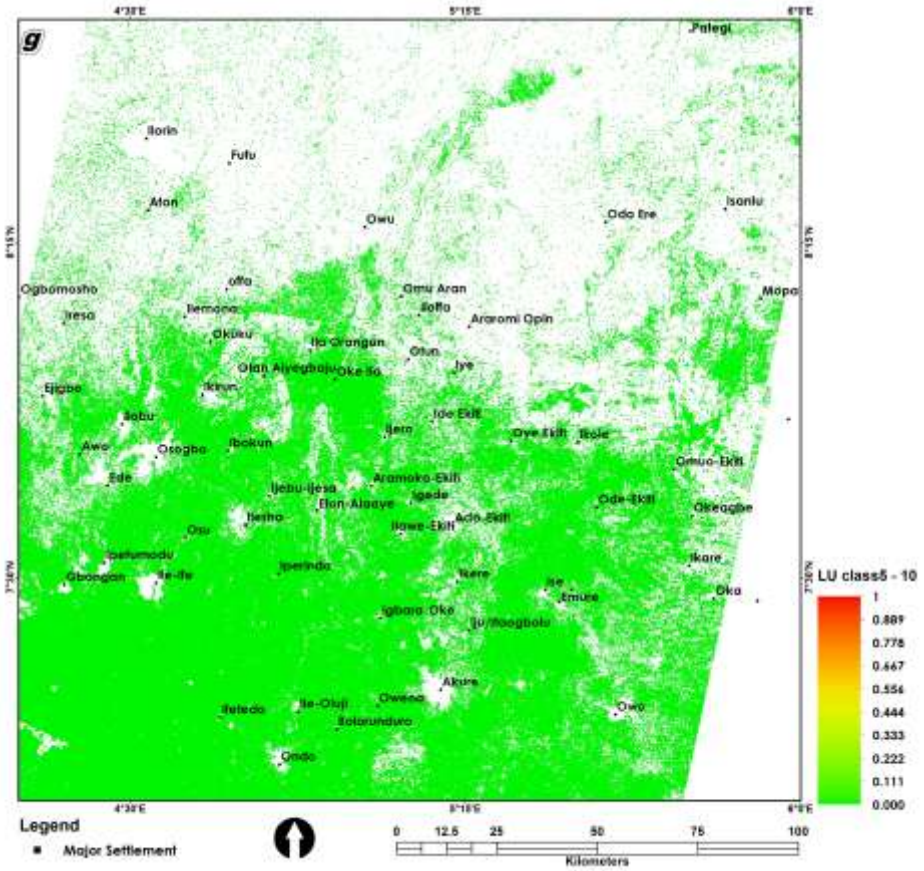

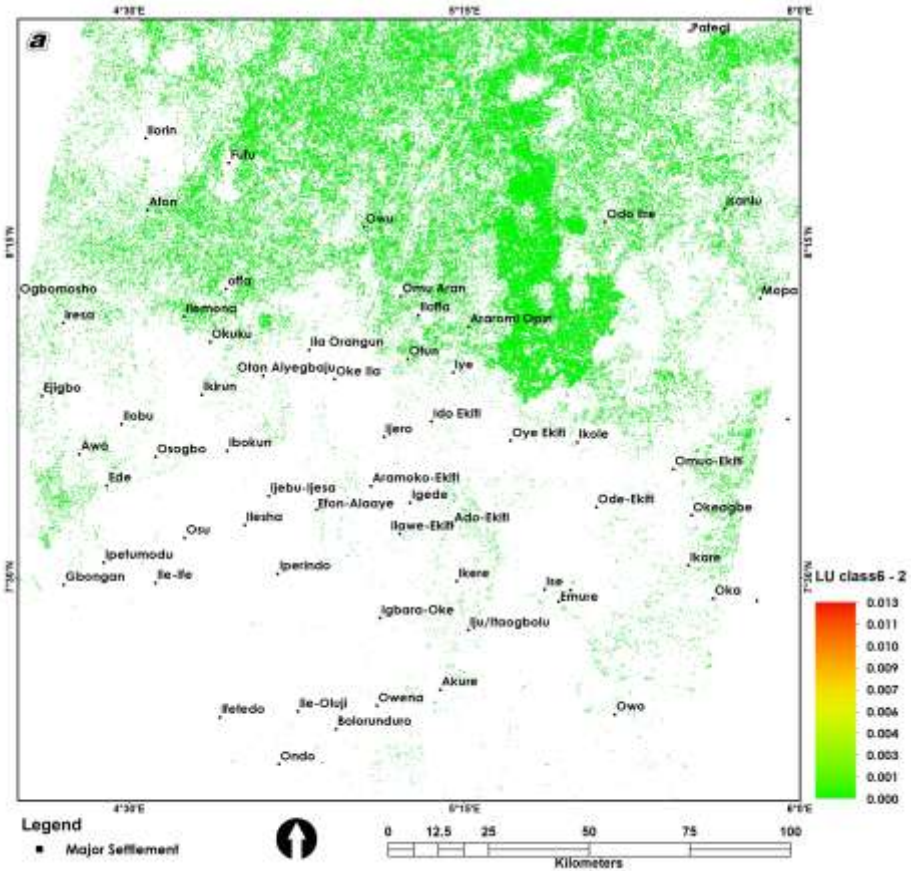

Figure 6.2: Transition potential from forest to (g) woodland; and **Figure 6.3:** Transition potential from grassland to (a) degraded surfaces (*Source: Author, 2015)*

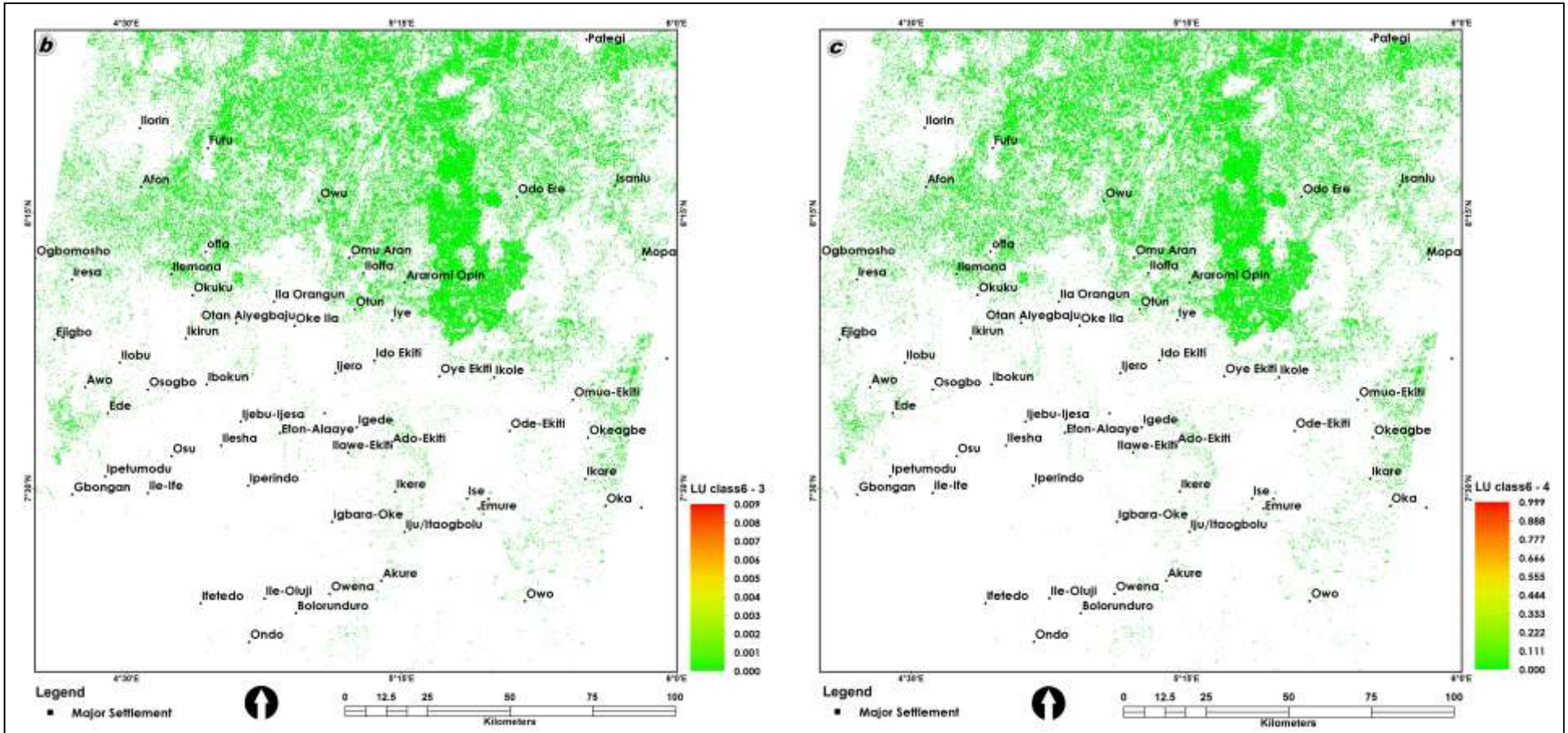

Figure 6.3: Transition potential from grassland to (b) fire scar and (c) farmland (*Source: Author, 2015)*

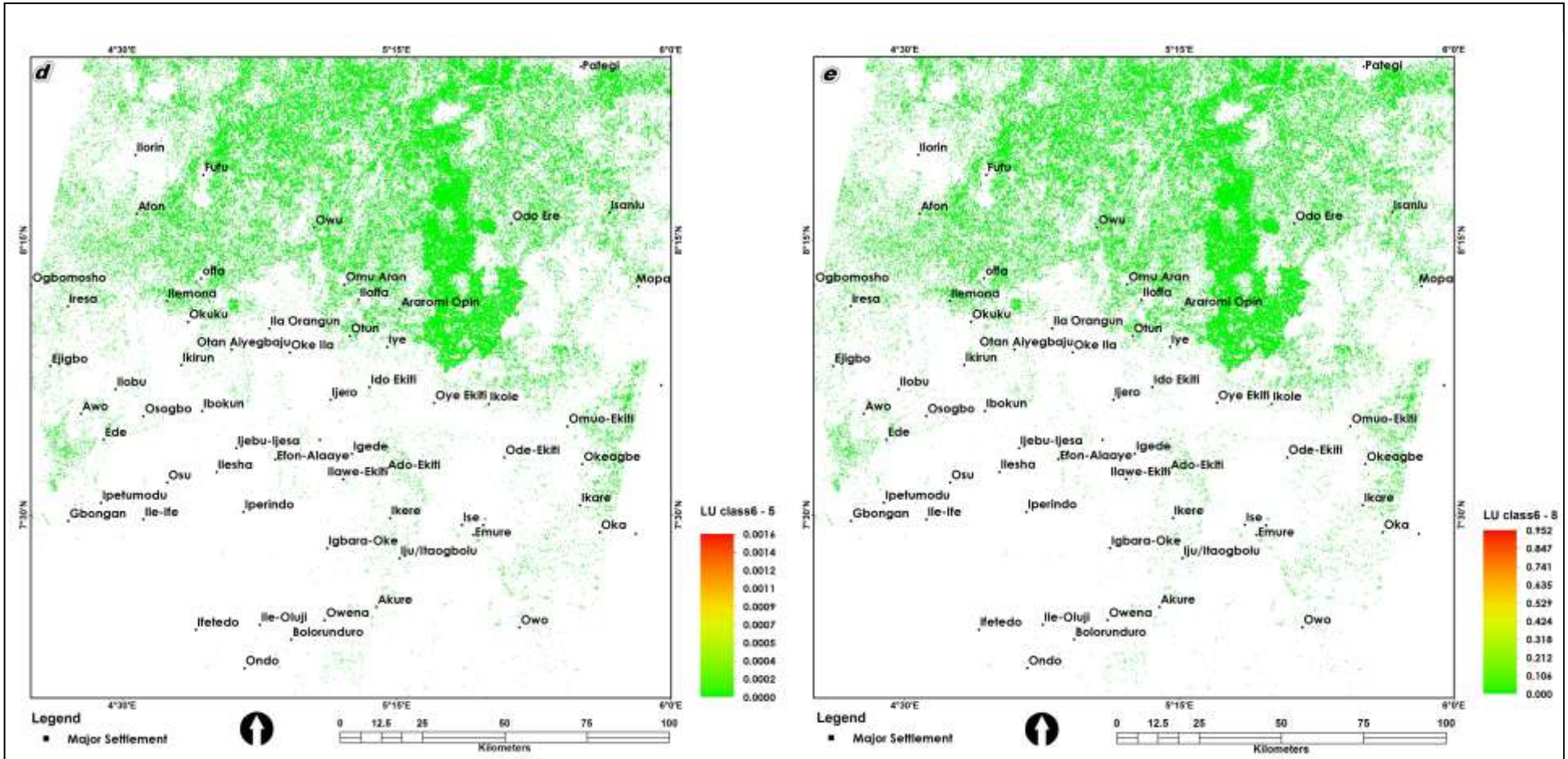

Figure 6.3: Transition potential from grassland to (d) forest and (e) urban (*Source: Author, 2015)*

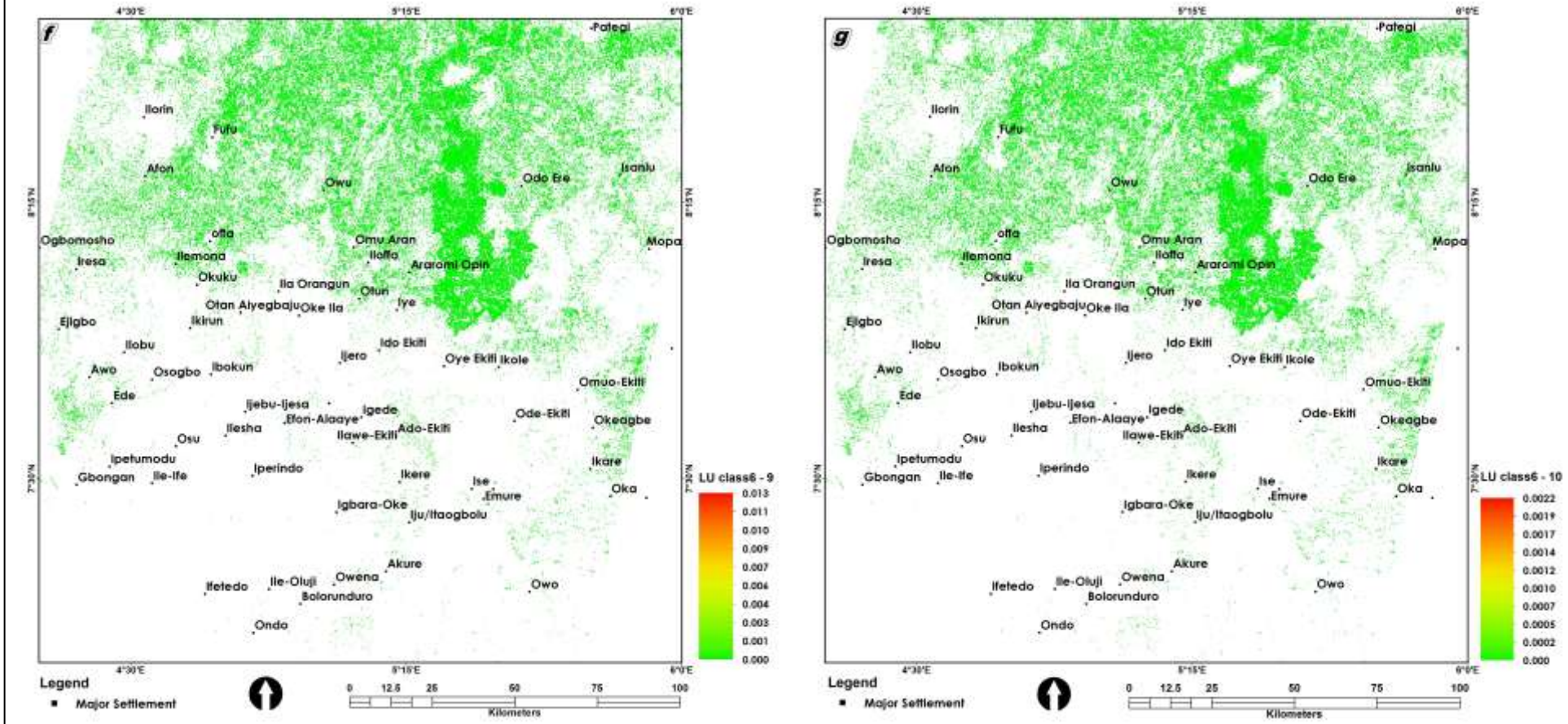

Figure 6.3: Transition potential from grassland to (f) waterbody and (g) woodland (*Source: Author, 2015)*

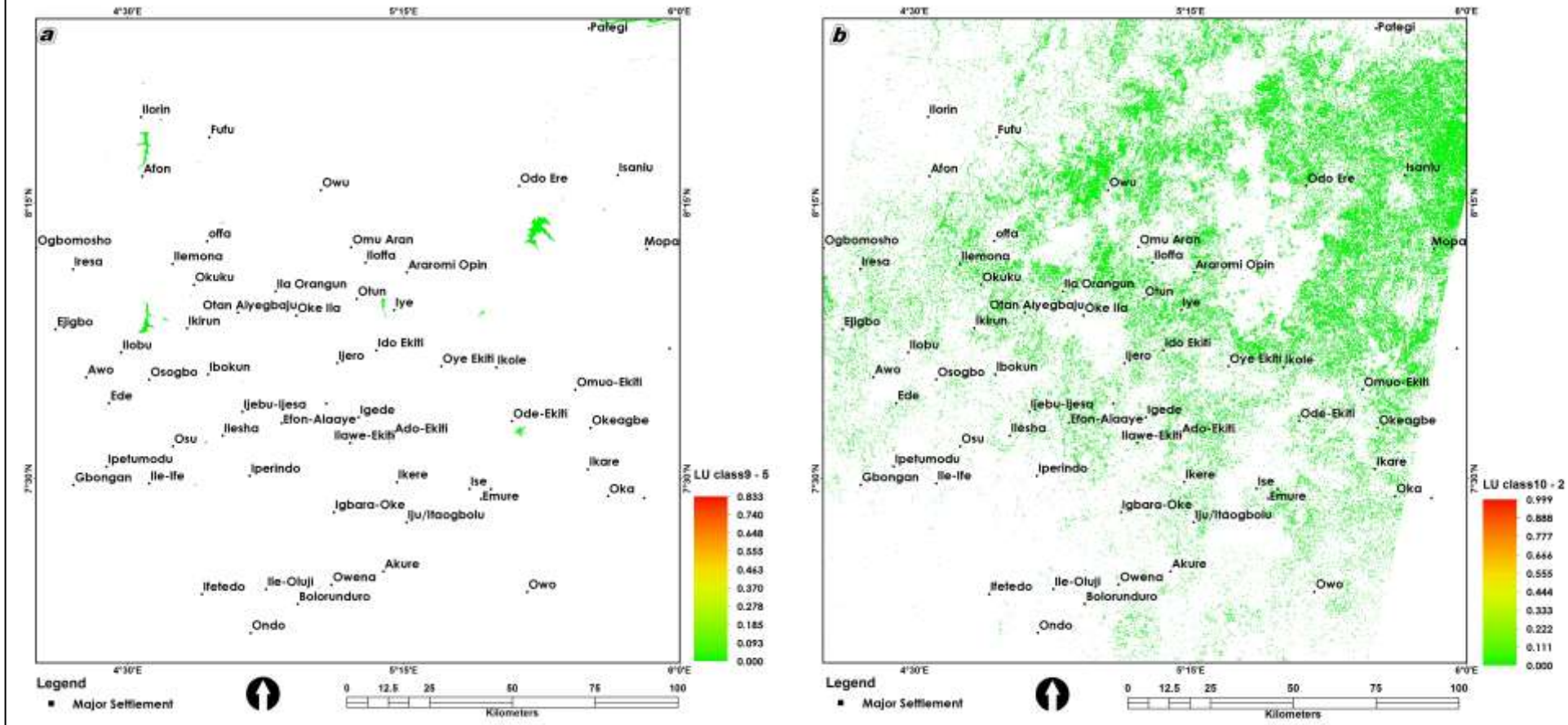

Fig. 6.4: Transition potential from waterbody to (a) forest; and **Figure 6.5:** Transition potential from woodland to (b) degraded surfaces *(Source: Author, 2015)*

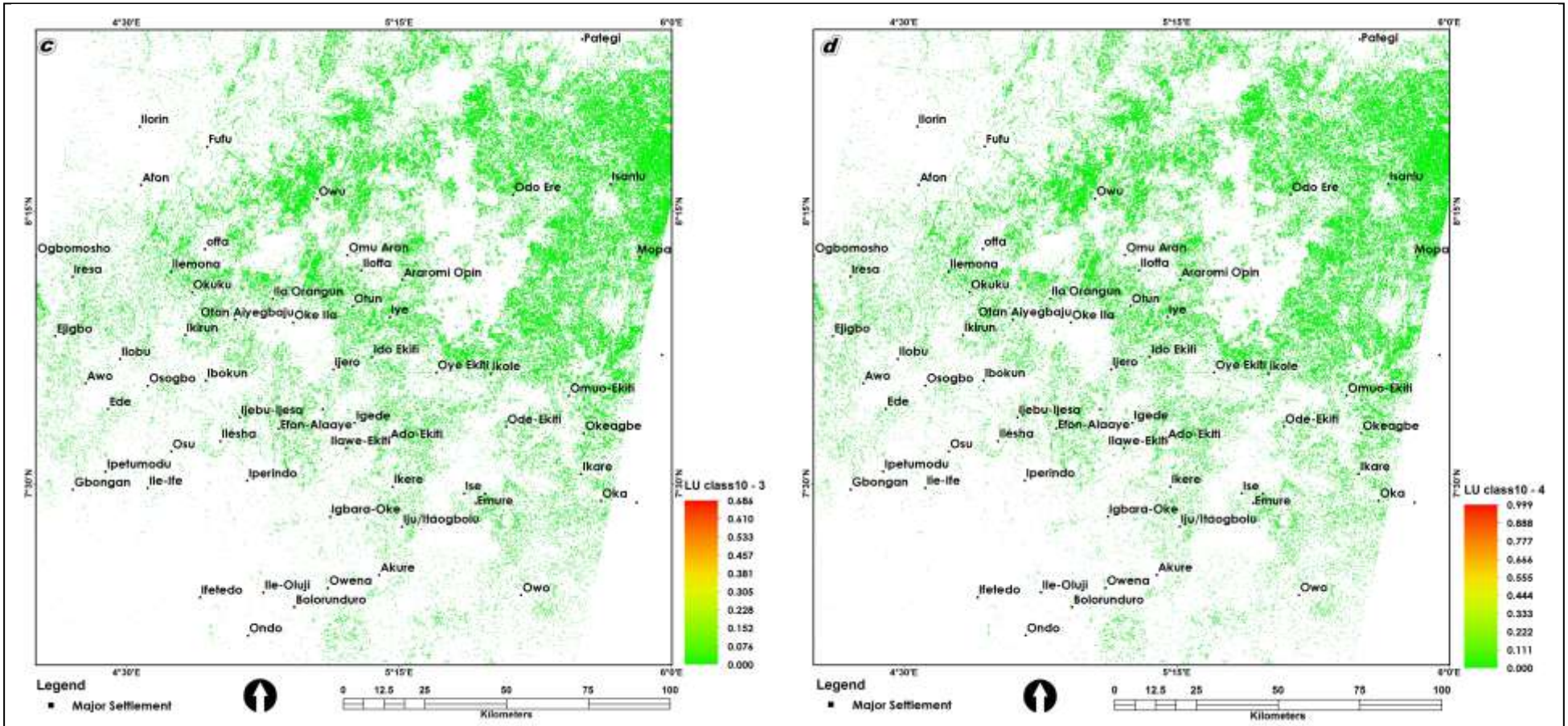

Figure 6.5: Transition potential from woodland to (c) farmland and (d) fire scar *(Source: Author, 2015)*

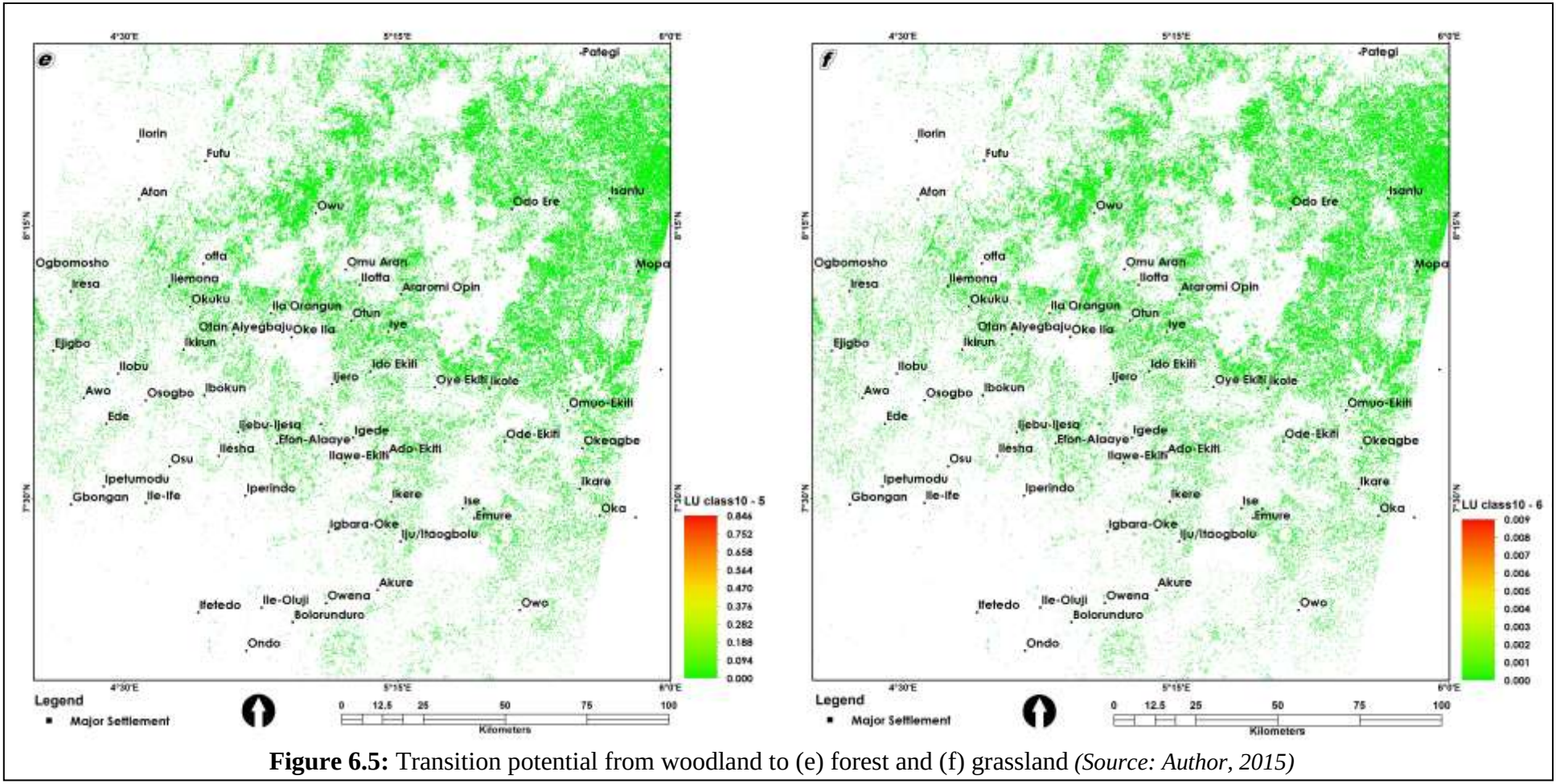

Figure 6.5: Transition potential from woodland to (e) forest and (f) grassland *(Source: Author, 2015)*

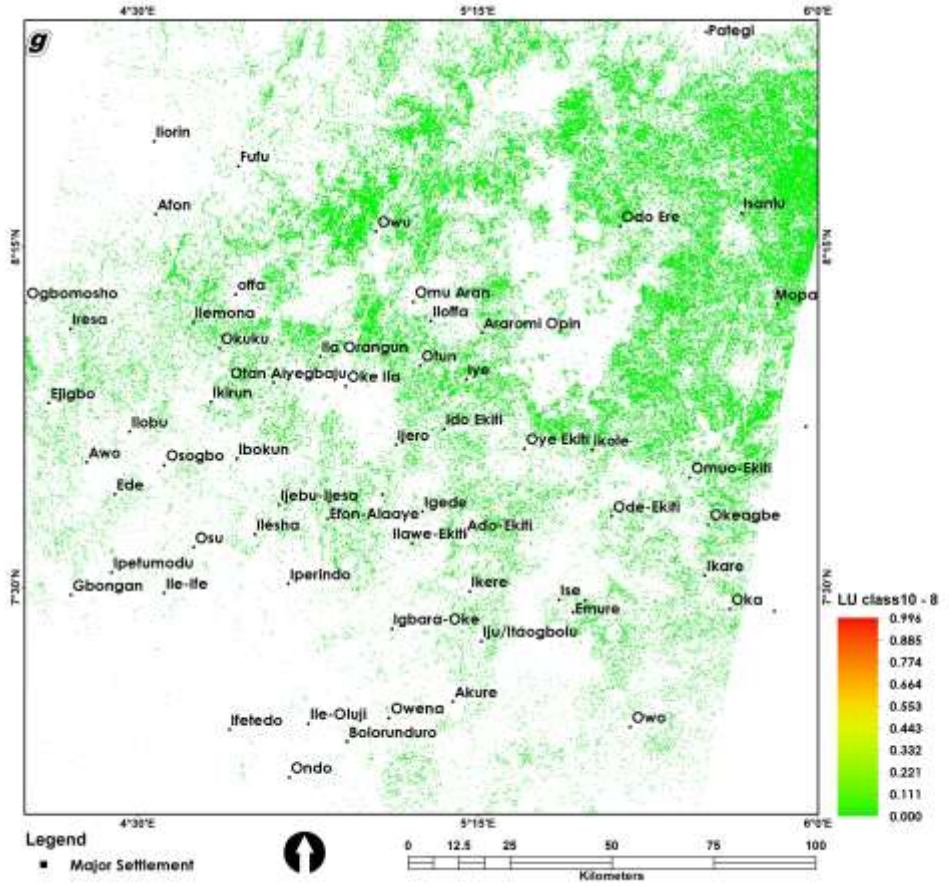

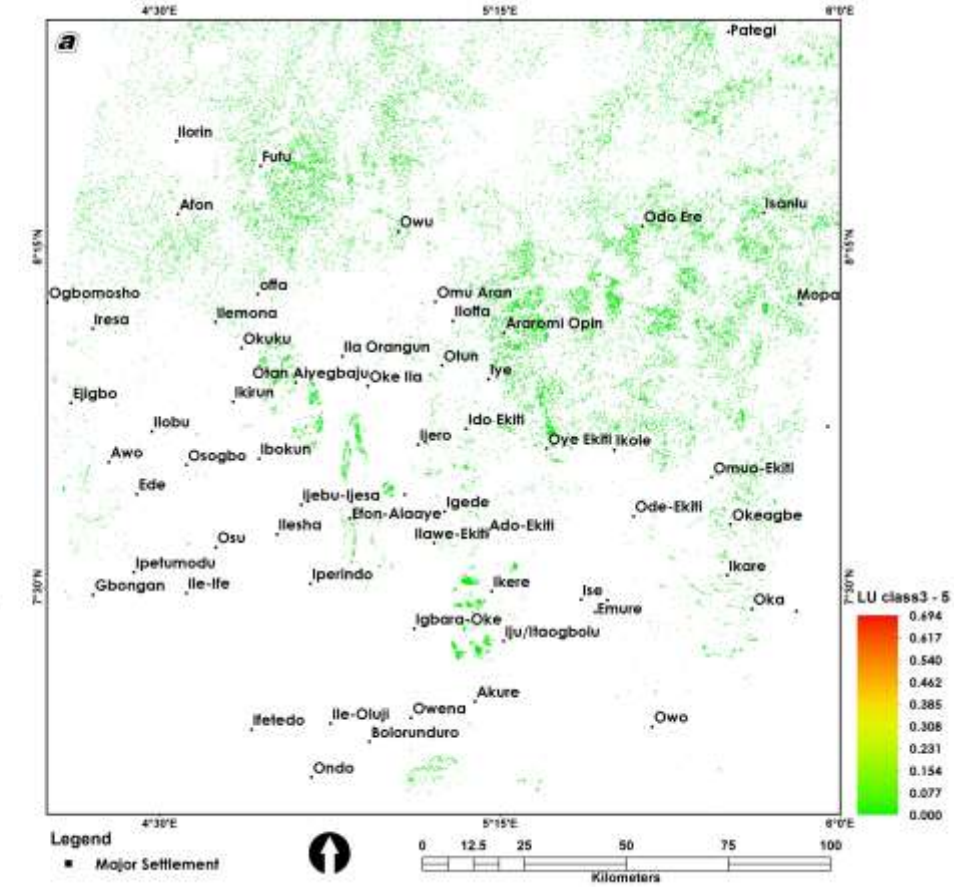

Figure 6.5: Transition potential from woodland to (g) urban and **Figure 6.6:** Transition potential from (a) farmland to forest *(Source: Author, 2015)*

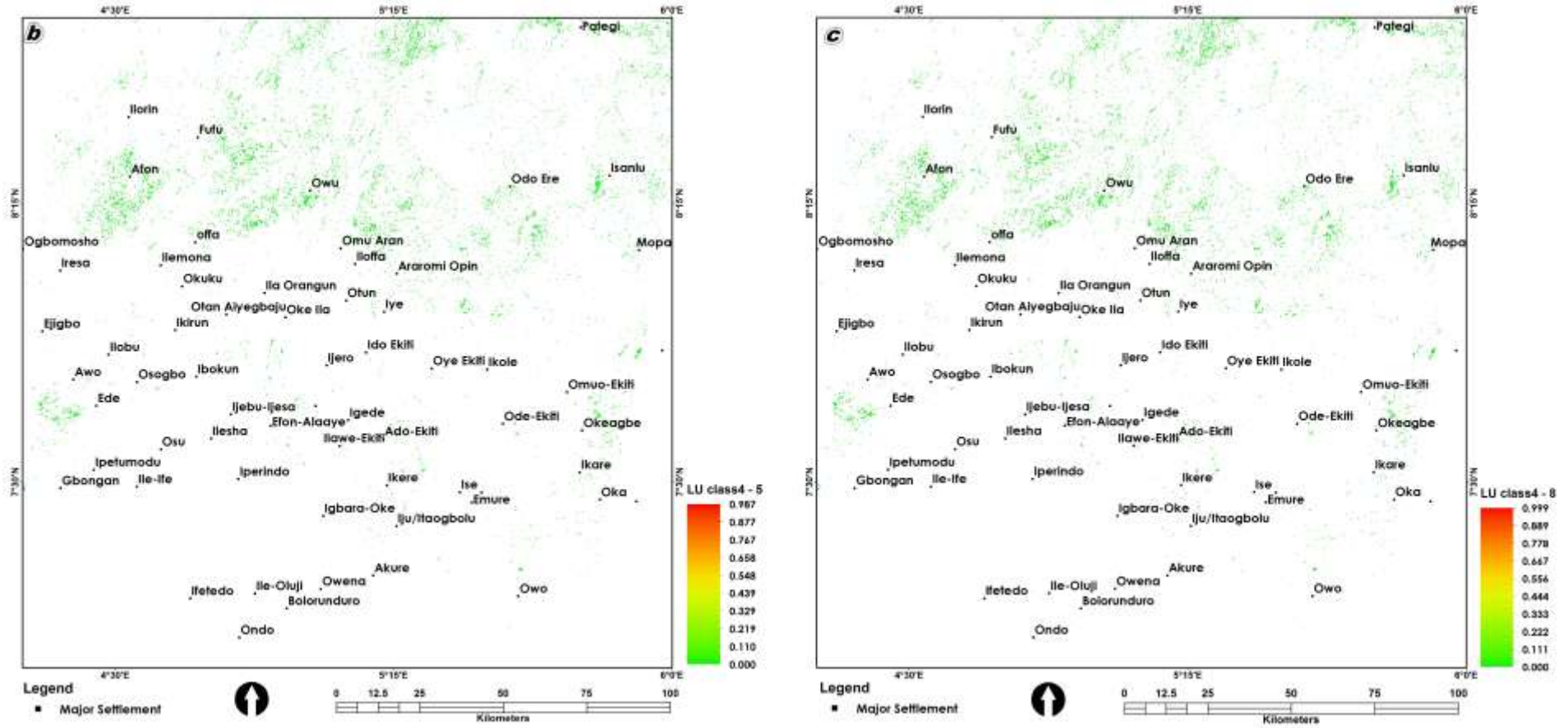

Figure 6.6: Transition potential from farmland to (b) forest and (c) urban *(Source: Author, 2015)*

6.3.2 Landuse/landcover for the present climate (2010)

The spatial pattern and nature of interaction of LULC and climate change within the derived savannah for the present climate was predicted by overlaying the transition potentials shown in figures.6.1 to 6.6 together with the combination of Markov probabilities in Table 6.5. Figure 6.7 shows the static characteristics and spatial distribution of the LULC predicted for the present climate, while Table 6.6 present statistics of the LULC.

Table 6.6: Static characteristics of the predicted LULC for 2010

S/n	LULC Class	Area (Km^2)	Area (Ha)	%
1	Cloud cover	0.00	0.00	0.00
2	Degraded Surfaces	2,340.14	234,014.10	6.20
3	Farmland	4,189.70	418,970.49	11.10
4	Fire Scar	737.97	73,797.14	1.95
5	Forest	15,354.33	1,535,432.73	40.67
6	Grassland	4,458.17	445,817.30	11.81
7	Area without data	2,783.65	278,365.47	7.37
8	Urban	1,455.53	145,553.33	3.86
9	Waterbody	93.84	9,384.17	0.25
10	Woodland	6,338.57	633,856.75	16.79
	Total (2010)	37,751.91	3,775,191.47	100.00

Source: Author, 2015

Forest occupies about 15,354km^2, which represents about 40.7% of the study extent during the present climate as revealed in figure 6.7 and table 6.6. During the present climate, woodland, grassland and farmland cover about 6,339km^2, 4,458km^2 and 4,190km^2 which account for about 17%, 12% and 11% of the study area, respectively. Figure 6.7 and table 6.6 further reveal that degraded surfaces, urban and waterbody take up about 6.2%, 3.9% and 0.3%, which amount to 2,340km^2, 1,456km^2 and 93.84km^2 of surface characteristics of the study area in that order were predicted for the present climate.

In comparing the spatial distribution and nature of the interaction of LULC with the climate change for the present climate, spatio-temporal characteristics of predicted 2010 LULC and 2002 LULC were assessed. Thus, Table 6.7 reveals that forest area reduced by about 9.5%

from 16,959.52km^2 to 15,354.33km^2; grassland while degraded surfaces lost about 18% and 39% from 5,437km^2 to 4,458km^2 and 3,828.60km^2 to 2,340.14km^2 of their area coverage during the period respectively. Furthermore, farmland, fire scar and urban area increased from 1,479km^2 to 4,190km^2, 5,398km^2 to 7,380km^2 and 1,087km^2 to 1,456km^2 amounting to

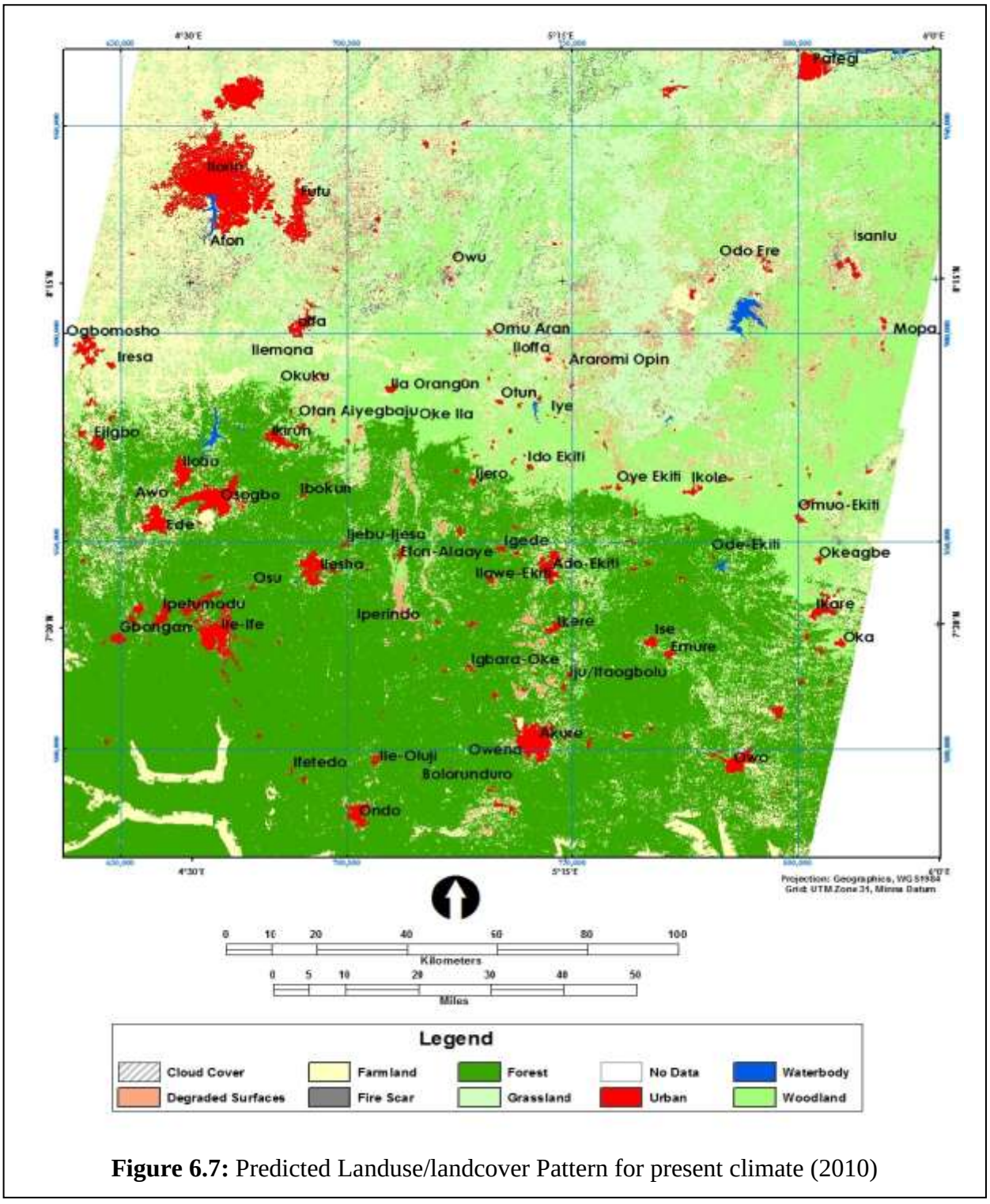

Figure 6.7: Predicted Landuse/landcover Pattern for present climate (2010)

Source: Author, 2015

about 183%, 37% and 34% of their extent. Similarly, waterbody and woodland gained about 22% and 14% to their previous extent during the present climate from 77km^2 to 94km^2 and 5,559km^2 and 6,339km^2 respectively as presented in Table 6.7.

Table 6.7: Spatio-temporal characteristics of LULC (2002 - 2010) predicted

S/n	LULC Class	LULC 2002 (ha)	LULC 2010 (ha)	Change(2002 - 2010)ha	% Change (2002 - 2010)
1	Cloud cover	0.00	0.00	0.00	0.00
2	Degraded Surfaces	382,859.15	234,014.10	-148,845.05	-38.88
3	Farmland	147,905.77	418,970.49	271,064.72	183.27
4	Fire Scar	53,981.97	73,797.14	19,815.17	36.71
5	Forest	1,695,952.74	1,535,432.73	-160,520.01	-9.46
6	Grassland	543,745.90	445,817.30	-97,928.60	-18.01
7	Area without data	278,365.47	278,365.47	0.00	0.00
8	Urban	108,737.94	145,553.33	36,815.39	33.86
9	Waterbody	7,702.24	9,384.17	1,681.93	21.84
10	Woodland	555,940.29	633,856.75	77,916.46	14.02
	Total	3,775,191.47	3,775,191.47	0.00	

Source: Author, 2015

6.4 LCM Modelling of Interaction of LULC and Climate Change in the Future Climate

6.4.1 Transition potential maps

The transition potential maps were modeled for the classes of the LULC with the underlying and proximate drivers of change so as to determine the nature and spatial distribution of interaction between LULC and climate change for the future climate (2050). These are presented in figures 6.8 to 6.11. In addition, Markov probabilities of change for the interaction are presented in Table 6.8.

As presented in the table, the forest class recorded the highest transition probabilities to other LULC classes in the order of woodland, 0.4176, degraded surfaces, 0.3533, fire scar, 0.3194, grassland, 0.3112, waterbody, 0.3108, farmland, 0.2762 and urban, 0.2255 in the future climate *(coloured red).* The figures on the main diagonal cells reveal the probabilities of each LULC class to remain in the same location during the present climate *(coloured yellow),*

while the figures on the right cells of the main diagonal show the chances of other LULC classes to transit to the LULC class from the main diagonal. In addition, the figures on the left cells of the main diagonal present the probabilities of the LULC classes to transit from LULC classes in the main diagonal cells.

Table 6.8: Markov transition probabilities of LULC for future climate

LULC Class	Cloud cover	Degraded Surfaces	Farmland	Fire Scar	Forest	Grassland	No Data	Urban	Waterbody	Woodland
Cloud cover	0.0000	0.1139	0.0396	0.0128	0.3399	0.1225	0.0207	0.2208	0.0110	0.1189
Degraded Surfaces	0.0000	0.1118	0.0527	0.0172	0.3533	0.1703	0.0343	0.0944	0.0045	0.1616
Farmland	0.0000	0.1319	0.0680	0.0200	0.2762	0.1927	0.0471	0.0920	0.0047	0.1675
Fire Scar	0.0000	0.1111	0.0643	0.0215	0.3194	0.2159	0.0216	0.0413	0.0054	0.1996
Forest	0.0000	0.0616	0.0220	0.0079	0.6685	0.0785	0.0069	0.0301	0.0028	0.1217
Grassland	0.0000	0.1076	0.0616	0.0215	0.3112	0.2187	0.0277	0.0435	0.0052	0.2031
No Data	0.0000	0.0569	0.0259	0.0095	0.3053	0.0869	0.3702	0.0159	0.0012	0.1282
Urban	0.0000	0.1199	0.0279	0.0084	0.2255	0.0736	0.0266	0.4355	0.0158	0.0669
Waterbody	0.0000	0.0695	0.0343	0.0215	0.3108	0.0767	0.0075	0.0263	0.3658	0.0875
Woodland	0.0000	0.0900	0.0493	0.0179	0.4176	0.1839	0.0171	0.0318	0.0046	0.1879

Source: Author, 2015

The transition potential from degraded surfaces to farmland, fire scar and urban are shown in figure 6.8 *(a, b & c)* with transition potentials ranging from 0 to 0.998, 0 to 0.953 and 0 to 0.866, respectively. In the period between 2002 and 2050, farmland has the greatest suitability of 0 to 99.8% to transit from degraded surfaces. Also, figure 6.9 (a - g) show the interaction between forest and other LULC classes during the future climate. In addition, transition from forest to degraded surfaces, farmland, fire scar, grassland, urban, waterbody and woodland are shown in figure 6.9 *(a – g)* with a transition potentials of 0 – 0.635, 0 – 0.208, 0 – 0.999, 0 – 0.999, 0 – 0.999, 0 – 0.018 and 0 – 0.981 correspondingly. During the future climate, transition potentials are higher between forest and fire scar, forest and grassland and forest and urban with a 0 – 99.9% chances as depicted in figure 6.9 *(c, d & e)*. Furthermore, lower transition potentials are recorded between forest and farmland and forest and waterbody having a 0 – 0.208 and a 0 – 0.018 transition potentials in that order.

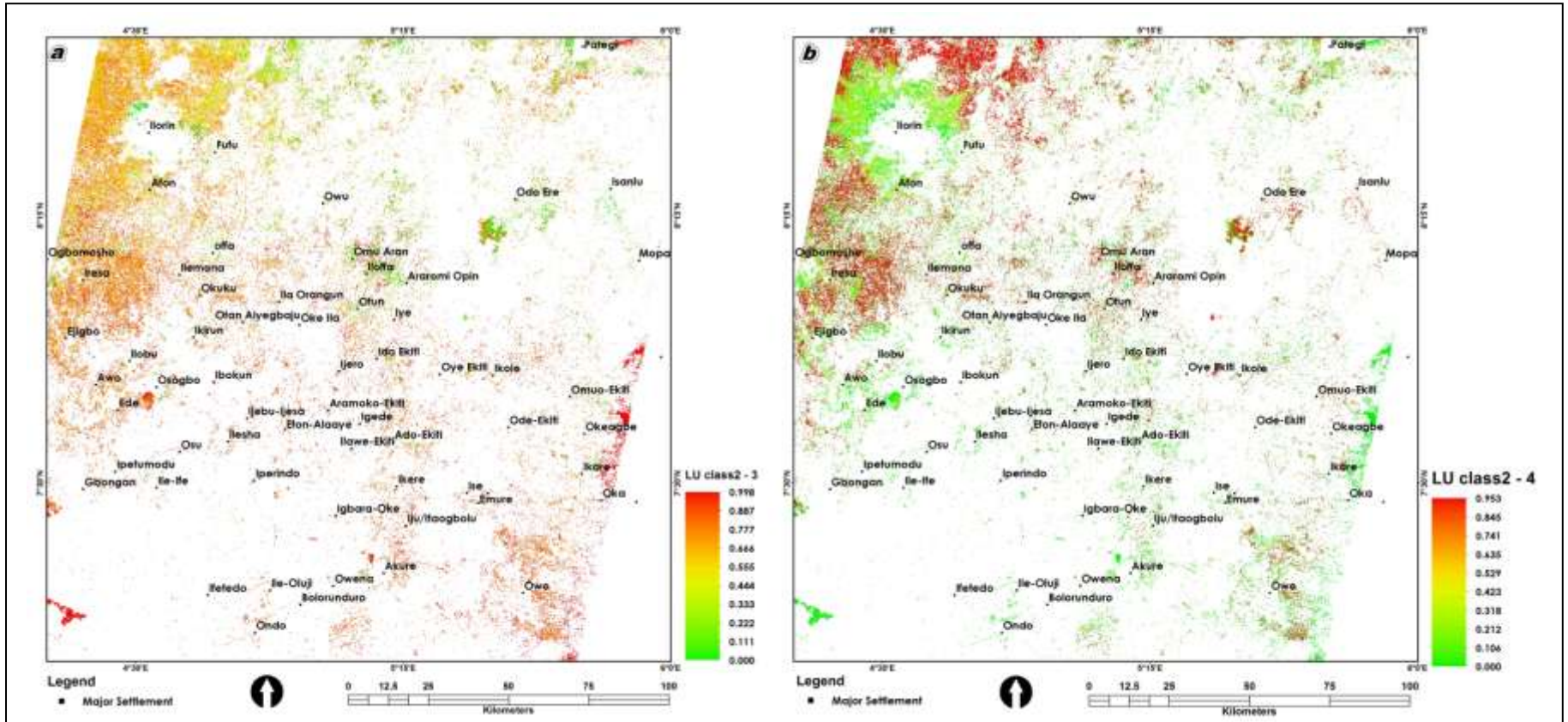

Figure 6.8: Transition potential from degraded surfaces to (a) farmland, (b) fire scar and (c) urban *(Source: Author, 2015)*

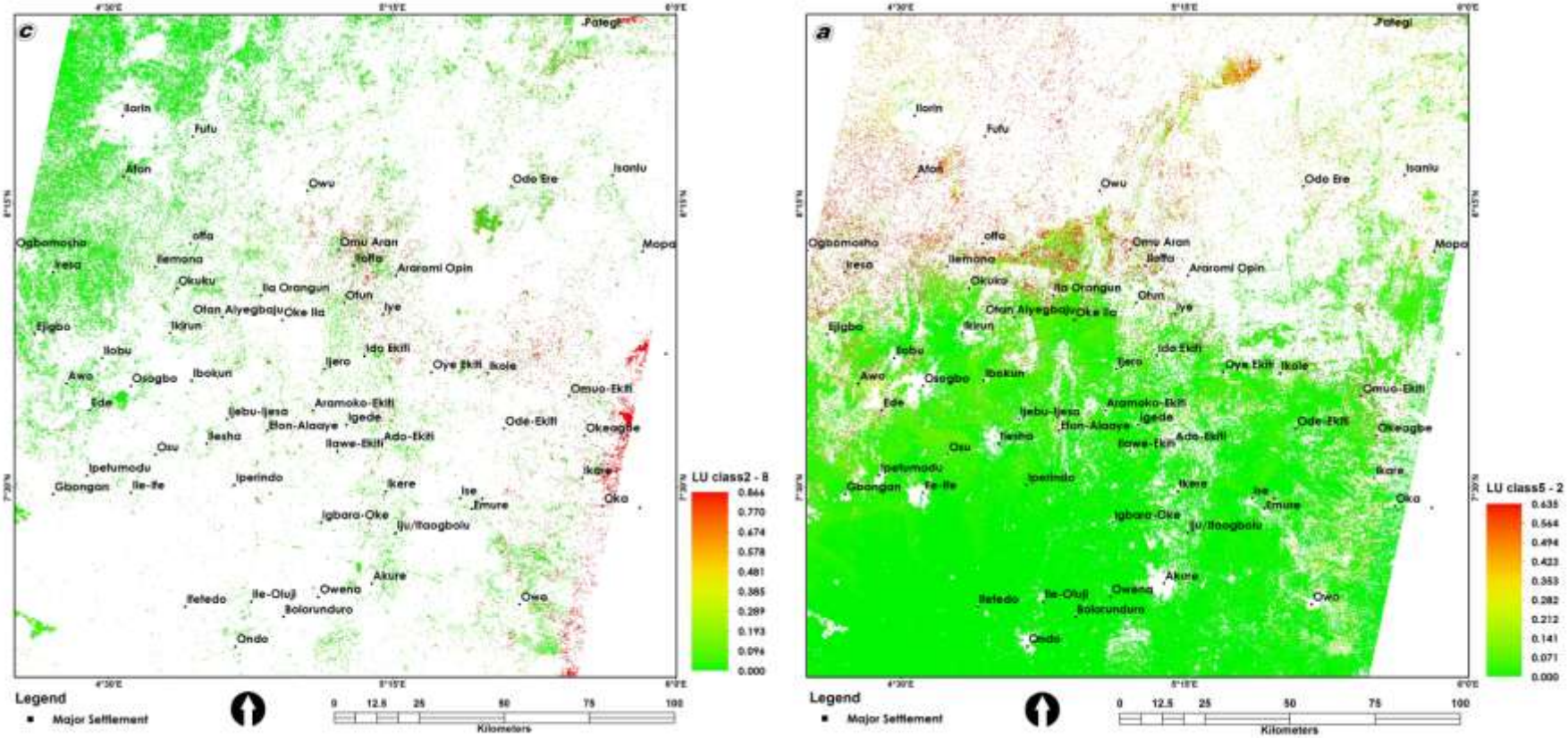

Figure 6.8: Transition potential from degraded surfaces to (c) urban and **Figure 6.9:** Transition potential from forest to (a) degraded surfaces *(Source: Author, 2015)*

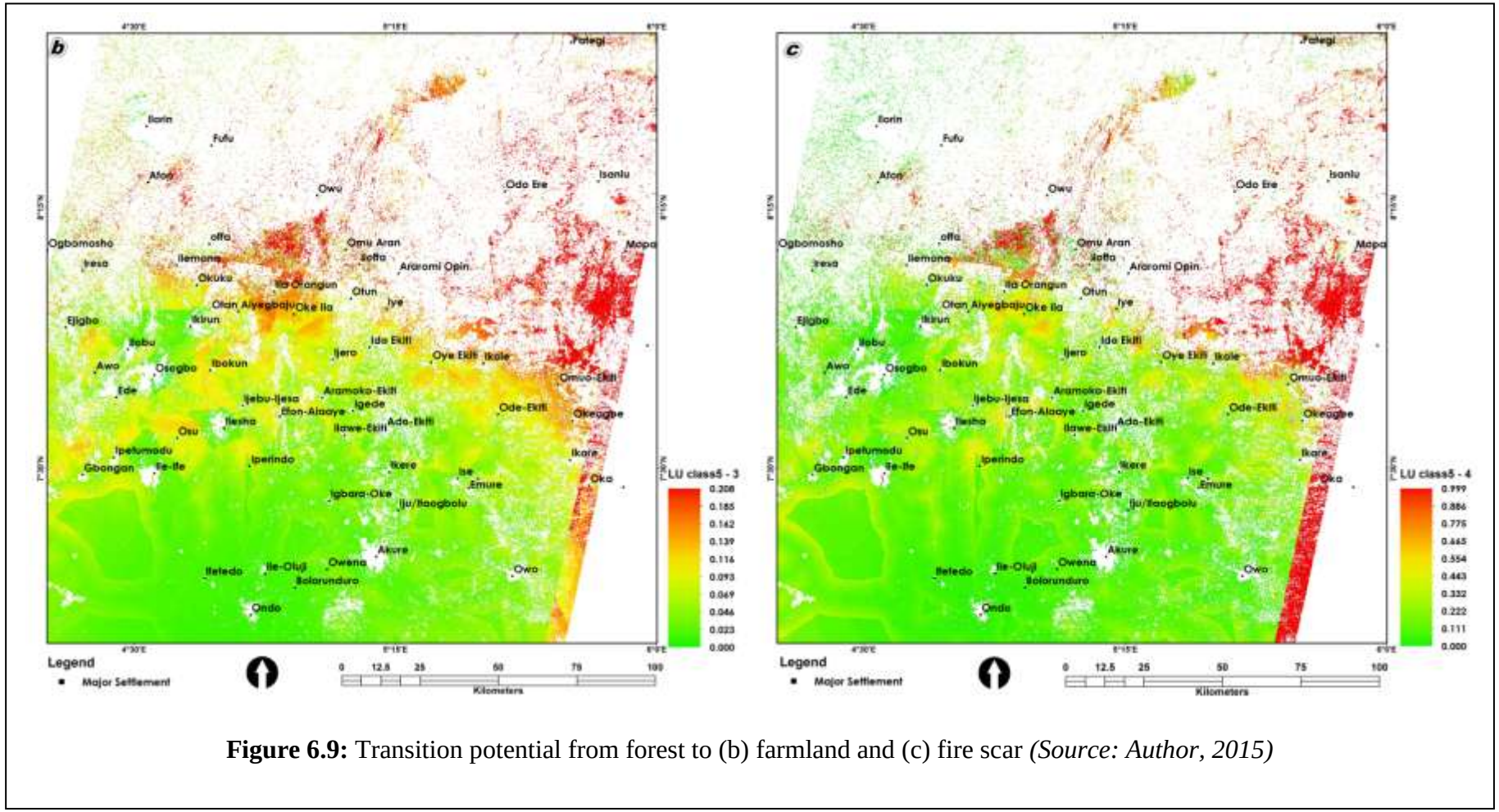

Figure 6.9: Transition potential from forest to (b) farmland and (c) fire scar *(Source: Author, 2015)*

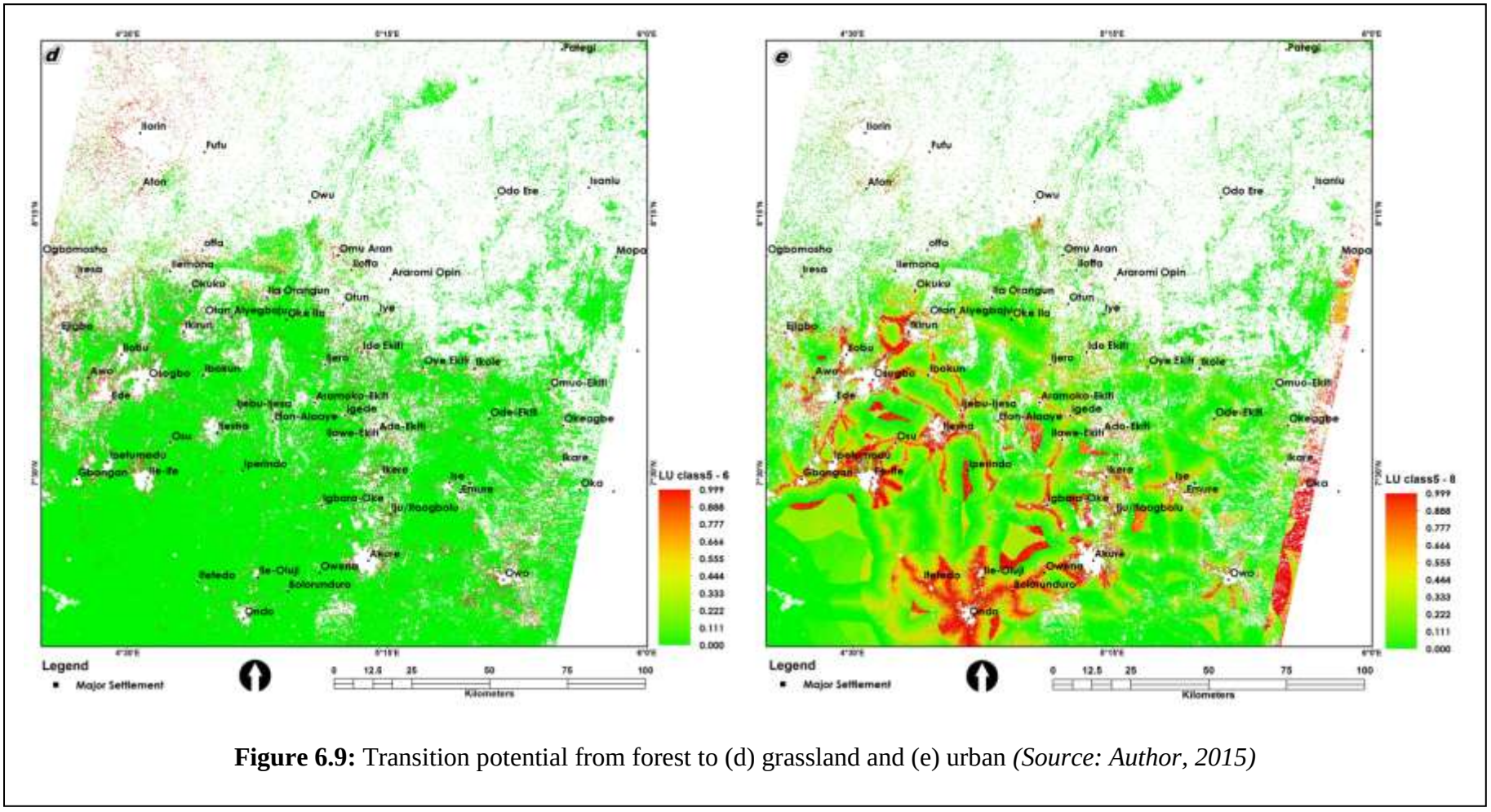

Figure 6.9: Transition potential from forest to (d) grassland and (e) urban *(Source: Author, 2015)*

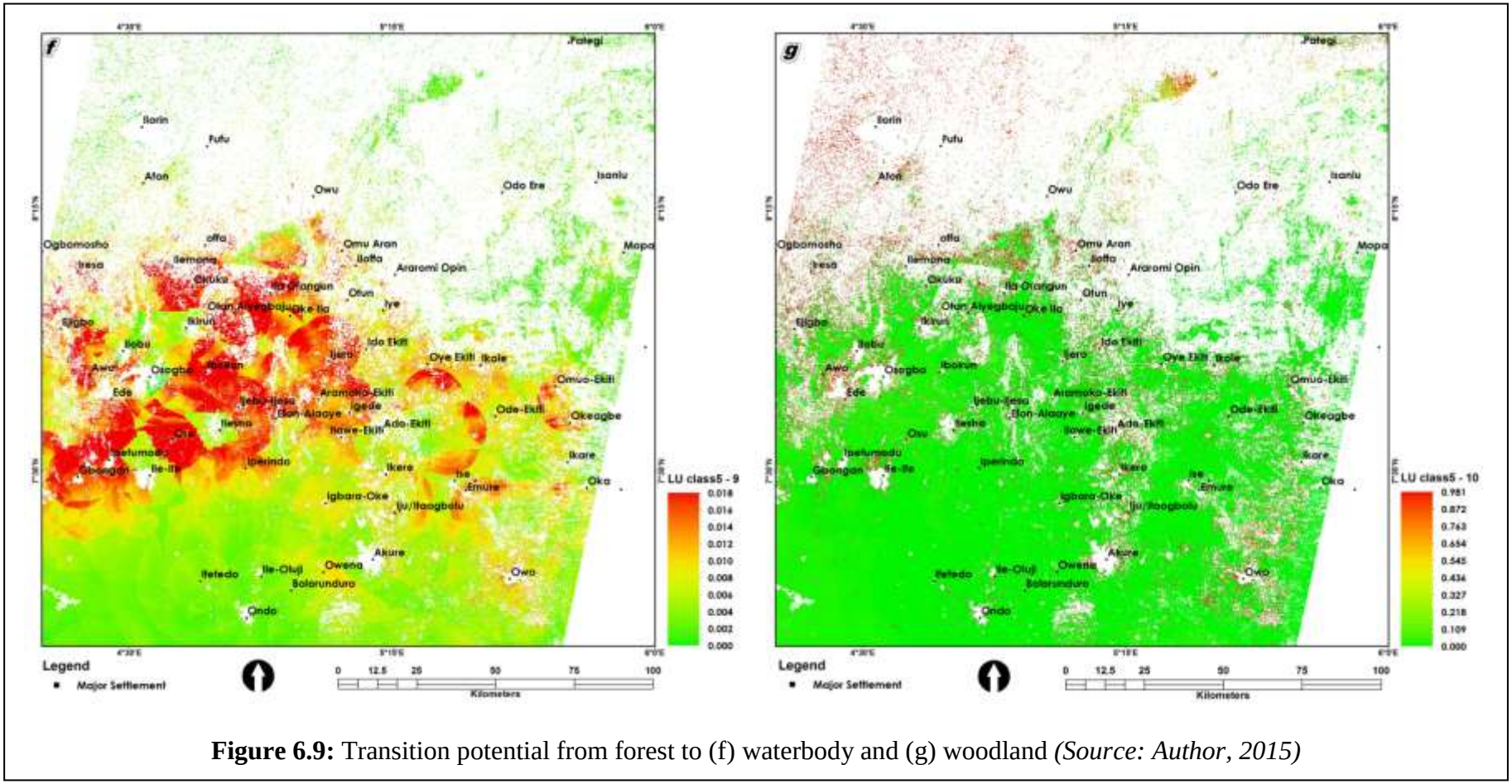

Figure 6.9: Transition potential from forest to (f) waterbody and (g) woodland *(Source: Author, 2015)*

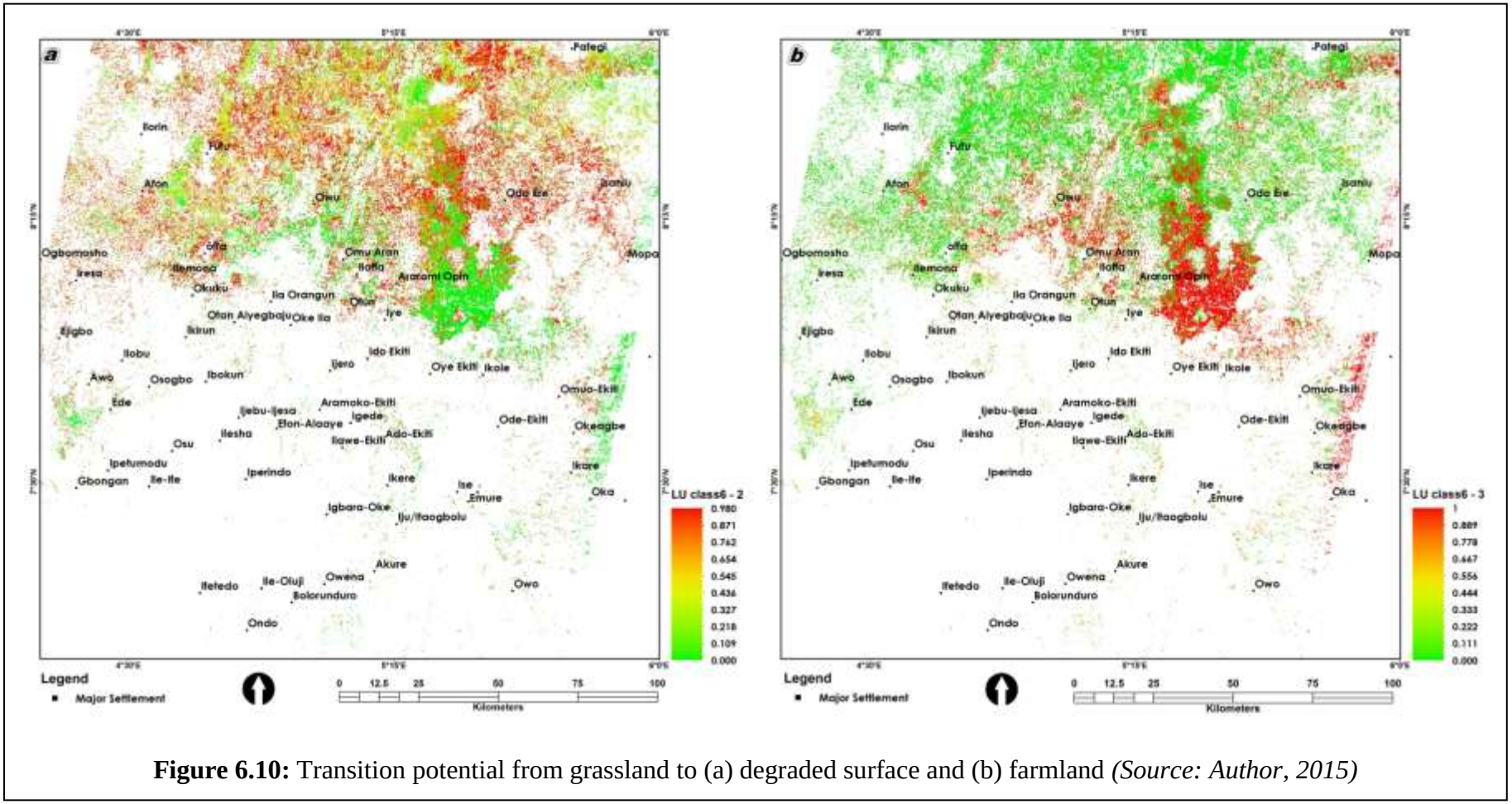

Figure 6.10: Transition potential from grassland to (a) degraded surface and (b) farmland *(Source: Author, 2015)*

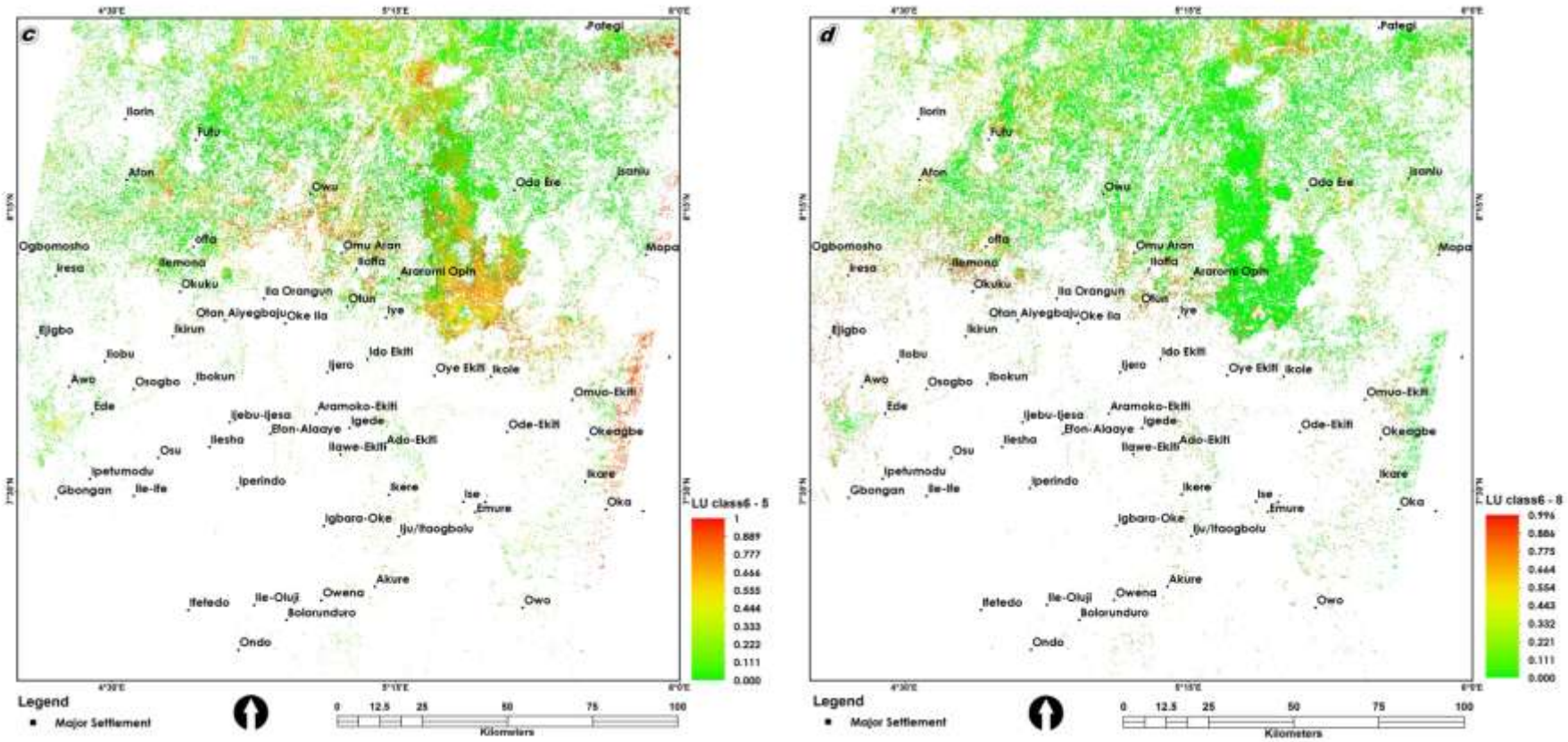

Figure 6.10: Transition potential from grassland to (c) forest and (d) urban *(Source: Author, 2015)*

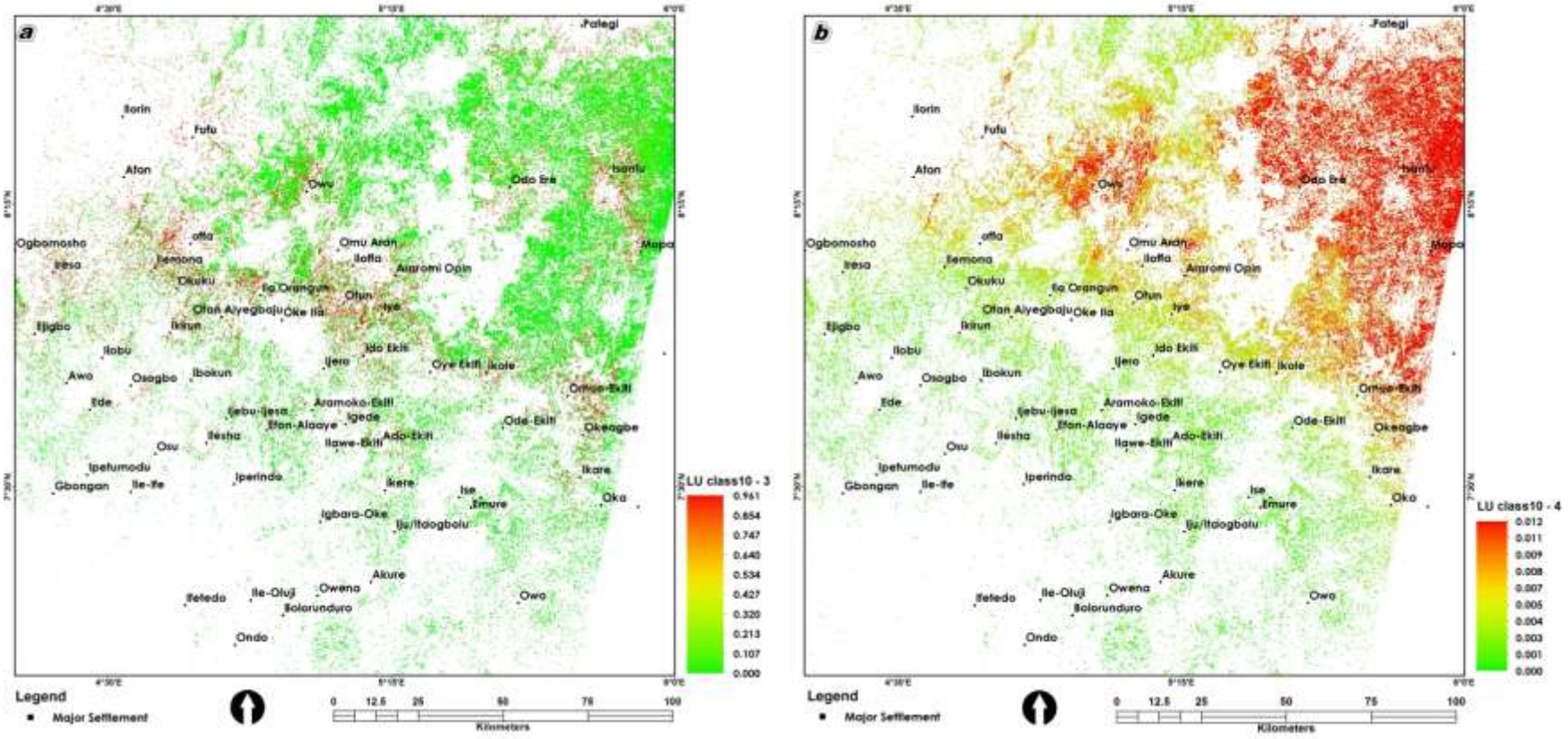

Figure 6.11: Transition potential from woodland to (a) farmland and (b) fire scar *(Source: Author, 2015)*

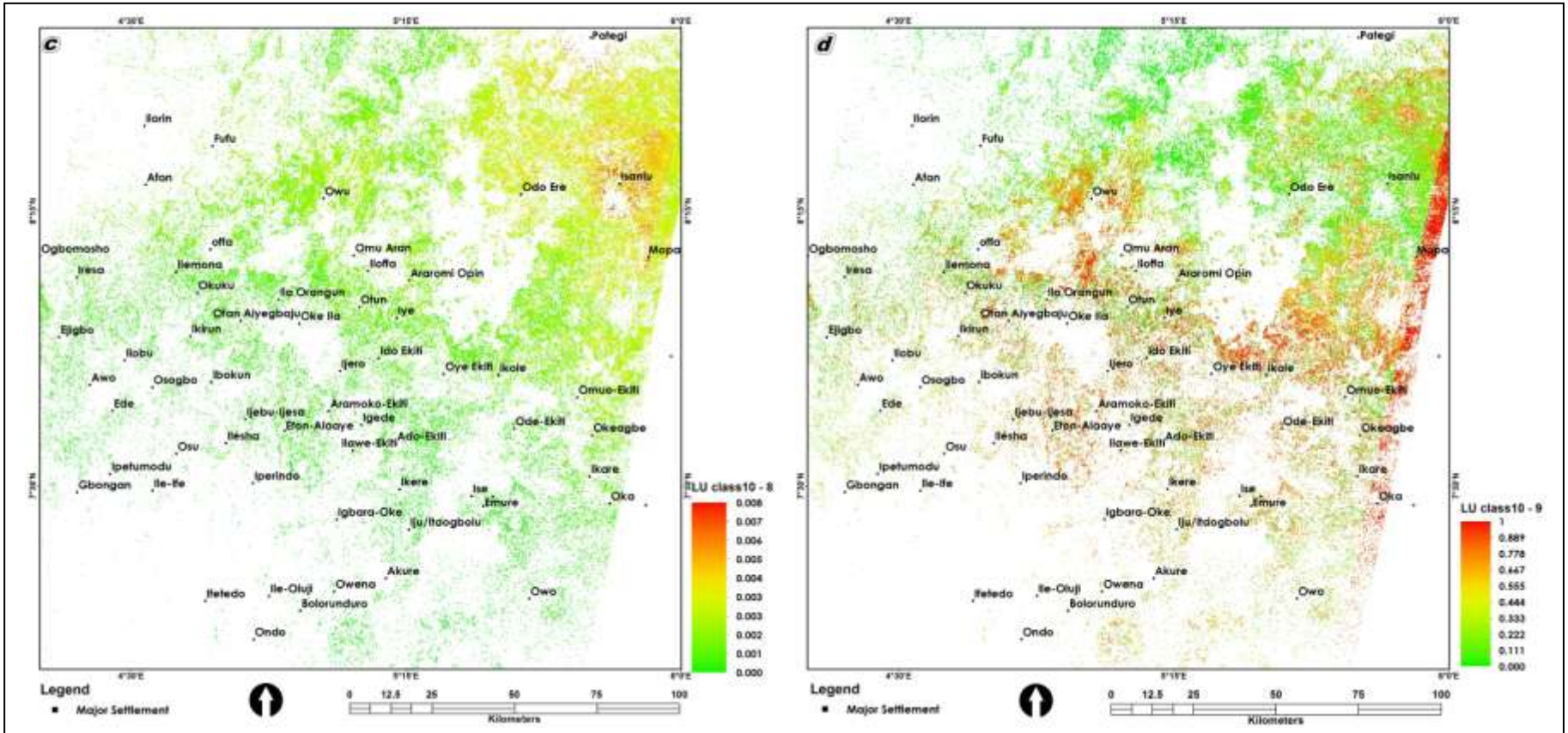

Figure 6.11: Transition potential from woodland to (c) urban and (d) waterbody *(Source: Author, 2015)*

Similarly, figure 6.10 shows the transition potential maps from grassland to other LULC classes during the future climate. Transition potentials from grassland to degraded surfaces, farmland, forest and urban are shown in figure 6.10 *(a – d)* with the transition potentials ranging from 0 – 0.980, 0 – 1, 0 – 1 and 0 – 0.996 respectively. The interaction between the grassland and farmland and grassland and forest will be very high as they recorded transition potentials of 0 – 1 during the future climate and so also with degraded surfaces and urban areas with suitability of 0 – 99.8% and 0 – 99.6% respectively. Finally, transition potential maps of woodland to transit to farmland, fire scar, urban and waterbody are illustrated in figure 6.11 *(a – d)* respectively. The transition potentials from woodland to farmland, fire scar, urban and waterbody are in the order of 0 – 0.961, 0 – 0.012, 0 – 0.008 and 0 – 1 as illustrated in figure 6.11. During the future climate, woodland will record the highest transition potentials to waterbody with a suitability of 0 – 100%, followed by farmland, 0 – 96.1%, fire scar, 0 – 1.2% and urban, 0 – 0.8% in that order.

6.4.2 Landuse/landcover for the future climate (2050)

The nature between the interaction of landuse/landcover (LULC) and climate change during the future climate (2050) is predicted by modelling the proximate and underlying drivers of LULC change and climatic parameters by cartographically overlaying the transition potential maps in figures 6.8 to 6.11. The spatial pattern and distribution of the nature of the interaction of LULC and climate change during the future climate is shown in figure 6.12 while the statistics are presented in Table 6.9. Figure 6.12 reveals that forest and woodland will be occupying about 13,146km^2 and 7,047km^2 which represent about 35% and 19% of the study area respectively during the future climate. Also, farmland, grassland and degraded surfaces will cover about 4,829.33km^2 (12.8%), 3,920km^2 (10.4%) and 2,663km^2 (7.1%) of 37,751.9km^2 covered by the entire area correspondingly. Furthermore, urban, fire scar and

waterbody covered 2,372.6km^2, 839.17km^2 and 150.1km^2, which represent about 6.3%, 2.22% and 0.4% of the study area in the future climate in that order.

Table 6.9: Static characteristics of the LULC for 2050

S/n	LULC Class	Area (Km^2)	Area (Ha)	%
1	Cloud cover	0.00	0.00	0.00
2	Degraded Surfaces	2,662.96	266,296.00	7.05
3	Farmland	4,829.33	482,933.23	12.79
4	Fire Scar	839.17	83,916.55	2.22
5	Forest	13,146.60	1,314,660.09	34.82
6	Grassland	3,920.10	392,009.72	10.38
7	Area without data	2,783.65	278,365.47	7.37
8	Urban	2,372.60	237,259.85	6.28
9	Waterbody	150.08	15,008.19	0.40
10	Woodland	7,047.42	704,742.38	18.67
	Total (2050)	37,751.91	3,775,191.47	100.00

Source: Author, 2015

In comparing the nature and spatial pattern of interaction between LULC and climate change in the future climate, LULC 2050 is predicted with the spatial distribution and pattern of LULC in 2002 presented in Table 6.10. Table 6.10 reveals that forest, grassland and degraded surfaces will reduce from 16,959.53km^2, 5,437.46km^2 and 3,828.60km^2 in 2002 to 13,146.60km^2, 3,920.10km^2 and 2,662.96km^2 in 2050, which amount to 22.5%, 27.9% and 30.5% reduction in their area extent respectively.

Table 6.10: Spatio-temporal characteristics of Landuse/Landcover (2002 - 2050)

S/n	LULC Class	LULC 2002 (ha)	LULC 2050 (ha)	Change(2002 - 2050)ha	% Change (2002 - 2050)
1	Cloud cover	0.00	0.00	0.00	0.00
2	Degraded Surfaces	382,859.15	266,296.00	-116,563.15	-30.45
3	Farmland	147,905.77	482,933.23	335,027.46	226.51
4	Fire Scar	53,981.97	83,916.55	29,934.58	55.45
5	Forest	1,695,952.74	1,314,660.09	-381,292.65	-22.48
6	Grassland	543,745.90	392,009.72	-151,736.18	-27.91
7	Area without data	278,365.47	278,365.47	0.00	0.00
8	Urban	108,737.94	237,259.85	128,521.91	118.19
9	Waterbody	7,702.24	15,008.19	7,305.95	94.85
10	Woodland	555,940.29	704,742.38	148,802.09	26.77
	Total	3,775,191.47	3,775,191.47	0.00	

Source: Author, 2015

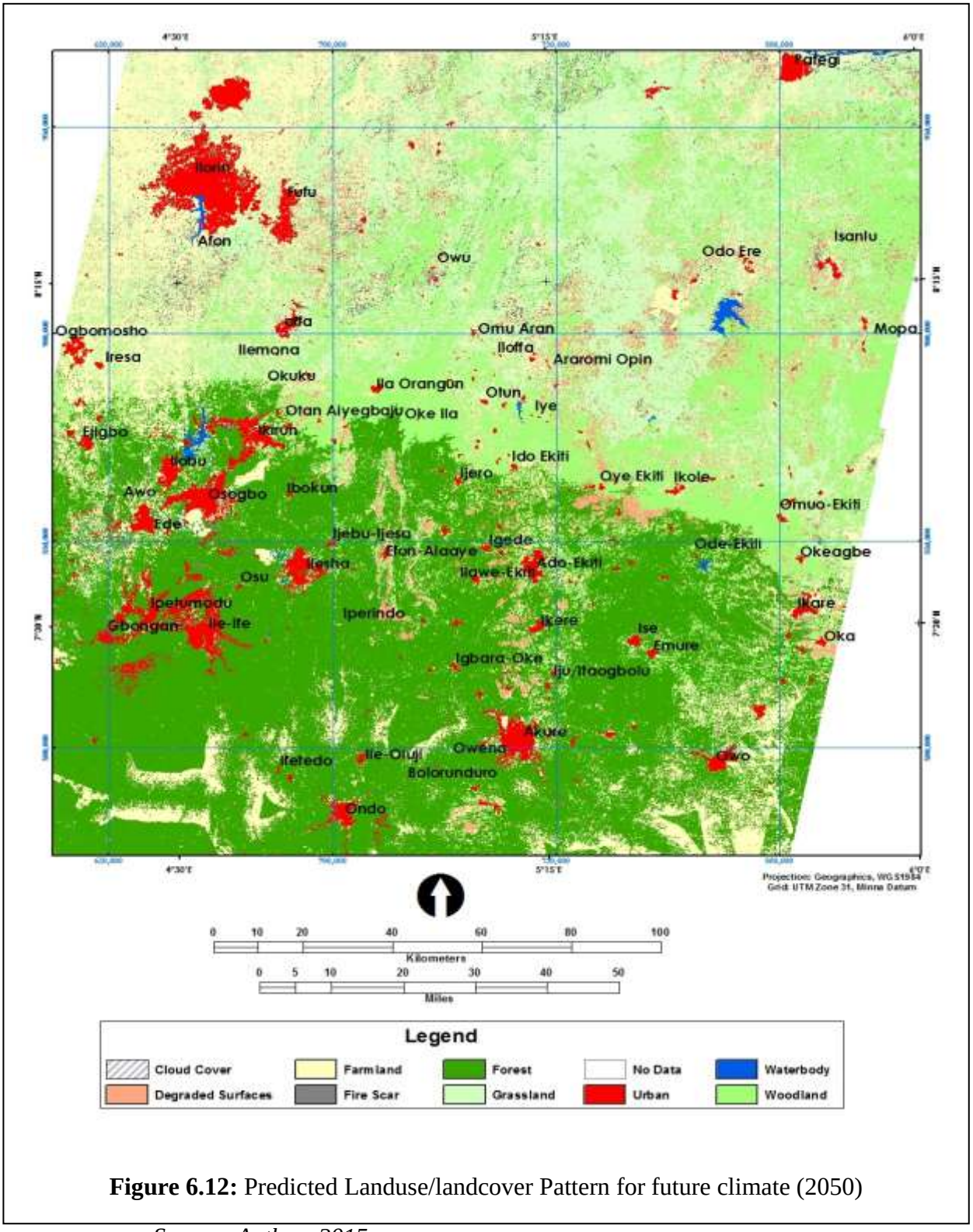

Figure 6.12: Predicted Landuse/landcover Pattern for future climate (2050)

Source: Author, 2015

However, farmland, urban and waterbody will expand from 1,497.06km^2, 1,087.38km^2 and 77.02km^2 in 2002 to 4,829.33km^2, 2,372.60km^2 and 150.08km^2 in 2050, which represent about 226.5%, 118.2% and 94.9% expansion into other LULC classes as presented in Table 6.10 respectively.

6.5 Spatio-Temporal Analysis of LULC in the Present and Future Climates

The spatial distribution and nature of interaction between LULC and climate change during the present climate (2010) and future climate (2050) are shown in figures 6.7 and 6.12 respectively. The statistics of spatio-temporal characteristics of LUCC between the present and future climates are presented in Table 6.11. During the period, forest and grassland lost about 14% and 12% respectively to other LULC classes, while urban and waterbody are main gainers of the future climate with 63% and 60% increase respectively. Similarly, farmland, degraded surfaces, fire scar and woodland will also increase by 15%, 14%, 14% and 11%, respectively, during the future climate as presented and shown in Table 6.10 and figure 6.13.

Table 6.11: Spatio-temporal characteristics of Landuse/Landcover (2010 - 2050)

S/n	LULC Class	LULC 2010 (ha)	LULC 2050 (ha)	Change(2010 - 2050)ha	% Change (2010 - 2050)
1	Cloud cover	0.00	0.00	0.00	0.00
2	Degraded Surfaces	234,014.10	266,296.00	32,281.90	13.79
3	Farmland	418,970.49	482,933.23	63,962.74	15.27
4	Fire Scar	73,797.14	83,916.55	10,119.42	13.71
5	Forest	1,535,432.73	1,314,660.09	-220,772.64	-14.38
6	Grassland	445,817.30	392,009.72	-53,807.58	-12.07
7	No Data	278,365.47	278,365.47	0.00	0.00
8	Urban	145,553.33	237,259.85	91,706.52	63.01
9	Waterbody	9,384.17	15,008.19	5,624.02	59.93
10	Woodland	633,856.75	704,742.38	70,885.63	11.18
	Total	3,775,191.47	3,775,191.47	0.00	

Source: Author, 2015

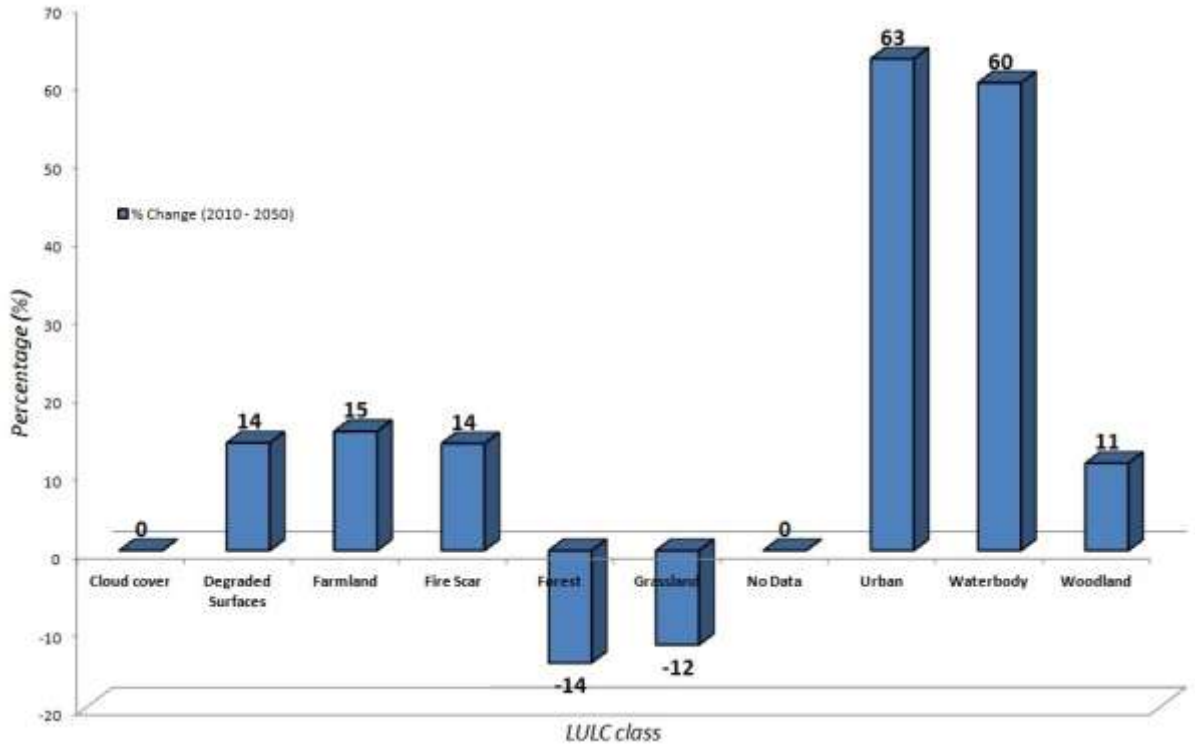

Figure 6.13: Spatio-temporal characteristics of Landuse/Landcover (2010 - 2050) *(Source: Author, 2013)*

6.6 Model Validation and Calibration

The static and temporal characteristics of LULC for 1972, 1986, 2002 and 2010 were generated from the Landsat satellite imageries of the corresponding years covering the study area. However, another set of LULC static characteristics for 2010 and 2050 were simulated due to the interaction of LULC and climate change during the present and future climates. Consequently, the simulated 2010 and 2050 LULC were validated using the generated (true) 2010 LULC against the simulated 2010 LULC. The generated and simulated LULC for 2010 have similar signals pattern as shown in figure 6.14. Therefore, the model simulated LULC patterns for 2010 and 2050 reasonably well as signals and pulses followed a similar trend as could be seen in figure 6.15. However, the computed kappa index and agreement between

generated and simulated LULC in terms of quantities and areal characteristics are poor when they are compared. Details of the Kappa index are contained in appendix III.

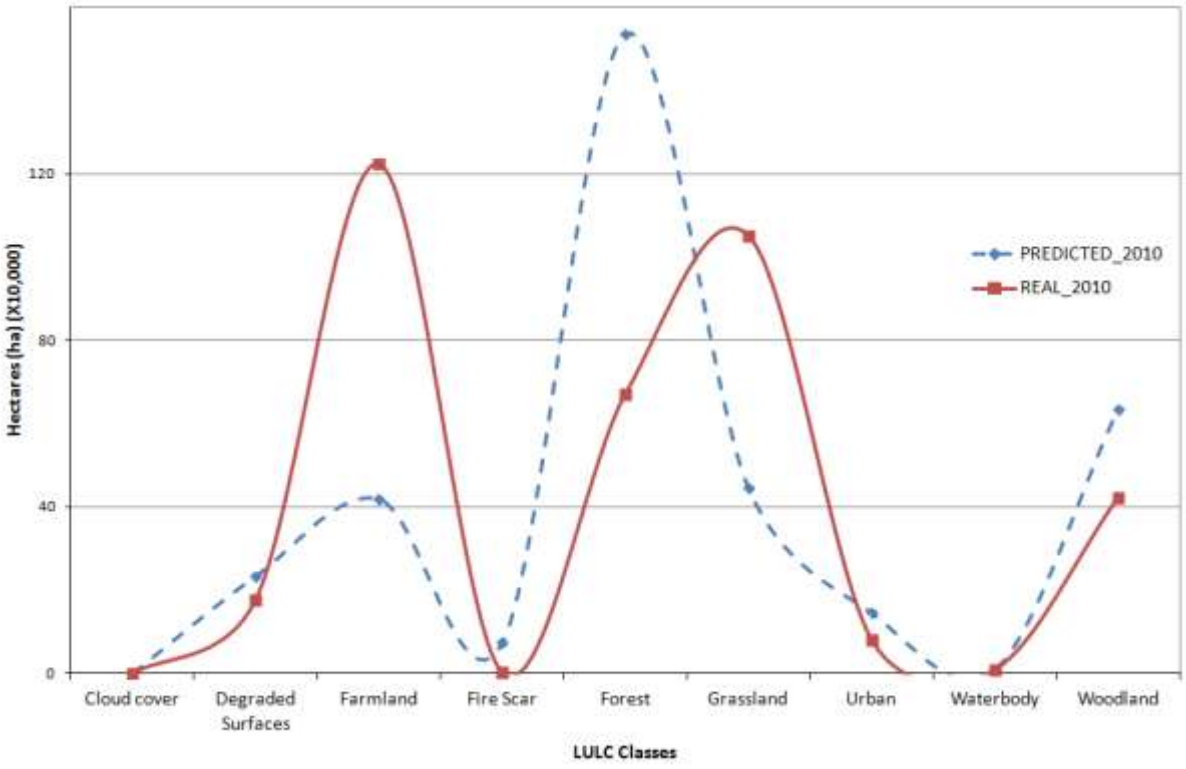

Figure 6.14: Comparison of areal characteristics of predicted and real LULC, 2010 *(Source: Author, 2013)*

This scenario is due to some problems in the image data used. The image used was one of Landsat 7 ETM+ imageries with SLC off error, it has gaps-like stripes and the gaps were filled before it was interpreted to generate the 2010 LULC. Also, the edges are not properly filled. The date of acquisition was in during the peak of the dry season (i.e. February) when farmlands are prepared and tree shed their leaves, while the images used to simulate was acquired in November/December at the end of the cessation of rainfall. Therefore, there was confusion between farmland in the simulated LULC map and forest in the generated LULC map.

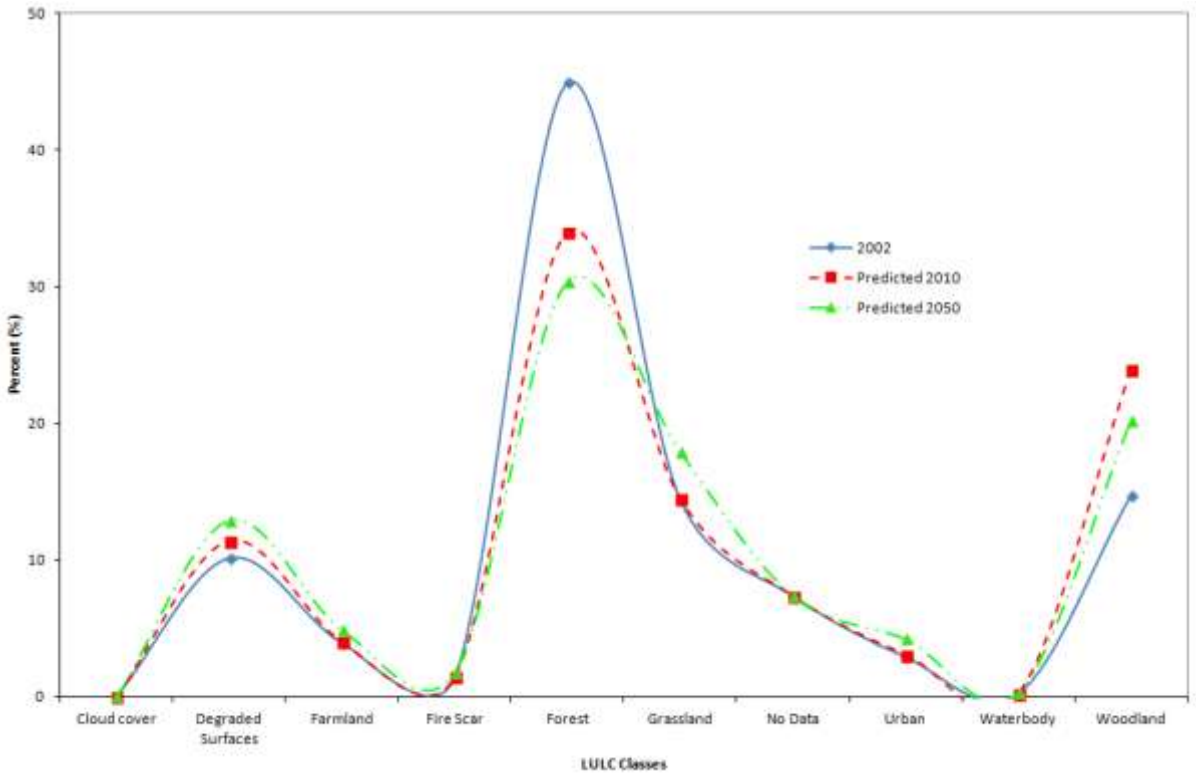

Figure 6.15: Agreement between classes of LULC 2002 and predicted 2010 and 2050 *(Source: Author, 2013)*

CHAPTER SEVEN

ESTIMATION OF THE CARBON DIOXIDE (CO_2) DUE TO INTERACTION OF LULC AND CLIMATE CHANGE

7.1 Introduction

This research has so far revealed that there are a number of implications arising from the interaction of LULC and climate change. These implications include flooding and wind storms, food security, water resources, air pollution, change in biodiversity, soil degradation, and so on. All these are fundamentally due to the extreme weather and climate events as well as the exposure to forest degradation and deforestation. However, the study assessed the implications of the interaction on the human activities emanating from continued forest degradation and deforestation vis-à-vis the quantity of the carbon dioxide (CO_2) that will be emitted in the future climate if the activities persist as it is currently within the study area.

Consequent upon the above, this chapter presents the result of the analysis carried out in order to estimate the quantity of CO_2 that will be emitted due to the interaction of LULC and climate change. The chapter is made up of three sections. Section one presents the spatial distribution and pattern of the reclassified Landuse/Landcover (LULC) for the base years, 1986 and 2002. Section two presents the result of modeling of the interaction of LULC and climate change for the present and future climates of derived savannah using the Land Change Modeler (LCM) techniques, while the last section discusses the quantification of the Carbon dioxide (CO_2) concentration that will be emitted during the future climate.

7.2 The Reclassified LULC (1986 – 2002)

The reclassified LULC for the savannah area of study is presented in figures 7.1 and 7.2 for 1986 and 2002. As shown by the generated statistics in Table 7.1, forests accounted for

1,598,409ha (42%) in 1986 and 1,695,953ha (45%) in 2002. Waterbody increased from 3,299ha in 1986 to 7,702ha in 2002, while the area covered with cloud cover decreased from 344,317ha in 1986 to 278,365% in 2002.

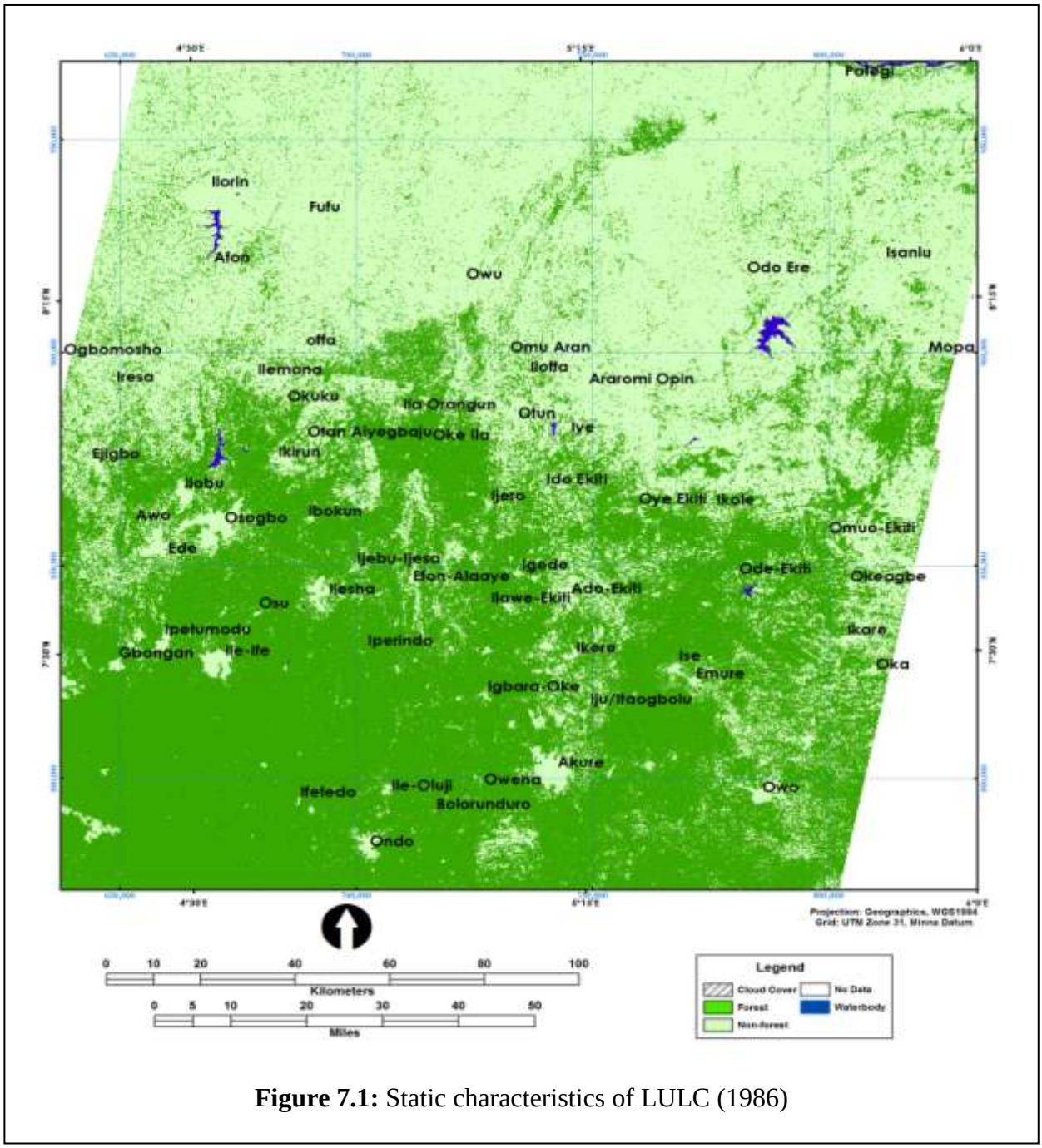

Figure 7.1: Static characteristics of LULC (1986)

Source: Author, 2015

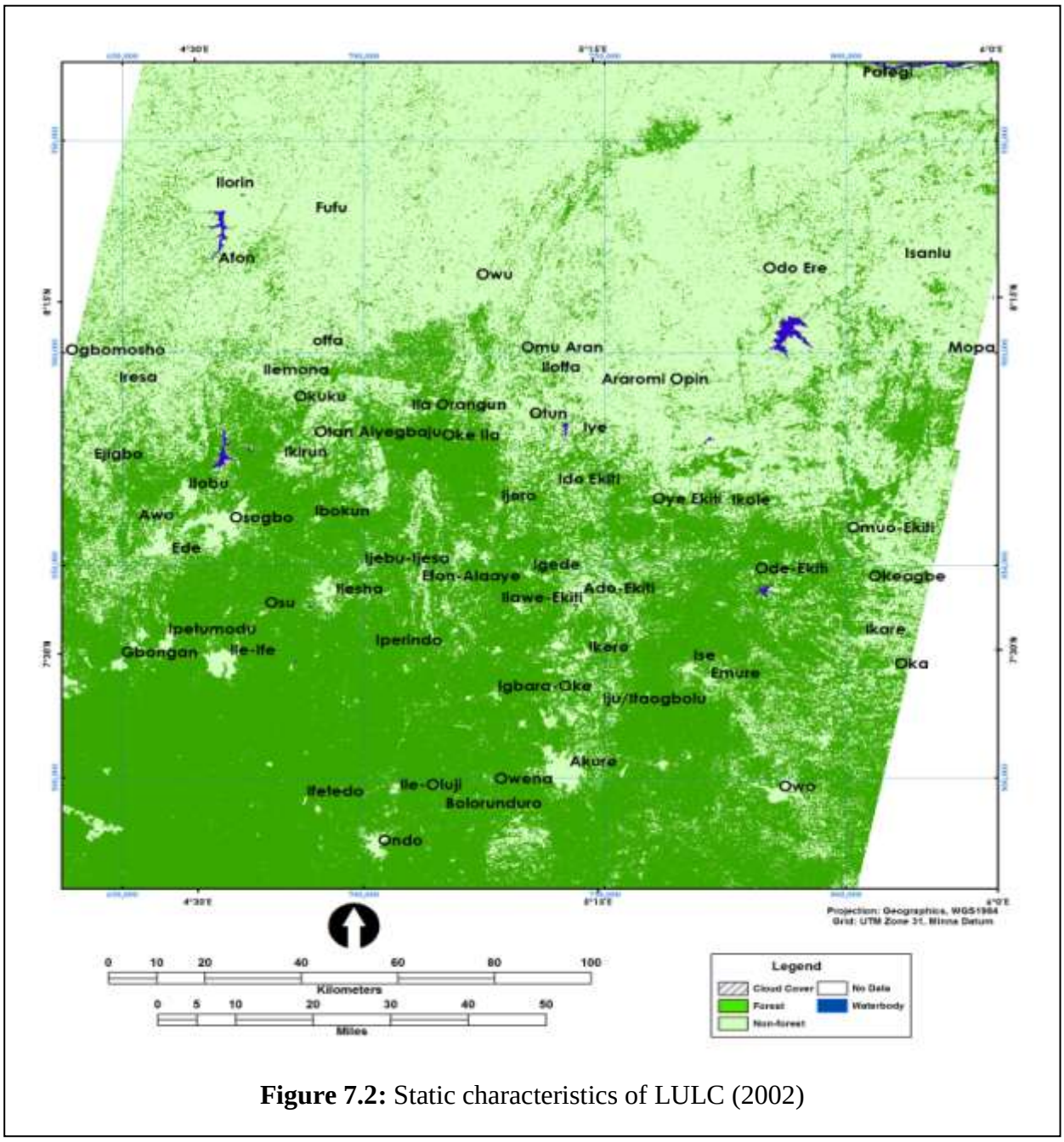

Figure 7.2: Static characteristics of LULC (2002)

Source: Author, 2015

Table 7.1: Spatio-temporal characteristics of re-classified LULC (1986 – 2002)

S/N	LU Classes	LULC (1986) ha	%	LULC (2002) ha	%	Change (1986 - 2002) (ha)	Change (1986 - 2002) (%)
1	Cloud Cover	344,417.3	9.1	278,365.5	7.4	-66,051.8	-19.18
2	Forest	1,598,408.8	42.3	1,695,952.7	44.9	97,543.9	**6.10**
3	Non-forest	1,829,066.7	48.4	1,793,171.0	47.5	-35,895.7	-1.96
4	Waterbody	3,298.6	0.1	7,702.2	0.2	4,403.6	133.50
	Total	3,775,191.5	100.0	3,775,191.5	100.0	0.00	

Source: Author, 2015

Also as presented in Table 7.1, the temporal characteristic of LULC over the two years show that forest areas gained about 97,543.9ha (6.10%) between that 1986 and 2002, while the non forest area lost about 1.96% which reduced from 1,829,067ha in 1986 to 1,793,171ha in 2002. In addition, some river networks in the area were dammed between the two periods, this accounted for about 133.5% increase in the waterbody from 3,298.6ha to 7,702.2ha. The dams include Egbe and Ero in Ekiti State and Ejiba in Kogi State as shown in figures 7.1 and 7.2.

7.3 The LULC and Climate Change for the Present and Future Climates

The nature and spatial pattern of the interaction between LULC and climate change for both the present and future climates as predicted are shown in figures 7.3 and 7.4 respectively, while the spatio-temporal characteristics of the interaction are presented in Table 7.2.

Table 7.2: Spatio-temporal characteristics of re-classified LULC (2010 – 2050)

S/N	LU Classes	LULC (2010) ha	LULC (2010) %	LULC (2050) ha	LULC (2050) %	Change (2010 - 2050) (ha)	Change (2010 - 2050) (%)
1	Cloud Cover	278,365.5	7.4	278,365.47	7.4	0.0	0.00
2	Forest	1,535,685.2	40.7	954,516.24	25.3	-581,168.9	**-37.8**
3	Non-forest	1,953,438.6	51.7	2,534,607.52	67.1	581,168.9	29.8
4	Waterbody	7,702.2	0.2	7,702.24	0.2	0.0	0.00
	Total	3,775,191.5	100.0	3,775,191.5	100.0	0.0	

Source: Author, 2015

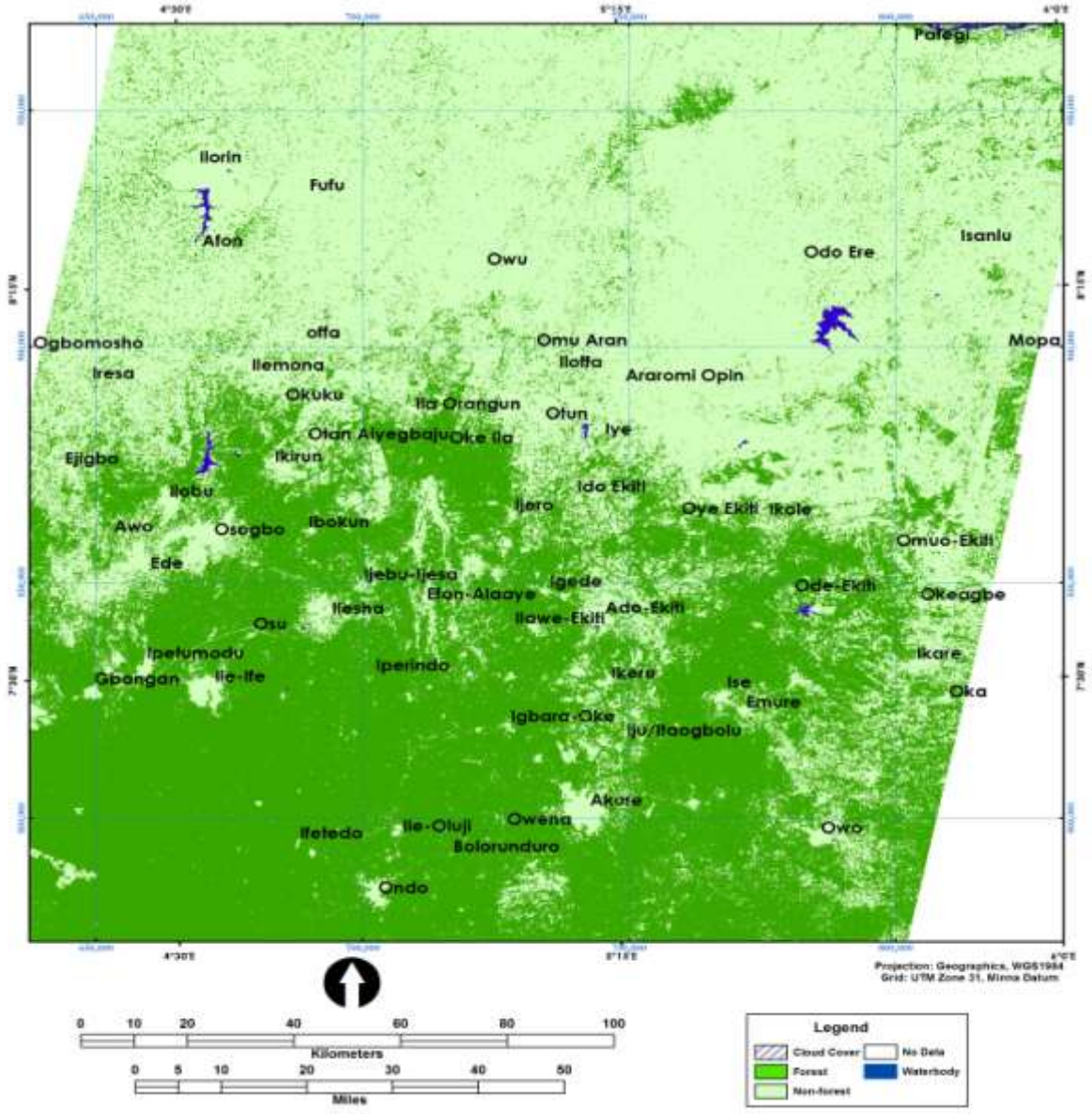

Figure 7.3: Static characteristics of LULC (2010)

Source: Author, 2015

Forest area covered about 1,535,685ha and 954,516ha during the present and future climates, which represent about 40.7% and 25.3% respectively. This means that the forest area lost about 37.84% of its extent during the period, while the non-forest area increased from 1,953,438.6ha (52%) to 2,543,607.5ha (67%) between 2010 and 2050. This shows that non-

forest area gained about 581,168ha (29.75%) to its area extent during the period under study as presented in Table 7.2.

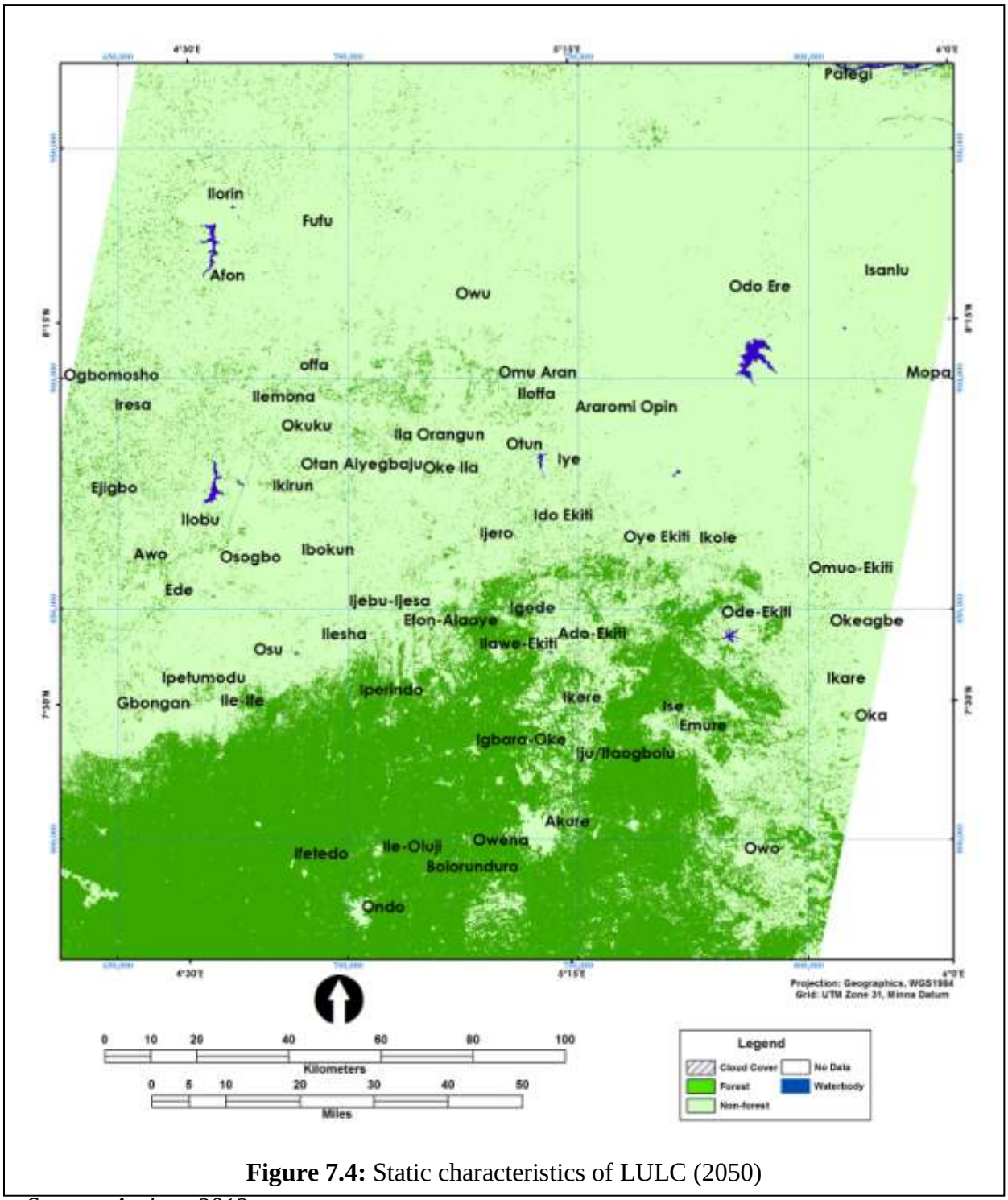

Figure 7.4: Static characteristics of LULC (2050)

Source: Author, 2013

The study reveals that the study area lost about 9.45% of the forests between 2002 and 2010 as presented in Table 7.3. The derived savannah is predicted to loss about 37.84% of forest

land between 2010 and 2050 due to the interaction of LULC and climate change within the study area.

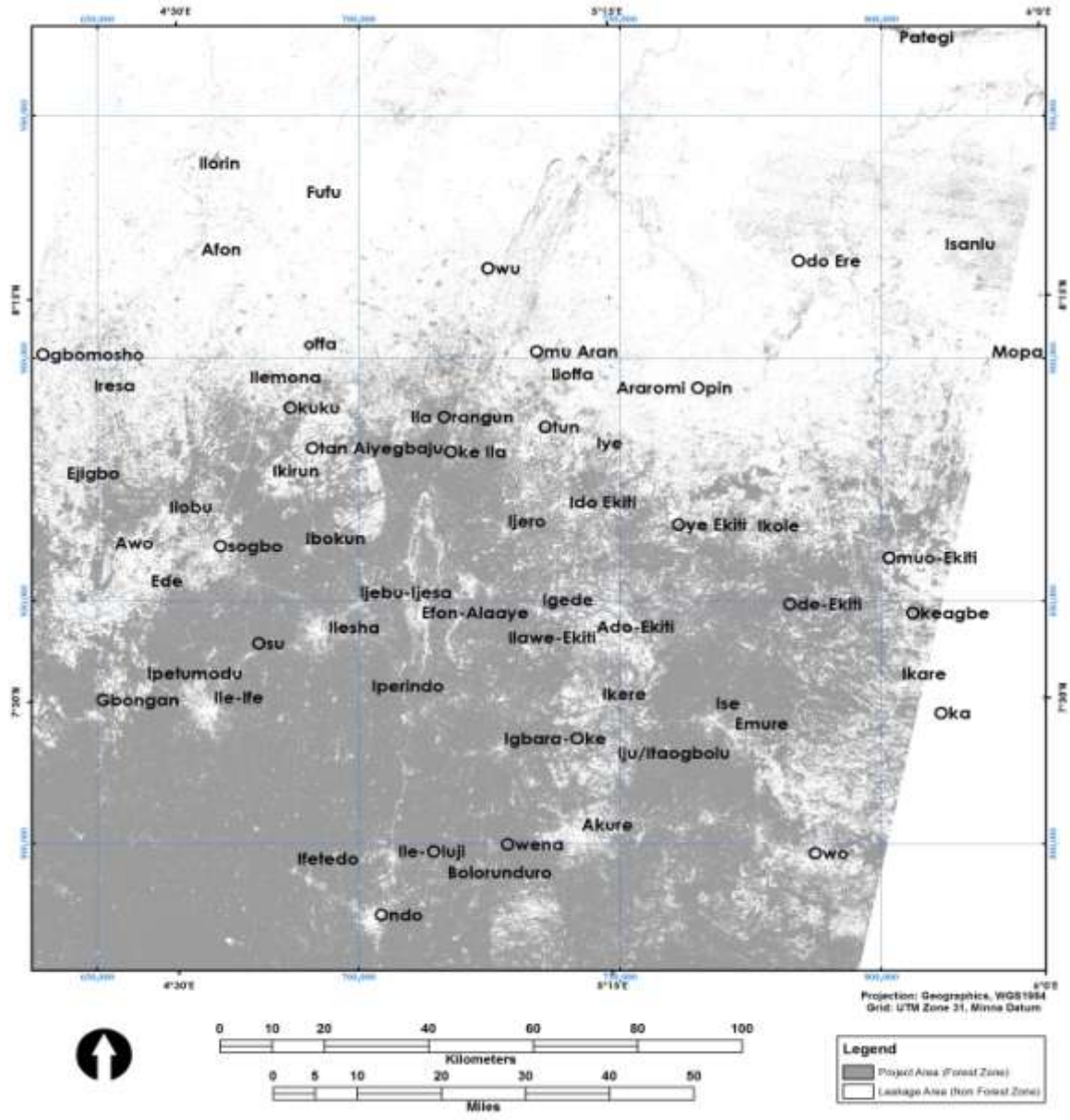

Figure 7.5: Spatial distribution of Project and leakage areas

Source: Author, 2015

Table 7.3: Spatio-temporal characteristics of LULC (1986 – 2050)

S/N	LU Classes	LULC (1986) ha	LULC (2002) ha	LULC (2010) ha	LULC (2050) ha	Change (1986 - 2002) (%)	Change (2002 – 2010) (%)	Change 2010 - 2050 (%)	Change 1986-2050 (%)
1	Cloud Cover	344,417.3	278,365.4	278,365.5	278,365.5	-19.2	0.00	0.00	-19.2
2	Forest	1,598,408.8	1,695,952.7	1,535,685.2	954,516.2	**6.1**	**-9.5**	**-37.8**	**-40.3**
3	Non-forest	1,829,066.7	1,793,171.0	1,953,438.6	2,534,607.5	-2.0	8.9	29.8	38.6
4	Waterbody	3,298.6	7,702.2	7,702.2	7,702.2	133.50	0.0	0.00	133.50
		3,775,191.5	**3,775,191.5**	**3,775,191.5**	**3,775,191.5**				

7.4 CO_2 Emission Due to the LULC and Climate Change Interaction

It is predicted that the study area will lose about 581,168.9ha of forests to the non-forest area between the period 2010 and 2050 as a result of deforestation and forest degradation. Tables 7.4, 7.5 and 7.5 present the statistics of the deforestation and forest degradation on yearly basis based on Biocarbon fund methods and estimated quantities of carbon dioxide emitted due to forest lost.

The project area lost about 450,0007ha and emitted about 254,000,000 metric tons of carbon dioxide equivalent *(tCO2e)* forest to the non forest area, while the non-forest area absorbed about 21,000,000*tCO2e* of carbon dioxide leaving a balance of 233,000,000*tCO2e* to the atmosphere as presented in Table 7.4. Furthermore, Table 7.5 reveals that within the leakage area about 127,332ha of forests were lost to the non-forest, and this accounts for 5,980,000*tCO2e* of the carbon dioxide out of the 71,000,000*tCO2e* released to the atmosphere due to forest degradation and deforestation within the study area. This thereby leaves a concentration of 65,000,000*tCO2e* of carbon dioxide lost to the atmosphere. Finally, the study area (reference area) will lose about 581,168.9ha of forest and emits 326,000,000*tCO2e* of carbon dioxide to the atmosphere during the future climate, while the non-forest area will gain same extent as a forest but will absorb about 27,000,000*tCO2e* of carbon dioxide as revealed in Table 7.6. This shows that 298,000,000*tCO2e* will be emitted to the atmosphere during the future climate. Finally, the study estimated about

298,767,072*tCO2e* (i.e. 233,308,456*tCO2e* and 65,458,685*tCO2e* from both the project and leakage area) of carbon dioxide will be emitted to the atmosphere due to deforestation and forest degradation occasioned by the modelled LULC and climate change interaction between 2010 and 2050.

Table 7.4: Estimated LULC and Carbon dioxide stock changes within the study area for project area

Year		Forest*			Non-forest**			Total***	
No	*Yr*	*Annual Activity Data (ha)*[+]	*Annual Change (tCO2e)*[++]	*Cumulative Change (tCO2e)*	*Annual Activity Data (ha)*[+]	*Annual Change (tCO2e)*[++]	*Cumulative Change (tCO2e)*	*Annual Change (tCO2e)*[++]	*Cumulative Change (tCO2e)*
1	2011	-8,652.95	-4,854,912.50	-4,854,912.50	8,652.94	406,604.91	406,604.91	-4,448,307.50	-4,448,307.50
2	2012	-8,652.95	-4,854,912.50	-9,709,825.00	8,652.94	406,604.91	813,209.81	-4,448,307.50	-8,896,615.00
3	2013	-8,652.95	-4,854,912.50	-14,564,738.00	8,652.94	406,604.91	1,219,814.75	-4,448,307.50	-13,344,923.00
4	2014	-8,652.95	-4,854,912.50	-19,419,650.00	8,652.94	406,604.91	1,626,419.63	-4,448,307.50	-17,793,230.00
5	2015	-8,652.95	-4,854,912.50	-24,274,562.00	8,652.94	406,604.91	2,033,024.50	-4,448,307.50	-22,241,538.00
6	2016	-8,652.95	-4,854,912.50	-29,129,474.00	8,652.94	406,604.91	2,439,629.50	-4,448,307.50	-26,689,844.00
7	2017	-8,652.95	-4,854,912.50	-33,984,388.00	8,652.94	406,604.91	2,846,234.50	-4,448,307.50	-31,138,154.00
8	2018	-8,652.95	-4,854,912.50	-38,839,300.00	8,652.94	406,604.91	3,252,839.50	-4,448,307.50	-35,586,460.00
9	2019	-11,032.75	-6,190,145.00	-45,029,444.00	11,032.76	518,433.53	3,771,273.00	-5,671,711.50	-41,258,172.00
10	2020	-11,032.75	-6,190,145.00	-51,219,588.00	11,032.76	518,433.53	4,289,706.50	-5,671,711.50	-46,929,880.00
11	2021	-11,032.75	-6,190,145.00	-57,409,732.00	11,032.76	518,433.53	4,808,140.00	-5,671,711.50	-52,601,592.00
12	2022	-11,032.75	-6,190,145.00	-63,599,876.00	11,032.76	518,433.53	5,326,573.50	-5,671,711.50	-58,273,304.00
13	2023	-11,032.75	-6,190,145.00	-69,790,024.00	11,032.76	518,433.53	5,845,007.00	-5,671,711.50	-63,945,016.00
14	2024	-11,032.75	-6,190,145.00	-75,980,168.00	11,032.76	518,433.53	6,363,440.50	-5,671,711.50	-69,616,728.00
15	2025	-11,032.75	-6,190,145.00	-82,170,312.00	11,032.76	518,433.53	6,881,874.00	-5,671,711.50	-75,288,440.00
16	2026	-11,032.75	-6,190,145.00	-88,360,456.00	11,032.76	518,433.53	7,400,307.50	-5,671,711.50	-80,960,152.00
17	2027	-12,087.25	-6,781,793.50	-95,142,248.00	12,087.25	567,984.13	7,968,291.50	-6,213,809.50	-87,173,960.00
18	2028	-12,087.25	-6,781,793.50	-101,924,040.00	12,087.25	567,984.13	8,536,276.00	-6,213,809.50	-93,387,760.00
19	2029	-12,087.25	-6,781,793.50	-108,705,832.00	12,087.25	567,984.13	9,104,260.00	-6,213,809.50	-99,601,568.00
20	2030	-12,087.25	-6,781,793.50	-115,487,624.00	12,087.25	567,984.13	9,672,244.00	-6,213,809.50	-105,815,376.00
21	2031	-12,087.25	-6,781,793.50	-122,269,416.00	12,087.25	567,984.13	10,240,228.00	-6,213,809.50	-112,029,184.00
22	2032	-12,087.25	-6,781,793.50	-129,051,208.00	12,087.25	567,984.13	10,808,212.00	-6,213,809.50	-118,242,992.00
23	2033	-12,087.25	-6,781,793.50	-135,833,008.00	12,087.25	567,984.13	11,376,196.00	-6,213,809.50	-124,456,816.00
24	2034	-12,087.25	-6,781,793.50	-142,614,800.00	12,087.25	567,984.13	11,944,180.00	-6,213,809.50	-130,670,624.00

Year		Forest			Non-forest			Total	
No	*Yr*	*Annual Activity Data (ha)*	*Annual Change (tCO2e)*	*Cumulative Change (tCO2e)*	*Annual Activity Data (ha)*	*Annual Change (tCO2e)*	*Cumulative Change (tCO2e)*	*Annual Change (tCO2e)*	*Cumulative Change (tCO2e)*
25	2035	-12,483.40	-7,004,060.50	-149,618,864.00	12,483.40	586,599.50	12,530,780.00	-6,417,461.00	-137,088,080.00
26	2036	-12,483.40	-7,004,060.50	-156,622,928.00	12,483.40	586,599.50	13,117,380.00	-6,417,461.00	-143,505,552.00
27	2037	-12,483.40	-7,004,060.50	-163,626,992.00	12,483.40	586,599.50	13,703,980.00	-6,417,461.00	-149,923,008.00
28	2038	-12,483.40	-7,004,060.50	-170,631,056.00	12,483.40	586,599.50	14,290,580.00	-6,417,461.00	-156,340,480.00
29	2039	-12,483.40	-7,004,060.50	-177,635,120.00	12,483.40	586,599.50	14,877,180.00	-6,417,461.00	-162,757,936.00
30	2040	-12,483.40	-7,004,060.50	-184,639,184.00	12,483.40	586,599.50	15,463,780.00	-6,417,461.00	-169,175,408.00
31	2041	-12,483.40	-7,004,060.50	-191,643,248.00	12,483.40	586,599.50	16,050,380.00	-6,417,461.00	-175,592,864.00
32	2042	-12,483.40	-7,004,060.50	-198,647,312.00	12,483.40	586,599.50	16,636,980.00	-6,417,461.00	-182,010,336.00
33	2043	-12,473.30	-6,998,392.50	-205,645,712.00	12,473.30	586,124.81	17,223,104.00	-6,412,267.50	-188,422,608.00
34	2044	-12,473.30	-6,998,392.50	-212,644,112.00	12,473.30	586,124.81	17,809,228.00	-6,412,267.50	-194,834,880.00
35	2045	-12,473.30	-6,998,392.50	-219,642,512.00	12,473.30	586,124.81	18,395,352.00	-6,412,267.50	-201,247,168.00
36	2046	-12,473.30	-6,998,392.50	-226,640,912.00	12,473.30	586,124.81	18,981,476.00	-6,412,267.50	-207,659,440.00
37	2047	-12,473.30	-6,998,392.50	-233,639,312.00	12,473.30	586,124.81	19,567,600.00	-6,412,267.50	-214,071,712.00
38	2048	-12,473.30	-6,998,392.50	-240,637,712.00	12,473.30	586,124.81	20,153,724.00	-6,412,267.50	-220,483,984.00
39	2049	-12,473.30	-6,998,392.50	-247,636,112.00	12,473.30	586,124.81	20,739,848.00	-6,412,267.50	-226,896,256.00
40	2050	-12,473.30	-6,998,392.50	-254,634,512.00	12,473.30	586,124.81	21,325,972.00	-6,412,267.50	-233,308,544.00
	Total	-453,837.19	-254,634,432.00		453,837.16	21,325,975.00		-233,308,456.00	

Source: Author, 2015

Table 7.5: Estimated LULC and Carbon dioxide stock changes within the study area for leakage area

Year		Forest			Non-forest			Total	
No	*Yr*	*Annual Activity Data (ha)*	*Annual Change (tCO2e)*	*Cumulative Change (tCO2e)*	*Annual Activity Data (ha)*	*Annual Change (tCO2e)*	*Cumulative Change (tCO2e)*	*Annual Change (tCO2e)*	*Cumulative Change (tCO2e)*
1	2011	-5,876.28	-3,297,006.25	-3,297,006.25	5,876.28	276,128.63	276,128.63	-3,020,877.50	-3,020,877.50
2	2012	-5,876.28	-3,297,006.25	-6,594,012.50	5,876.28	276,128.63	552,257.25	-3,020,877.50	-6,041,755.00

Year		Forest			Non-forest			Total	
No	*Yr*	*Annual Activity Data (ha)*	*Annual Change (tCO2e)*	*Cumulative Change (tCO2e)*	*Annual Activity Data (ha)*	*Annual Change (tCO2e)*	*Cumulative Change (tCO2e)*	*Annual Change (tCO2e)*	*Cumulative Change (tCO2e)*
3	2013	-5,876.28	-3,297,006.25	-9,891,019.00	5,876.28	276,128.63	828,385.88	-3,020,877.50	-9,062,633.00
4	2014	-5,876.28	-3,297,006.25	-13,188,025.00	5,876.28	276,128.63	1,104,514.50	-3,020,877.50	-12,083,510.00
5	2015	-5,876.28	-3,297,006.25	-16,485,031.00	5,876.28	276,128.63	1,380,643.13	-3,020,877.50	-15,104,388.00
6	2016	-5,876.28	-3,297,006.25	-19,782,038.00	5,876.28	276,128.63	1,656,771.75	-3,020,877.50	-18,125,266.00
7	2017	-5,876.28	-3,297,006.25	-23,079,044.00	5,876.28	276,128.63	1,932,900.38	-3,020,877.50	-21,146,144.00
8	2018	-5,876.28	-3,297,006.25	-26,376,050.00	5,876.28	276,128.63	2,209,029.00	-3,020,877.50	-24,167,020.00
9	2019	-3,496.46	-1,961,759.38	-28,337,810.00	3,496.47	164,300.36	2,373,329.25	-1,797,459.00	-25,964,480.00
10	2020	-3,496.46	-1,961,759.38	-30,299,570.00	3,496.47	164,300.36	2,537,629.50	-1,797,459.00	-27,761,940.00
11	2021	-3,496.46	-1,961,759.38	-32,261,330.00	3,496.47	164,300.36	2,701,929.75	-1,797,459.00	-29,559,400.00
12	2022	-3,496.46	-1,961,759.38	-34,223,088.00	3,496.47	164,300.36	2,866,230.00	-1,797,459.00	-31,356,858.00
13	2023	-3,496.46	-1,961,759.38	-36,184,848.00	3,496.47	164,300.36	3,030,530.25	-1,797,459.00	-33,154,318.00
14	2024	-3,496.46	-1,961,759.38	-38,146,608.00	3,496.47	164,300.36	3,194,830.50	-1,797,459.00	-34,951,776.00
15	2025	-3,496.46	-1,961,759.38	-40,108,368.00	3,496.47	164,300.36	3,359,130.75	-1,797,459.00	-36,749,236.00
16	2026	-3,496.46	-1,961,759.38	-42,070,128.00	3,496.47	164,300.36	3,523,431.00	-1,797,459.00	-38,546,696.00
17	2027	-2,441.98	-1,370,122.00	-43,440,248.00	2,441.97	114,749.01	3,638,180.00	-1,255,373.00	-39,802,068.00
18	2028	-2,441.98	-1,370,122.00	-44,810,368.00	2,441.97	114,749.01	3,752,929.00	-1,255,373.00	-41,057,440.00
19	2029	-2,441.98	-1,370,122.00	-46,180,488.00	2,441.97	114,749.01	3,867,678.00	-1,255,373.00	-42,312,808.00
20	2030	-2,441.98	-1,370,122.00	-47,550,608.00	2,441.97	114,749.01	3,982,427.00	-1,255,373.00	-43,568,180.00
21	2031	-2,441.98	-1,370,122.00	-48,920,728.00	2,441.97	114,749.01	4,097,176.00	-1,255,373.00	-44,823,552.00
22	2032	-2,441.98	-1,370,122.00	-50,290,848.00	2,441.97	114,749.01	4,211,925.00	-1,255,373.00	-46,078,924.00
23	2033	-2,441.98	-1,370,122.00	-51,660,968.00	2,441.97	114,749.01	4,326,674.00	-1,255,373.00	-47,334,296.00
24	2034	-2,441.98	-1,370,122.00	-53,031,088.00	2,441.97	114,749.01	4,441,423.00	-1,255,373.00	-48,589,664.00
25	2035	-2,045.82	-1,147,850.63	-54,178,940.00	2,045.83	96,134.22	4,537,557.00	-1,051,716.38	-49,641,384.00
26	2036	-2,045.82	-1,147,850.63	-55,326,792.00	2,045.83	96,134.22	4,633,691.00	-1,051,716.38	-50,693,100.00
27	2037	-2,045.82	-1,147,850.63	-56,474,644.00	2,045.83	96,134.22	4,729,825.00	-1,051,716.38	-51,744,820.00

Year		Forest			Non-forest			Total	
No	*Yr*	*Annual Activity Data (ha)*	*Annual Change (tCO2e)*	*Cumulative Change (tCO2e)*	*Annual Activity Data (ha)*	*Annual Change (tCO2e)*	*Cumulative Change (tCO2e)*	*Annual Change (tCO2e)*	*Cumulative Change (tCO2e)*
28	2038	-2,045.82	-1,147,850.63	-57,622,496.00	2,045.83	96,134.22	4,825,959.00	-1,051,716.38	-52,796,536.00
29	2039	-2,045.82	-1,147,850.63	-58,770,348.00	2,045.83	96,134.22	4,922,093.00	-1,051,716.38	-53,848,256.00
30	2040	-2,045.82	-1,147,850.63	-59,918,200.00	2,045.83	96,134.22	5,018,227.00	-1,051,716.38	-54,899,972.00
31	2041	-2,045.82	-1,147,850.63	-61,066,052.00	2,045.83	96,134.22	5,114,361.00	-1,051,716.38	-55,951,692.00
32	2042	-2,045.82	-1,147,850.63	-62,213,904.00	2,045.83	96,134.22	5,210,495.00	-1,051,716.38	-57,003,408.00
33	2043	-2,055.93	-1,153,518.25	-63,367,424.00	2,055.92	96,608.53	5,307,103.50	-1,056,909.75	-58,060,320.00
34	2044	-2,055.93	-1,153,518.25	-64,520,944.00	2,055.92	96,608.53	5,403,712.00	-1,056,909.75	-59,117,232.00
35	2045	-2,055.93	-1,153,518.25	-65,674,464.00	2,055.92	96,608.53	5,500,320.50	-1,056,909.75	-60,174,144.00
36	2046	-2,055.93	-1,153,518.25	-66,827,984.00	2,055.92	96,608.53	5,596,929.00	-1,056,909.75	-61,231,056.00
37	2047	-2,055.93	-1,153,518.25	-67,981,504.00	2,055.92	96,608.53	5,693,537.50	-1,056,909.75	-62,287,968.00
38	2048	-2,055.93	-1,153,518.25	-69,135,024.00	2,055.92	96,608.53	5,790,146.00	-1,056,909.75	-63,344,880.00
39	2049	-2,055.93	-1,153,518.25	-70,288,544.00	2,055.92	96,608.53	5,886,754.50	-1,056,909.75	-64,401,788.00
40	2050	-2,055.93	-1,153,518.25	-71,442,064.00	2,055.92	96,608.53	5,983,363.00	-1,056,909.75	-65,458,700.00
		-127,331.80	-71,442,052.00		127,331.75	5,983,365.94		-65,458,685.00	

Source: Author, 2015

Table 7.6: Estimated LULC and Carbon dioxide stock changes within the study area

Year		Forest*			Non-forest**			Total***	
No	*Yr*	*Annual Activity Data (ha)*	*Annual Change (tCO2e)*	*Cumulative Change (tCO2e)*	*Annual Activity Data (ha)*	*Annual Change (tCO2e)*	*Cumulative Change (tCO2e)*	*Annual Change (tCO2e)*	*Cumulative Change (tCO2e)*
1	2011	-14,529.22	-8,151,908.50	-8,151,908.50	14,529.22	682,733.31	682,733.31	-7,469,175.00	-7,469,175.00
2	2012	-14,529.22	-8,151,908.50	-16,303,817.00	14,529.22	682,733.31	1,365,466.63	-7,469,175.00	-14,938,350.00
3	2013	-14,529.22	-8,151,908.50	-24,455,726.00	14,529.22	682,733.31	2,048,200.00	-7,469,175.00	-22,407,526.00
4	2014	-14,529.22	-8,151,908.50	-32,607,634.00	14,529.22	682,733.31	2,730,933.25	-7,469,175.00	-29,876,700.00

Year		Forest			Non-forest			Total	
No	*Yr*	*Annual Activity Data (ha)*	*Annual Change (tCO2e)*	*Cumulative Change (tCO2e)*	*Annual Activity Data (ha)*	*Annual Change (tCO2e)*	*Cumulative Change (tCO2e)*	*Annual Change (tCO2e)*	*Cumulative Change (tCO2e)*
5	2015	-14,529.22	-8,151,908.50	-40,759,544.00	14,529.22	682,733.31	3,413,666.50	-7,469,175.00	-37,345,876.00
6	2016	-14,529.22	-8,151,908.50	-48,911,452.00	14,529.22	682,733.31	4,096,399.75	-7,469,175.00	-44,815,052.00
7	2017	-14,529.22	-8,151,908.50	-57,063,360.00	14,529.22	682,733.31	4,779,133.00	-7,469,175.00	-52,284,228.00
8	2018	-14,529.22	-8,151,908.50	-65,215,268.00	14,529.22	682,733.31	5,461,866.50	-7,469,175.00	-59,753,400.00
9	2019	-14,529.22	-8,151,908.50	-73,367,176.00	14,529.23	682,734.13	6,144,600.50	-7,469,174.50	-67,222,576.00
10	2020	-14,529.22	-8,151,908.50	-81,519,088.00	14,529.23	682,734.13	6,827,334.50	-7,469,174.50	-74,691,752.00
11	2021	-14,529.22	-8,151,908.50	-89,671,000.00	14,529.23	682,734.13	7,510,068.50	-7,469,174.50	-82,160,928.00
12	2022	-14,529.22	-8,151,908.50	-97,822,912.00	14,529.23	682,734.13	8,192,802.50	-7,469,174.50	-89,630,112.00
13	2023	-14,529.22	-8,151,908.50	-105,974,824.00	14,529.23	682,734.13	8,875,537.00	-7,469,174.50	-97,099,288.00
14	2024	-14,529.22	-8,151,908.50	-114,126,736.00	14,529.23	682,734.13	9,558,271.00	-7,469,174.50	-104,568,464.00
15	2025	-14,529.22	-8,151,908.50	-122,278,648.00	14,529.23	682,734.13	10,241,005.00	-7,469,174.50	-112,037,640.00
16	2026	-14,529.22	-8,151,908.50	-130,430,560.00	14,529.23	682,734.13	10,923,739.00	-7,469,174.50	-119,506,824.00
17	2027	-14,529.23	-8,151,918.00	-138,582,480.00	14,529.22	682,733.31	11,606,472.00	-7,469,184.50	-126,976,008.00
18	2028	-14,529.23	-8,151,918.00	-146,734,400.00	14,529.22	682,733.31	12,289,205.00	-7,469,184.50	-134,445,200.00
19	2029	-14,529.23	-8,151,918.00	-154,886,320.00	14,529.22	682,733.31	12,971,938.00	-7,469,184.50	-141,914,384.00
20	2030	-14,529.23	-8,151,918.00	-163,038,240.00	14,529.22	682,733.31	13,654,671.00	-7,469,184.50	-149,383,568.00
21	2031	-14,529.23	-8,151,918.00	-171,190,160.00	14,529.22	682,733.31	14,337,404.00	-7,469,184.50	-156,852,752.00
22	2032	-14,529.23	-8,151,918.00	-179,342,080.00	14,529.22	682,733.31	15,020,137.00	-7,469,184.50	-164,321,936.00
23	2033	-14,529.23	-8,151,918.00	-187,494,000.00	14,529.22	682,733.31	15,702,870.00	-7,469,184.50	-171,791,136.00
24	2034	-14,529.23	-8,151,918.00	-195,645,920.00	14,529.22	682,733.31	16,385,603.00	-7,469,184.50	-179,260,320.00
25	2035	-14,529.22	-8,151,908.50	-203,797,824.00	14,529.22	682,733.31	17,068,336.00	-7,469,175.00	-186,729,488.00
26	2036	-14,529.22	-8,151,908.50	-211,949,728.00	14,529.22	682,733.31	17,751,070.00	-7,469,175.00	-194,198,656.00
27	2037	-14,529.22	-8,151,908.50	-220,101,632.00	14,529.22	682,733.31	18,433,804.00	-7,469,175.00	-201,667,824.00
28	2038	-14,529.22	-8,151,908.50	-228,253,536.00	14,529.22	682,733.31	19,116,538.00	-7,469,175.00	-209,136,992.00
29	2039	-14,529.22	-8,151,908.50	-236,405,440.00	14,529.22	682,733.31	19,799,272.00	-7,469,175.00	-216,606,176.00

Year		Forest			Non-forest			Total	
No	*Yr*	*Annual Activity Data (ha)*	*Annual Change (tCO2e)*	*Cumulative Change (tCO2e)*	*Annual Activity Data (ha)*	*Annual Change (tCO2e)*	*Cumulative Change (tCO2e)*	*Annual Change (tCO2e)*	*Cumulative Change (tCO2e)*
30	2040	-14,529.22	-8,151,908.50	-244,557,344.00	14,529.22	682,733.31	20,482,006.00	-7,469,175.00	-224,075,344.00
31	2041	-14,529.22	-8,151,908.50	-252,709,248.00	14,529.22	682,733.31	21,164,740.00	-7,469,175.00	-231,544,512.00
32	2042	-14,529.22	-8,151,908.50	-260,861,152.00	14,529.22	682,733.31	21,847,474.00	-7,469,175.00	-239,013,680.00
33	2043	-14,529.22	-8,151,908.50	-269,013,056.00	14,529.22	682,733.31	22,530,208.00	-7,469,175.00	-246,482,848.00
34	2044	-14,529.22	-8,151,908.50	-277,164,960.00	14,529.22	682,733.31	23,212,942.00	-7,469,175.00	-253,952,016.00
35	2045	-14,529.22	-8,151,908.50	-285,316,864.00	14,529.22	682,733.31	23,895,676.00	-7,469,175.00	-261,421,184.00
36	2046	-14,529.22	-8,151,908.50	-293,468,768.00	14,529.22	682,733.31	24,578,410.00	-7,469,175.00	-268,890,368.00
37	2047	-14,529.22	-8,151,908.50	-301,620,672.00	14,529.22	682,733.31	25,261,144.00	-7,469,175.00	-276,359,520.00
38	2048	-14,529.22	-8,151,908.50	-309,772,576.00	14,529.22	682,733.31	25,943,878.00	-7,469,175.00	-283,828,704.00
39	2049	-14,529.22	-8,151,908.50	-317,924,480.00	14,529.22	682,733.31	26,626,612.00	-7,469,175.00	-291,297,856.00
40	2050	-14,529.22	-8,151,908.50	-326,076,384.00	14,529.22	682,733.31	27,309,346.00	-7,469,175.00	-298,767,040.00
Total		-581,168.88	-326,076,416.00		581,168.88	27,309,339.00		-298,767,072.00	

Source: Author, 2015

*Annual Change *(tCO2)* = Annual activity data (ha) X 561.07*tCO2e/ha* for forest
**Annual Change *(tCO2)* = Annual activity data (ha) X 46.99*tCO2e/ha* for Non forest
***Total *(tCO2)* = Annual Change (Forest) + Annual Change (Non forest)
[+]Annual activity data (ha) = Estimated forest area lost or Non forest gain per annual
[++]Annual Change (*tCO2*) = estimated CO2 emitted or absorbed by forest area lost or Non forest

CHAPTER EIGHT

SUMMARY OF FINDINGS, CONCLUSION AND RECOMMENDATIONS

8.1 Summary Of Findings and Discussion

The interaction between LULC and climate change in a region is complex and interwoven. Studies have shown that LULC is both a factor and effect of climate change. The interaction of LULC and climate change can be considered from three dimensions, interaction of LULC on climate change, interaction of climate change on LULC and interaction and feedbacks of climate change and LULC. This study emphasized the interaction of climate change on LULC of the Derived Savannah so as to predict the nature and spatio-temporal patterns of LULC in the future climate, with a view to evaluate the interactions between landuse/landcover and climate change in the derived savannah region of Nigeria using Satellite Remote Sensing and GIS techniques. The following specific objectives were pursued: assessment of the changes in the LULC patterns within the study area for the periods 1972, 1986, 2002 and 2010; evaluation of the variability in Rainfall and Temperature over the area between 1941 and 2010 for present climate and 2011 and 2050 for future climate; modeling of the impact of the climate change on landuse/landcover changes within the study area; and estimation of the changes in carbon stock resulting from landcover changes.

Remote sensing and GIS techniques were adopted for the interpretation and generation of the basemap for LULCC for the period between 1972 and 2010. Multivariate statistical and factor analysis were used to assess the climate variability and change and to identify the controlling variables for both the present and future climates. GIS techniques provided the environment for the integration, manipulation and analysis of all data to generate results and statistics. In addition, the Land Change Modeler (LCM) was used for the selection of

variables for modeling of the interaction between LULCC and climate change to simulate the nature and patterns of LULC during both the present and future climates.

The study revealed that the interaction of LULC and climate change within the derived savannah is complex in nature and that climate is one of the key drivers of global environmental change, especially the LULCC. Hence, the findings of the study are summarized as follows:

- The study showed that the area experienced LULCC and revealed the trend, direction and location of this change between 1972 and 2002. The built up area witnessed a rapid increase of about 1,134.69% from 8,806.90ha to 108,737ha between 1972 and 2002. This is due to population increases and the establishment of a new urban area and administration centres arising from the creation of states and local government areas. For example, Osun and Ekiti states were carved out of the existing states in 1991 and 1996, respectively (Omotoso, 2009). Also, waterbody increased by about 6,649ha from just 1,052.92ha in 1972 to 7,702.24 in 2002, which represent about 631.5% expansion in its area extent. This is attributed to the massive dam construction during the period under study. For examples, Egbe, Ejiba, Ero and other were constructed during the period for both irrigation and domestic water supply. In addition, farmland gained about 1,202% between 1972 and 2002 from 29,386.39ha to 382,859.15ha, respectively. However, there was a decline of agricultural activities between 1986 and 2002, thus, the study recorded a 48.4 % drop in farmland land. Meanwhile, it is recorded that the forest and grassland lost about 19.32% and 0.05%, respectively within the period between 1972 and 2002. For instance, forest area lost about 49,308ha and 235,406ha to urban and woodland between 1972 and 2002. Similarly, degraded surface lost about 22,188ha, 30,735ha and 116,671ha to urban,

grassland and woodland respectively, during the period between 1972 and 2002, which amount to about 72.8% overall within the period under study.

- The study confirmed the sinusoidal nature of the climatic pattern (i.e. Rainfall & temperature) that shows the increasing trend of rainfall and temperature during both climates (present [1941-2010] & future [2011-2050]). The study further revealed an increasing trend, which is at the rate of 2.03mm (0.02%) and 0.15mm (0.01%) per annum for mean annual rainfall and rainfall anomaly, respectively. In the same token annual mean rainfall of 1,316mm for the present climate was recorded, while the future climate will be increasing at a rate of 3.13mm (0.2%) and 0.23mm (0.02%) per annum for both parameters, having an annual mean of 1,393mm. In addition, the mean annual temperature for both the present and future climates was increasing annually at a rate of 0.007^{o}C and 0.014^{o}C. The study also predicted that 28.2^{o}C and 26.4^{o}C will be received as the highest and lowest annual temperature in the future climate, which represent about 3.0% and 3.5% above and below mean annual temperature, respectively. Furthermore, rainfall variability index during the present climate ranges between 15 and 23% in Akure area having the highest index, while the range in the future climate will be 9 – 13% with Oshogbo axis recording the highest. With this narrow variability index and increasing rainfall, rainfall will be more stable in the future climate than in the present climate, which has a wider variability index range (Akinsanola and Ogunjobi, 2014).

- The study also confirmed the established spatial pattern of rainfall that mean annual rainfall was increasing towards the southern part of the study area in north to south direction within the present climate (1941-2010). It is confirmed that this will continue in the same direction in future climate (2011 – 2050). The study further shows that temperature is increasing in the south – north direction across the study

area and affirmed that the trend will continue during the future climate. The rainfall trend follows the predicted trends and spatial pattern of rainfall in tropical region as established in Odjugbo (2011); Efe (2011) and Fasona, *et al.* (2008).

- The temporal variability and trend analysis revealed that the study area is experiencing dryness as from 1981 - 1990 decade upward, the highest being the decade of 2001 – 2010. Also, the annual rainfall and temperature variability indices varied from -2.00 to 2.38 and -1.64 to 2.64 during the present climate. However, the decadal variability indices for the study area during the present climate varied from -1.64 to 1.45 and -1.36 to 1.75 for both rainfall and temperature. This is in agreement with the findings of previous studies on the trend and variability of rainfall and temperature in Nigeria including Oguntunde *et al.,* (2011) and Akinsanola and Ogunjobi (2014).

- Furthermore, four and three factors were extracted for both the present and future climates, respectively. Climate and topography are the main controlling variables of the cover type as they constitute component one of the PCA, with a sum of square loadings of 43.35% and 40.97% for both the present and future climates, respectively. In the future climate, climate will have more influence than terrain on the cover as it has a higher correlation of 0.78 with the cover than 0.65 for the topography. Also, the study revealed that rainfall will be a dominant climatic parameter and will determine the nature and spatial distribution of the cover during the climate (Fasona, *et al.*, 2008; Abiodun, *et al.*, 2012).

- The LCM predicted suitability of forest to transit to degraded surfaces, farmland, fire scar, grassland, urban, waterbody and woodland during the present climate with transition potential ranges from 0 – 0.938, 0 – 0.989, 0 – 0.999, 0 – 0.009, 0 – 0.999, 0

– 0.021 and 0 – 1.0, respectively. This means that there are higher chances of forest to change to woodland, urban, farmland than waterbody and grassland. However, during the future climate, potentials transition from forest to transit to degraded surfaces, farmland, fire scar, grassland, urban, waterbody and woodland ranging from 0 – 0.635, 0 – 0.208, 0 – 0.999, 0 – 0.999, 0 – 0.999, 0 – 0.018 and 0 – 0.981 respectively are predicted. The trend shows that it would be more suitable for forest to be converted to grassland, urban, woodland and degraded surfaced than farmland and waterbody, which showed higher transition potential probabilities.

- Also, the LCM predicted that forest and grassland lost 9% and 18% of their area extent between 2002 and 2010, respectively and deforestation at 2.25% per annum. Between 2002 and 2050, however, grassland and forest were predicted to decrease to 22% and 28%. In addition, urban and woodland expanded by 34% and 14% between 2002 and 2010, while between 2002 and 2050, urban and woodland would increased by 118% and 28%, respectively. The result further showed that the intensity of climate induced deforestation and forest degradation will continue in the future, which accounts for about 63% and 15%, increase in urban area and agricultural expansion, while grassland and forest areas will lose about 14% and 12% of their area extent between 2010 and 2050, respectively.

- Finally, the study further predicted that the forested area will reduce with about 37.84% between 2010 and 2050 as against 40.28% of forest land that will be lost between 1986 and 2050. This suggests that the rate of forest degradation and deforestation will be more rapid than it was initially. One of the major implications of the interaction of LULC and climate change is that about 298,767,040 tCO_2e of carbon dioxide will be emitted from about 581,168.9ha of forest lost between 2010 and 2050. The breakdown showed that 326,076,416tCO_2e of carbon dioxide were

actually emitted due to 581,168ha of forest lost to other LULC classes, at the rate of 561.07tCO_2e per hectare. Also, the non-forest area of 581,168ha absorbed about 27,309,339 tCO_2e of carbon dioxide due to the interaction between the forest and the non forest classes. This is at the rate of 46.99tCO_2e per hectare. This showed that a total of 298,767,040 tCO_2e concentration will be emitted to the atmosphere, which comfirmed the contribution of LULC change to the continue increase in the amount of CO_2 in the atmosphere .

8.2 Conclusion

This study has been able to evaluate the interaction between landuse/landcover and climate change in the derived savannah zone of Nigeria by determining the extent, magnitude, direction and location of LULCC (1972 – 2010). The study also assesses the climate variability for the period between 1941 and 2010. In addition, the interaction between LULC and climate change was modeled and predicted for future climate (2011 – 2050) statistically and through Land Change Modeler (LCM) technique. Finally, an evaluation of the possible future implications of the interaction was carried out. The research revealed that climate change and variability within the study area has been transformed to an extent that it has effects on spatial pattern and distribution LULC within the area. In addition, the study revealed that climate is one main underlying driver of LULCC. The interaction between the LULC and climate change has led to the uncontrollable processes of deforestation and forest degradation within the study area. The processes of deforestation and forest degradation have altered the composition atmospheric of concentration of carbon dioxide (CO_2) being emitted and absorbed within the study area and means of livelihood of the inhabitants of the area.

8.3 Recommendations

The objectives of the research have been achieved, results and data analyses and summary of findings presented above, the study, therefore, recommends the following:

i. It has already been identified in the Nigerian REDD+ programme that woodland savannah is declining, the study revealed that the trend will continue during the future climate.

ii. Deforestation and forest degradation within the area was predicted at 2.25% per annum for the period of study. In view of this, government should not limit the REDD+ programme to the forest Zone and identified forest reserves, but, to other ecological Zones in the country as there are increasing carbon stocks in vast islands and savannah grassland. Government should intensify the tree planning programme.

iii. The forest reserves in the study area are reduced in size, degraded and it is difficult to identify their boundaries due to over exploitation and encroachment. The study recommends that an inventory of all forest reserves should be conducted so as to help in determining the extent of deforestation, forest degradation and fragmentation. This will enable government to take concise decisions on how to strengthen the existing policies, legislative framework programs and instruments to checkmate over-exploitation.

iv. The continuing increase in deforestation, forest degradation and carbon stocking occasioned by logging, lumbering, charcoal production and bush burning will affect the livelihood and economic development in the long run. There is a need for further research on the socioeconomic implications of climate and LULC interaction in the Derived Savannah.

v. The study shows that there is an increase in the annual distribution of temperature and rainfall towards the northern and southern parts during the future climate respectively.

Due to the shift in spatio-temporal distribution and pattern and predicted trend, there is a need for more climatic research in order to adopt appropriate adaptation and mitigation strategies.

8.4 Contributions to Knowledge

Firstly, the study generated an inventory of the spatial distribution of LULC patterns between 1972 and 2010 within the study area and provides the baseline information for planning and climate change adaptation and mitigation strategies, and sustainable development in the derived Savannah region of Nigeria.

Secondly, it has confirmed the predicted climate, spatial pattern and trend for the zone in which rainfall will continue to increase in a north-southward direction and temperature in opposite directions with high climate variability. The study also affirmed the characteristics of rainfall to remain as double maxima with the highest recorded in September, which makes it to have a single peak period.

In addition, the study predicted that the dominant climatic parameters dictate the nature and cover types in the study area. Based on this premise, rainfall and temperature will combine to drive the direction, trend and magnitude of LULC change in the future climate. However, the influence of rainfall on the LULC change during the future climate will be more than that of the temperature. It must be included here that this is one of the studies out of many that used rainfall and temperature to predict future LULC.

Finally, the study provides quantitative information on the nature of the complex interaction between LULC and climate change in the future climate and estimated the quantity of carbon dioxide (CO_2) that will be emitted due to continued forest degradation and deforestation as one of the major implications of the interaction. In conclusion, this study forms part of the

pioneer research on carbon trading and Reducing Emissions from Deforestation and forest Degradation (REDD) in Nigeria.

REFERENCES

Abiodun, B. J., Lawal, K. A., Salami, A. T., & Abatan, A. A. (2012). Potential Influences of Global Warming on Future Climate and Extreme Events in Nigeria. *Reg. Environ Change*, 1-15. doi: 10.1007/s10113-012-0381-7

Adam, J. C., & Lettenmaier, D. P. (2003). Adjustment of Global Gridded Precipitation for Systematic Bias. *Journal of Geophysics Resources*, 108, 1–14.

Adegbola, A.A., & Onayinka, E.A.O. (1976). A Review of Range Management Problems in the Southern Guinea and Derived Savanna zones of Nigeria. *Tropical Grasslands*, 10(1), 41–51.

Adejuwon, J. (2006). Food security, Climate Variability and Climate Change in Sub Saharan West Africa. *A Final Report Submitted to Assessments of Impacts and Adaptations to Climate Change (AIACC), Project No. AF23.* Pp156. Washington, USA: The International START Secretariat. Retrieved from 2009, June 30 from http://www.aiaccproject.org/Final%20Reports/Final%20Reports/FinalRept_AIACC_AF23.pdf

Adeniyi, P. O. (1978). The Role of Remote Sensing in Land Use Planning. In N. Musisi (Ed.). *Application of Remote Sensing Techniques in Nigeria* (2, pp19-33). Nigerian Society of Remote Sensing, Ilesa.

Adeniyi, P. O., & Omojola, A. (1999). Land Use/Land Cover Change Evaluation in Sokoto – Rima Basin of NW Nigeria Based on Archival Remote Sensing and GIS Techniques. In P.O. Adeniyi (Ed.). *Geoinformation Technology Applications for Resources and Environmental Management in Africa* (pp143-172). AARSE, Nigeria: Wura - Kay Press.

Adeniyi, P. O., Omojola, A. S. & Soneye, A. S. O. (I992). Applications of Remote Sensing and GIS in the Mapping, Evaluation and Monitoring of Agricultural Resources in Northwestern Nigeria. In S. Frank and H. J. Onsrudg (Eds.). *Proceedings, Canadian Conference on GIS.* 1: 803 – 820. Ottawa: Amazon Publishers.

Adger, N. W. (2000). Social and Ecological Resilience: Are They Related? *Progress in Human Geography*, 24(3**),** 347–364.

Akinsanola, A. A., & Ogunjobi, K. O. (2014). Analysis of Rainfall and Temperature Variability over Nigeria. *Global Journal of Human Social Science*, 14(3), 1-17.

Anyamba, A., Tucker, C. J., & Mahoney, R. (2002). From El Nino to La Nina: Vegetation Response Patterns Over East and Southern Africa during the 1997–2000 Period. *Journal of Climate*, 15, 3096 – 3103.

Armston, J.D., Danaher, T.J., Goulevitch, B.M., & Byrne, M.I. (2002). Geometric Correction of Landsat MSS, TM, AND ETM+ Imagery for Mapping of Woody Vegetation Cover and Change Detection in Queensland; *In proceedings of the 11th Australasian Remote Sensing and Photogrammetry Conference, (11ARSPC).* Pp.1-23. Retrieved on June 30, 2011. *http://www.scribd.com/doc/135823836/Geometric-Correction-for-Landsat-Imaginary*

Aronoff, S. (1989). *Geographic Information Systems: A Management Perspective*; Ottawa-Canada: WDL Publications.

Baede, A.P.M., Ahlonsou, E., Ding, Y., & Schimel, D.S. (2001). The Climate System: An Overview. In J.J Maccarthy, O.F Canziani, & N.A Leary (Eds). *Climate Change 2001: Impacts, Adaptation and Vulnerability* (pp. 87-98). New York: Cambridge University Press.

Ball, J.B. (2001). Global Forest Resources: History and Dynamics. In J. Evans (Ed.). *Forests Handbook.* (1st ed., pp. 3-22). Oxford: Blackwell Science

Barker, T. (2003) Representing Global Climate Change, Adaptation and Mitigation. *Global Environmental Change*, 13, 1–6.

Bell, B (1953). Solar Variation As An Explanation of Climate Change. In Shapley H. (Ed.), *Climate Change* (pp123 – 136). Cambridge: Harvard University Press.

Betts, R., Sanderson, M., & Woodward, S. (2008) Effects of Large-Scale Amazon Forest Degradation on Climate and Air Quality through Fluxes of Carbon Dioxide, Water, Energy, Mineral Dust and Isoprene. *Phil. Trans. R. Soc. B*, 363, 873–1880. doi:10.1098/rstb.2007.0027. *http://rstb.royalsocietypublishing.org/*

Birkett, C. M. (2000). Synergistic remote sensing of Lake Chad: Variability of basin inundation. *Remote Sensing Environment*, 72, 218 – 236.

Braganza, k., Karoly, D.J., Hirst, A.C. Mann, M.E., Stott, P., Stouffer, R.J., & Tett, S.F.B. (2002). Simple Indices of Global Climate Variability and Change: Part I – Variability and Correlation Structure. *Climate Dynamics* 20, 491–502.

Burrough, P. A. (1986). *Principles of Geographical Information Systems for land Resources Assessment*. Oxford: Clarendon Press.

Campbell, J. B. (2007). *Introduction to Remote Sensing* (4th ed.). New York: The Guilford Press, 622p.

Campbell, J.B., & Wynne, R. H. (2011). *Introduction to Remote Sensing* (5th ed.). New York: The Guilford Press, 667p.

Clayton, D. (1961). Derived Savanna in Kabba Province, Nigeria. *Samaru Research Bulletin*, 15. Northern Nigeria: Ministry of Agriculture.

Clayton, W. D. (1961). Derived Savanna in Kabba Province. *Journal of Ecology*, 49(3), 595-604

Clayton, W. D. (1958). Secondary Vegetation and the Transition to Savanna near Ibadan. *Journal of Ecology*, 46(2), 217-238.

Cofer, W. R., Levine, J. S., Winstead, E. L., & Stocks, B. J. (1991). New Estimates of Nitrous Oxide Emissions from Biomass Burning. *Nature*, 349, 689-691.

Cook, K. H. & Vizy, E. K. (2006). Coupled Model Simulations of the West African Monsoon System: Twentieth- and Twenty-First-Century Simulations. *Journal of Climate*, 19, 3681 - 3703.

Crutzen, P. J., & Andreae, M. O. (1990). Biomass Burning in the Tropics: Impact on Atmospheric Chemistry and Biogeochemical Cycles. *Science*, 250, 1669-1678.

Dai, A. (2006). Precipitation Characteristics in Eighteen Coupled Climate Models. *Journal of Climate*, 19, 4605 – 4630.

Dale, V. H. (1997). The Relationship between Landuse Change and Climate Change. Ecological Applications. *Ecological Society of America*, 7(3), 753-769.

Department of Environment (1987). Handling Geographic Information. *Report of the Enquiry Chaired by lord Chorley.* London; HMSO.

de Smith, M.J., Goodchild, M.F., & Longley, P.A. (2007). *Geospatial Analysis – A Comprehensive Guide to Principles, Techniques and Software Tools*. UK: The Winchelsea Press. 394P

Efe, S. I. (2011). Climate Change: A Challenge to Our Generation. In A. T. Salami & O. I. Orimoogunje (Eds.), *Environmental Research and Challenges of Sustainable Development in Nigeria* (pp.165 – 189). Ile Ife, Nigeria: Obafemi Awolowo University Press.

Eastman, R. (2012). *IDRISI Selva Manual Guide to GIS and Image Processing* (17, Pp 332).Worcester, MA, USA: Clark University.

ESRI (1990). *Understanding GIS - The ARC/INFO Method*. Redlands, CA: ESRI (Environmental Systems Research Institute Incorporations);

Fasona, M. J. (2007). Land Degradation and Environmental Change in Ondo State Coastline, Southwest, Nigeria. *Ph.D. Thesis (unpb).* University of Lagos: Department of Geography.

Fasona, M. J., Tadross, M., Abiodun, B. J., & Omojola, A. S. (2010). Climate Change, Terrestrial Ecology Imprints and Adaptation Options in Semi-Dry Environments: A Case of the Nigerian Savannah. Proceeding of 2nd International Conference: *Climate, Sustainability and Development in Semi-arid Regions.* ICID+18, August 16 - 20, 2010, Fortaleza - Ceará, Brazil.

Fasona, M.J., & Omojola, A.S. (2005). Climate Change, Human Security and Communal Clashes in Nigeria. *Proceeding of International Workshop on Human Security and Climate Change*, Holmen Fjord Hotel, Asker, near Oslo, 22–23 June 2005. Accessed on 2007, August 10. Retrieved from: www.gechs.org/activities/holmen/Fasona_Omojola.pdf.

Federal Ministry of Environment (FME) (2004). *National Biodiversity Strategy and Action Plan* (Pp 1-144). Abuja-Nigeria: FME.

Fitzpatrick-Lins, K. (1981). Comparison of Sampling Procedure and Data Analysis for a Land-Use and Land-Cover Map. *Photogrammetric Engineering and Remote Sensing*. 47(3), 343–351.

Folland, C.K., Karl, T.R., Christy, J.R., Clarke, R.A., Gruza, G.V., Jouzel, J., ...Wang, S.W. (2001). Observed Climate Variability and Change. In J.T. Houghton, Y. Ding, D.J. Griggs, M. Noguer, P.J. van der Linden, X. Dai, K. Maskell, and C.A. Johnson (Eds.). *Climate change 2001: The scientific Basis. Contribution of Working Group I to the Third Assessment Report of the Intergovernmental Panel on Climate Change* (pp. 99-181). UK: Cambridge University Press.

Gao, J. (2009). *Digital Analysis of Remotely Sensed Imagery* (Pp 645). New York: McGraw-Hill Companies, Inc.

Geist, H. J., & Lambin, E. F. (2002). Proximate Causes and Underlying Driving Forces of Tropical Deforestation. *Bio Science,* 52(2), 143-150.

Geist, H. J., & Lambin, E. F. (2004). Dynamic Causal Patterns of Desertification. *BioScience*, 54(9), 817-829.

Glantz, M. H., Betsill, M., & Crandall, K. (1997). Food Security in Southern Africa. Assessing the Use and Value of ENSO Information. *National Center for Atmospheric Research,* CO. USA.

Global Landcover Facility (2004). *Landsat Technical Guide;* Accessed on June 11, 2013. Retrieved from *http://glcf.umd.edu/library/guide/techguide_landsat.pdf*

Harrison, B.A. and Jupp, D. L. B. (1997): *Introduction to Remotely Sensed Data* (2nd ed.). France: CNES. *http://ceos.cnes.fr*

Harvey, L. D. D. (2013). Climate and Climate-System Modelling. In J. Wainwright and M. Mulligan (Eds.). *Environmental Modelling: Finding Simplicity in Complexity* (2nd ed., Ch.9). Chichester, UK: John Wiley & Sons, Ltd. doi: 10.1002/9781118351475

Harvey, L. D. D. (2000). *Global Warming: The Hard Science* (Chp 2. pp81-91). Harlow: Prentice Hall

Hewitson, B.C., & Crane, R. G. (1996). Climate Downscaling: Techniques and Application; *Climate Research*; 7, 85-95

Holling, C. S., & Sanderson, S. (1996). Dynamics of (Dis)harmony in Ecological and Social Systems. In S. Hanna, C. Folke, K. G. Maler, and A. Jansson (Eds.). *Rights to Nature: Ecological, Economic, Cultural, and Political Principles of Institutions for the Environment* (pp. 57–86). Washington, Island Press.

Houghton, R.A., & Goodale, C.L. (2004). Effects of Land-Use Change on the Carbon Balance of Terrestrial Ecosystems. *Ecosystems and Land Use Change, Geophysical Monograph Series, 153,* 85 – 98. American Geophysical Union, 10.1029/153GM08.

Houghton, R. A., Hobbie, J. E., Melillo, J. M., Moore, B., Peterson, B. J., Shaver, G. R., & Woodwell, G. M. (1983). Changes in Carbon Content of Terrestial Biota and Soil between 1860 and 1980: A Net Release of CO_2 to the Atmosphere. *Ecological Monographs,* 53, 235-262

Iloeje, N.P. (2001). *A New Geography of Nigeria* (New Revised Edition, Pp200.). Nigeria: Longman Plc.

IPCC (Intergovernmental Panel on Climate Change) (2001) *Climate Change 2001: Synthesis Report. A Contribution of Working Groups I, II, and III to the Third Assessment Report of the Intergovernmental Panel on Climate Change* (Pp 398). Cambridge, UK: Cambridge University Press.

IPCC (Intergovernmental Panel on Climate Change) (2007). *Climate Change 2007: Synthesis Report. Contribution of Working Groups I, II and III to the Fourth Assessment Report of the Intergovernmental Panel on Climate Change* [Core Writing Team, Pachauri, R.K and Reisinger, A. (Eds.). Pp 104]. Geneva, Switzerland: IPCC.

Jensen, J. R. (2007). *Remote sensing of the Environment: An Earth Resource Perspective (2nd e*d. Pp 592). Upper Saddle River, NJ: Pearson Education, Inc.

Jones, H. G., & Vaughan, R. A. (2010). *Remote Sensing of Vegetation: Principles, Techniques and Applications (*Pp 353). UK: Oxford University Press

Kandji, S. T., Verchot, L., & Mackensen, J. (2006). *Climate Change and Variability in the Sahel Region: Impacts and Adaptation Strategies in the Agricultural Sector* (Pp58). Nairobi: UNEP & ICRAF.

Kandji, S. T., Verchot, L. & Mackensen, J. (2006). *Climate Change and Variability in the Southern Africa Region: Impacts and Adaptation Strategies in the Agricultural Sector* (pp42). Nairobi: UNEP & ICRAF.

Keay, R.W.J. (1959). *An Outline of Nigerian Vegetation.* Lagos: Government Printer, Pp 54.

Kiehl, J. T. & Trenberth, K. E., (1997). Earth's Annual Global Mean Energy Budget. *Bull. Amer. Meteor. Soc.*, 78, 197-208.

Kim J. 1970. Factor Analysis. In Nie N.H., Hull C.H., Jenkins J.G., Steinberger, K., and Bent, D.H. (Eds.). *Statistical package for the social sciences*. New York, USA: McGraw Hill.

Lambin, E. F., Helmut, J. G., & Erika, L. (2003). Dynamics of Land Use and Land Cover Change in Tropical Regions. *Annual Review: Environmental Resources*, 28, 205-241.

Landsat - A Global Land-Imaging Mission (n.d.); Accessed on June 11, 2013; Retrieved from: *http://pubs.usgs.gov/fs/2012/3072/fs2012-3072.pdf*

Langdon, C., Broecker, W.S., Hammond, D.E., Glenn, E., Fitzsimmons, K., Nelson, S.G., ... Bonani, G. (2003). Effect of Elevated CO_2 on the Community Metabolism of an Experimental Coral Reef. *Global Biogeochem. Cy.* 17, 1011, doi: 10.1029/2002GB001941

Laymon, C. (2003). Satellite Remote Sensing of Land Use Change. *www.directionsmag.com\article.php*

Lesschen, J. P., Verburg, P. H., & Staal, S. J. (2005). *Statistical Methods for Analysing the Spatial Dimension of Changes in Land Use and Farming Systems – LUCC Report Series 7 (*Chapter 3, pp26-51). LUCC Focus 3 Office, the Netherland and ILRI 2005, Kenya

Le Treut, H., Somerville, R., Cubasch, U., Ding, Y., Mauritzen, C., Mokssit, A., Peterson, T., & Prather, M. (2007). Historical Overview of Climate Change. In: S. Solomon, D. Qin, M. Manning, Z. Chen, M. Marquis, K.B. Averyt, M. Tignor and H.L. Miller (Eds.). *Climate Change 2007: The Physical Science Basis. Contribution of Working Group I to the Fourth Assessment Report of the Intergovernmental Panel on Climate Change* (Chp.1, pp93-128). Cambridge, UK: Cambridge University Press.

Lillesand, T. M., and Kieffer, R. W. (1987). *Remote Sensing and Image Interpretation* (2nd ed.). New York: John Wiley and Sons.

Loucks, O. L. (1977). Emergence of Research on Agro-Ecosystems. *Annual Review of Ecology and Systems*, 8, 173–192.

Loveland, T., Gutman, G., Buford, M., Chatterjee, K., Justice, G., Roger, C., Stokes, B., & Thomas, J. (2003). Land-Use/Land-Cover Change. In Mahoney et al., (Eds.). *Strategic plan for the US Climate Change science program – A report by the Climate Change Science Program and Subcommittee on Global Change Research (*Pp61-70). Washington, DC, USA: National Academy Press.

Lu, D., P., Mausel, E. B., & Moran, E. (2004). Change Detection Techniques. *International Journal of Remote Sensing*, 26, 2365–2401.

Luizao, F., Matson, P., Livingston, G., Luizao, R., & Vitousek, P. (1989). Nitrous Oxide Flux following Tropical Land Clearing. *Global Biogeochemical Cycles*, 3, 281-285

Mahoney, J. R., Asrar, G., Leinen, M. S., Andrews, J., Glackin, M., Groat, C., … Wuchte, E. (2003) *Strategic Plan for the US Climate Change science program – A report by the Climate Change Science Program and Subcommittee on Global Change Research* (pp211). Washington, DC, USA: National Academy Press. Retrieved from http://climatescience.gov/ Library/stratplan2003/default.htm

Maguire, D. J. (1989). *Computers in Geography.* London: Longman.

Matthews, E. (1983). Global Vegetation and Landuse: New High Resolution Data Bases for Climate Studies. *Journal of Climate and Applied Meteorology*, 22, 474-487

Maurer, E. P., Adam, J. C., & Wood, A. W. (2009). Climate Model Based Consensus on the Hydrologic Impacts of Climate Change to the Rio Lempa Basin of Central America. *Hydrology and Earth System Sciences*, 13, 183–194.

Meehl, G. A., Covey, C., McAvaney, B., Latif, M., & Stouffer, R. J. (2005). Overview of the Coupled Model Intercomparison Project, B. *Am. Meteor. Soc.,* 86, 89–93.

Mitchell, B. (1989). *Geography and Resources Analysis* (2nd ed. pp186). UK: Longman Group.

National Bureau of Statistics (NBS) (2006). *Federal Republic of Nigeria: 2006 Population Census.* Pp10. www.nigerianstat.gov.ng

NCAR (2005). A Continent Split by Climate Change: New Study Projects Drought in Southern Africa, Rain in Sahel. *National Center for Atmospheric Research Press Release*, May 24, 2005, Boulder, CO.

Odeyemi, S.O (1998). Plant – The Renewal Green Gold. *Inaugural Series*. Lagos: University of Lagos Press.

Odjugo, P. A. O. (2011). Climate Change: Evidence, Impacts and Adaptation Strategies in Nigeria. In A. T. Salami & O. I. Orimoogunje (Eds.), *Environmental Research and Challenges of Sustainable Development in Nigeria* (pp.142 – 164). Ile Ife, Nigeria: Obafemi Awolowo University Press.

Odjugo P. A. O. & Ikhuoria I. A. (2005). An Analysis of Rainfall Pattern in Nigeria. *Global Journal of Environmental Sciences*, 4(2), 139 – 146

Oguntunde, P. G., Abiodun, B. J., &. Gunnar, L (2011). Rainfall Trends in Nigeria, 1901–2000. *Journal of Hydrology*, 411, 207 - 218. doi:10.1016/j.jhydrol.2011.09.037

Oguntunde, P. G., Abiodun, B. J., & Gunnar, L. (2012). Spatial and Temporal Temperature Trends in Nigeria, 1901–2000. *Meteorology and Atmospheric Physics*, 118, 95–105.

Ojo, S.O. (1987). The Climatic Drama. *Inaugural Series*. Lagos: University of Lagos Press.

Ojo, S.O., Ojo, K. & Oni, F. (2001) *Fundamentals of Physical and Dynamic Climatology*. Lagos: Sedec Publishers.

Omojola, A.S. (1997). Use of Remote Sensing and Geographic Information Techniques in Land Use and Land Cover Inventory and Change Assessment in a Semi-Arid Region of Nigeria. *Ph.D Thesis* (*Unpl).* University of Lagos: Department of Geography. 184p

Omojola, A., & Soneye, A. S. O. (1993). Applications of Remote Sensing and GIS Subsystem Techniques for Land Use and Land Cover Mapping in the Middle Sokoto River, North Western Nigeria. *Nigerian Journal of Remote Sensing*, 1(1), 52-57.

Omotoso, F. (2009). Administrative Problems of State Creation in Ekiti State, Nigeria. *African Journal of Political Science and International Relations*. **3(3),** 107-116. Retrieved from http://www.academicjournals.org/article/article1379786015_Omotosho.pdf

Oyenuga, V.A. (1967). *Agriculture in Nigeria*. Rome, Italy: Food and Agriculture Organization of the United Nations (FAO).

Pickles, J. (Ed.). (1995). *Ground Truth: The Social Implications of Geographic Information Systems*. New York: The Guilford Press.

Pielke Sr, R. A., Adegoke, J., Beltran-Przekurat, A., Hiemstra, C. A., Lin, J., Nair, U. S., ... Nobis, T. E. (2007). An Overview of Regional Land-Use and Land-Cover Impacts on Rainfall. *Tellus*, 59B, 587 – 601.

Pielke Sr, R. A., Marland, G., Betts, R. A., Chase, T. N., Eastman, J. L., Niles, J. O., ... Running S. W. (2002). The Influence of Land-Use Change and Landscape Dynamics on the Climate System: Relevance to Climate-Change Policy beyond the Radiative Effect of Greenhouse Gases. *Phil. Trans. R. Soc. Lond. A* 360, 1705 – 1719.

Pielke, Sr. R. A. (2001). Influence of the Spatial Distribution of Vegetation and Soils on the Prediction of Cumulus Convective Rainfall. *Rev. Geophys.* 39, 151 - 177.

Pielke, R. A. (1997). The Role of Land Cover as a Driving for Regional Climate Change. In S.J. Hassol, and J. Katzenberger (Eds., 1998) electronic edition 2008, *Scaling from Site-Specific Observations to Global Model Grids* (pp.89-92). Proceeding of an Aspen Global Change Institute Workshop 7-17 July 1997, Elements of Change series, AGCI.

Pielke, R. A., & Avissar, R. (1990). Influence of Landscape Structure on Local and Regional Climate. *Landscape ecology*, 4(2/3), 133 – 155.

Pitman, A. J. (2003). The Evolution of, and Revolution in, Land Surface Schemes Designed for Climate Models. *Int. J. Climatol.*, 23, 479 - 510.

Pitman, A., Pielke Sr., R., Avissar, R., Claussen, M., Gash J., & H. Dolman (2000). The Role of the Land Surface in Weather and Climate: Does the Land Surface Matter? *IGBP Newsletter*, 39, 4 - 11

Pontius, G. R., & Malanson, J. (2005). Comparison of the Structure and Accuracy of Two Land Change Models. *International Journal of Geographical Information Science*, **19**, 43–265.

Randall, D.A., Wood, R.A., Bony, S., Colman, R., Fichefet, T., Fyfe, J., ... Taylor, K.E. (2007). Climate Models and Their Evaluation. In Solomon, S., D. Qin, M. Manning, Z. Chen, M. Marquis, K.B. Averyt, M.Tignor and H.L. Miller (Eds.), *Climate Change 2007: The Physical Science Basis. Contribution of Working Group I to the Fourth Assessment Report of the Intergovernmental Panel on Climate Change* (Ch.8, Pp589 – 662). Cambridge, UK and New York, NY, USA: Cambridge University Press.

Roberts, D. A., Batista, G. T., Pereira, J., Waller, E. K., & Nelson, B. W. (1998). Change Identification Using Multitemporal Spectral Mixture Analysis: Applications in Eastern Amazonia. In: C. Elvidge, & R. Lunetta (Eds.). *Remote Sensing Change Detection: Environmental Monitoring Applications and Methods* (pp. 137–161). Ann Arbor, MI: Ann Arbor Press

Rosenzweig, C., Parry, M. L., Fischer, G. & Frohberg, K. (1993). *Climate Change and World Food Supply*. Research Report No. 3. Oxford: University of Oxford, Environmental Change Unit.

Sabin, F. F. (2007). *Remote sensing: Principles and interpretation* (3rd ed. pp494). Long Groove, IL: Waveland Press, Inc.

Simpson, G. C. (1959). World Temperatures during the Pleistocene. *Quarterly Journal of Royal Meteorological Society*, 85, 332 – 49.

Simpson, G. C. (1957). Further Studies in World Climate. *Quarterly Journal of Royal Meteorological Society*, 83, 358, 459 – 81.

Shine, K. P., Derwent, R. G., Wuebbles, D. J. & Morcrette, J .J. (1990). Radiative forcing of climate. In J. T. Houghton, G. J. Jenkins, and J. J. Ephranums (Eds.). *Climate Change: The IPCC Scientific Assessment* (pp. 40-68). New York, USA: Cambridge University Press.

Solomon, S., Qin, D., Manning, M., Alley, R.B., Berntsen, T., Bindoff, N.L. … Wratt, D. (2007). Technical Summary. In Solomon, S., D. Qin, M. Manning, Z. Chen, M. Marquis, K.B. Averyt, M. Tignor & H.L. Miller (Eds.), *Climate Change 2007: The Physical Science Basis. Contribution of Working Group I to the Fourth Assessment Report of the Intergovernmental Panel on Climate Change (pp*19–92). Cambridge, UK: Cambridge University Press

Soneye, A.S.O (2012) Concentrations of GHGs around Tankfarms and Petroleum Tankers Depots, Lagos, Nigeria. *Journal of Geography and Regional Planning.* 5(4), 108-114.

Soneye A.S.O., & Akintuyi, A. (2013). Nigeria Remote Sensing and Topographical Mapping, 1937 - 2010: A Critical Appraisal. *Lagos Journal of GIS,* University of Lagos. 1(2), 16 – 27.

Soneye, A.S.O. (2004). Fadama Resources Management in Nigeria: Implications for Sustainable Agricultural Development in the Sokoto-Rima Basin. In O. Badejo, and A. Omitogun (Eds.). *Strategies and Tactics for Sustainable Agriculture in the Tropics* (2 (1), 209 – 226). Ibadan: College Press.

Soneye, A. S. O. (2000). The Application of Satellite Remote Sensing and GIS in the Evaluation and Revision of Nigerian Topographical Maps (pp284). *Ph.D. Thesis, (unpb).* University of Lagos, Lagos: Department of Geography.

Soneye, A.S.O. (1999). Creating GIS Spatial Database from the Nigerian 1:25,000 Topographical Map Series: A Technical Appraisal. In O.Y. Balogun, and A.S.O. Soneye (Eds.). *Cartography in the Service of Government* (Ch. 6, Pp. 50 – 60). Lagos: Nigeria Cartographic Association.

Stephenne, N., & Lambin, E. F. (2001a). A Dynamic Simulation Model of Landuse Changes in Sudano-Sahelian Countries of Africa (SALU). *Agric. Ecosyst. Environ.*, 85, 145-161.

Strahler, A.H (1980). The Use of Prior Probabilities in Maximum Likelihood Classification of Remotely Sensed Data. *Remote Sensing of Environment*, 10, 135-163

Swanson, K. L., Sugihara, G., & Tsonis, A. A. (2009). Long-term natural variability and 20th century climate change. *PNAS,* 106(38), 16120 - 16130. Retrieved from www.pnas.org_cgi_doi_10.1073_pnas.0908699106

Taylor, C. M., Lambin, E. F., Stephenne, N., Harding, R., & Essery, R. L. H. (2002). The Influence of Landuse Change on Climate in the Sahel. *American Meteorological Society*, 15, 3615-3628

Thiam, A., & Eastman, J. R. (2009). Vegetation Indices. In J. Ronald Eastman (Ed.). *Idrisi Taiga guide to GIS and image processing* (Pp. 213 – 224). Worcester, Ma: Clarks Lab, Clarks University.

Turner II, B. L., Meyer, W. B., & Skole, D. L. (1994). Global Land-Use/Land-Cover Change: Towards an Integrated Study. *Ambio,* 23(1), 91-95

Turner, B. L; Moss, R. H. & Skole, D. L. (1993). Relating Landuse and Global Landcover Change. *A Proposal for an IGBP-HDP Core Project, HDP Report No 5* (pp.1-13). Stockholm, Sweden: International Geosphere-Biosphere Programme

Veldkamp, A. & Fresco, L. O. (1996). CLUE-CR: An Integrated Multi-Scale Model to Simulate Landuse Change Scenarios in Costa Rica. *Ecological Modelling*, 91, 231-248.

Verburg, P. H., Soepboer, W., Limpiada, R., Espaldon, M. V. O., & Sharifa, M. (2002). Land Use Change Modelling at the Regional Scale: The CLUE-S model. E*nvironmental Management;* 30(3), 391-405

Verburg, P. H., Veldkamp, A., de Koning, G. H. J., Kok, K., & Bouma, J. (1999). A Spatial Explicit Allocation Procedure for Modeling the Pattern of Landuse Change Based Upon Actual Landuse. *Ecological Modelling*, 116, 45-61.

Vine, H., Weston, V. J., Montgomery, R. F., Smyth, A: J. & Moss, R. P. (1954). Progress of Soil Surveys in South-Western Nigeria. *2nd Inter-African Soils Conf.*, Leopoldville, 211.

Wang, G. (2004). A Conceptual Modeling Study on Biosphere-Atmosphere Interactions and its Implications for Physically Based Climate Modeling. *Journal of Climate*, 17, 2572-2583

Wang, Y., Woodcock, C. E., Buermann, W., Stenberg, P., Voipio, P., Smolander, H., …. Myneni, R. B. (2004). Evaluation of the MODIS LAI Algorithm at a Coniferous Forest Site in Finland. *Remote Sensing of Environment*, 91, 114–127

Wang, G. L., & Eltahir, E. A. B. (2000).The Role of Ecosystem Dynamics in Enhancing the Low-Frequency Variability of the Sahel Rainfall. *Water Resources Res* 36: 1013–1021.

Willett, H.C. (1953). Atmospheric and Oceanic Circulation as Factors in Glacial Interglacial Changes of Climate. In H. Shapley (Ed.). *Climate Change* (pp51–71). Cambridge: Harvard University Press

Wood, A. W., Leung, L. R., Sridhar, V., & Lettenmaier, D. P. (2004). Hydrologic Implications of Dynamical and Statistical Approaches to Downscaling Climate Model Outputs. *Clim. Change*, 62, 189–216.

Xue, Y. (1997). Biosphere Feedback on Regional Climate in Tropical North Africa. *Quarterly Journal Royal Meteorological Society*, 123, 1483–1515.

Xue, Y., & Shukla, J. (1993). The Influence of Land Surface Properties on Sahel Climate. Part I: Desertification. *J Climate*, 6, 2232 – 2245

Zeng, N., Neelin, J. D., Lau, K. M. & Tucker, C. J. (1999). Enhancement of Interdecadal Climate Variability in the Sahel by Vegetation Interaction. *Science*, 286, 1537–1540.

Zheng, X., & Eltahir, E. A. B. (1997). The Response to Deforestation and Desertification in a Model of West African Monsoons. *Geophysical Research Letters*, 24(2), 155 – 158.

http://www.suratclimatechange.org/upload/image/global_climate_system.jpg

http://www.fao.org/ag/agp/AGPC/doc/Counprof/PDF%20files/Nigeria.pdf (26/01/2014)

https://unfccc.int/files/methods/redd/submissions/application/pdf/redd_20090425_biocarbon_fund.pdf

http://www.usgs.gov

Appendix I: Raster data of the LULC change drivers

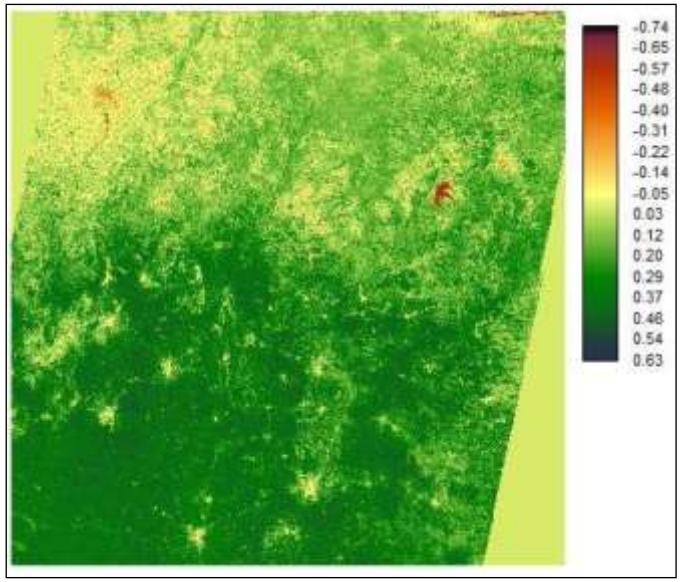

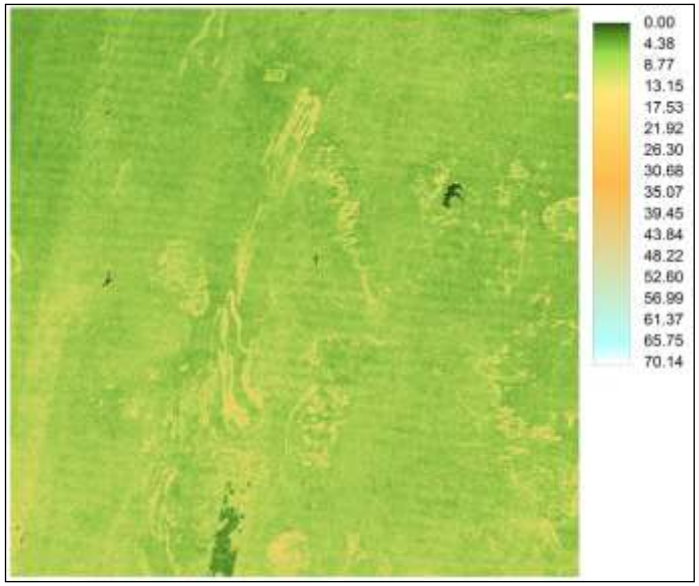

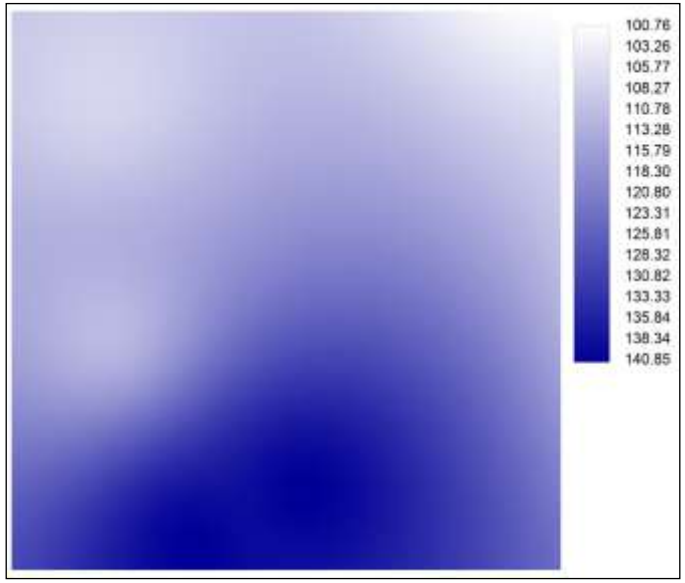

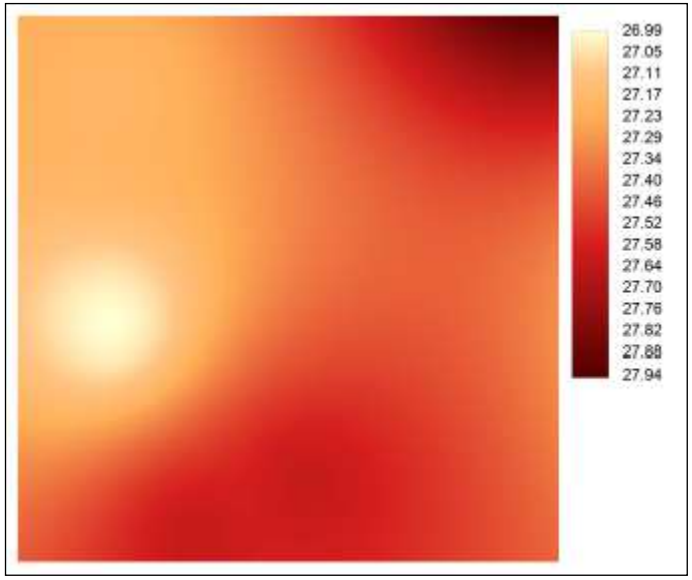

Appendix I: Raster data of the LULC change drivers

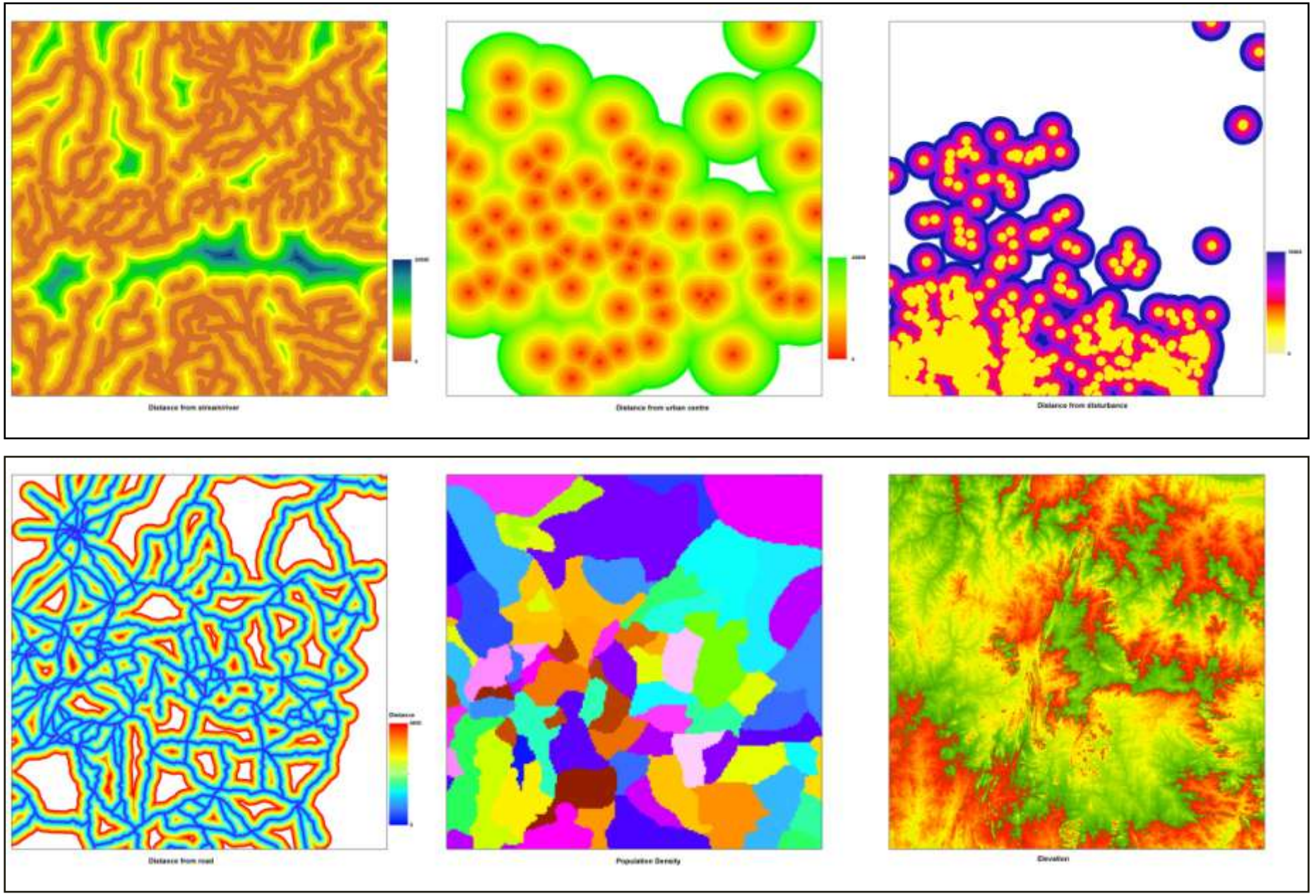

Appendix IIa: Result of Factor Analysis - Present Climate

Correlation Matrix[a]

		Cover	Aspect	Disturb	Elev31	NDVI31	Pop31
Correlation	Cover	1.000	.186	.652	.256	.699	-.222
	Aspect	.186	1.000	.087	.841	.812	-.389
	Disturb	.652	.087	1.000	.246	.504	.367
	Elev31	.256	.841	.246	1.000	.797	-.285
	NDVI31	.699	.812	.504	.797	1.000	-.367
	Pop31	-.222	-.389	.367	-.285	-.367	1.000
	Rain31	.643	.243	.656	.255	.621	.045
	Road	.394	-.451	.375	-.179	-.084	-.082
	Slope	.513	.536	.411	.494	.745	-.484
	Stream	.272	.670	.457	.758	.705	.066
	Temp31	-.147	-.421	-.635	-.450	-.439	-.487
	Urban31	-.068	.275	-.687	.004	.078	-.871
	Tmax31	-.543	-.361	-.737	-.377	-.651	-.220
	Tmin31	.159	-.354	-.356	-.374	-.181	-.493

a. This matrix is not positive definite.

Correlation Matrix[a]

		Rain31	Road	Slope	Stream	Temp31	Urban31
Correlation	Cover	.643	.394	.513	.272	-.147	-.068
	Aspect	.243	-.451	.536	.670	-.421	.275
	Disturb	.656	.375	.411	.457	-.635	-.687
	Elev31	.255	-.179	.494	.758	-.450	.004
	NDVI31	.621	-.084	.745	.705	-.439	.078
	Pop31	.045	-.082	-.484	.066	-.487	-.871
	Rain31	1.000	-.157	.724	.568	-.387	-.222
	Road	-.157	1.000	-.034	-.378	.199	-.224
	Slope	.724	-.034	1.000	.396	-.087	.175
	Stream	.568	-.378	.396	1.000	-.815	-.202
	Temp31	-.387	.199	-.087	-.815	1.000	.554
	Urban31	-.222	-.224	.175	-.202	.554	1.000
	Tmax31	-.935	.236	-.598	-.770	.686	.373

	Tmin31	.071	.149	.250	-.608	.892	.478

a. This matrix is not positive definite.

Correlation Matrix[a]

		Tmax31	Tmin31
Correlation	Cover	-.543	.159
	Aspect	-.361	-.354
	Disturb	-.737	-.356
	Elev31	-.377	-.374
	NDVI31	-.651	-.181
	Pop31	-.220	-.493
	Rain31	-.935	.071
	Road	.236	.149
	Slope	-.598	.250
	Stream	-.770	-.608
	Temp31	.686	.892
	Urban31	.373	.478
	Tmax31	1.000	.284
	Tmin31	.284	1.000

a. This matrix is not positive definite.

Total Variance Explained

Component	Initial Eigenvalues		
	Total	% of Variance	Cumulative %
1	6.070	43.355	
2	3.325	23.750	
3	2.402	17.155	
4	1.220	8.715	
5	.431	3.082	96.056
6	.307	2.189	98.245
7	.227	1.620	99.865
8	.019	.135	100.000
9	8.251E-16	5.894E-15	100.000
10	4.931E-18	3.522E-17	100.000
11	-1.006E-16	-7.188E-16	100.000
12	-3.362E-16	-2.401E-15	100.000

13	-6.067E-16	-4.333E-15	100.000
14	-1.272E-15	-9.085E-15	100.000

Extraction Method: Principal Component Analysis.

Total Variance Explained

Component	Initial Eigenvalues	Extraction Sums of Squared Loadings		
	Cumulative %	Total	% of Variance	Cumulative %
1	43.355	6.070	43.355	43.355
2	67.105	3.325	23.750	67.105
3	84.260	2.402	17.155	84.260
4	92.974	1.220	8.715	92.974

Extraction Method: Principal Component Analysis.

Total Variance Explained

Component	Rotation Sums of Squared Loadings		
	Total	% of Variance	Cumulative %
1	3.880	27.716	27.716
2	3.852	27.512	55.227
3	3.608	25.768	80.996
4	1.677	11.979	92.974

Extraction Method: Principal Component Analysis.

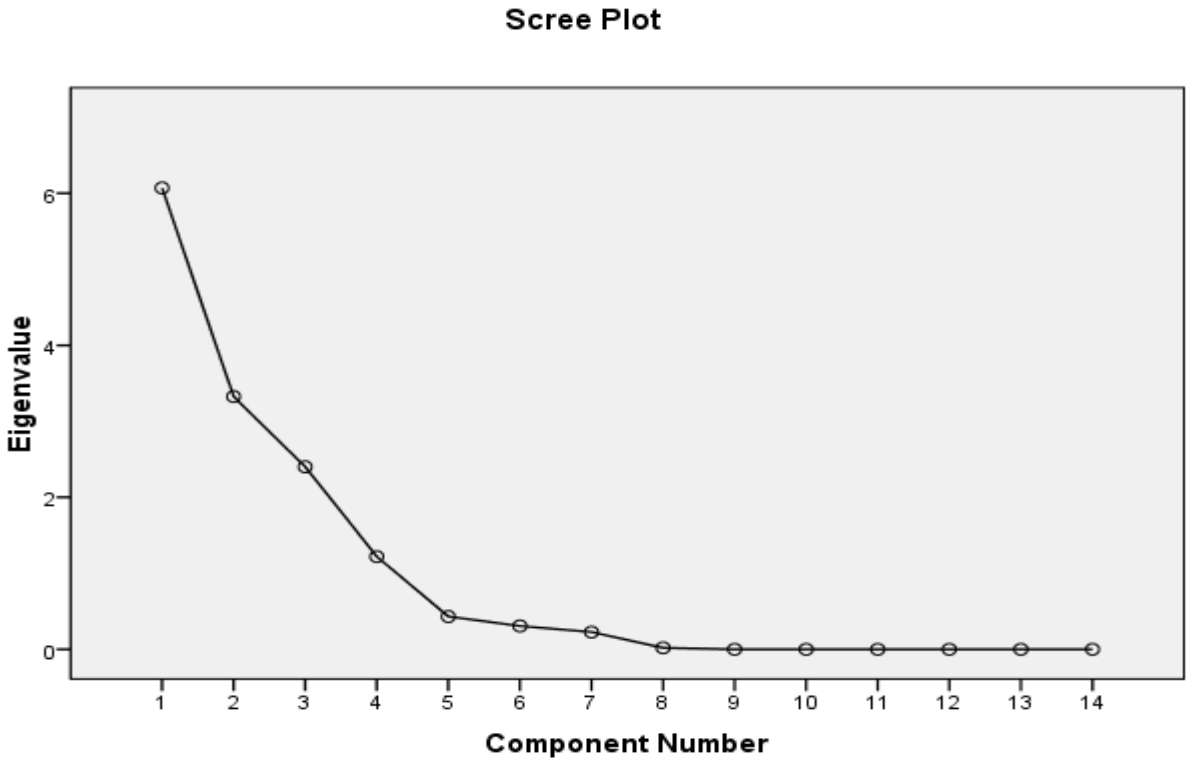

Rotated Component Matrix[a]

	Component			
	1	2	3	4
Cover	.704	.185	.081	.552
Aspect	.172	.916	.147	-.223
Disturb	.635	.156	-.575	.461
Elev31	.169	.913	-.004	.030
NDVI31	.592	.766	.097	.152
Pop31	-.039	-.347	-.899	-.142
Rain31	.979	.098	-.127	-.096
Road	-.057	-.215	-.010	.955
Slope	.760	.373	.346	.058
Stream	.413	.735	-.381	-.240
Temp31	-.226	-.530	.781	.102
Urban31	-.159	.163	.888	-.212
Tmax31	-.854	-.283	.393	.151
Tmin31	.236	-.539	.773	.072

Extraction Method: Principal Component Analysis.

Rotation Method: Varimax with Kaiser Normalization.

Rotated Component Matrix[a]

	Component			
	1	2	3	4
Cover	.704	.185	.081	.552
Aspect	.172	.916	.147	-.223
Disturb	.635	.156	-.575	.461
Elev31	.169	.913	-.004	.030
NDVI31	.592	.766	.097	.152
Pop31	-.039	-.347	-.899	-.142
Rain31	.979	.098	-.127	-.096
Road	-.057	-.215	-.010	.955
Slope	.760	.373	.346	.058
Stream	.413	.735	-.381	-.240
Temp31	-.226	-.530	.781	.102
Urban31	-.159	.163	.888	-.212
Tmax31	-.854	-.283	.393	.151
Tmin31	.236	-.539	.773	.072

Extraction Method: Principal Component Analysis.

Rotation Method: Varimax with Kaiser Normalization.

a. Rotation converged in 6 iterations.

Component Transformation Matrix

Component	1	2	3	4
1	.678	.659	-.325	.010
2	.172	.289	.942	-.015
3	.557	-.546	.076	.621
4	-.447	.430	-.038	.783

Extraction Method: Principal Component Analysis.

Rotation Method: Varimax with Kaiser Normalization.

Component Plot in Rotated Space

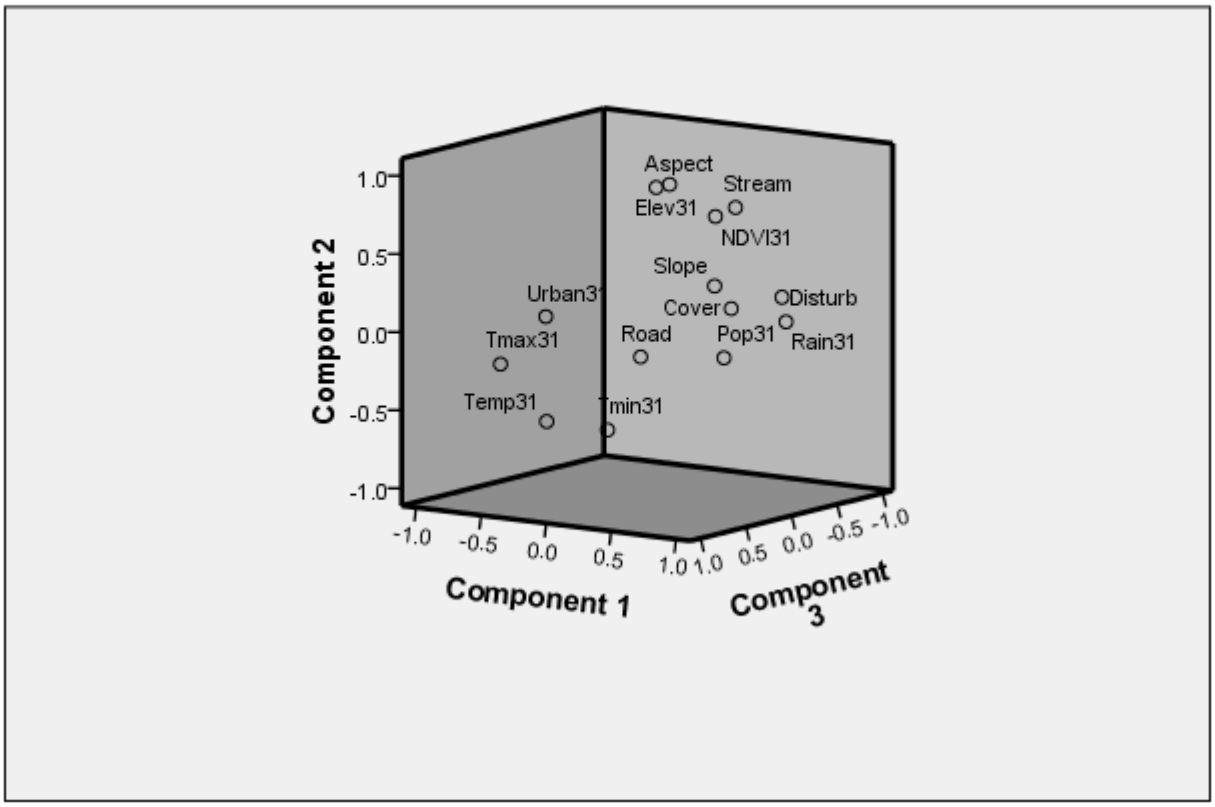

Appendix IIb: Result of Factor Analysis - Future Climate

Correlation Matrix

		Cover	Aspect	Disturb	Mravg	Mtavg	Elev31
Correlation	Cover	1.000	.186	.652	.607	.375	.256
	Aspect	.186	1.000	.087	.298	-.462	.841
	Disturb	.652	.087	1.000	.643	-.014	.246
	Mravg	.607	.298	.643	1.000	-.046	.299
	Mtavg	.375	-.462	-.014	-.046	1.000	-.387
	Elev31	.256	.841	.246	.299	-.387	1.000
	NDVI31	.699	.812	.504	.641	-.126	.797
	Pop31	-.222	-.389	.367	.060	-.354	-.285
	Road	.394	-.451	.375	-.220	.610	-.179
	Slope	.513	.536	.411	.716	.231	.494
	Stream	.272	.670	.457	.626	-.684	.758
	Urban31	-.068	.275	-.687	-.222	.186	.004

Correlation Matrix

		NDVI31	Pop31	Road	Slope	Stream	Urban31
Correlation	Cover	.699	-.222	.394	.513	.272	-.068
	Aspect	.812	-.389	-.451	.536	.670	.275
	Disturb	.504	.367	.375	.411	.457	-.687
	Mravg	.641	.060	-.220	.716	.626	-.222
	Mtavg	-.126	-.354	.610	.231	-.684	.186
	Elev31	.797	-.285	-.179	.494	.758	.004
	NDVI31	1.000	-.367	-.084	.745	.705	.078
	Pop31	-.367	1.000	-.082	-.484	.066	-.871
	Road	-.084	-.082	1.000	-.034	-.378	-.224
	Slope	.745	-.484	-.034	1.000	.396	.175
	Stream	.705	.066	-.378	.396	1.000	-.202
	Urban31	.078	-.871	-.224	.175	-.202	1.000

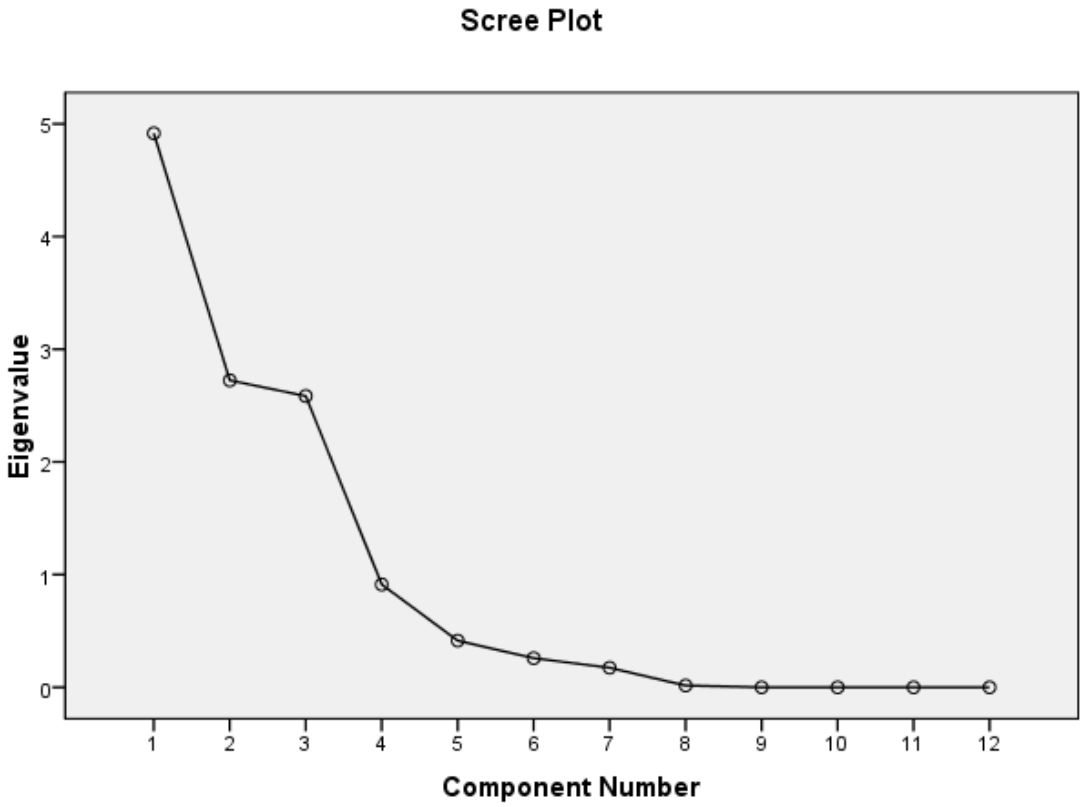

Total Variance Explained

Component	Extraction Sums of Squared Loadings	
	Total	% of Variance
1	4.916	40.970
2	2.724	22.701
3	2.585	21.538

Extraction Method: Principal Component Analysis.

Total Variance Explained

Component	Extraction Sums of Squared Loadings	Rotation Sums of Squared Loadings		
	Cumulative %	Total	% of Variance	Cumulative %
1	40.970	4.602	38.351	38.351
2	63.672	2.944	24.531	62.881
3	85.210	2.679	22.328	85.210

Extraction Method: Principal Component Analysis.

Rotated Component Matrix[a]

	Component		
	1	2	3
Cover	.810	-.409	.049
Aspect	.584	.655	-.357
Disturb	.700	-.186	.653
Mravg	.784	.086	.251
Mtavg	.063	-.911	-.282
Elev31	.652	.540	-.155
NDVI31	.934	.245	-.162
Pop31	-.280	.129	.929
Road	.111	-.805	.141
Slope	.832	-.038	-.285
Stream	.638	.675	.220
Urban31	-.083	.037	-.957

Extraction Method: Principal Component Analysis.

Rotation Method: Varimax with Kaiser Normalization.

a. Rotation converged in 7 iterations.

Component Transformation Matrix

Component	1	2	3
1	.928	.370	-.034
2	.242	-.531	.812
3	.283	-.762	-.582

Extraction Method: Principal Component Analysis.

Rotation Method: Varimax with Kaiser Normalization.

Component Plot in Rotated Space

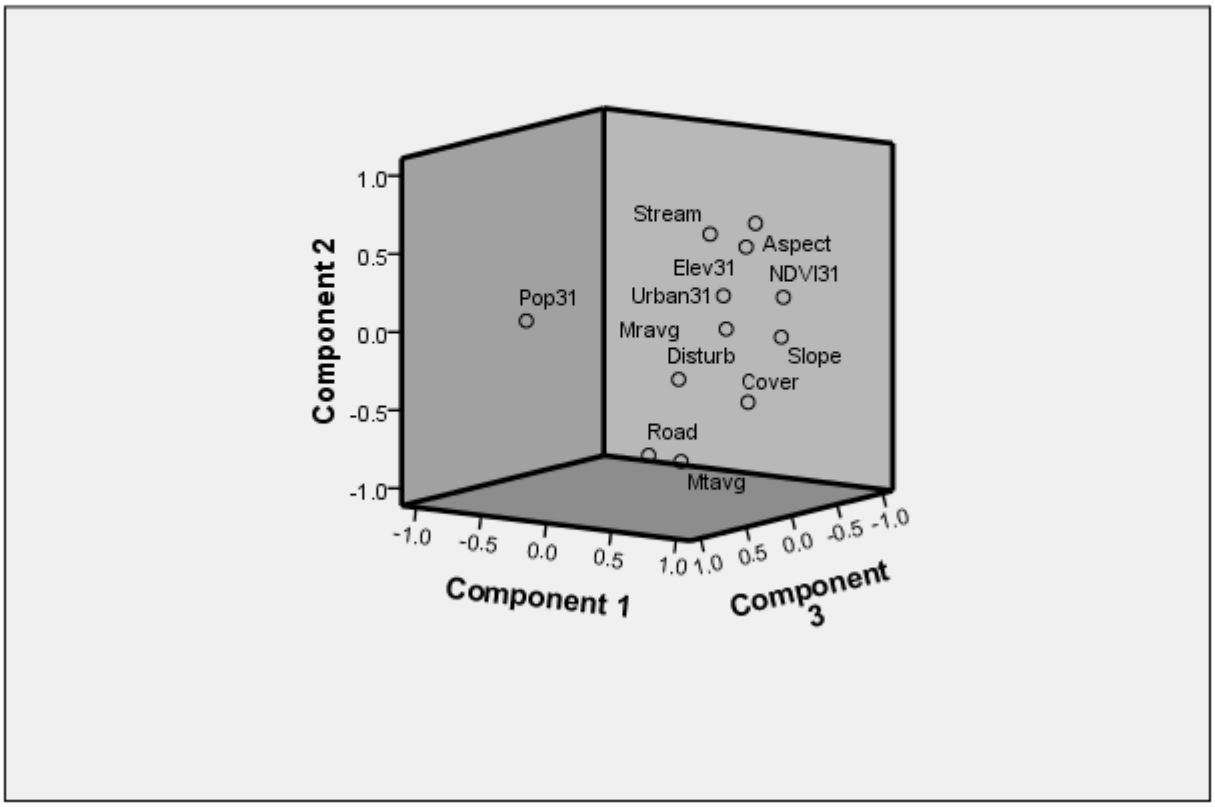

Appendix III: Confusion Matrix and Kappa Index of Agreement

Table 1: Proportional Crosstabulation between predicted and real LULC, 2010

LULC	Cloudcover	Degraded Surface	Farmland	Fire scar	Forest	Grassland	Area without Data	Urban	Waterbody	Woodland	**Total**
Degraded Surface	0	0.0576	0.0069	0.0001	0.0021	0.0375	0	0.0037	0	0.003	0.111
Farmland	0	0.0296	0.0063	0.0001	0.0007	0.0232	0	0.0014	0	0.0006	0.062
Fire scar	0	0.008	0.0019	0	0.0004	0.0085	0	0.0005	0	0.0002	0.0195
Forest	0	0.0891	0.002	0.0001	0.1643	0.053	0	0.0015	0.0002	0.0965	0.4067
Grassland	0	0.0501	0.0079	0.0002	0.0008	0.0571	0	0.0012	0	0.0007	0.1181
Area without Data	0	0.0143	0.0102	0	0.0012	0.0072	0.0367	0.0025	0.0004	0.0012	0.0737
Urban	0	0.0119	0.0028	0	0.001	0.0098	0	0.012	0	0.0011	0.0386
Waterbody	0	0.0002	0.0001	0	0.0002	0.0002	0	0.0001	0.0016	0.0001	0.0025
Woodland	0	0.0629	0.0055	0.0001	0.0071	0.0818	0	0.0021	0	0.0083	0.1679
Total	0	0.3238	0.0435	0.0007	0.1779	0.2783	0.0367	0.025	0.0023	0.1118	1

Table 2: Kappa Index of Agreement (KIA)

Using real LULC 2010 as the reference image

LULC	KIA
Cloud cover	0
Degraded Surface	0.0753
Farmland	0.0893
Fire scar	0.0462
Forest	0.8713
Grassland	0.0989
Area without Data	1
Urban	0.4595
Waterbody	0.675
Woodland	-0.1121
Overall Kappa	0.2132

Using predicted LULC 2010 as the reference image

Category	KIA
Degraded Surface	0.2887
Farmland	0.0615
Fire scar	0.0016
Forest	0.2751
Grassland	0.2848
Area without Data	0.479
Urban	0.2933
Waterbody	0.6339
Woodland	-.0699
Overall Kappa	0.2132